2010/2011

Mapping of Nitrate Reduction Capacities on a Small Scale

Lundgårds Bæk Catchment Area

Master Thesis by Denitza Voutchkova

Department of Civil Engineering
Aalborg University
Denmark

[empty page]

Title: Mapping of Nitrate Reduction Capacities on a Small Scale: Lundgårds Bæk Catchment Area

Theme: Groundwater – Surface Water Interaction, Nitrate Reduction

Project period: Autumn 2010, Spring 2011

Synopsis:

This master thesis aims to research and develop a way for estimating the nitrate reduction capacities of a small agriculture-dominated catchment area of first-second order stream (Lundgårds bæk). From landuse management point of view, it would be economically more efficient to use small scale maps instead of the existing national big scale nitrate reduction potential map.

More specific, the goals of this thesis are: to understand the nitrate fate in the catchment area of Lundgårds bæk; to develop a method for estimating the nitrate reduction capacities on a sub-catchment level; and to map critical zones from the catchment area, contributing to the nitrate pollution of Lundgårds bæk.

It was found that the high NO_3^- concentrations in Lundgårds bæk are caused by NO_3^- contaminated groundwater and that the measured concentrations differ significantly in the different part of the stream.

The developed nitrate reduction capacity map showed that only around 30% of Lundgårds bæk catchment area has less than 80% NO_3^- reduction capacity. While, according to the big scale national map the whole catchment falls in the 50-75% reduction potential zone

The mapping of the critical zones illustrated that the leaching from 80% of Lundgårds bæk catchment area is not affecting the water quality of the stream.

Project group: no *[individual work]*

Participant:

_____
Denitza Voutchkova

Supervisors:

Jacob Birk Jensen

Morten Lauge Pedersen

Copies: 5
Page Numbers: 113
Appendixes: 14
Delivery date: 07.06.2011

The content of this report is freely accessible but any publication must be proper referenced and the acceptance of the authors must be given.

[empty page]

Preface and Acknowledgments

This report regards the final thesis for the autumn semester 2010 and spring semester 2011 (60ECTS) of the Master program "Water and Environment" within the Department of Civil Engineering at Aalborg University. The thesis has been made in close collaboration with NIRAS and Nature Agency (Aalborg) as part of their partnership on the Aquarius project.

The chapters of this report are alphabetically marked and the appendixes are numbered according to the order of their appearance. Whenever an appendix is mentioned in the text, it will include its title and the page, for example (Appendix: Base Flow Separation, p.135). As for the chapters, only their heading letter and the page is given, for example (Chapter B, p.13). If there is a reference made to a specific part in the chapter, then the page of that part is given. All figures and tables in the report are numbered in the order they appear in it. Captions regarding figures are given below them and captions of tables are given above them. When referring to a figure or table from different part of the report, the page is also given. All references present in the report include, in brackets, the name of the author (person or organization) and the year of publication, for example (Hansen et al., 2011). In addition, whenever a reference is made, it refers to the information presented before it. The source of the used images is given as a reference in the caption for the respective figure. The only exception is the picture on the cover, which is taken from Stephan S. Lund as part of the Aquarius project (Miljøcenter Alborg, 2010).

I wish to thank my supervisors, Jacob Birk Jensen and Morten Lauge Pedersen, for their fruitful supervision through the last year. I'm grateful for the given opportunity to work on that project in a close collaboration with NIRAS and Nature Agency (Aalborg). It has been an honour for me to be part of their teams and to have the chance to get an inside view on the working atmosphere in those two organisations. I would like to express my special gratitude to Jørgen Bidstrup and Kirsten Elisabeth Broch for sharing their knowledge, for the inspiring advises, and for the help through the field work. Also, I would like to thank to Martin Skjøtt Linneberg and Morten Westergaard for the pleasant teamwork on the 3D geological model; and, to Jacob Skødt Jensen and Ole Munch Johansen for their help in one or other point of the project work. Further, I'm thankful for the proof-reading, the moral support and patience to Niels Claes; and to Ina Ibro, with whom we've shared a group-room, for her friendship. And last but not least, I wish to thank to my parents for their financial support and for making it possible for me to attend an education in Aalborg University.

[empty page]

Table of Contents

A. Project Objective 11

B. Literature Study on Nitrogen Dynamics: the Fate of Nitrate in Three Zones of Interest 13

Introduction 13

Introduction to Nitrogen Cycle 14

1st Zone of Interest: Upland 15

2nd Zone of Interest: Groundwater 19

Groundwater Flow System 19

Microbial Metabolism in the Soil and Nitrate Reduction in Deep Aquifers 21

3rd Zone of Interest: Riparian Zone 23

Stream and Hyporheic Zone Characteristics 23

Wetlands and Riparian Buffer Zone Characteristics 25

Nitrogen (N) Storage in Wetlands 26

Nitrogen Cycling in Wetlands 26

Groundwater - Surface Water Interactions (Connection between 2nd and 3rd Zone of Interest) 28

Types of Water Flow through the Riparian Zone and Attenuation Capacity of the Riparian Zone 28

Examples for Conceptualising the GSI 30

C. Project Site Description 35

Project Site Location and Land Use 35

Nitrate Leaching to the Groundwater 36

Regional Geomorphology 40

Regional Hydrogeology 42

Regional Hydrology and Hydrochemistry 44

D. Monitoring Data Analysis 45

Rainfall Data Analysis 45

Base Flow Analysis for Lundgårds Bæk 47

Introduction 47

Method 47

Results 48

Discussion 48

Analysis of the Relation between the Nitrate Concentration and the Flow Rate 50

Introduction 50

Initial Data Analysis 51

Pearson's Correlation 53

Regression Analysis 54
Conclusions 57
E. Field work 59
Used Methods and Results 59
Flow Rate Measurements along Lundgårds Bæk 60
Nitrate-N and Nitrite-N concentrations in the stream 61
Water Temperature Measurements in the Stream 62
Field Investigation and Sampling from the Sources (Groundwater Springs, Diffuse Groundwater Flow, Pipes etc. in Lundgårds bæk's Riparian Zone) 63
Overview and discussion of the results from the field work 67
F. Analysis of the Catchment and the Sub-catchment Areas 69
Introduction 69
Method 69
Topographical Sub-catchment Areas 69
Hydrogeological Sub-Catchment Areas 69
Results 73
Catchment Areas of Lundgårds Bæk 73
Sub-catchment Areas 74
Groundwater-flow Residence Time 76
G. Estimation of the Nitrate Leaching from the Sub-catchment Areas 79
Introduction 79
Method 79
Results 82
H. Application of Two Methods, Found in Literature Sources, for Estimating Reduction Capacities ... 85
Application of the Dahl's GSI Typology as a Tool for Estimating the Reduction Capacities of the Riparian Zone for the Sub-catchment Areas 85
Introduction 85
Critical Sub-catchments 85
GSI 2nd Level: Riparian Hydrogeological Types 86
GSI 3rd Level: Riparian Flow Path Types 88
Reduction Capacities of the Riparian Zone (Based on Dahl's GSI Typology) 89
Application of the Vidon & Hill Conceptual Model as a Tool for Estimating the Reduction Capacities of the Riparian Zones for the Sub-catchment Areas 90
Introduction 90
Needed Width of the Riparian Buffer Zone for 90% Removal of the Nitrate Removal 91

Conclusion 93
I. Reduction Capacity on Sub-catchment Scale 95
Introduction 95
Method 95
Results 101
Overview and Discussion 102
J. Critical Areas for Nitrate Pollution 105
Introduction 105
Where Does the Calculated Nitrate Reduction Take Place? 105
Method 105
Results and Discussion 106
K. Summary and Conclusions 107
L. Future Perspectives 109
M. Bibliography 111
N. Appendixes 115
Appendix: Nitrate Reduction Potential Map 117
Appendix: Rosgen Stream Bed Classification 119
Appendix: Six Geological Profiles (Initial Geological Study) 121
Appendix: Building a 3D Geological Model of the Project Area 123
Introduction 124
Method 124
Conceptual Geological Model 129
Results 130
Appendix: Base Flow Separation 135
Appendix: Basic Theory for the Statistical Analysis (after TGP, 2005) 139
Appendix: Nitrate Concentrations Plotted vs. Flow Rate (Annually and Monthly) 143
Appendix: Regression Analysis (Additional Figures) 149
Appendix: Field Observations and Thermo Imaging 155
Appendix: Field Measurements 167
Appendix: Residence Times 171
Appendix: Stream Valley Characteristics 177
Appendix: Non-agricultural Sources for Nitrate Leaching 181
Appendix: Correction Coefficients Calculations 183

[empty page]

A. Project Objective

The goals of this project are:

- to understand the nitrate fate in a small agricultural area – the catchment area of Lundgårds bæk ;
- to develop a method for estimating the nitrate reduction capacities on a small scale (sub-catchment level);
- to map critical zones from the catchment area, contributing to the nitrate pollution of Lundgårds bæk;

Why focusing on nitrate and on the reduction capacities on a small scale?

Nitrate is one of the two readily available for direct assimilation forms of Nitrogen. It is, as a part of the Nitrogen cycle, one of the most important nutrients responsible for the growth of microbes, algae, plants etc. The large input of Nitrogen and Phosphorus to a freshwater or marine water bodies, especially when all other factors are present (favourable temperatures, high oxygen content, bad mixing of the water column etc.), can cause algal blooms, oxygen depletion and extinction of species. Hence, the eutrophication, which is caused by human activities, has a negative impact on the aquatic environment. One of the main pathways of Nitrogen, reaching the surface bodies, is recognised to be the nitrate leaching from the root zone to the groundwater.

As part of the European Union legislation, the EU Water Frame Directive (WFD), which objective is to establish a frame work for protecting the surface and groundwater bodies from further pollution, was accepted by all EU members. With the acceptance of the WFD, Denmark has set a goal to achieve a good ecological status for all surface and ground water bodies until 2015. For the region of Mariager fjord, in which catchment area the project area is situated, fulfilling the goals of the WFD means that the negative human impact on the ecosystem should be reduced. As part of the plan, a reduction of nitrate input from the agricultural sources is needed. Further, a big scale nitrate reduction map is provided on a national level. According to that map the project area falls in a region, where the reduction capacity is from 50-75% (see Figure 98, p.118). However, using this big-scale map to take land-use management decisions might be economically inefficient. That's why as part of this project, an attempt to develop a new small scale reduction map is made.

Taking into account this very general information, the final goal of this project is to find a more effective way to define critical areas on a smaller scale, where a reduction of the nitrate input would be efficient.

In each part of this report something new is added to the knowledge about Lundgårds bæk catchment area or in general about the nitrate fait in a dominantly agricultural land. The report is divided in eleven chapters and each of them contributes in the following way:

- **Literature Study**: a better understanding on the chemical and physical processes happening in the system is obtained;
- **Project Site Description**: an information on the regional geomorphology and hydrogeology is given; as addition, the land use and the historical aspect of the nitrate leaching from the agricultural land is discussed;

- **Monitoring Data Analysis**: the available hydrological and hydrochemical data for the project site are analysed; the base flow separation shows what part of the water feeding the stream is with groundwater origin; the correlation analysis shows the correlation between the flow rate and the nitrate concentration;
- **Field Work**: the distribution of flow rate and nitrate concentrations along the stream is studied; the sources of nitrate pollution are investigated; the water quality of the groundwater spring is analysed;
- **Catchment and Sub-catchment Analysis**: two methods for delineating the sub-catchment areas are used and the areas are compared; additionally, the travelling times of the groundwater flow particles (modelled in GMS, by NIRAS) between the recharge and discharge area are analysed and the "age" distribution of the groundwater for each sub-catchment area is determined;
- **Estimating the Nitrate Leaching from the Sub-catchments:** weighted average and total nitrate leaching from each sub-catchment is calculated, taking into account also the non-agricultural sources of nitrate leaching
- **Application of Different Methods for Conceptualising the GSI in Order to Estimate Reduction Capacities:** it is found which sub-catchments are "critical" and which are "not critical" for the nitrate load to the stream and the dependant eco-system; Dahl's GSI typology is used to determine the reduction capacities of the riparian zones for each sub-catchment area; the width of the riparian buffer zone along the stream to have 90% nitrate removal is found, based on the Vidon & Hill conceptual model;
- **Estimation of the Reduction Capacities on Sub-catchment Scale**: a new methodology is established, so the reduction capacities of each sub-catchment were calculated; as part of the method, the "lag" time in the response of the system, the calculated total leaching, and the findings from the measurements for the flow and nitrate concentration distribution along the stream are taken into account; the developed method combines all the gathered information about the system through the project period. With the knowledge build as part of the initial literature study was possible the method and its weaknesses to be assessed;
- **Critical Areas for Nitrate Pollution:** the zones contributing to the nitrate pollution of the stream are mapped by using the estimated reduction capacities and the residence times of the groundwater flow particles, simulated with GMS;
- **Summary and Conclusions:** the results presented in this report are summarised and conclusions about the potential nitrate reduction measures are made;
- **Future Perspectives:** ideas about further investigation in the field of nitrate reduction on a small scale are presented.

B. Literature Study on Nitrogen Dynamics: the Fate of Nitrate in Three Zones of Interest

Introduction

The purpose of this part of the project is to obtain a better understanding on the physical and chemical nature of the processes and of the system, where they are happening.

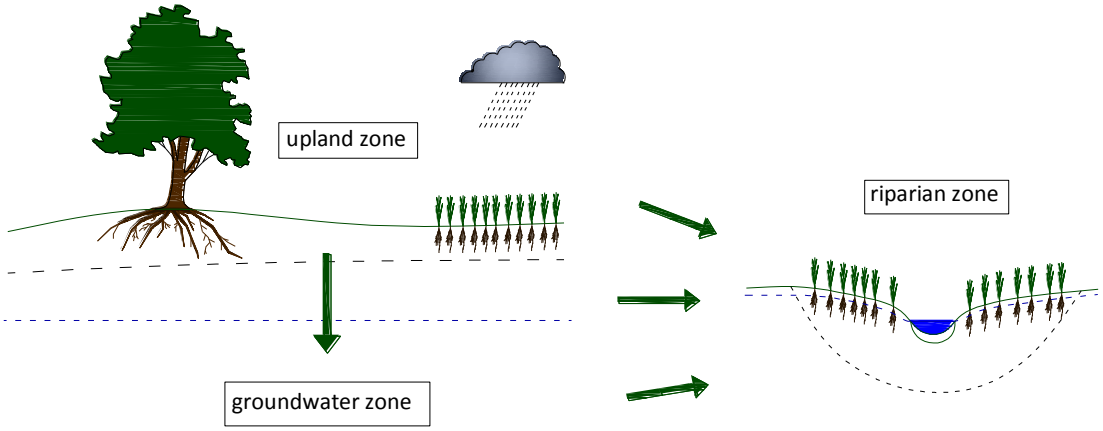

Figure 1: Zones of interest

When speaking about Nitrogen dynamics (nitrate is part of it), the system where it takes place can be roughly divided in a 3 main zones of interest (see Figure 1):

- Upland zone
- Groundwater zone
- Riparian zone (including the wetlands and stream beds)

The streams carry the Nitrogen to lakes, fjords, seas and the ocean, meanwhile the Nitrogen cycles from inorganic to organic form and back. This project studies small agricultural catchment area of a first-second order stream and the focus of interest is limited to what happens in the upland zone, groundwater zone and riparian zone. The processes occurring in the lake/estuary sediments or water column are not discussed.

The same logic of zone division is used for the structure of the literature study. First a basic explanation on the Nitrogen cycle is made, and then, the processes happening in the three zones of interest are discussed.

Introduction to Nitrogen Cycle

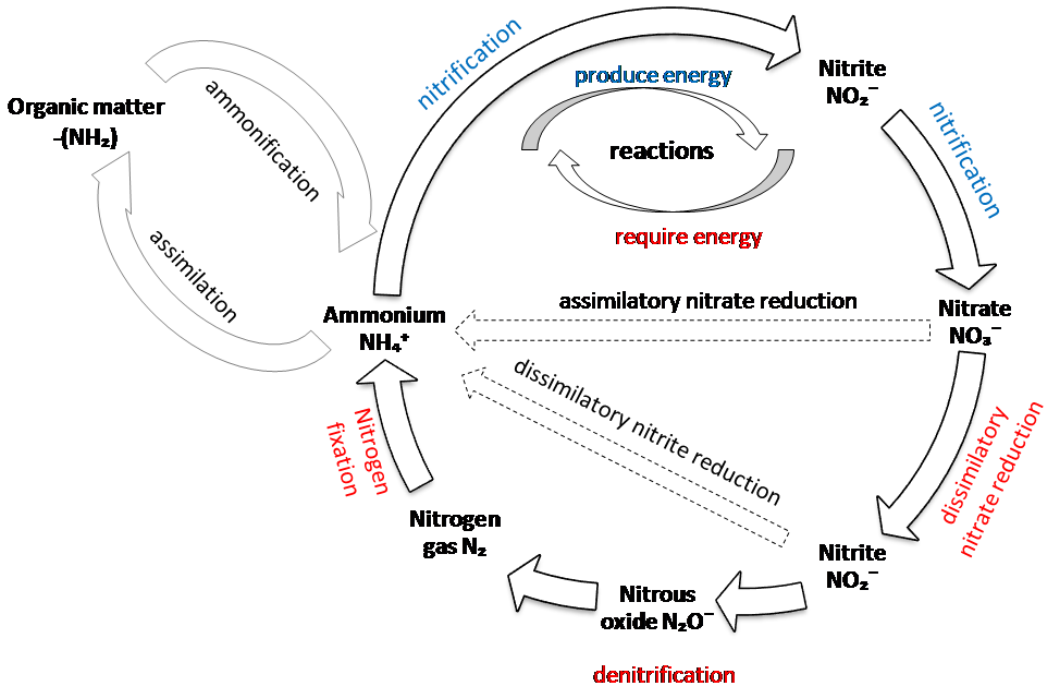

Figure 2: Nitrogen cycle (modified (Duff & Triska, 2000))

The processes taking part into the Nitrogen cycle are schematically presented on *Figure 2.*

Ammonium (NH_4^+), nitrate (NO_3^-) and nitrite (NO_2^-) are the dissolved inorganic Nitrogen (N) forms and nitrous oxide (N_2O^-) and Nitrogen gas (N_2) are the gaseous forms. From all these forms of N, the biologically available ones, which can be assimilated directly, are NO_3^- and NH_4^+. NH_4^+ is used preferably over NO_3^- for assimilation of N by green plants, algae, bacteria, fungi.(CAB International, 2008)(Duff & Triska, 2000). Most of the N in the aquatic systems is bond in organic matter and it is inaccessible for assimilation until it is mineralized to NH_4-N.(Duff & Triska, 2000)

There are two main types of biological transformation in the Nitrogen cycle:

- obtaining Nitrogen for structural synthesis;
- energy-yielding reactions (e.g.: nitrification and denitrification). (CAB International, 2008)

Between the N in NH_4^+ and NO_3^- there are 8 electrons difference in the valence (large range in the redox potential). As a result, the reactions transforming the Nitrogen from reduced (-3) to oxidized state (+5) are producing energy, which is used by the chemolitothrophic bacteria. Opposite, the reactions which transform the Nitrogen from oxidised to reduced state require energy.(Duff & Triska, 2000)

The nitrification-denitrification pathways result in loss of NH_4^+, which is first converted to NO_3^-, then to N_2. Nitrification and denitrification are processes driven by microbial metabolism. The nitrification process is carried out by two types of organisms: Nitrosomonas (NH_4^+ to NO_2^-) and Nitrobacter ($NO_2^-$to NO_3^-). Nitrification is oxygen-demanding process, the efficiency of which is dependent on the oxygen concentrations, pH, and temperature.(CAB International, 2008).

Denitrification occurs largely in sediments and is controlled by both oxygen supply and available energy provided by the organic matter. Factors which control the rate of denitrification:

- oxygen depletion (favours denitrification);
- organic carbon (or other compound, see "Microbial Metabolism in the Soil and Nitrate Reduction in Deep Aquifers", p. 21)
- pH (low pH favours N_2 production).
- Temperature (denitrification decreases at low temperatures)
- Other inhibiting compounds (for example: Sulphide (S_2^-) depresses N_2 production, but stimulates the reduction of NO_3^- to NH_4^+). (CAB International, 2008)

Denitrification occurs in anoxic sediments (estuary, lake, river, stream sediments), in riparian zones, and in deep subsurface layers. It is considered as the main mechanism for reducing the concentration of NO_3^-. Several studies on NO_3^- profiles in depth have shown on a meters-scale some correlation with both groundwater and sediment characteristics. (Pedersen et al., 1991)

There are big differences in the N dynamics between the upland and wetland zones/riparian zones(Nieder & Benbi, 2008). The nitrification, denitrification and the other processes will be further discussed in the next parts.

1st Zone of Interest: Upland

The upland soils have a tendency to be better aerated than the wetland soils and in general the decomposition rates of organic materials are higher. The landscape position of upland soils results in drainage and transport of nutrients and particles to lower areas. The periodic shifts between wet and dry cycles causes decrease and increase of the oxygen availability, which influences the direction of the processes. (Nieder & Benbi, 2008)(Shaffer & Ma, 2001).

The N in upland zone occurs together with a carbon in the soil organic matter (SOM) and also as inorganic NO_3^--N, NH_4^+-N, urea, plant residues, and as gaseous forms. Usually the relative amounts of N found in the upland soils are in the following order (Nieder & Benbi, 2008)(Shaffer & Ma, 2001), (see Figure 3):

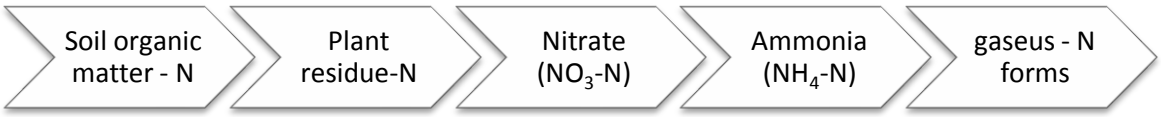

Figure 3: Occurrence of Nitrogen in different forms (decreasing amounts from left to right direction)

The most mobile and with the most negative effects on the environment are the NO_3-N and the gaseous forms of N. (Shaffer & Ma, 2001)

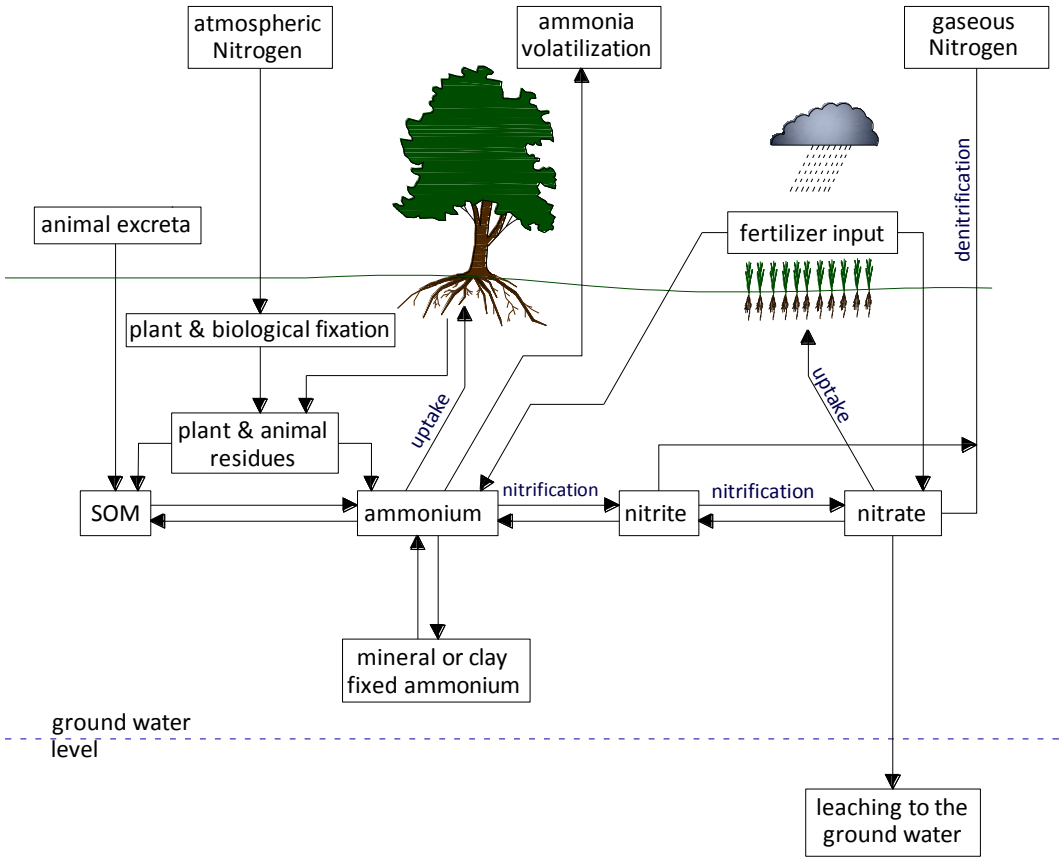

Figure 4: Nitrogen cycle in upland soils (after(Nieder & Benbi, 2008))

The Nitrogen cycle in upland soils is presented on Figure 4. The sources for N in the upland soil are: plant residues, organic fertilizers (manure, sewage sludge, and compost), synthetic fertilisers, biological and plant fixation of N from the atmosphere, and N in the precipitation. The processes when there is N loss are: erosion and runoff, NO_3^- leaching to the groundwater, ammonia (NH_3) volatilization, plant uptake, and denitrification. (Nieder & Benbi, 2008)

For the agricultural areas in Denmark, the average total load of N in 1991 has been 235 kgN/ha/year (Pedersen et al., 1991):

Table 1: Nitrogen load in Denmark *(Pedersen et al., 1991)*

Fertilizers [kg/ha/yr]	Manure [kg/ha/yr]	Atmospheric depositions [kg/ha/yr]
~130	~85	~20

From which around 85% should be lost in the environment trough the following processes:

- volatilization as NH_3,
- accumulation as ion-exchanged NH_3,
- organic N in the topsoil,
- denitrification in the top soil,
- leakage of NO_3^- to the ground water (Pedersen et al., 1991).

The fertiliser application in Denmark has been decreasing significantly since 1991, as will be shown in Chapter C (p.36). The present annual N cycle for the agricultural areas, based on the monitoring program of 5 representative sites for Denmark, is shown on Figure 5:

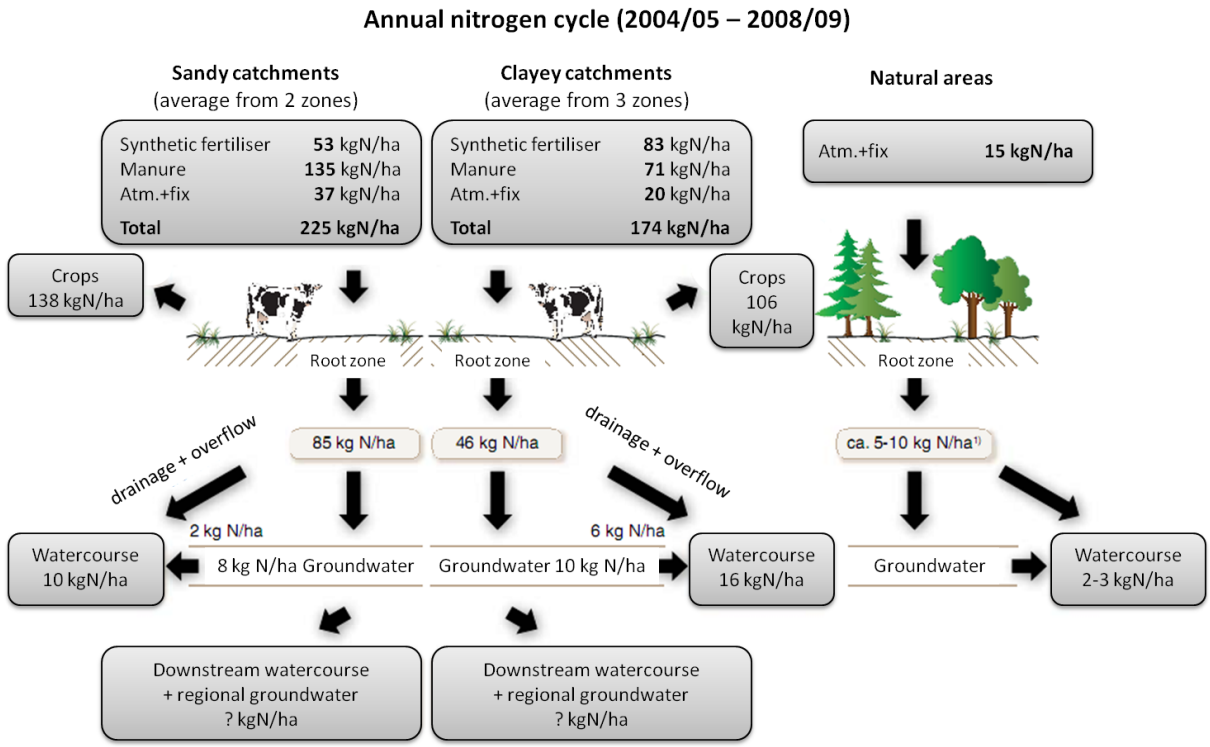

Figure 5: Annual Nitrogen cycle for the hydrogeological years 2004/05 - 2008/09 (translated from(Grant et al., 2010)) The data for the fertiliser application is based on interview survey for the period 2003-2007 and the leaching from the root zone is calculated with using the N-LES4 and averaged climate data for the period 1990-2005

The annual N cycle of Denmark is made for two types of catchments taking into account the different soil types – sandy soils or clayey soils. For the studied period the fertiliser application (synthetic and natural) equals to 188kg N/ha for sandy catchments and 154kg N/ha for clayey catchments. This results in 85kg N/ha and 46kg N/ha leaching from the root zone respectively from sandy and clayey catchments.(Grant et al., 2010)

Typically, the **plant uptake** of N is an important sink for agricultural areas. The uptake rates of NO_3^--N and NH_4^+-N by crops may range vastly – from 50kg N/ha/y to more than 400kg N/ha/y (Shaffer & Ma, 2001)(Nieder & Benbi, 2008). For Denmark it has been estimated to equal to 138kg N/ha/y for sandy catchments and 106kg N/ha/y for clayey catchments (Grant et al., 2010). The pre-applying of big amounts of fertilizers (to protect the crops from nutrient deficiency) can result in loosing significant amounts of N through NO_3^--N leaching to the ground water, denitrification, and NH_3 volatilization.(Shaffer & Ma, 2001).

The N from the decomposing organic material and the NO_3^--N and NH_4^+-N from the inorganic pool are used by the heterotrophic organisms to build a biomass. This immobilized N is remobilised when the microbes die(Shaffer & Ma, 2001). N is cycling rapidly between inorganic and organic forms: a complete turnover can happen in a few weeks. However, some forms of organic N (e.g.: humus) might have an age of thousands of years.(Nieder & Benbi, 2008)

As it was mentioned before, the **nitrification** process converts NH_4^+ to NO_3^- and it is carried out by small group of autotrophic nitrifies (CAB International, 2008). As addition, it is not anymore believed that these are the only organisms responsible for this process: it can occur by the activity of a heterotrophic bacteria and fungi capable of oxidising NH_4^+.(Nieder & Benbi, 2008)

Usually 2 to 3 weeks are needed (in the warmer months) to nitrify an application of NH_3-based fertiliser. If the process is not 100% effective, instead of NO_3^-, greenhouse gasses are produced. The nitrification process is sensitive to soil pH (reduction in the rates when ph is bellow 6 and above 8(Shaffer & Ma, 2001)) and also depends on the NH_4^+ concentration, temperature and soil-water content. (Nieder & Benbi, 2008).

The **denitrification** is a very fast pulse process and as a result (if the right conditions are present) a big Nitrogen loss can occur in a single day. These preferable conditions involve presence of sufficient NO_3^- amounts, fresh carbon source (manure, residue SOM), warm temperatures, and precipitation, irrigation or temporary flooding. These conditions are common in upland soils in early spring and summer and result in production of N_2 and greenhouse gasses.(Shaffer & Ma, 2001)

NO_3^- leaching is the main N loss process from the upland soils and contributes to pollution of underlying shallow aquifers. The NO_3^- leaching can vary greatly depending on the climatic, soil, plan and management factors(Nieder & Benbi, 2008)(Shaffer & Ma, 2001). Rates from less than 25 to greater then 300kg N/ha/y are common(Shaffer & Ma, 2001).Generally NO_3^- is leached faster from sandy soils than from silt and clay soils(Nieder & Benbi, 2008). As it is shown on Figure 5, the leaching from sandy soils (85kg N/ha/yr) is almost twice bigger than from clayey soils (46kg N/ha/yr) for Denmark.

The main form of N available for transport from the soil is NO_3^-. NO_3^- is not usually absorbed by the soil particles, is highly soluble and is characterized by high diffusion rates. The export of N from the catchment and its availability in water bodies is linked to hydrological processes and represents mostly transport-limited system. (CAB International, 2008)

Once leached bellow the root zone, the reduction of NO_3^- is difficult, and further movement downward can result in ground water contamination. Groundwater contamination from agricultural NO_3^- occurs in localised “hotspot” regions within shallow underlying groundwater aquifers.(Shaffer & Ma, 2001)(the authors give example with South Platte River in USA, where due to the coarse soil texture and bad management of some of the agricultural areas, the underplaying shallow groundwater was NO_3^- polluted)

The major routes for the transport of N are surface runoff, deep and shallow lateral groundwater flow. The importance of these pathways depends on the amount and pattern of precipitation, the surface water level, the specific retention time of groundwater systems, and the composition and slope of the soil. Agricultural drainage, in particular when using drains, favours transport in subsurface flow; this is recognized as the main pathway of NO_3^- transport from hill slopes to streams. (CAB International, 2008) This topic will be further discussed in the next part, where the focus is on the groundwater system and the processes in the deep subsurface.

2nd Zone of Interest: Groundwater

After the NO_3^- leaches to the groundwater the most important process which takes place is the transport. For fully understanding the nature of the NO_3^- fate in the groundwater, first a characteristic of the groundwater flow system should be done.

Groundwater Flow System

Different systems for characterising the groundwater flow system exist and 3 of them are presented.

The most used is the **Toth's classification** for unconfined groundwater systems up to 100km^2 with a small slope and lower order outlet streams. Differentiation is made between local, intermediate and regional flow systems. (see Figure 6)

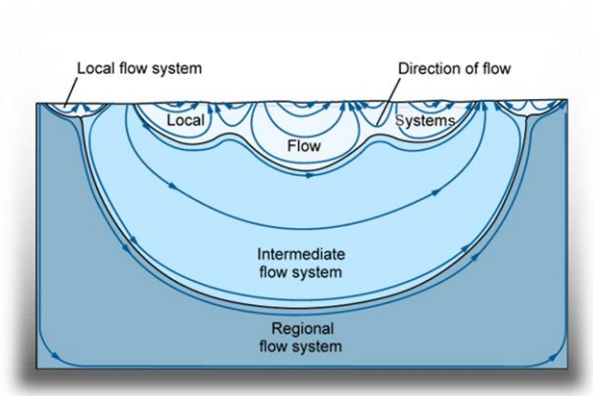

Figure 6: Groundwater flow systems of varying scale - local, intermediate and regional (Toth, 1963) *(Commonwealth of Australia, 2006)*

Groundwater from the local scale, which recharges at a topographic high and discharges to a topographic low, has high rates of recharge (1-30cm/yr) and high rates of groundwater flow (1-100m/yr).

The groundwater from an intermediate flow system, where the recharge and discharge points are separate by at least 1 topographical high, has a rate of recharge 0.01-1cm/yr and groundwater flow rate 0.1-1m/yr.

When it comes to the regional flow systems, which recharge only at a ground water divide and discharge only at the bottom of the basin, the flow rate is very, very low. (Chapelle & Lovely, 1995)

The water from a regional flow, at the point of discharge, should have relatively higher mineralisation and temperature. The local flow systems are shallower and the flow paths are shorter than the regional ones. The size of the recharge area is bigger with the respect of the volume water in the aquifer. The temperature of the groundwater is close to the year average air temperatures. The discharge shows wide fluctuations linked to the precipitation and great changes in the water quality. (Fetter, 2001)

There is a significant difference in the residence time of the local and regional flow systems. A schematic overview on the time scale is shown in Figure 7:

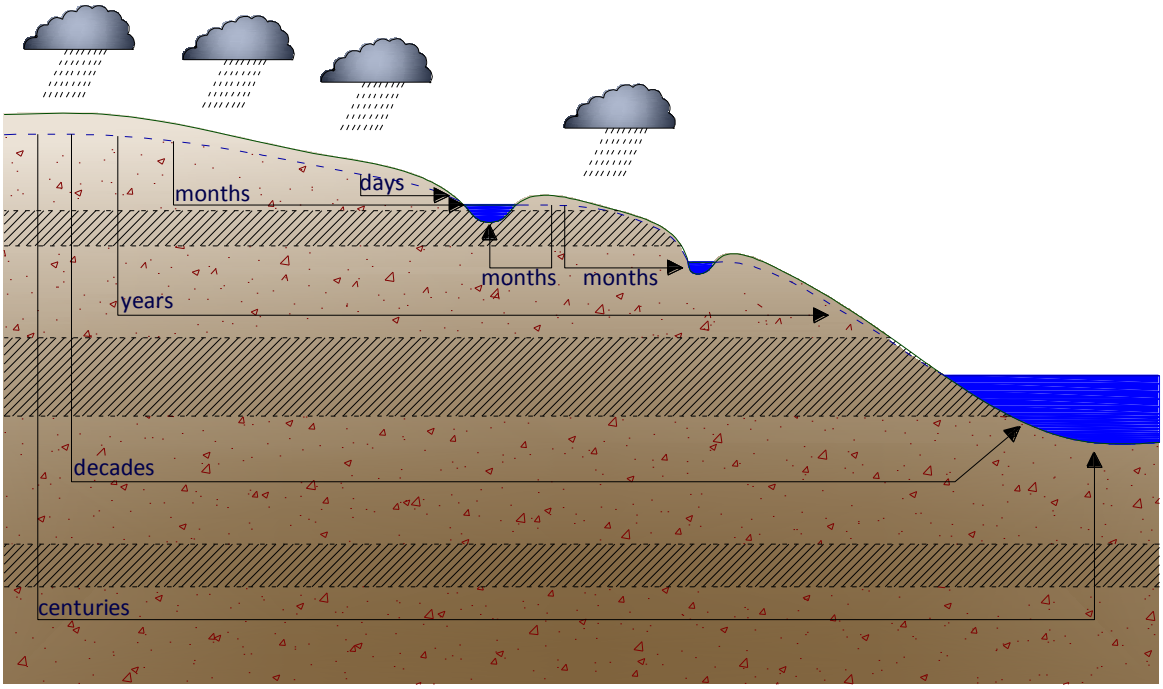

Figure 7: Schematic overview of groundwater residence times in large regional systems (after (K. M. van der Heijde, 1988))

Groundwater originating from regional and deep groundwater bodies is most likely to be reduced and NO_3^- free. The opposite is expected for a groundwater from shallow local groundwater bodies, where water is presumed to be oxidised and probably NO_3^- polluted depending on the land use(Dahl et al., 2007)

Heath (1982) has proposed a two level classification of the groundwater system, where on the first level, the groundwater system is classified by taking into account the number of aquifers and on the second level a further characteristic of the dominant aquifer is made.

On the first level the system can be classified as:

- single dominant unconfined aquifer;
- two interconnected aquifers of equal importance;
- three unit system : confined, confining and unconfined aquifer;
- complex system of interbedded aquifers and confining layers.

According to (Dahl et al., 2007), this way of classifying the regional systems gives useful information about the characteristics and the regional discharge patterns.

Milijøstyrelsen's system (Dahl et al., 2007) is another way to describe the groundwater flow system. This system is based on Toth's classification but also takes into account other factors which are affecting the groundwater body. In this system the ground water body is defined as a reactor, which is recharged, and discharges into the adjacent ecosystem and in between some processes are happening. The groundwater body is characterised by the lithology, redox state and the contact with the surface bodies (the absence or presence and the duration) (see Figure 8):

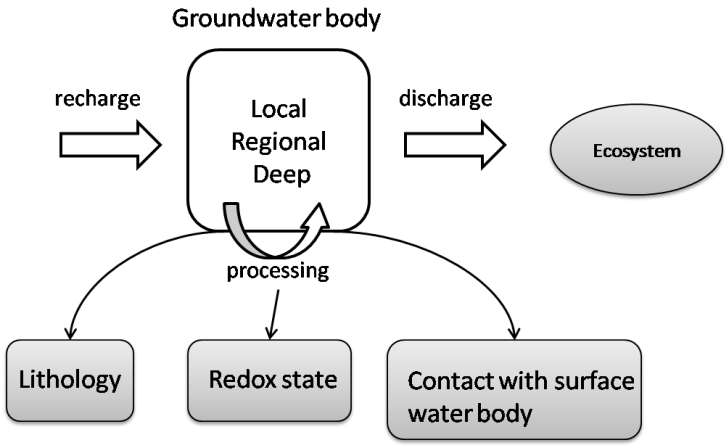

Figure 8: Miljøstyrelsen classification system

The different types of contact with the surface water bodies are discussed in the "Groundwater - Surface Water Interactions (Connection between 2nd and 3rd Zone of Interest)" (p.28).

When speaking about processes happening in the groundwater body, a brief review on the microbial metabolism in soil is needed, as most of the processes are governed by microorganisms.

Microbial Metabolism in the Soil and Nitrate Reduction in Deep Aquifers

Since there is no light available in the deep subsurface, the photosynthesis is not possible and the microorganisms depend on energy sources like organic matter and other reduced compounds (Mn^{4+}, Fe^{3+}, NH_3, sulphate (SO_4^{2-})). Energy is released with their oxidation. Microorganisms have evolved different ways for conserving the energy from the oxidations to support their growth. Each of these types of metabolisms is part of complex series of electron transfers. The most significant, from an environmental point of view, is the final electron transfer to an electron acceptor (terminal electron accepting process (TEAP). The dominating TEAP in sediment environment are:

- O_2 reduction – aerobic respiration,
- NO_3^- reduction – denitrification and dissimilatory NO_3^- reduction,
- Mn^{4+} reduction, Fe^{3+} reduction, SO_4^{2-} reduction,
- CO_2 reduction (methane production)(Chapelle & Lovely, 1995).

Aerobic Respiration

The oxidation of organic matter (aerobic respiration or metabolism) yields the most energy to support microbial growth followed by the denitrification. (Chapelle & Lovely, 1995)(see Table 2)

Table 2: Relative energy yield of different metabolisms (Chapelle & Lovely, 1995)

	Aerobic respiration	Denitrification	Mn^{4+} reduction	Fe^{3+} reduction	SO_4^{2-} reduction	Methane production
Relative energy yield	100	93	87	84	6	3

The only source of O_2 in the deep subsurface is the one which enters the groundwater body dissolved in the recharge water. If organic matter or other reduced compounds are present in the soil, then this

O_2 is consumed fast by the aerobic metabolism. Some aerobic microorganisms can switch and catalyze oxidation of the other inorganic compounds. (Chapelle & Lovely, 1995)

Because of the fast consumption of O_2, the regional flow systems are usually anoxic (oxygen depleted). O_2 could be found in deep aquifers only when there's no microbial activity. (Chapelle & Lovely, 1995)

Figure 9: Typical distribution of TEAPs in deep aquifers, modified after(Chapelle & Lovely, 1995)

Anaerobic Respiration

Anaerobic metabolism is a metabolism in anoxic or oxygen depleted conditions. The NO_3^- reduction metabolism (denitrification) is the anaerobic metabolism, which is most similar to the aerobic one. NO_3^- can replace O_2 in most of the reactions with organic and inorganic donors.(Chapelle & Lovely, 1995)

The microorganisms which have both aerobic and anaerobic metabolism typically regulate their metabolism to use only O_2, when it is available. The organisms, which can respire only anaerobically, are usually inhibited in presence of O_2. (Chapelle & Lovely, 1995)

The deep subsurface is extremely nutrient poor environment. The rates of the catalysed reactions are in orders of magnitude slower than those in the surface environments. (Chapelle & Lovely, 1995). Even though, according to Pedersen et al. (1991) there are different possibilities for NO_3^- reduction in the deep aquifers:

- by microbial **oxidation of organic matter**. The number of NO_3^- -reducing bacteria and the amount of organic carbon in deep soil layers, as compared with the conditions known in top soils, are expected to be too low to support any significant biological NO_3^- reduction by organic matter oxidation. Representing the organic matter by CH_2O, the overall denitrification process may be expressed by the following reaction showing that 1mg NO_3^--N corresponds to 1.1mg of organic C:

  $$5/4CH_2O + NO_3^- + H^+ \rightarrow 5/4CO_2 + 1/2N_2 + 7/4H_2O$$

  Shallow groundwater may have a significant content of dissolved organic carbon (e.g. 1-10mgC/l), which may support denitrification corresponding to a comparable decrease in NO_3^- concentration. Many coarse-grained aquifer materials contain very little organic carbon (supposedly in the range of 0.005-0.5%). Assuming a content of 0.05 organic C in an aquifer material available for denitrification, this would mean that 2.2g of aquifer material is needed for denitrification of 1mg NO_3^-- N. (Pedersen et al., 1991)

- by **ferrous iron oxidation**:

  $$5Fe^{2+} + NO_3^- + 12H_2O \rightarrow 5Fe(OH)_3 + 1/2N_2 + 9H^+$$

  NO_3^- reduction by chemical oxidation of Fe^{2+} has been considered a major factor in some of the early studies of NO_3^- reduction in deep soil profiles.(Pedersen et al., 1991)

For anoxic Danish aquifer material, the content of extractable reduced iron is estimated to vary between 0.001 and 0.1%. If 0.05% reduced iron in an aquifer material is available for NO_3^- reduction, this would indicate, that 40g of aquifer material is needed to reduce 1mg of NO_3^--N.

- by **oxidation of reduced Sulphur compounds** such as iron sulphide and pyrite

$$5/14FeS_2 + NO_3^- + 2/7H_2O \rightarrow 5/7SO_4^{2-} + 5/14Fe^{2+} + 1/2N_2 + 1/7\ H_2O$$

Pyrite has been found in many aquifers at a level of 1-2% in association with lignite. In most aquifers the amount of reduced Sulphur is believed to be much lower, supposedly in the range <0.001-0.1%. If 0.01% reduced Sulphur as pyrite is available for NO_3^- reduction, this would mean that 16g of aquifer material is needed to reduce 1mg of NO_3^-- N.

These reactions and the estimated capacities show that aquifers contain a significant potential for reducing NO_3^- concentrations. (Pedersen et al., 1991)

Total reduction capacity (TRC), which includes in one analysis all the reduced species, is used to quantify the sediment profiles with respect to reduction capacity. Denitrification takes place above this reduction front in small anaerobic microenvironments.(Pedersen et al., 1991)

3rd Zone of Interest: Riparian Zone

The third zone of interest for this literature study is named riparian zone, but in fact it consists of different elements: the stream with its hyporheic zone, the wetland/riparian buffer zone, and the connection between the groundwater and the surface water (see Figure 10). Description of these elements and their characteristics are following.

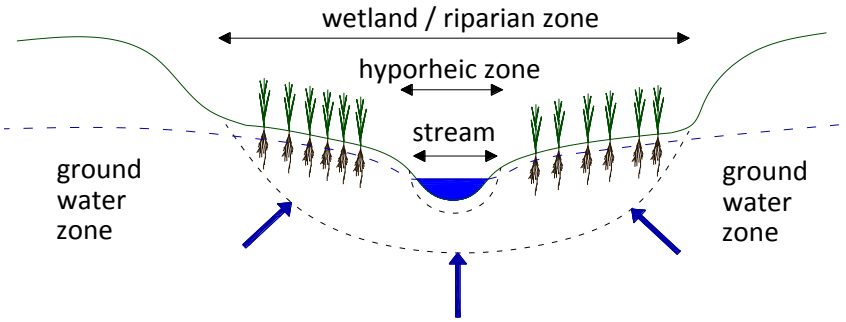

Figure 10: Elements of the 3rd zone of interest

Stream and Hyporheic Zone Characteristics

There are different criteria for characterising a stream. The stream could be young, mature or old, based on the landscape age and the erosion stage, according to the classification of William Morris Davis (1889). One of the earliest classifications of the streams is based on the channel type. According to it, the stream can be straight, meandering or braided. Rosgen's qualification (1994) uses letters and numbers to qualify the stream based on geomorphological profile, dimensions and the channel material. In general, the letters from that system describe the stream type (see Figure 99, p.120) and the numbers characterise the type of dominating bed material (see Figure 100, p.120). Longitudinal, cross-sectional and plan views of the major stream types, according to the Rosgen's

system are presented on Figure 99 (p.120). On Figure 100 (p.120), the different stream channel types together with the bed material are presented.(Endreny, 2003)

Other classification is the Strahler's (1957) classification for the order of the stream or/and river. According to that system, the streams can be first, second, third etc. order (see Figure 11).

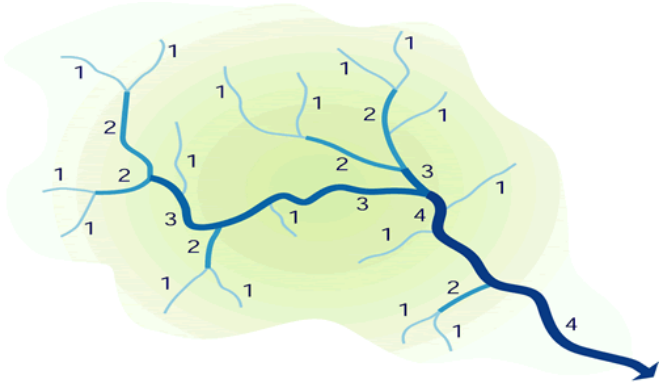

Figure 11: Strahler's stream order classification (Endreny, 2003)

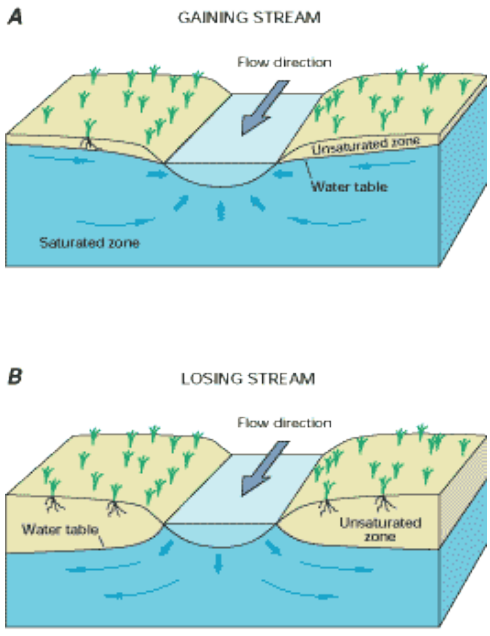

Figure 12: Cross-sections of gaining (A) and losing (B) streams.(Alley et al., 1999)

When taking into account the hydrological status, a stream or parts of it can be losing or gaining.

Gaining stream is typical for humid regions, where the groundwater table is above the water table in the stream. The gaining stream receives groundwater discharge and even though there might not be tributaries, the base flow increases downstream (see A on Figure 12). (Fetter, 2001)

Opposite, the loosing stream is usually situated in arid regions and the bottom of the stream is higher than the water table. As stream goes downstream, less and less water is found in the stream channel (see B on Figure 12). (Fetter, 2001)

It is also possible if the stream is losing during low-flow periods to become temporarily a gaining stream during flood stage. (Fetter, 2001).

Next to the interaction between the groundwater flow and the stream, another interaction is also presented – the one between the stream and its hyporheic zone. The hyporheic zone is the subsurface zone, where the stream water flows through parts of the adjacent bed and banks and where a mixing between groundwater and stream water occurs(Ranalli & Macalady, 2010). By

definition the hyporheic flow paths differ from the ground water flow paths, because they can leave and return the streams couple of times for a study reach (see example on Figure 13). The importance of that exchange between the streams and hyporheic zone is that keeps the surface water in close contact with the chemical and bioactive sediments, which influences the downstream water quality.(Harvey & Wagner, 2000)

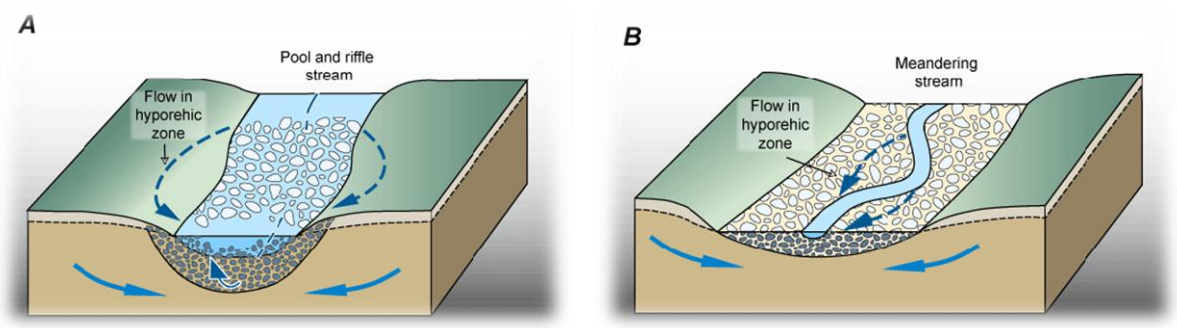

Figure 13: Examples of hyporheic flow paths *(Commonwealth of Australia, 2006)*

The length of the hyporheic flow path (from the point, where the stream flow enters the subsurface to the point where returns to the stream) can vary from centimetres to hundreds of meters. It is dependent on the streambed slope and its variation, the hydraulic conductivity of the sediment, and the curvature of the stream. (Harvey & Wagner, 2000)

In general the highest rates of denitrification occur at the soil-stream interface (hyporheic zone) and at the upslope edge of the riparian zone, where the ground water recharges (Ranalli & Macalady, 2010)(Dahl et al., 2007). However, for Denmark the hyporheic zone has a minor importance than the hilltop part of the riparian zone in respect to the denitrification rates.(Dahl et al., 2007)

Wetlands and Riparian Buffer Zone Characteristics

The term “riparian zone” is used for the stripe of undisturbed natural land in the stream valley, which has both the characteristics of aquatic and terrestrial environment. For the purposes of this literature study, the riparian zone is further discussed in the meaning of a wetland or taking into account the conditions similar to the one existing in the wetlands. Different systems for classifying the riparian zones exist. The ones which are of particular interest for this study are the classifications which criterion is the NO_3^- attenuation capacity (see “Groundwater - Surface Water Interactions (Connection between 2nd and 3rd Zone of Interest)”, p.28) or the source of water. According to the source, they can be mainly fed by: precipitation (bogs), groundwater (fens), surface water (swamps, marshes, etc)(Dahl et al., 2007). The classification of riparian zones is usually included in the wetland classifications, where the characteristics of the wet land are:

- Groundwater table is near or above the land surface,
- The soil has reduced conditions and accumulates organic matter,
- Communities adapted to these special conditions are presented;(Dahl et al., 2007)

Wetlands differ from the upland system, because they have aerobic/anaerobic interface in:

- the water column;
- the soil-water zone;
- the root-soil zone.(DeBusk et al., 2001)

The retention of the flood water in wetlands results in high decomposition rates and in increased accumulation of organic matter. In addition, wetlands have Nitrogen storages in different forms.

Nitrogen (N) Storage in Wetlands

The stored N in wetlands has organic or inorganic form. The organic N storage consists of: living matter – vegetation, fauna, microbial biomass; non-living matter – standing dead, detrital plant matter, peat, and soil-organic matter. The percentage N stored in microbial mass is 0.3-3% from the TN in the wetland. However, the microbial activity is one of the greatest regulators of the stability of N. Organic N pool is the most stable and the biggest one in wetlands, but it is not readily available for cycling. The inorganic storage consists of NH_4^+-N, NO_3^--N, and NO_2^--N. In flooded soils the NO_3^- and NO_2^- are found only in a trace amounts and the dominating form is NH_4^+. NO_3^- amounts are higher only in the aerobic interface. The inorganic stores are not stable over time and in general are presenting less than 1% of the TN in the wetland.(DeBusk et al., 2001)

Nitrogen Cycling in Wetlands

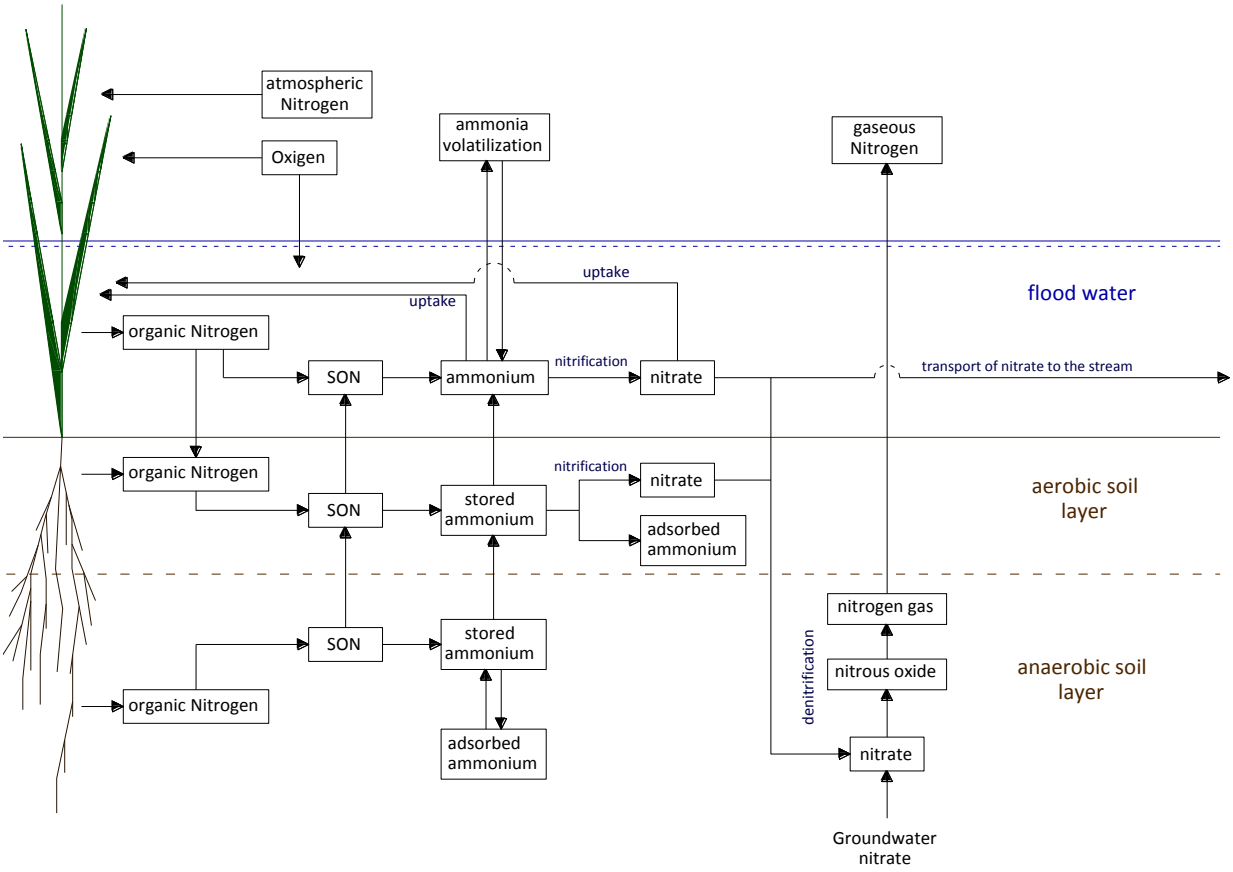

Figure 14: Wetland Nitrogen cycle (modified from(DeBusk et al., 2001)

The N cycle in wetlands is presented on Figure 14. The inorganic N can be effectively processed through denitrification, nitrification, plant uptake, and NH_3 volatilization. NH_3 volatilization is abiotic process, which is dependent on the pH of the soil-water system. The rates of volatilization are increasing significantly at pH ranging from 8.5 to 10. At pH below 7.5 the N losses due to volatilisation are insignificant. The sources of NH_4^+ in the water column are: the addition of NH_4^+ from external

sources, the mineralisation of organic N to NH_4^+ in the water column, and diffusion of NH_4^+ from the anaerobic soil layer to the water. (DeBusk et al., 2001)

The uptake by the vegetation and the immobilisation by microorganisms are only temporary storage of N, because it will be returned to the ecosystem upon the death and decomposition. (Ranalli & Macalady, 2010)

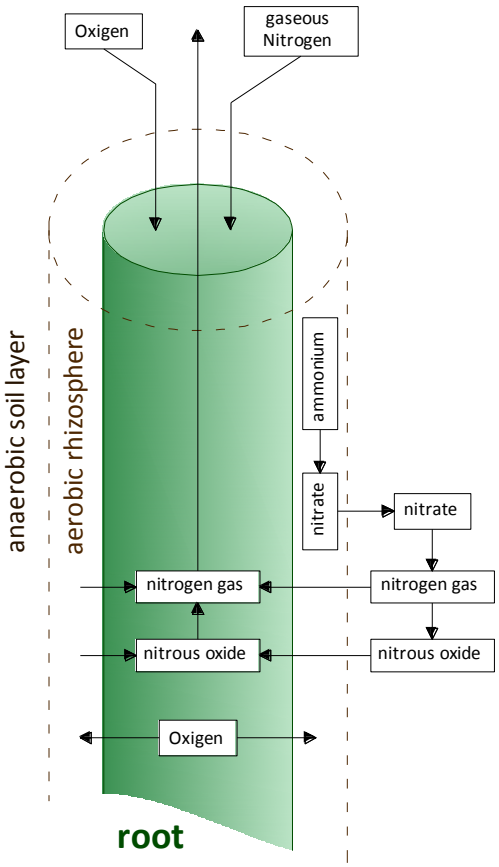

Figure 15: Nitrogen cycle in the root/soil interface (after (DeBusk et al., 2001))

Nitrification occurs in three zones of the wetland: in the water column, in the aerobic soil layer (see Figure 14) and in the rhizosphere (see Figure 15). Nitrification is mostly happening at the water column and at a very thin aerobic soil layer. Very little nitrification occurs within flooded soil and then it is only within the rhizosphere of some wetland plants that create aerobic microclimate.

The limiting factors are the O_2 availability and the NH_4^+ supply. Other factors regulating the nitrification are NH_3 concentration, pH, alkalinity, wind velocity, density of the wetland plants, the photosynthetic activity in the water column, and the soil cation exchange capacity. Rates of nitrification in constructed wetlands range from 0.01 to 0.161g $N/m^2/d$.(DeBusk et al., 2001).

NO_3^- diffuses into anaerobic soil layers, where it is reduced to gaseous products (**denitrification**) or to NH_4^+ (dissimilatory NO_3^- reduction to NH_4^- - DNRA). The denitrification occurs at higher redox levels (Eh= 200-300mV) and DNRA occurs when Eh is bellow 0mV. The more reduced the soil becomes, the more favourable are the conditions are for DNRA. The reduction potential of the wetland soil can play a critical role to the rate of NH_4^+ production. The redox potential of the soil decreases from aerobic (Eh=+600mV) to NO_3^- reduction (Eh=+300mV), SO_4^{2-} reduction (Eh=-100mV), and methanogenic conditions (Eh=-250mV). The major limiting factor for denitrification is the NO_3^- supply. Denitrification rates in wetlands can range from 0.003 to 1.02g $N/m^2/d$.(DeBusk et al., 2001). Redox gradients can have daily fluctuations as a result of plant growth (Nieder & Benbi, 2008).

The presence of vegetation can play an important role in the N cycling by: assimilating inorganic N into plant tissue, and by providing environment in the root zone for nitrification-denitrification to take place (DeBusk et al., 2001). During the growing season NO_3^- concentrations in surface water are lowered by denitrification and plant uptake (Shabaga & Hill, 2010). During the dormant season attenuation results exclusively because of microbial processes(Dahl et al., 2007). The most effective

period for NO_3^- removal for the groundwater-fed surface flow is in the summer when plant uptake occurs and warm temperatures increase the rates of denitrification (Shabaga & Hill, 2010). NO_3^- removal is less effective in landscapes where cold temperatures in the non-growing season restrict biotic removal. (Shabaga & Hill, 2010)

The wetland can function in the watershed as either a nutrient sink or source, providing a retention or release of nutrients to downstream waters. Which one will be depends on the biogeochemical characteristics: soil and vegetation in the wetland, rate of nutrient input from surface or groundwater sources. Wetlands are also functioning as transformers of nutrients from inorganic to organic forms. Nutrient export from wetlands is mainly in organic form.(DeBusk et al., 2001)

Groundwater - Surface Water Interactions (Connection between 2nd and 3rd Zone of Interest)

Types of Water Flow through the Riparian Zone and Attenuation Capacity of the Riparian Zone

The interactions between the groundwater and the surface water determine the NO_3^- attenuation capacity of the riparian zone and the capability of the riparian zone to maintain the good quality of the water in the stream and the adjacent area.

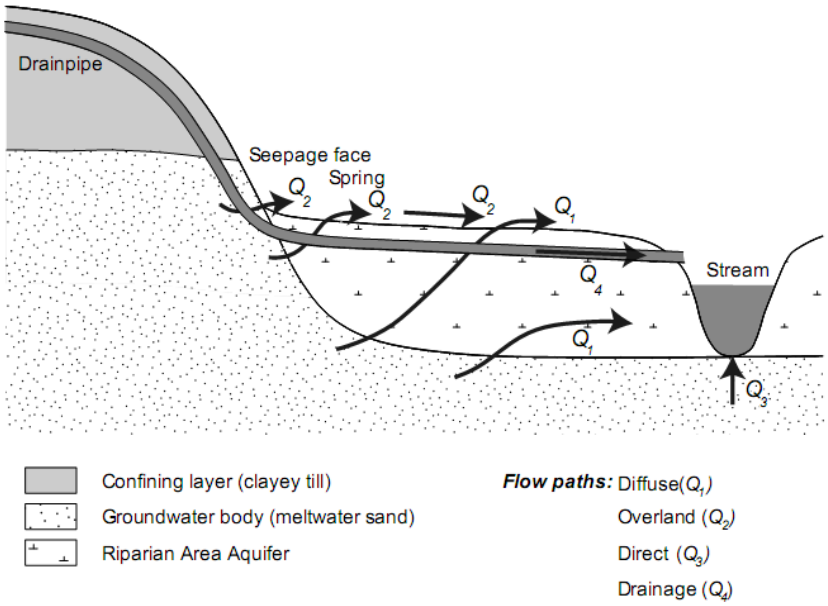

Figure 16: Flow paths through the riparian zone (Dahl et al. 2007)

The different flow paths and their interaction with the riparian zone can be grouped in four categories (see Figure 16):

- Shallow subsurface groundwater, passing through the riparian zone, because of a shallow aquiclude(Ranalli & Macalady, 2010) or diffuse flow path type (Dahl et al., 2007);
- Deep groundwater flow, bypassing the riparian zone and discharging directly in the stream or river (Ranalli & Macalady, 2010) or direct flow path type (Dahl et al., 2007);
- Ground water seep (the ground water surface is above the land surface)(Ranalli & Macalady, 2010) or overland flow path type (Dahl et al., 2007) or groundwater-fed surface flow paths(Shabaga & Hill, 2010);

- Artificial drainage(Ranalli & Macalady, 2010) or drainage flow path (Dahl et al., 2007).

As a part of Dahl's GSI typology (p.32) and after reviewing many riparian zones in Denmark, Dahl found that the reduction capacity of:

- the diffusive (Q1) and direct (Q3) flow paths is close to 100% if the organic content of the riparian zone is more than 3% and it is close to 0% if the organic content is below 3%. For the direct flow this is the case only when the water contacts the riparian deposits below the stream bed. If not, then the reduction capacity is close to 0%;
- the overland (Q2) water flow is approximately 50%;
- the drainage (Q_2) water flow is close to 0%.(Dahl et al., 2007)

Dahl proposes to estimate the denitrification capacity of the riparian area through multiplying the flow path distribution by the respective path-specific reduction capacities(Dahl et al., 2007).

Next to the shallow subsurface or deep groundwater flows discharging directly in the stream, a third major riparian flow path is the overland flow produced by groundwater discharging as springs or seeps (Shabaga & Hill, 2010).(Shabaga & Hill, 2010) suggest to not classify all riparian zones with groundwater-fed surface flow paths as sites which are ineffective in NO_3^- depletion. They are first to examine in detail the hydrodynamics of the groundwater-fed surface flow paths in relation to the NO_3^- removal effectiveness.

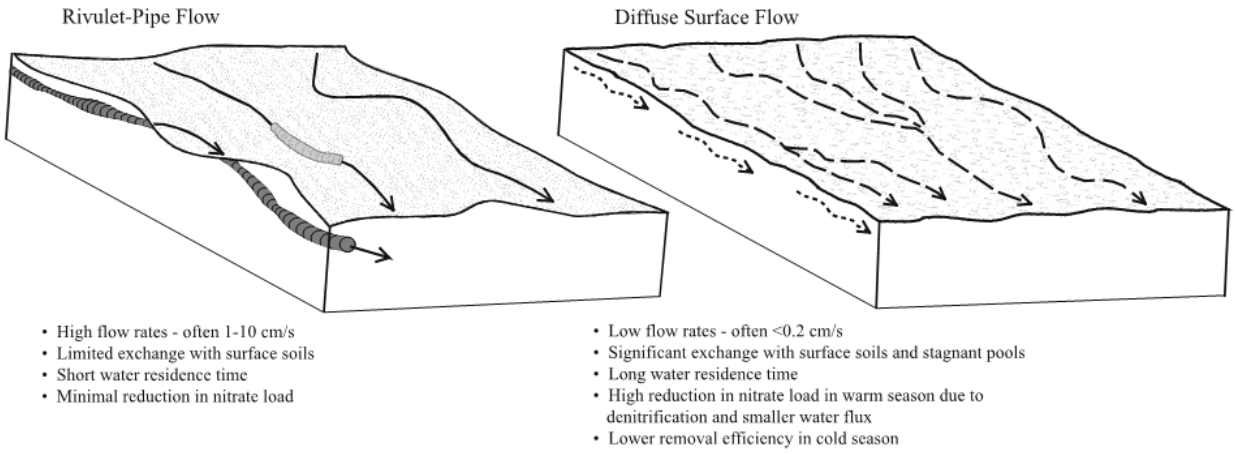

Figure 17: Conceptual model linking riparian zone groundwater-fed surface flow path hydrodynamics to the NO3-N removal efficiency (Shabaga & Hill 2010)

Figure 17 presents the conceptual model on the attenuation capacity of different types groundwater-fed surface flow. The left side shows an area where the small rivulets flowing rapidly across the surface or linked to a shallow horizontal pipe networks have a minimal interaction with the riparian soils and low water residence times that result in ineffective NO_3^- removal. On the other side, there are the diffusive surface flows, where repeated exchanges of water between the main flow zones and areas of slower flowing water in surface pools and sediments pore-water zones greatly increase residence times and the potential for NO_3^- removal.(Shabaga & Hill, 2010)

According to (Ranalli & Macalady, 2010) if the soil in the riparian zone is saturated or flooded long enough during the growing season so anaerobic conditions are developed (hydric soil), the NO_3^- removal is bigger than 80%. Opposite, if the soils are non-hydric, the groundwater NO_3^- removal is less than 30%(Ranalli & Macalady, 2010).

Although NO_3^- attenuation in groundwater occurs in riparian zones, the degree to which this attenuation affects stream concentrations and loads has to be assessed on a watershed scale. In agricultural watersheds the increase in NO_3^- concentration in streams is observed during the snow melt and/or rainfall events. Peaks in NO_3^- concentration usually occur before peaks in stream discharge. This can be explained with the rise of the water table to the soil surface and flushing the NO_3^- stored near or in the surface. When the saturated zone is deep below the soil surface, NO_3^- accumulates in the soil, which results in a small export to the surface water bodies. When the groundwater surface rises the stored NO_3^- is flushed out. Riparian zones function as a net source during high flows because that "flushing" of NO_3^- happens primarily there.(Ranalli & Macalady, 2010). Low concentrations of NO_3^- in the riparian zone of a small headwater catchment can be a sign of originally low NO_3^- concentrations in a regional groundwater system.(Ranalli & Macalady, 2010)

(Ranalli & Macalady, 2010) suggest that NO_3^- attenuation strategies should be focused mostly in riparian zones in 1st order streams, because:

- The small streams often represent up to 85% of the total stream length and collect most of the water and dissolved nutrients;
- In agricultural watersheds the in-stream attenuation process is not sufficient to reduce the NO_3^- loads;
- The groundwater flow is most likely to be local in small watersheds.

Variety of studies on the attenuation capacity of the riparian zones has been made. As a result, different conceptual frames, models or systems for classifying were developed. Presentation of two of them follows.

Examples for Conceptualising the GSI

The conceptual model of (Vidon & Hill, 2006) and the GSI typology of (Dahl et al., 2007) are presented bellow.

Vidon & Hill's Conceptual Model (2006)

According to Allan Hill, because the riparian zones affect the stream chemistry in significant way, it is important to be developed a conceptual framework. In that way it could be explained why the riparian zones differ in their influence on the stream chemistry. Moreover, that understanding will be useful if there are to be made generalizations which could be applied from one riparian zone to other. (Hill, 2000)

Vidon and Hill developed and validated a conceptual model for riparian zones, that links landscape hydrogeological characteristics to riparian groundwater hydrology and NO_3^- removal efficiency. (see Figure 18)

Data from several studies in the US and Europe have shown that a width less than 15m is necessary to achieve a 90% NO_3^- removal from subsurface flows at these sites with loam and silt loam soils despite the significant variation in riparian sediment depth (1 to 4m). In riparian zones with sand and gravel sediments the distance necessary to achieve 90% removal is generally more than 25m. For sites with less than 4m of permeable sediments in the riparian zone, the distance for a 90% removal remains below 40m. But for zones with more than 4m permeable sediments in the riparian zone the distance for a 90% NO_3^- removal could be more than 40m.(Vidon & Hill, 2006)

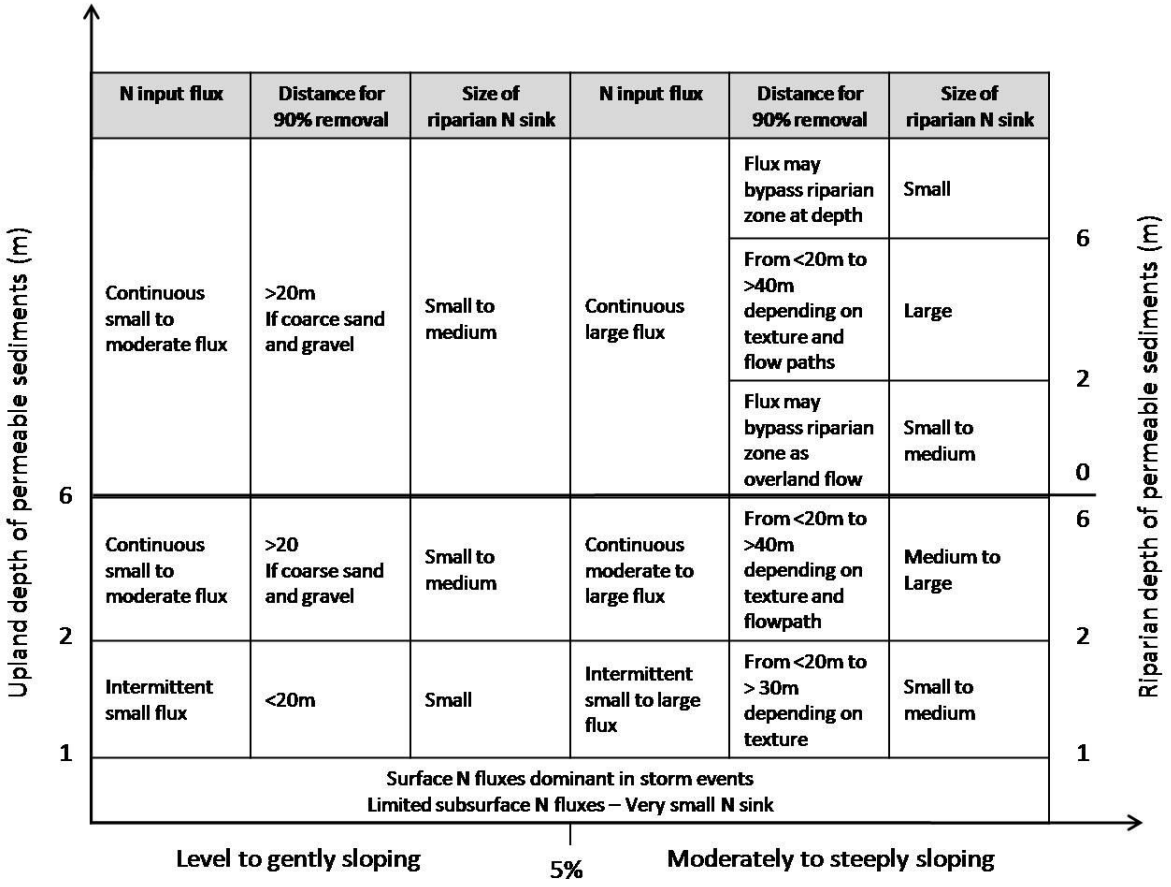

Figure 18: Conceptual model, linking the NO3- removal with the topography, the upland depth of permeable sediments and riparian depth of permeable sediments (Vidon & Hill, 2006)

Dahl's GSI Typology (2004)

A new process-orientated multi-scale typology of the groundwater – surface water interactions was developed by Dahl et al. (2004). This classification is made for different scales and it is based on geomorphology, hydrogeological setting and flow paths, where eco-hydrological approach is used for characterizing the processes. The typology distinguishes between three scales (types of groundwater flow): catchment scale (landscape type), reach scale (riparian hydrogeological type), and local (riparian flow path type). (Figure 19)

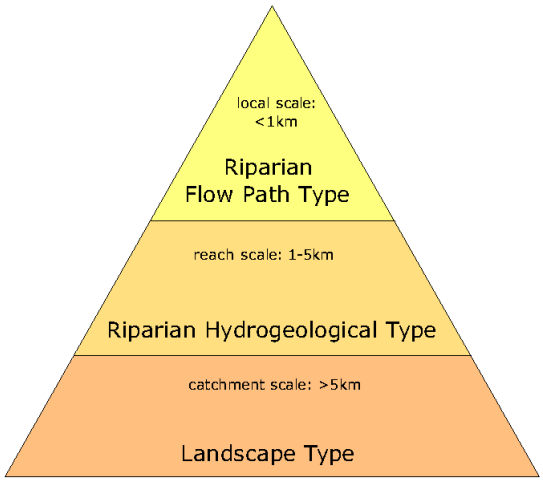

Figure 19: Dahl's GSI typology: the 3 scales

Landscape type – catchment scale (>5km). The regional geomorphology and hydrogeological setting are taken into account. It is used Heat's system (see Groundwater flow systems) for classifying the system where different interactions between confined, confining and unconfined aquifers are possible. In Figure 20 is presented an example of groundwater system and its complexity:

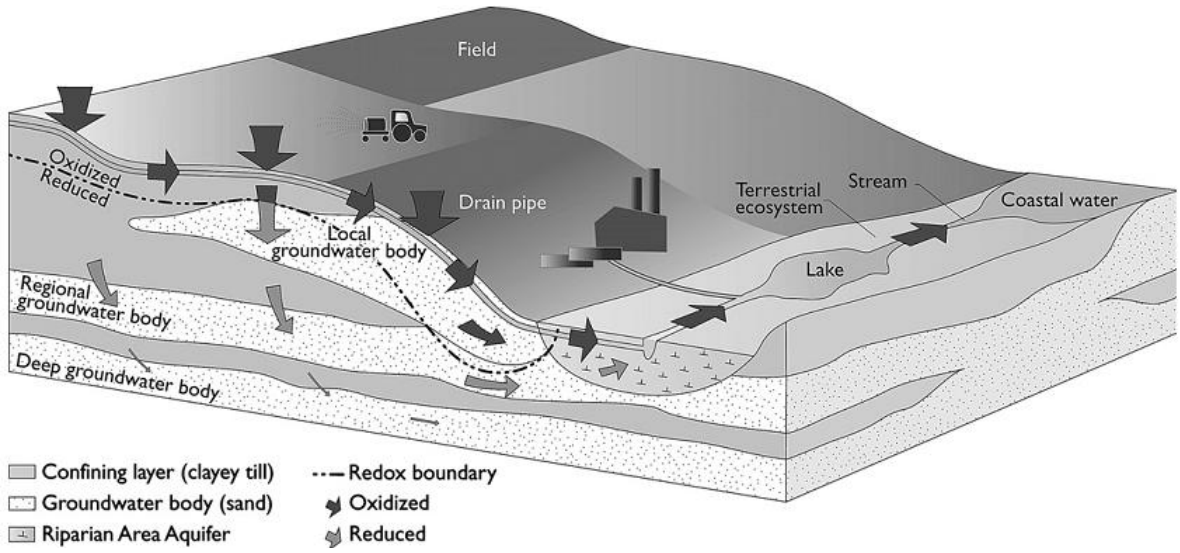

Figure 20: Landscape characteristics (Dahl et al., 2007)

Riparian hydrogeological type – reach scale (1-5km). The exchange of groundwater between the groundwater body and the riparian zone aquifer is to be characterized in this stage. Mainly two hydrological settings are taken into account: the physical contact between the groundwater body and the riparian zone aquifer, and the groundwater body type. The different types of contact are shown below:

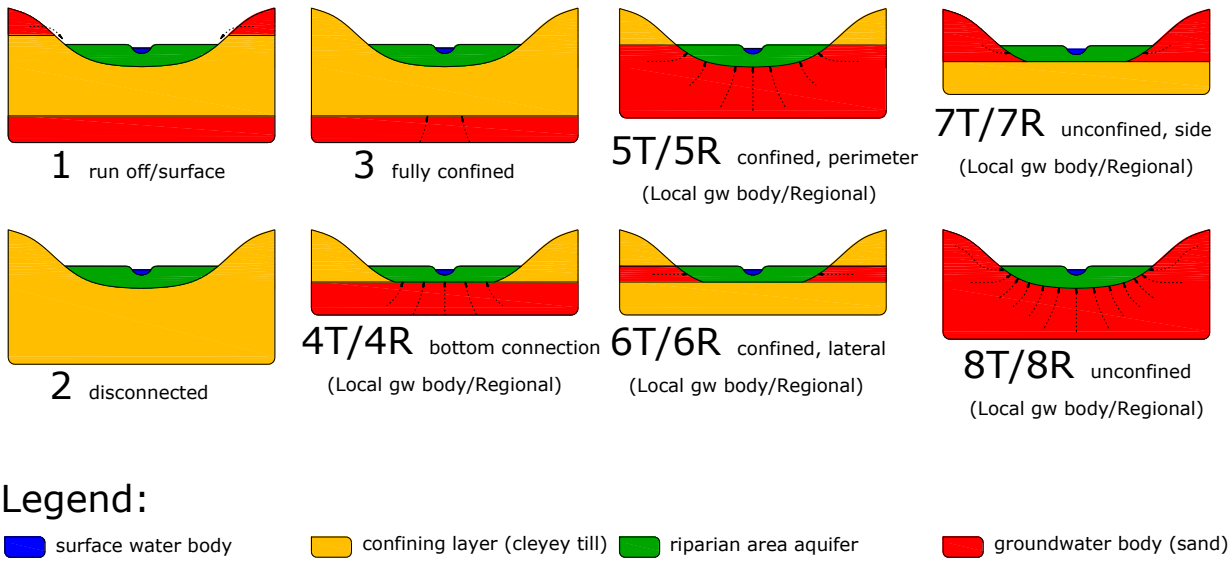

Figure 21: Dahl's GSI typology: types of contact

The groundwater body type could be local and regional. The local type is defined as a shallow, small groundwater body with large recharge rates, short flow paths and respectively short residence times and the seasonal discharge is unsteady. When the regional type is with longer flow paths and longer residence times, deep penetration, smaller recharge rate and the discharge is stable in the year. The groundwater from this groundwater body usually connects with riparian zones along medium sized streams and big rivers.

Riparian flow path type – local scale (0.01-1km). The dominant flow type through the riparian zone is characterised. In that classification four flow paths have been found to be the most important for the transport of groundwater to the stream (trough the riparian zone). These flow paths control also the attenuation processes and the capability of the riparian zone to maintain the good quality of the water in the stream and the adjacent area. These four flow types and their attenuation capacities were presented in the beginning of this part of the project (p.28).

The GSI typology is useful tool for delineating the critical zones in a catchment in respect to the NO_3^- loads to the endangered ecosystem. The GSI typology can be used for conceptualising the catchment area by dividing it on smaller zones with similar characteristics. However, one shortcoming of this typology is that it can't be used for quantification analysis of the interactions and for further calculation of the rates for NO_3^- reduction of the zones.

[empty page]

C. Project Site Description

Project Site Location and Land Use

The project site is situated in North Jutland (Denmark). It includes the catchment area of Lundgårds bæk (see Figure 22), a small tributary to Villestrup Å, which is one of the two biggest streams in the catchment area of Mariager Fjord.

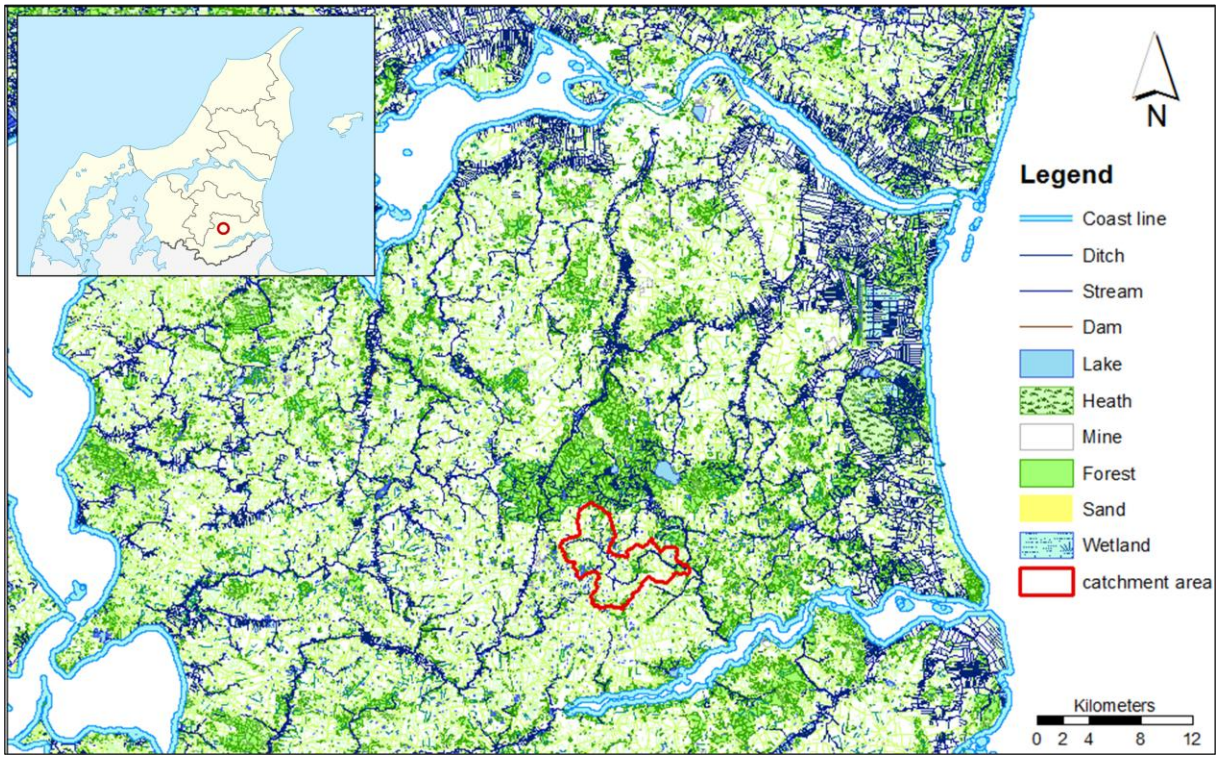

Figure 22: Location of the project site - the catchment area of Lundgårds bæk (author of the small picture: Erik Frohne)

The catchment area of Lundgårds bæk is 35km^2 from which around 80% is potential agricultural land. The rest is distributed to forests (10.05%), urban areas (6.8%), shrubs, lakes and wetlands (see Figure 23).

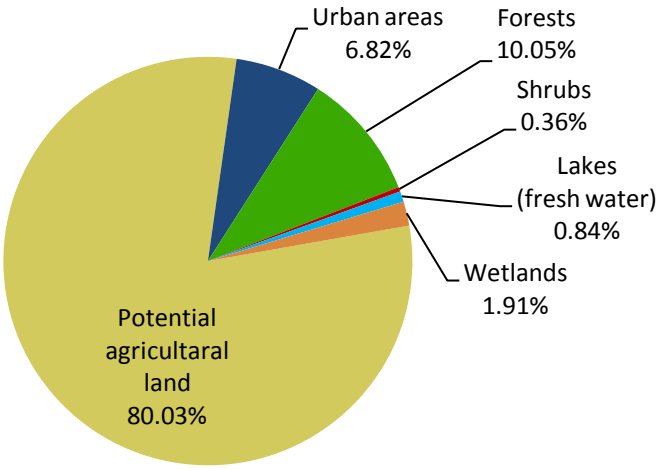

Figure 23: Land use distribution

Figure 24 shows the land use map of the catchment area of Lundgårds bæk:

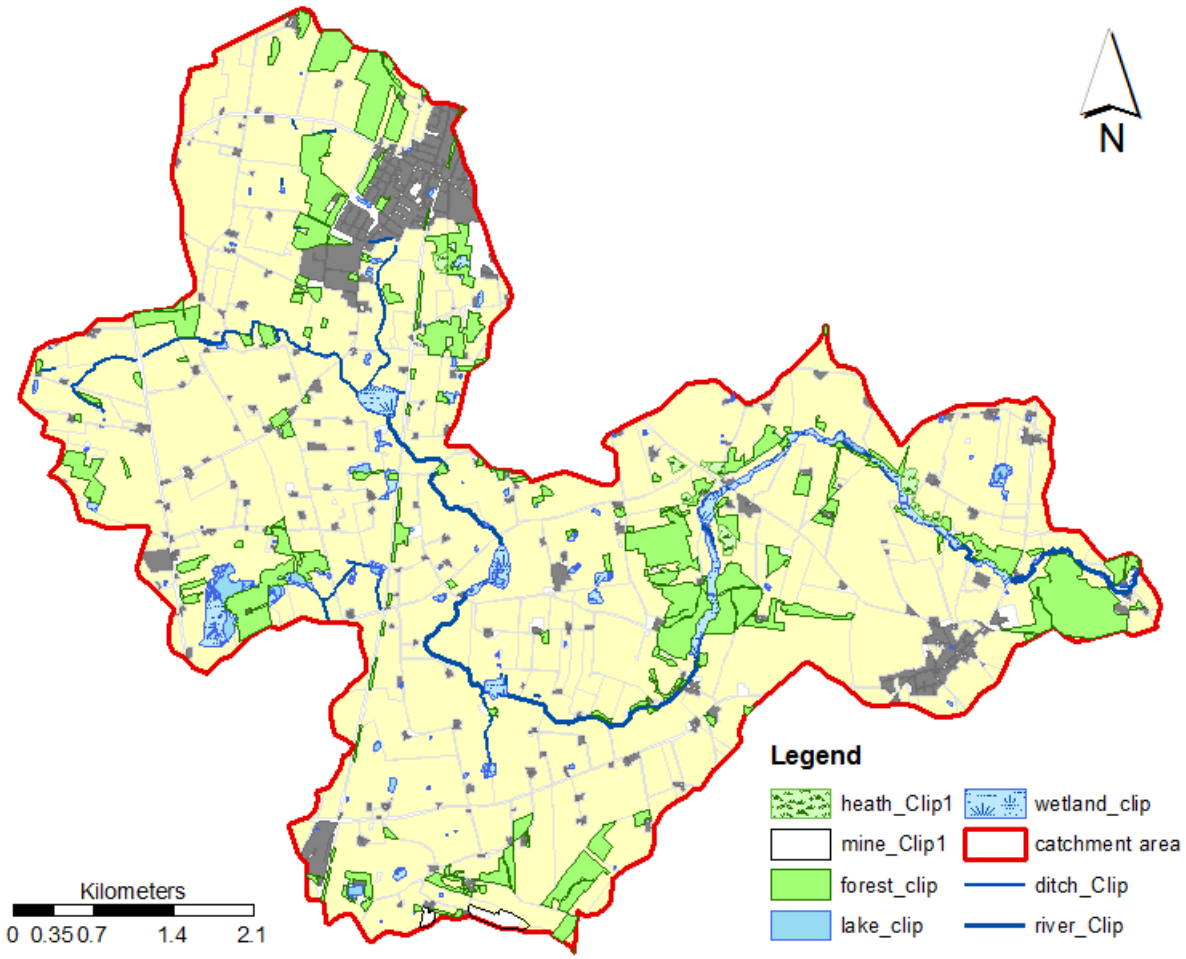

Figure 24: Landuse map (the urban areas are presented with gray colour)(source of GIS theme: AAU)

It can be said that the landuse distribution of Lundgårds bæk is not an exception from the rest of Denmark. According to (Hansen et al., 2011) two thirds of the total land area of Denmark is under agricultural use, which results in high N fertilisation rate and high livestock density if compared to the European and global averages. The average livestock density in Denmark is about 0.8 animal units per hectare and the average input of N to agricultural land is around 180 kgN/ha/yr in 2008.(Hansen et al., 2011)

Nitrate Leaching to the Groundwater

The majority of the studies conducted on NO_3^- leaching (not only for Denmark but in general) focus on the leaching from agricultural land. Before presenting the available data for the leaching from the agricultural land in the catchment area of Lundgårds bæk for 2008, the historical context of this issue has to be looked at.

The Danish farming (particularly the livestock farming) has gone through significant structural changes by developing larger and more intensive farms after the Second World War. This growing process has been encouraged by the rising use of synthetic fertilisers and imported feed and has resulted in higher nutrient turnover. The crop yield per hectare has risen and the yearly milk yield per cow has grown almost 5 times for the period 1950 to 2007. Besides, the production time of pigs and chickens has shortened nowadays. The pig production has risen dramatically: 3.5 times for the period

1950-1967 and almost 2 times between 1967 and 2007. This intensive farming causes N leaching because of mineralisation of the soil's pools and because the amount of N used exceeds the nutrient demand of the crops.(Hansen et al., 2011)

Following the large increase in the consumption of N in chemical fertilisers during the 60s and 70s, the TN input to the Danish arable land has reached its maximum in the early 1980s. Since the early 90s, the usage of chemical fertilisers has decreased in Denmark as a result of the major national environmental plan from 1985 and the following plans in 1987, 1991, 2000, 2001, 2004, and forward. All these plans have focused on the reduction of the N-pollution from agriculture as this is one of the main and most important sources of NO_3^--N leaching in Denmark. (Hansen et al., 2011)(Kronvang et al., 2002) As part of the plans, restrictions to the farmers were applied, especially on the storage facilities and the application times for the liquid manure, and also on the application of fertilisers (Kronvang et al., 2002).

Logically the decrease in N fertilisers should result in decrease in the NO_3^- leaching and therefore the groundwater quality. A recent study (Hansen et al., 2011) based on the data from the Danish groundwater monitoring program investigates the trends in the groundwater quality, related to the changes in the landuse and the management practices from the last 50 years. The groundwater age had been determined, which allowed relating the measured concentrations of NO_3^- to the time of the recharge of the groundwater instead to the sampling time. As a result, the authors have proved that there is a statistically significant trend reversal in 1980 ($\pm 3.4\ years$) of the NO_3^- concentration of the Danish oxic groundwater (Figure 25) .(Hansen et al., 2011)

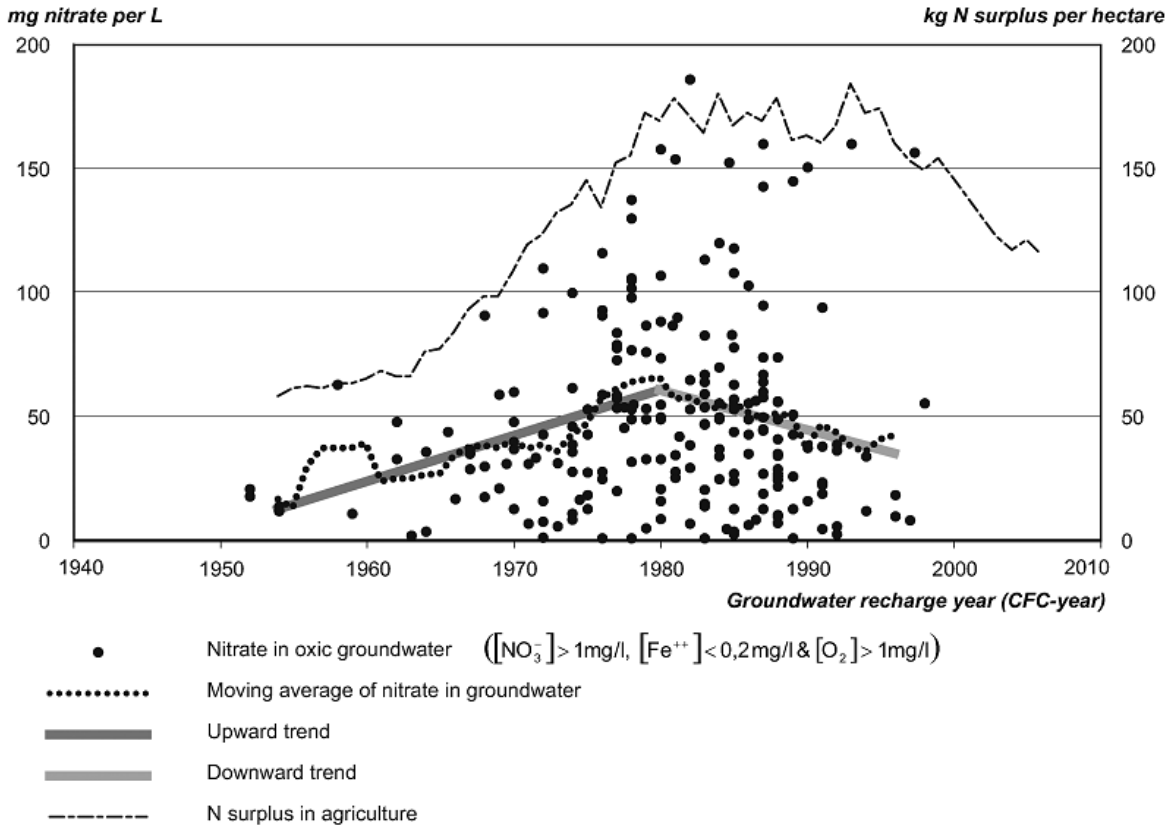

Figure 25: Time-series of N surplus in agriculture and NO3-N in oxic ground water versus recharge age (CFC age) on annual mean level (Hansen et al., 2011)

The leaching trends from the root zone on a smaller scale were modelled for 6 agriculture-dominated catchment areas (see Figure 26) as part of the national monitoring program of Denmark (see (Grant et al., 2010)).

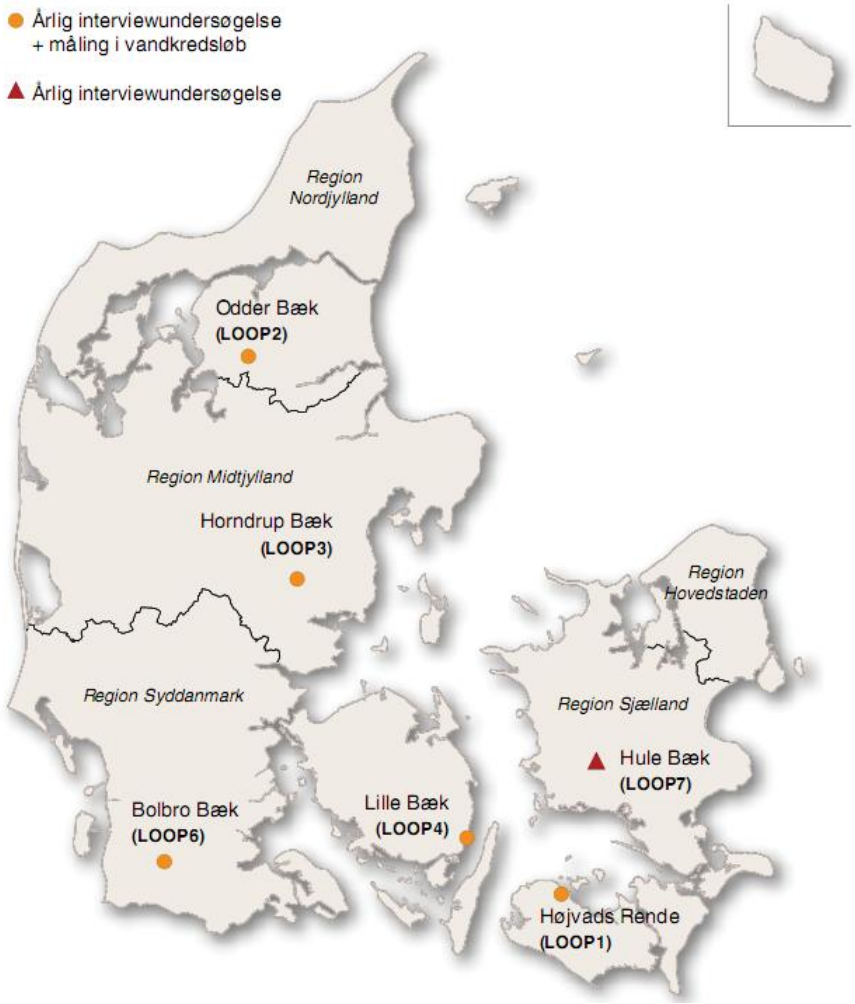

Figure 26: Overview of the 6 agriculture-dominated catchments, part of the national monitoring program, representative for Denmark (Grant et al., 2010)

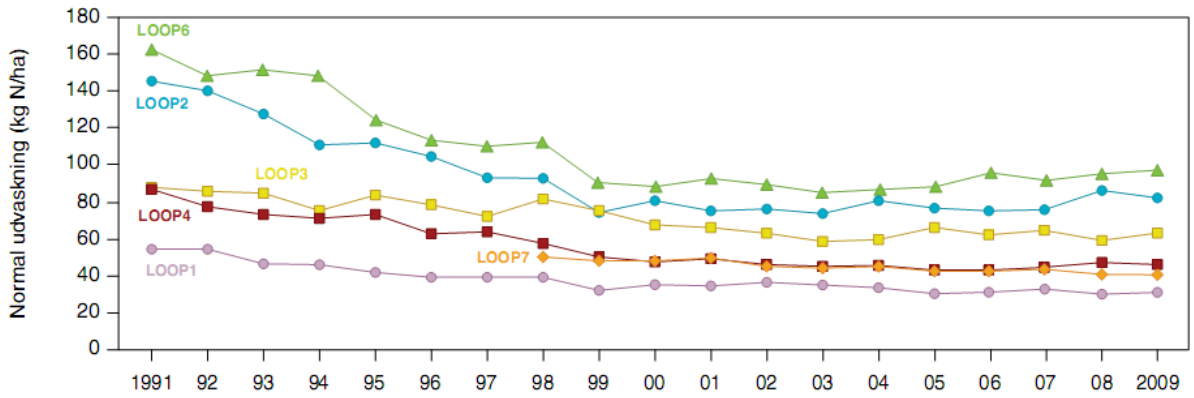

Figure 27: Results from the modelling study for the annual leaching (kg/ha) from the root zone of the 6 representative catchments; LOOP2 and LOOP6 are mainly sandy soil catchments and the rest are mainly clayey soils (Grant et al., 2010)

Those 6 sites are believed to be representative for Denmark, where two of them have mainly sandy soils and the rest are with clayey soils. The LOOP2 site Odder Bæk (see Figure 26) is situated in Region North Jutland, as the project area, so it can be assumed that the trends for the two catchments will be alike. From Figure 27 for LOOP2 can be seen that there is a big decrease in the annual leaching from 1991 to 1999, almost 1.8 times, followed by more or less constant leaching over the end of the study period (2009). Furthermore, another study based on the national monitoring program shows the measured NO_3^--N concentrations for two streams in the catchment area of Mariager fjord (Villestrup Å and Kastbjerg Å) together with the data for the applied chemical fertilizer for the same period (from the 30s to the first decade of 2000) (see Figure 28). It can be seen that the observed upward trend at the chemical fertilizer application is followed by similar upward trend at the measured NO_3^--N concentrations in the two streams with delay of 10-15 years. It can be expected that, as Lundgårds bæk is a tributary to Villestrup Å, there would be similar delay in the response.

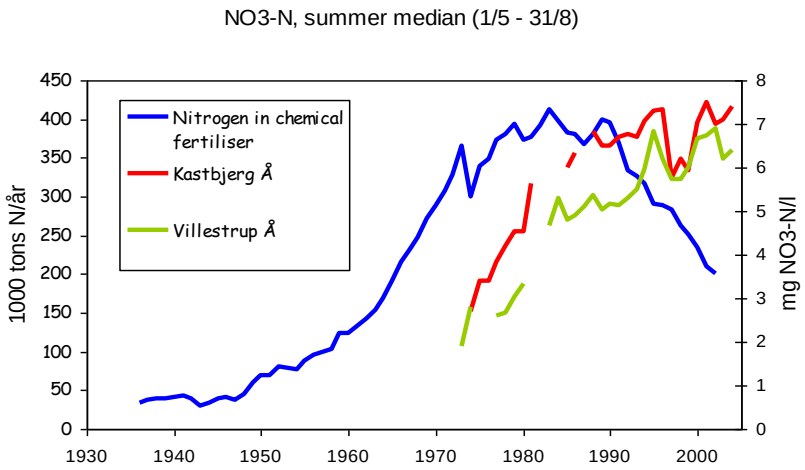

Figure 28: Time "lag" for 2 streams in the catchment area of Mariager fjord (source: Miljøcenter Aalborg)

Unfortunately there is no such study made on even smaller scale – the catchment areas of the first order streams in the region. However, a GIS theme about the NO_3^--N leaching under the root zone from the agricultural land on a parcel scale exists. Figure 29 presents the map of the NO_3^--N leaching from the root zone in the area for 2008. The potential NO_3^--N leaching is calculated from the "potential outwash" and the net precipitation for the area. The "potential outwash" [kg N/ha] is calculated by the equation:

$$Pot.outwash = kgN^{(seed)} + kgN^{(manure)} + kgN^{(fertilizer)} + kgN^{(other\ org.fertiliser)} + kgN^{(atm.deposition)} + kgN^{(fixation)} - kgN^{(volatilization)} - kgN^{(denitrification)} - kgN^{(harvest)}$$

Where the input sources of N (+) [kg] are:

- from the sowing ($kgN^{(seed)}$);
- from the applied manure ($kgN^{(manure)}$), fertilisers ($kgN^{(fertilizer)}$), and other organic fertilisers ($kgN^{(other\ org.fertiliser)}$);
- from atmospheric deposition ($kgN^{(atm.deposition)}$);
- from N-fixation ($kgN^{(fixation)}$).

The part of the equation presenting the N loss (-) includes volatilisation ($kgN^{(volatilization)}$), denitrification ($kgN^{(denitrification)}$), and harvest ($kgN^{(harvest)}$). The harvest is calculated as 50% of the kg N it the secondary yield (straw).

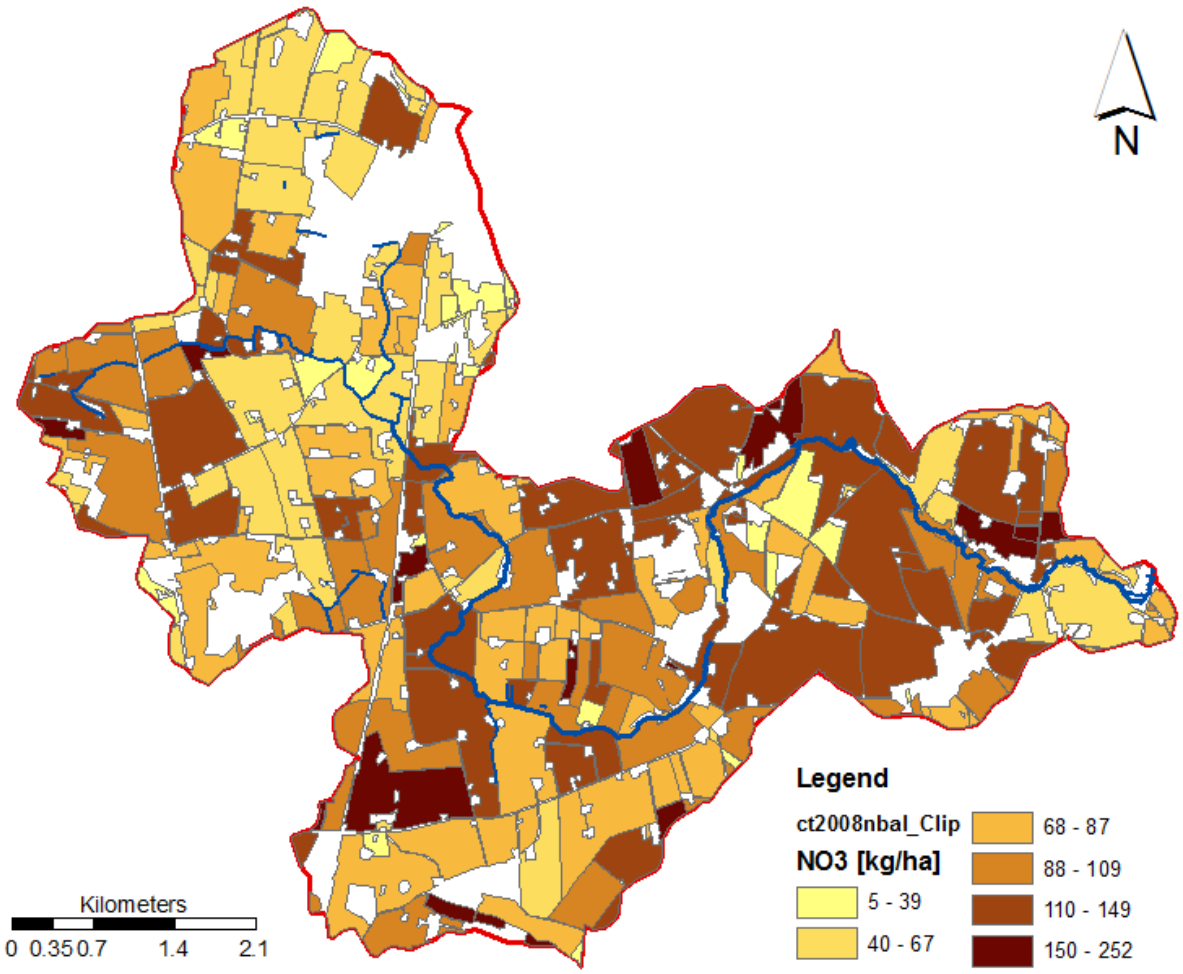

Figure 29: NO3-N leaching from the root zone(there is no leaching from the urban areas, from the forests, and from the laces presented – the white parts of the map)(GIS theme provided by NIRAS)

Regional Geomorphology

The Lundgårds Bæk's catchment area is located in a moraine landscape from the Weichselian glaciation (the last glacial period). The landscape in the area is mainly characterised by clayey or sandy soils and is hummocky or pitted due to dead-ice formation. A tunnel valley is registered in South direction from the catchment area (see Figure 30).

Figure 30: Landscape formation map (Per Smed, 1979); the site is located in the red circle (provided by NIRAS)

The regional geomorphology is characterised by regional sloping and small local rises of the terrain. The highest point is 116m above the sea level in north-west part of the project site; and the lowest point is 10m above the sea level in the East direction, where the stream valley of Villestrup Å is.

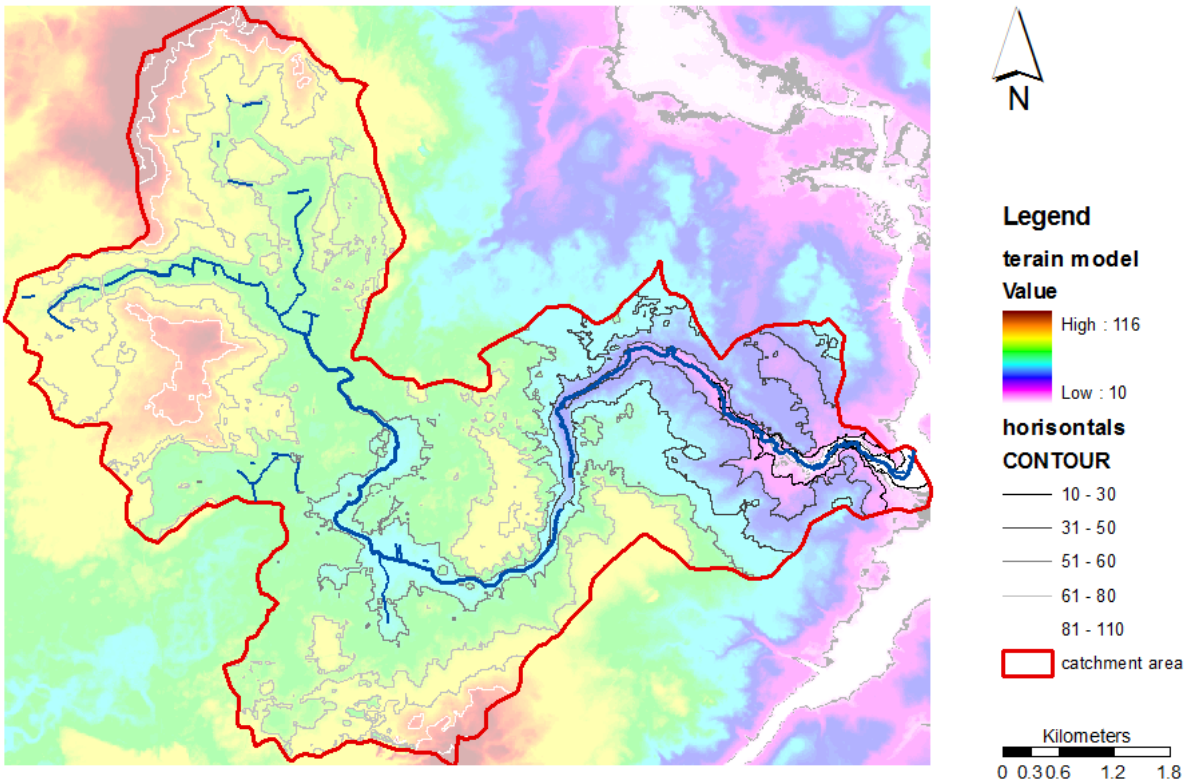

Figure 31: Terrain map (the lowest part of the area around 10-20m above sea level – white/pink colours; the highest parts are yellow and red)(GIS theme provided by NIRAS)

Regional Hydrogeology

The area can be described as a moraine landscape with a complexly interbedded sequence of sand/gravel aquifer layers and clay/silt aquitard layers (mainly from glacial-melt-water origin or glacial origin) and underlying limestone/chalk aquiclude. Data from Jupiter (GEUS, n.d.) is analysed for the initial understanding of the geology of the area (see Figure 32):

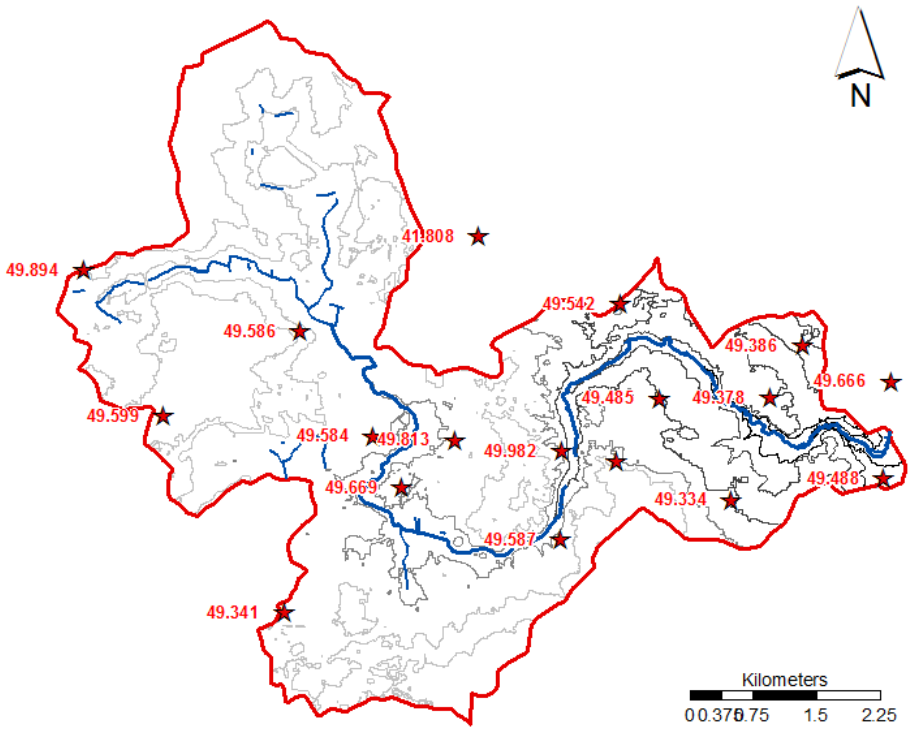

Figure 32: Map with the wells (DGU numbers (GEUS, n.d.)) in the area, which were used for drawing the geological profiles;

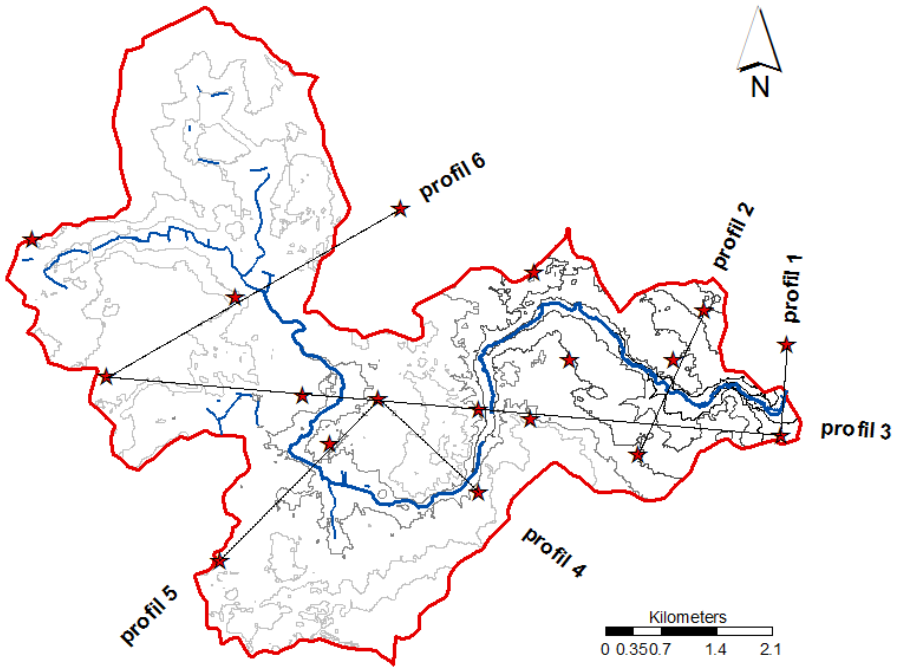

Figure 33: Geological profiles based on the data from the drilling reports of the wells (Appendix: Six Geological Profiles (Initial Geological Study), p.121)

Based on that data and the terrain model, 6 geological profiles were drawn (see Figure 33 for their location and p.121 for the profiles). Further, a stratigraphic 3D model of the area is created with GeoScene3D (I-GIS, n.d.). This stratigraphic model is based on the conceptual understanding of the geology for the region, the drilling reports from Jupiter data base(GEUS, n.d.), and the geophysical data for the region. See "Appendix: Building a 3D Geological Model of the Project Area" (p.123) for a detailed explanation.

Also a surface soil map is used as an addition to the Jupiter data, (see Figure 34). Four types of surface soils are presented in the area according to it: coarse sand, fine sand, loamy sand and humus.

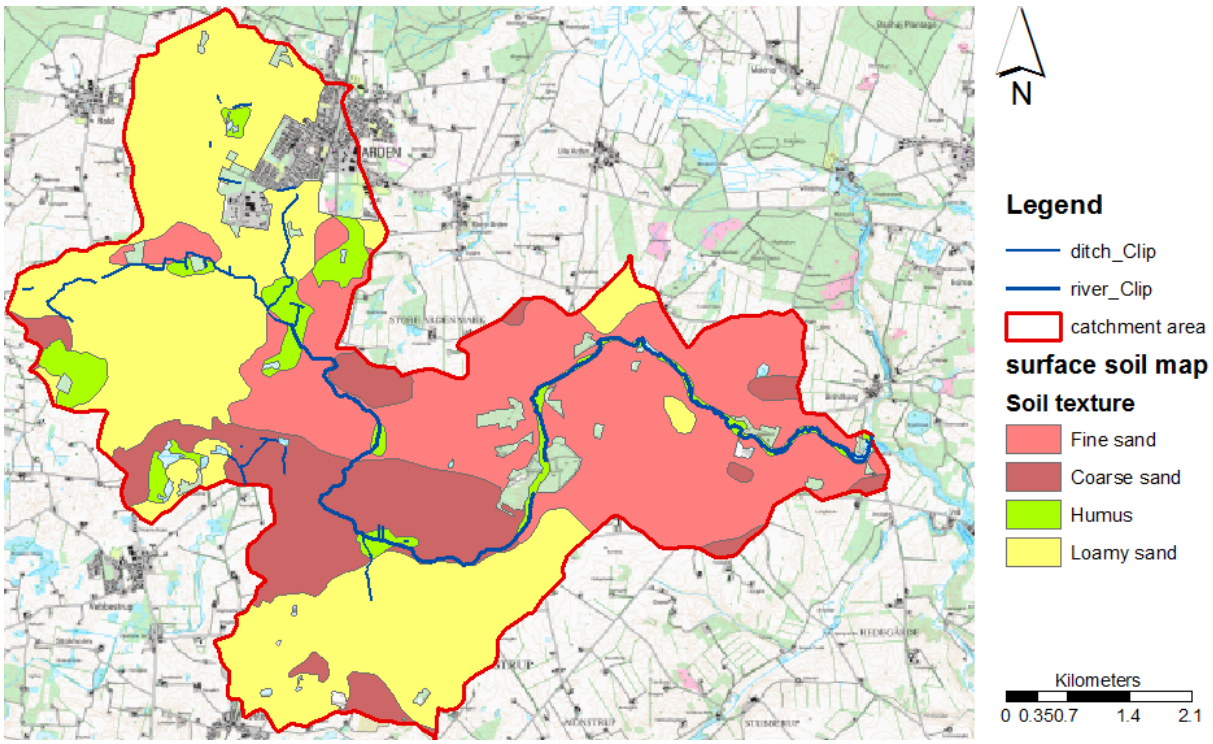

Figure 34: Surface soil map (GIS theme provided by NIRAS)

According to the soil textural classes (USDA, 1987):

- Sand soil is a soil which consists of 85% or more sand and the percentage of silt plus 1.5x clay should not exceed 15%.
    - Coarse sand contains at least 25% of very coarse and coarse sand and less than 50% of any other subdivision of sand.
    - Fine sand contains at least 50% fine sand or less than 25% of very coarse, coarse, and medium sand and less than 50% very fine sand.
- Loamy sand must contain between 70% and 90% sand and between 15% and 30% of silt plus 1.5x or 2x clay. It should contain at least 25% very coarse, coarse and medium sand and less than 50% of fine or very fine sand.(USDA, 1987)

Where the diameter range for the sand is 2.0-0.005mm, for silt 0.05-0.002mm, and for clay – less than 0.002mm. The sand is subdivided into very coarse sand (2.0-1.0mm), coarse sand (1.0-0.5mm), medium sand (0.5-0.25), fine sand (0.25-0.1mm), and very fine sand (0.10-0.05mm).(USDA, 1987).

The humus is any soil with organic content more than 10%. This humus soil can be found mainly in the wetlands, around the lakes and in the stream valley of Lundgårds Bæk in this region (see Figure 168, p.179).

From the topography and stratigraphy of the area it could be assumed that there are present different groundwater flows in the different parts of the catchment area: local, intermediate or/and regional. The groundwater table in the area is measured to be deeper than 10m below the surface, which probably belongs to a secondary aquifer. The ground flow direction, determined from the potential map (see Figure 35), is from West or South-West to the direction of Villestrup Å.

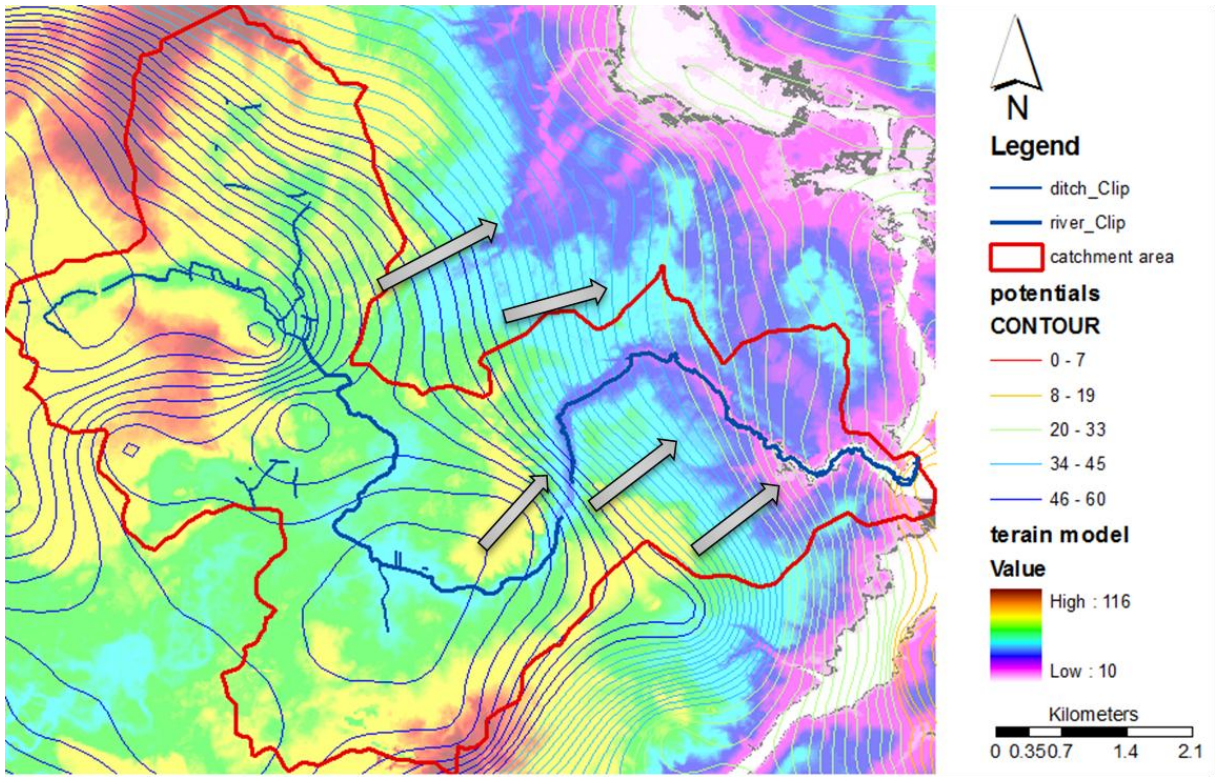

Figure 35: Potential map (GIS theme provided by NIRAS) with ground water flow direction

Another feature of the area is the deep redox front, which is located between 20m and 39m below the surface (based on the soil colour and the big-scale redox GIS theme). As a result, it is expected that the intermediate and part of the regional groundwater flow is not reduced before it reaches the riparian zone of Lundgårds Bæk. This means that denitrification is not happening unless the groundwater flow enters the deep redox zone or the anoxic, high in organic matter, soil in the riparian zone of the stream and of the wetlands in the area.

Regional Hydrology and Hydrochemistry

Lundgårds Bæk is a second order stream, tributary to Villestrup Å in the bigger catchment area of Mariagerfjord. It is formed by two small tributaries, which are characterised with almost no flow. Further, the stream has formed two big meanders before it discharges in Villestrup. The hydrology and hydrochemistry of the project site is further discussed in Chapter D (p.45) and Chapter E (p.59).

D. Monitoring Data Analysis

Monitoring data for the measured flow rate and NO_3^--N and NO_2^--N concentration at the station on Lundgårds Bæk (Egelund) are analyzed in this part of the project. The analysis contains two parts:

- Base flow separation and base flow index calculation – this gives information about the natural sources feeding the stream;
- Analysis of the relation between the NO_3^--N and NO_2^--N concentration and the flow rate – it is studied if and how these two sets of data are correlated, and additionally, a regression analysis is performed.

The rainfall data is analysed next to this, in order to help understand the results from the above mentioned analysis.

The purpose of this part is to add some more information about the project site, based on the available data.

Rainfall Data Analysis

The precipitation data from the Danish national 40x40km climate grid for the cell covering the catchment area of Lundgårds Bæk (1985-2000) are analyzed. The precipitation values have been corrected for evaporation loss and wind loss. Because in the next part (p.47) the base flow separation is made for 5 years: 1991, 1994, 1997, 2000, and 2003, the following calculations are made for 4 of the years, excluding 2003 (not present precipitation data after 31.12.2000). From these 4 years the driest is 1997, with 175 days with no precipitation, followed by 1991, with 167 days without precipitation. 2003 is the wettest year (from the chosen 4 years) with 233 days with rainfall (see Figure 36).

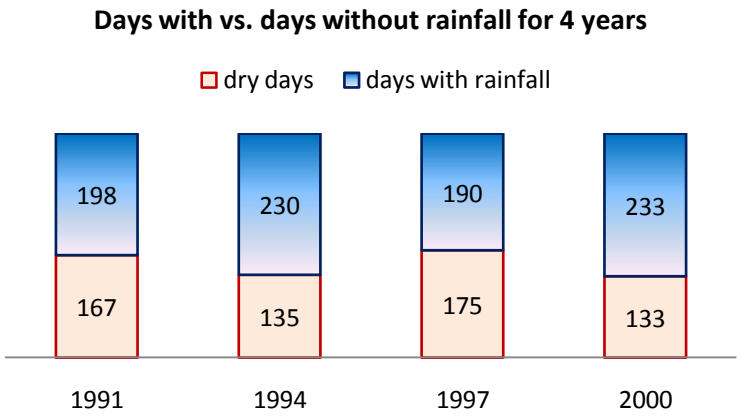

Figure 36: Dry vs. wet days in 1991, 1994, 1997, 2000

The maximum and the average rainfall for the 4 years are presented in Figure 37, where the maximum rainfall for 1991 is on 2nd of November (29.27mm), for 1994 is on 16th of September (53.13mm), for 1997 is on 28th of July (41.71mm), for 2000 is on 13th of September (32.745mm).

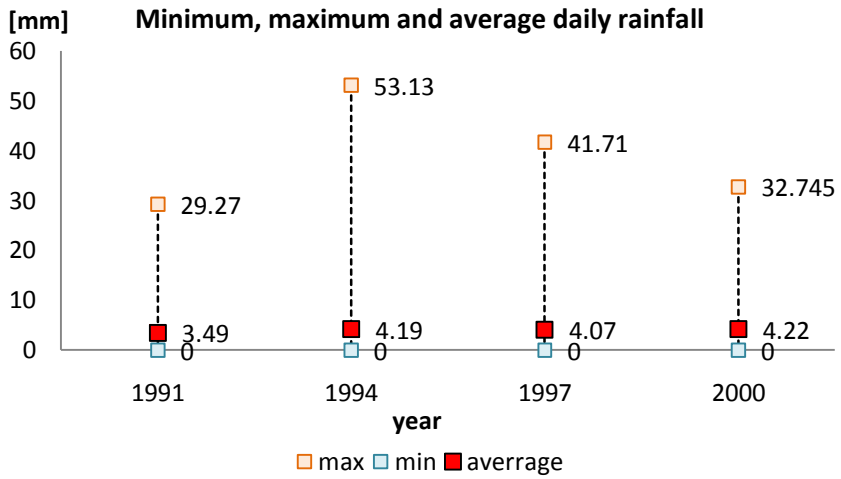

Figure 37: Maximum and average daily rainfall for 1991, 1994, 1997, and 2000

As addition, the NO_3^--N and NO_2^--N load at the stream (calculated from the flow and the concentrations) is plotted together with the precipitation for the period (Figure 38).

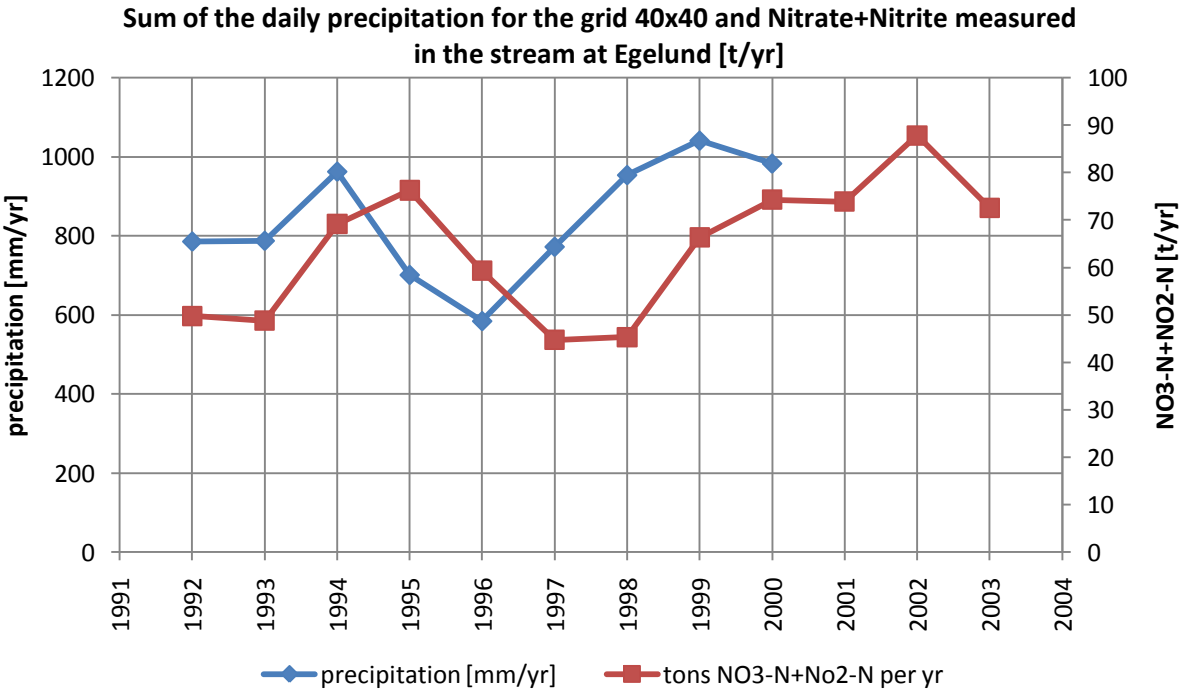

Figure 38: Sum of the daily precipitation plotted together with the NO_3-N and NO_2-N load measured in the stream at Egelund

From Figure 38 can be seen that the same trends are observed for both data sets, which could mean that there is delay of one 1 or more years in the precipitation-flow system at Egelund.

Base Flow Analysis for Lundgårds Bæk

Introduction

The stream hydrograph is a time-series record for the stream flow at a gauging site. The hydrograph represents a sum of different water sources, contributing to the flow, which can be:

- Quick flow – the result of a rainfall event (runoff, interflow and direct precipitation),
- Base flow – long-term discharge from a natural storages.(Brodie & Hostetler, n.d.)

The base flow separation analysis gives information about the natural sources feeding the stream and it can be used for determining the dominating source. The main contributor to the base flow is usually assumed to be the groundwater discharge from adjacent aquifer. This aquifer should be unconfined, with a relatively shallow groundwater table (higher than the stream water level) and should have the needed storage and transport properties to be able to maintain the discharge to the stream. However, other sources are possible to be the reason for dominating base flow, such as: connected lakes and wetlands; snow; glaciers; caverns in karst terrains; bank storage. In addition, the base flow could be affected by some specific activities, like: stream regulation (where there are dams, locks or weirs); direct pumping from the stream; direct discharge into the stream (from sewage treatment plants, industrial outfalls etc.); seasonal return flows from drainage of irrigation areas; artificial drainage of the floodplain and others.(Brodie & Hostetler, n.d.)

Method

There are different methods for analysing the base flow, which can be divided by the used approach into 3 groups: recession analysis, frequent analysis and base flow separation methods. The base flow separation methods are either graphical, or filtering. (Brodie & Hostetler, n.d.)

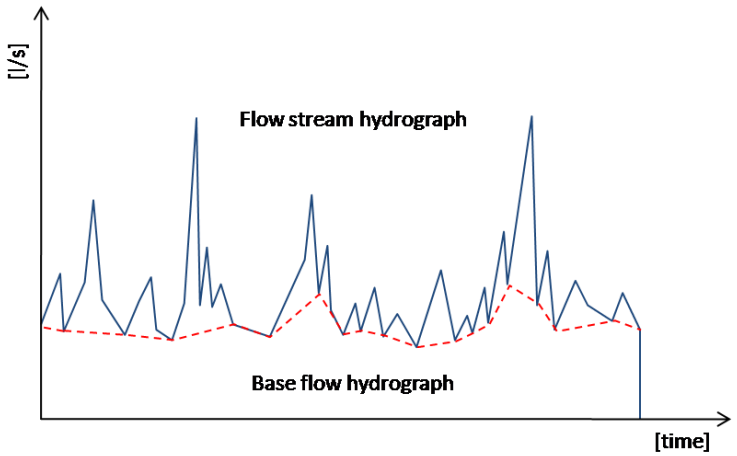

Figure 39: Scheme of the base flow separation

For finding the base flow index (BFI), filtering method, based on the smoothed minima technique is used. It has been described by the Institute of Hydrology (1993) and the procedure (Grant et al., 2000) is briefly explained below:

1. The minima of each 5 day non-overlapping period from the stream flow hydrograph are marked.

2. Only the ones of the minima (multiplied by 0.9), which are smaller than the two closest marked minima, are connected with a straight line and the result is the base flow hydrograph. The period in between the chosen minima is varying.
3. The BFI is number between 0 and 1 and it is calculated by subtracting the areas under the base flow hydrograph and the stream flow hydrograph.

Results

The daily averaged values of the flow rate from the database of Lundgårds Bæk (1989-2003) are used for calculating the BFI. Five years are chosen randomly and the base flow separation is made for each of them (see from Figure 115 to Figure 119). The minimum, maximum and average base flow are calculated for each of the 5 years (see Figure 40).

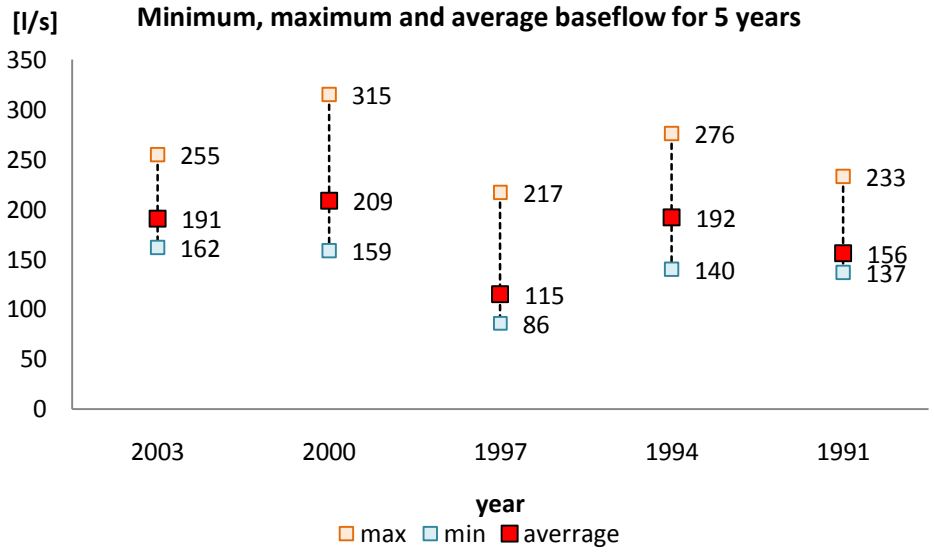

Figure 40: Minimum, maximum and base flow for 1991, 1994, 1997, 2000, 2003

Further, the BFI are calculated for each of the years. The results are given in Table 3:

Table 3: Base flow indexes of Lundgårds Bæk for the chosen 5 years:

year	BFI
1991	0.922
1994	0.831
1997	0.965
2000	0.928
2003	0.921

Discussion

As it is seen from Table 3 the average BFI for Lundgårds Bæk is around 0.92 with the exception of 1994 (BFI=0.83) and 1997 (BFI=0.97). In dry years (like 1997) the BFI is expected to be higher than 0.93 and in wet years (like 1994 and 2000) it is expected to drop below the 0.93. These results imply that the stream flow has its origin mostly from groundwater discharge from an unconfined aquifer (around 90% of the stream flow).

Figure 41: Gauging sites

For a comparison of the results a BFI is calculated for Villestrup Å (for two gauging sites: Møldrup bro and Ouegård bro) (see Figure 41). Data from the monitoring of Villestrup Å at Møldrup bro is available for the period 1989-1997 and the years with almost the same BFI for Lundgårds Bæk are 1991, 2000 and 2003. That is the reason why year 1991 was chosen for this comparison (see Figure 41):

Table 4: Base flow indexes for 1991 for 3 gauging sites in the region

gauging site	**BFI for 1991 [-]**
Lundgårds Bæk	0.922
Villestrup Å (Møldrup bro)	0.915
Villestrup Å (Ouegård bro)	0.936

From the base flow separation ("Appendix: Base Flow Separation", p.135) it is seen that the base flow is more or less constant in the year. And from the comparison between the stream flow hydrographs of the tree gauging sites (see "Appendix: Base Flow Separation", Figure 115, Figure 120, Figure 121*)* is seen that the pattern is almost the same. The only difference is in the magnitude, which is seen also from the calculated average values of the flow rate for the 3 sites (see Table 5*):*

Table 5: Average flow rate for 1991 for 3 gauging sites int he region

gauging site	**average flow rate1991 [l/s]**
Lundgårds Bæk	176.82
Villestrup Å (Møldrup bro)	311.52
Villestrup Å (Ouegård bro)	1254.09

Analysis of the Relation between the Nitrate Concentration and the Flow Rate

Introduction

The used data for the following analysis is from the monitoring station on Lundgårds bæk (Egelund). The NO_3^--N and NO_2^--N concentrations are measured once per month; there are 147 measurements for the period 1992-2003. From the available daily measurements of the flow rate (Q) the ones, which correspond to the NO_3-N and NO_2-N concentration data, are chosen.

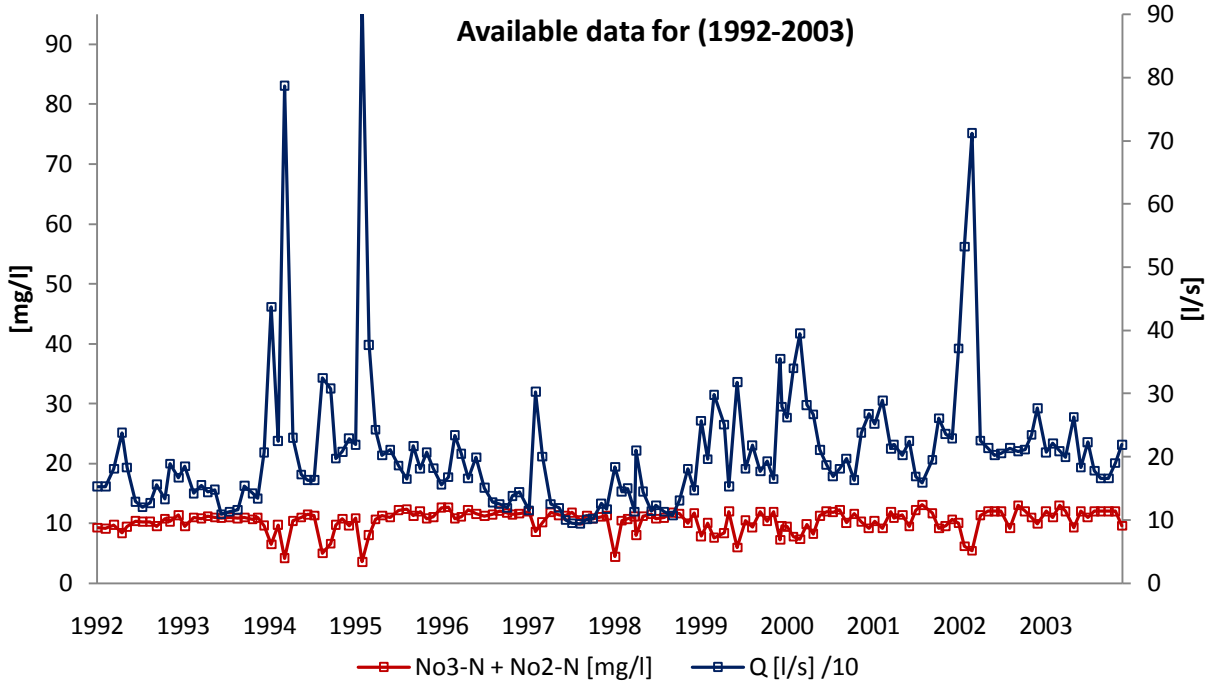

Figure 42: Measured Flow rate and NO3-N and NO2-N concentrations for the period (1992-2003) (data provided by AAU)

When plotting the data together (see Figure 42), a pattern is observed: the high flow corresponds to a lower concentration, which could be explained by the dilution when a big amount of "clean" water enters the stream.

The purpose of the following calculation is to find if there is any correlation between the concentration and the flow and to evaluate how strong the dependence is. Some correlation coefficients are calculated for achieving that goal. Next to this, linear and nonlinear regression analyses are performed. A brief explanation of the theoretical basis and the used methods is given in "Appendix: Basic Theory for the Statistical Analysis (after TGP, 2005)", p.139.

Initial Data Analysis

The flow rate is plotted against NO_3^--N and NO_2^--N concentration and a linear trend line is fitted to the data (see Figure 43). From the Figure 43 can be concluded two things: first, there isn't a good linear correlation between the two data-sets; second, the quality of at least 4 measurements can be questioned. These 4 measurements are marked with red and blue ellipses, where the blue circle is for a winter measurement (8th of January 1998) and the low flow corresponds to one of the smallest concentrations (4.4mg/l) - the average January concentration for the 1992-2003 period is 9.92mg/l. The red ellipse is drawn around 3 summer measurements (18th August 1994, 10th June 1999, 22nd September 1994) which aren't following the pattern high flow-low concentration and the opposite. On Figure 44 are plotted the data without these 4 measurements; a different trend-lines are fitted, from which the 2nd order polynomial function fits the best (R^2=0.8443).

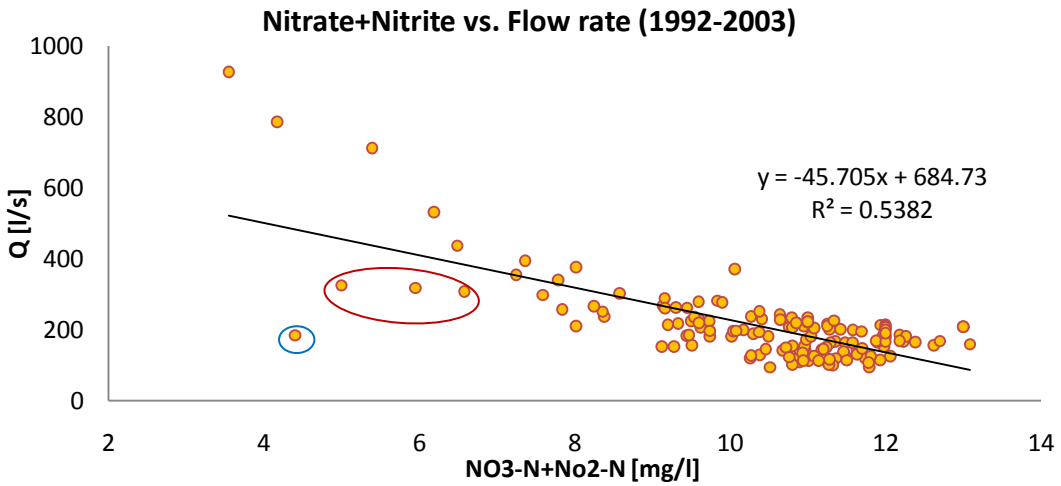

Figure 43: NO_3-N and NO_2-N concentrations plotted versus flow rate for the period (1992-2003); Pearson's correlation coefficient R=-0.569 for this period. In the red ellipse: the measurements on 18th August 1994, 10th June 1999, 22nd September 1994; In the blue ellipse: measurement on 8th of January 1998

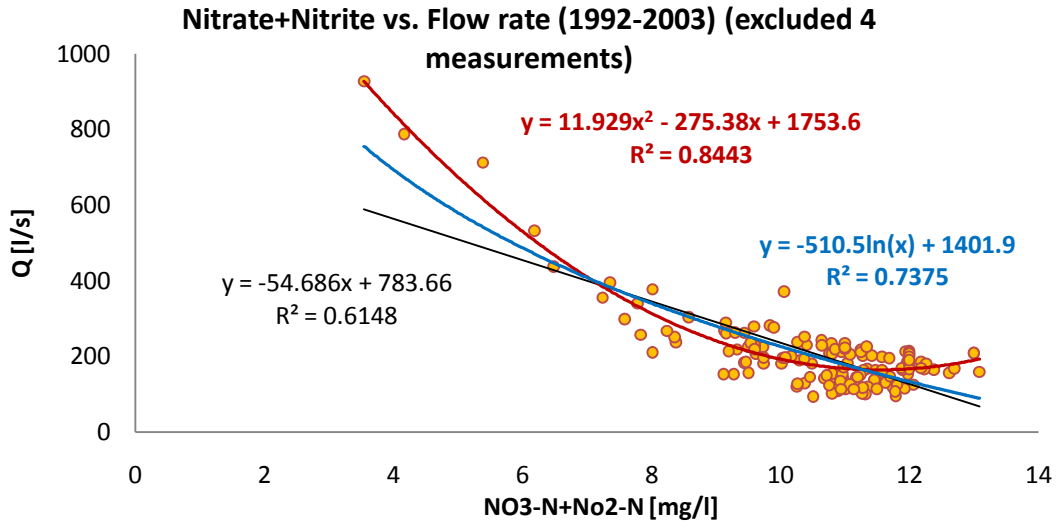

Figure 44: NO_3-N and NO_2-N concentrations plotted versus flow rate for the period (1992-2003), where the 4 measurements are excluded; Pearson's correlation coefficient R= -0.784, Polynomial trend line with r^2=0.844, logarithmic trend line with r^2=0.738

Before any correlation coefficients are calculated, the data is plotted in such a way that it is possible to find if there is an obvious dependency between the data and the period for which it is.

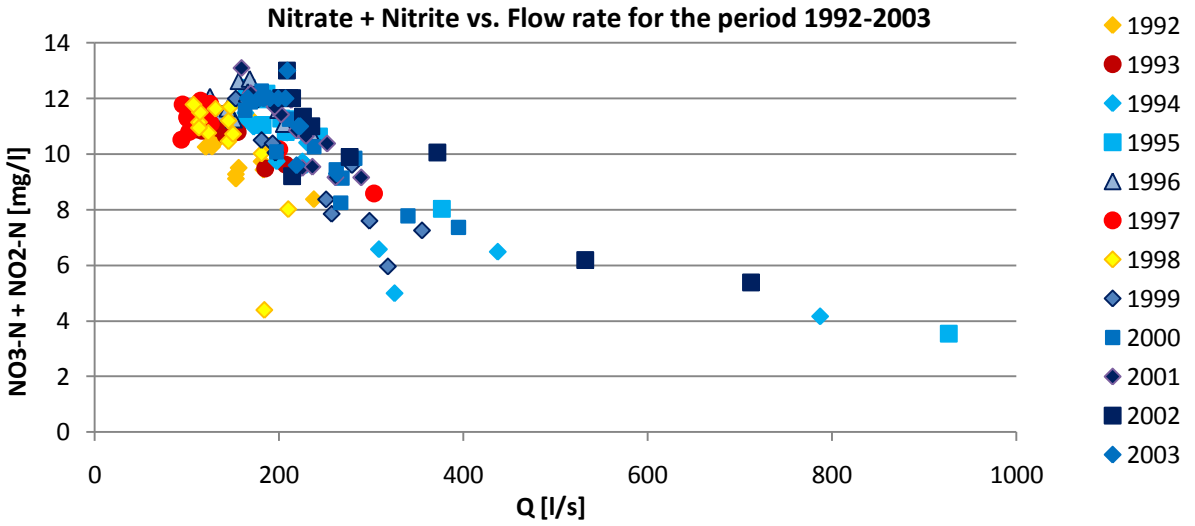

Figure 45: NO_2-N and NO_3-N plotted versus the flow rate for the period 1992-2003, where each year is presented with different colour

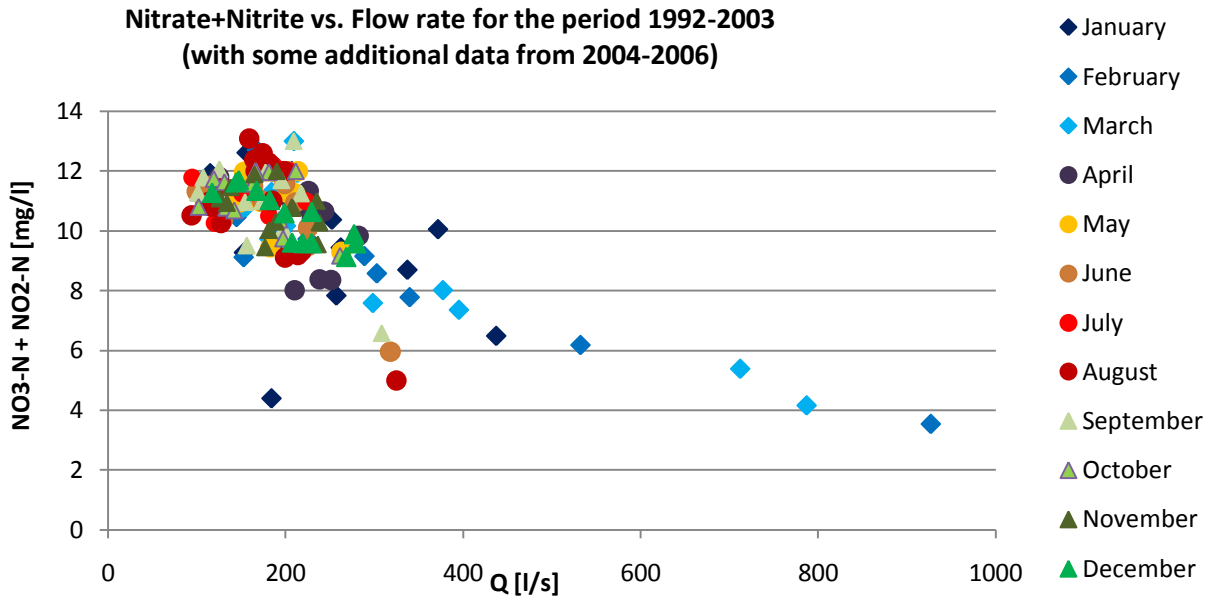

Figure 46: NO_2-N and NO_3-N plotted versus the flow rate for the period 1992-2003 (with some additional data from 2004-2006), where each month is presented with different colour

From Figure 46 and Figure 45 it can be seen that there is a need for further analysis to be able to conclude if there is any connection between the period for which is the data.

Further, Pearson's correlation coefficients are calculated and a regression analysis is performed in order to describe the relation between the NO_3^--N and NO_2^--N concentration and the flow rate in the 1992-2003 period.

Pearson's Correlation

The Pearson's correlation coefficient (R) is calculated for each year and the results are presented in Figure 47. From the results can be concluded that in some years a strong linear relation is present - with a coefficients higher than 0.9. In other years there is no correlation, or the coefficient is too low to be able to conclude that there is negative correlation between the concentration and the flow.

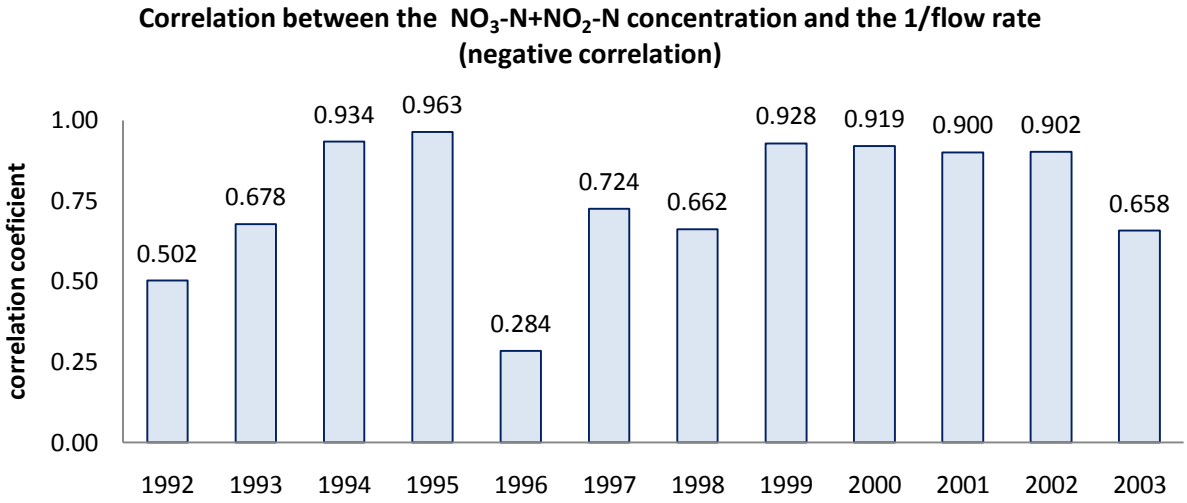

Figure 47: Pearson's correlation coefficient calculated for each year (1992-2003)

The same calculations are done on a monthly basis and the results can be seen on Figure 48. Relatively high correlation coefficients are calculated only for February, March and December, because the significant high flow rates (storm flows) are more often observed in these months.

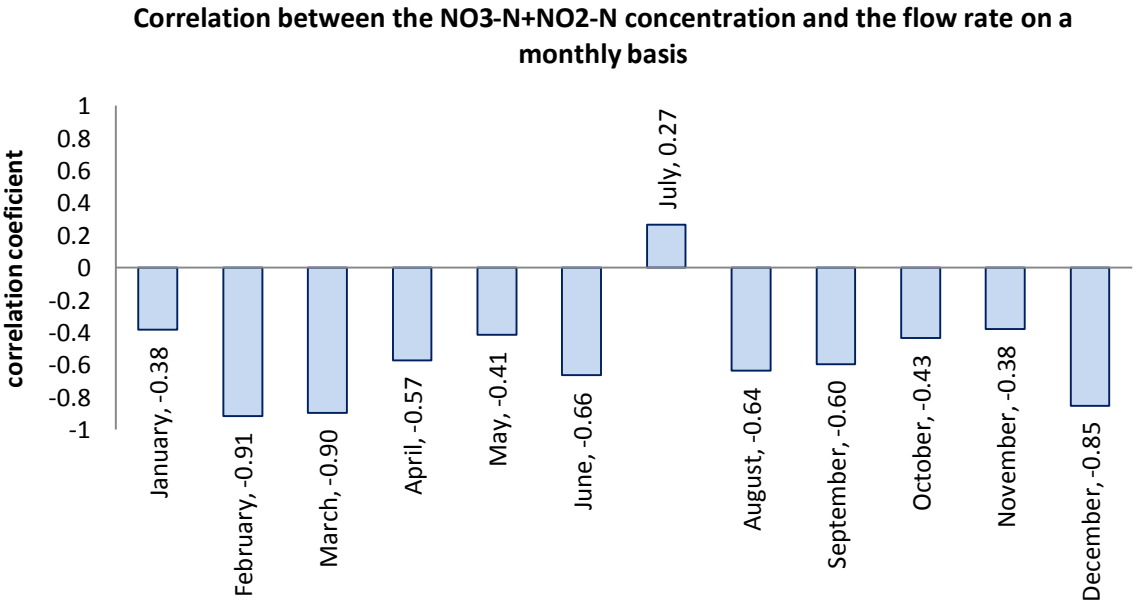

Figure 48: Pearson's correlation coefficient calculated for each month from the measurements done in the period (1992-2006)

In appendix (p.143) can be seen the monthly separated (Figure 131 - Figure 136) and annually separated (Figure 125 - Figure 130) plots of the data with fitted linear trend line and the coefficient of determination (R^2).

Regression Analysis

Both linear and non-linear regression analysis are performed with the original data (see Figure 49) and with the changed data (excluded 4 measurements, see Figure 50).

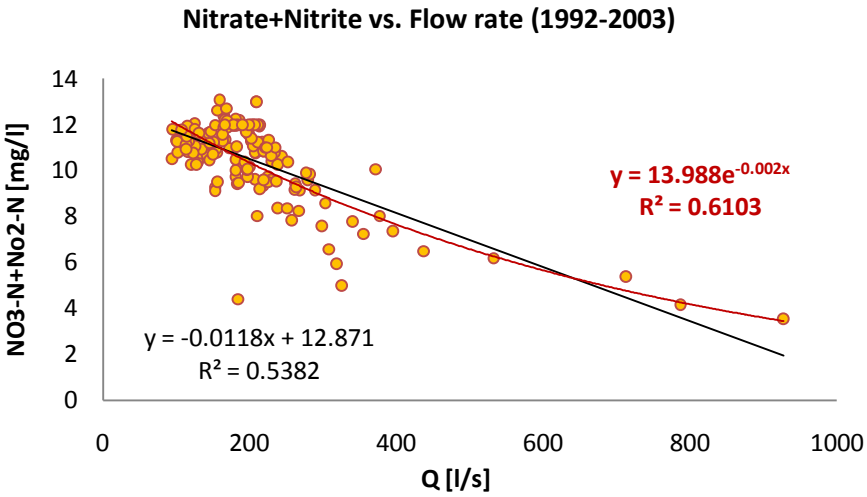

Figure 49: NO_3-N and NO_2-N concentration vs. Flow rate for the period 1992-2003 with linear (R^2=0.538) and exponential trend line (R^2=0.61) fitted to the data.

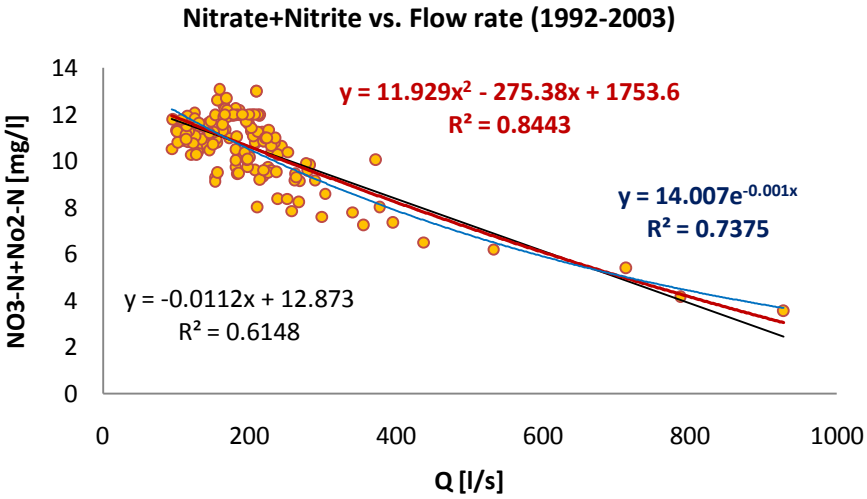

Figure 50: NO_3-N and NO_2-N concentration vs. Flow rate for the period 1992-2003 without the 4measurements with fitted different trend lines: linear (R^2=0.615), exponential (R^2=0.748), and 2nd order polynomial (R^2=0.844)

Below are presented the best fits from the performed regression analysis: first from the linear, and then from the non-linear.

Linear Regression

The best fit of the original data set is given by the equation:

$$y_{i,est} = Ax_i + B + \varepsilon_i = -0.012x_i + 12.871 + \varepsilon_i,$$

Where,

- $y_{i,est}$ - the estimated NO_3-N + NO_2-N concentrations
- x_i - the measured flow rate
- $A = -0.012$ is a fitting constant
- $B = 12.871$ - fitting constant
- ε_i – residuals (the deviations from the fitted line); the residuals for each data point are presented on Figure 137 (p.150)

On Figure 138 (p.150) the estimated concentrations versus the measured ones are plotted and from Table 17 (p.150) the regression summary output is given, where can be seen that the calculated RMSE equals 1.225 and the R^2 equals 0.538.

The same analysis is carried out for the changed data set, where the 4 measurements are deleted. The best linear fit to the data is given below:

$$y_{i,est} = Ax_i + B + \varepsilon_i = -0.011x_i + 12.873 + \varepsilon_i,$$

The plot of the residuals for the changed data-set is given on Figure 139 (p.150).

From the presented results for both (the changed and the original data set) it is seen that a linear function doesn't give a good fit to the measured data. It can also be said that there is no strong linear correlation between the NO_3^--N and NO_2^--N concentration and the flow rate. Even though, the changed set gives a better regression parameters (Table 18, p.151).

Non-linear Regression

The non-linear regression is performed also for both, the original and the changed data sets. First are presented the results for the original data set.

Different equations are used for the non linear regression analysis from which best fits are presented in Table 19 (p.151). Even though the RMSE are still high, the best fitting equation is with RMSE equals 1.181 and reads:

$$y_{i,est} = 13.899\ e^{(-0.0017x_i)} + 0.0026x_{i-1},$$

On Figure 141 (p.151) the measured concentrations and the one found by the exponential regression (the best fitted one with RMSE=1.181) are plotted together. Also, an exponential trend line is shown with the R^2.

The same procedure is repeated for the changed data set. The best fits are presented in Table 22 (p.153), from which the equation with the smallest RMSE=0.993 is:

$$y_{i,est} = 13.175\ e^{(-0.0007x_i)} + 0.0043x_i,$$

On Figure 143 (p.152) the measured concentrations and the one found by the exponential regression (the best fitted one with RMSE=0.993) are plotted together. Also, an exponential trend line is shown with the R^2.

Summary

A summary of the regression analysis is provided in Table 6, where the goodness of the fit could be examined by comparing the RMSE. Also, the R, R^2, and the used equation are given.

Table 6: Summary of the regression analysis

type of regression	**Linear regression**		**Non-linear regression**	
data-set	**original**	**changed**	**original**	**changed**
N	147	143	147	143
equation	$y_{i,est} = -0.012x_i + 12.871$	$y_{i,est} = -0.011x_i + 12.873$	$y_{i,est} = 13.899\, e^{(-0.0017x_i)} + 0.0026x_{i-1},$	$y_{i,est} = 13.175\, e^{(-0.0007x_i)} + 0.0043x_i$
R	0.734	0.784	0.788	0.853
R^2	0.538	0.615	0.621	0.728
RMSE	1.225	1.003	1.181	0.993

From Table 6 is seen that for both the linear and the non-linear regression better results give the changed data set. From the chosen models the one that describes best the relation between the NO_3^--N and NO_2^--N concentration with the flow rate is the exponential model (see Figure 51).

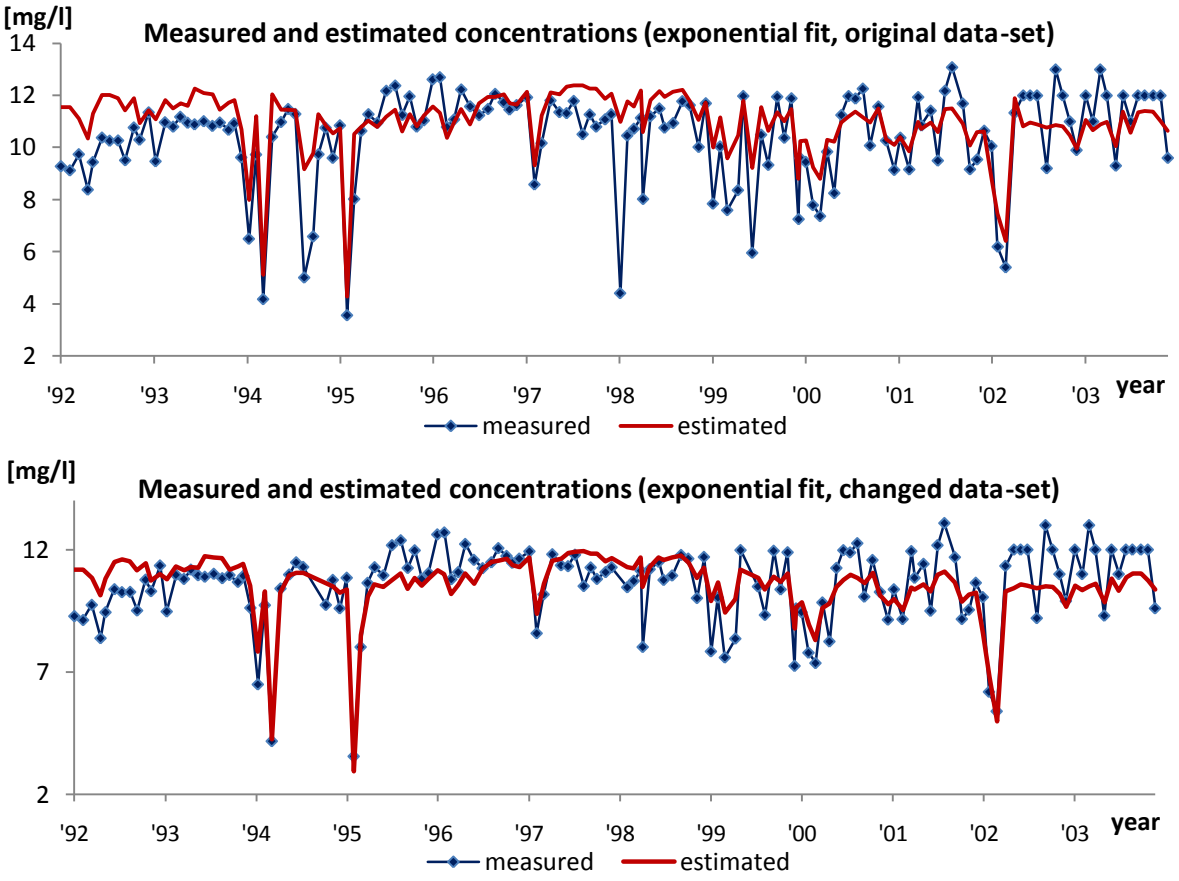

Figure 51: Measured and estimated concentrations for the period 1992-2003

Conclusions

From the presented data analysis can be concluded:

- A relation between the observed NO_3^--N and NO_2^--N concentration and the flow rate exists;
- The best fit of the data is where the extreme values are; Next to other unstudied factors, most probably the high fast flow (storm flow) is one of the reasons for the low concentrations. An explanation for the observed relation could be that the high background concentrations are diluted when a high less-contaminated flow enters the stream.
- The process(es), which is(are) controlling the NO_3^--N and NO_2^--N concentration in the stream can't be modelled by simple one variable non-linear regression. Other factors like temperature, organic content and pH of the soil/sediment etc. should be included for obtaining better results.

[empty page]

E. Field work

A great amount of field work was planned in order to gather data for building an understanding about the area. The purpose of the field work is:

- to study how the flow and the concentrations are distributed along the stream;
- to investigate what is the origin of the NO_3^- pollution;
- to detect the zones, where the groundwater is the main source;
- to obtain a valuable information about the NO_3^--N and NO_2^--N concentrations in the groundwater springs in the area.

As part of the field work, different measurements are performed:

- Flow rate and NO_3^--N and NO_2^--N concentration measurements at chosen measuring stations in the stream;
- Water temperature measurements in the stream (each 70-100m) (Miljøcenter, Aalborg);
- NO_3^--N and NO_2^--N concentrations, oxygen and temperature measurements in the groundwater sources (mainly in groundwater springs directly discharging at Lundgårds bæk).

In addition, a field observation is conducted and thermo imaging is used for detection of warmer groundwater discharging to the stream (as a diffusive or direct flow). The field work is done in the winter period mainly because of two reasons: (1st) the temperature difference of the surface water and the groundwater is used; and (2nd) the dormant period of the plants and the low microbial activity in the winter is providing a preferable conditions in order to exclude the NO_3^- uptake from the analysis.

Further the gathered from the field work information is used in the application of the Dahl's GSI typology and for calculating the reduction capacities of the area.

All the field work was done with the kind support of the Nature Agency (former Miljøcenter Aalborg).

Used Methods and Results

For the purposes of the project, eleven points along the stream are used as sampling stations (see Figure 52, next page). Sampling station 1 is located at the same place, where the monitoring station "Egelund" is and stations 9 and 10 are located further upstream, closer to Arden.

Samples for measuring NO_3^--N and NO_2^--N concentrations are taken from those stations, and the flow rate is measured several times in the project period at them. The results from the field work are presented further.

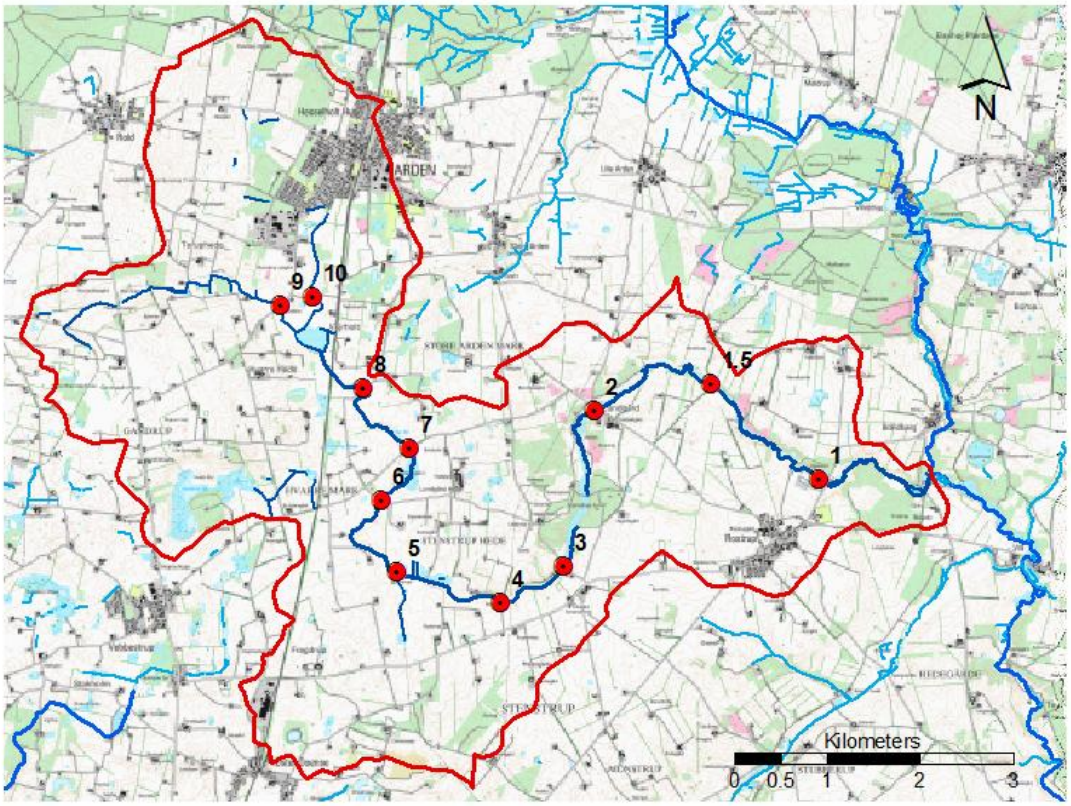

Figure 52: Sampling stations

Flow Rate Measurements along Lundgårds Bæk

Flow rate measurements at the sampling stations (st.) are carried out 4 times for the period September 2010 – February 2011, with the exception of st. 1,5 (see Figure 52), which was added later in this period, so only one measurement was made there.

The results from these measurements are presented on Figure 53 and Figure 54 (next page). From the calculated average values, it is seen that downstream from st. 10 to st. 8 the flow rate is increasing, then from st.8 to st.6 is decreasing, and finally, from st.6 to st.1 is increasing again.

Based on that, it can be concluded that Lundgårds bæk is gaining from st.10 to st.8 and from st.6 to st.1 and loosing from st.8 to st.6. It should be remarked that the flow rate at st.1 ($Q_{average}$=178l/s) is around three times bigger than the flow rate at st.2 ($Q_{average}$=51.43l/s).

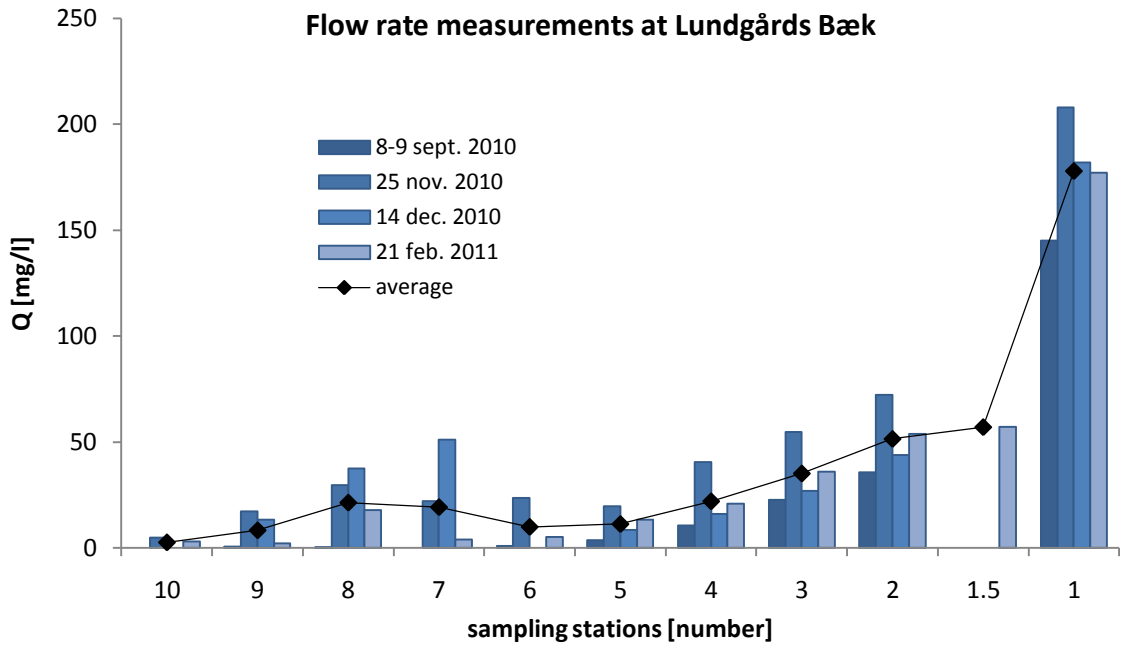

Figure 53: Results from the flow rate measurements at the 11 sampling stations of Lundgårds bæk

Nitrate-N and Nitrite-N concentrations in the stream

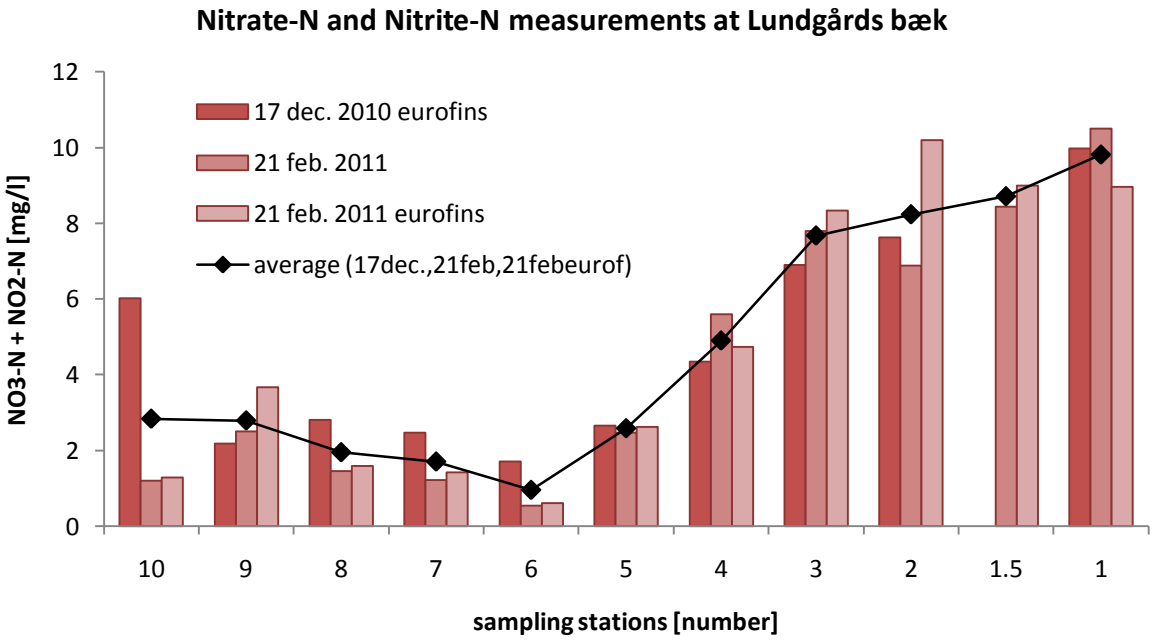

Figure 54: Results from the NO_3-N and NO_2-N measurements at the 11 sampling stations of Lundgårds bæk (17th December 2010, 21st February 2011)

The NO_3^- concentrations are measured 5 times (Figure 155, p.168) through the period from September 2010 to February 2011:

1. On 8-9th September 2010 by using in-situ (on-site) sensor, measuring NO_3^- concentrations;
2. On 25th November, 14th December, 21st December 2010 with photometer, measuring NO_3^--N and NO_2^--N, NH_3 and TN concentrations (also PO_4-P);
3. On 17th February and on 21st February 2011 are analyzed in licensed laboratory (Eurofins);

Only the results from 17th of December 2010 and 21st of February 2011 are presented On Figure 54, because they are the most reliable. The samples from 17th of December are tested in a licensed lab. The samples, taken on 21st February, are tested with the photometer, but also independently in the licensed laboratory. The difference in the results from 21st February is shown in Figure 156 (p.168).

From Figure 54 it can be seen that the NO_3^--N and NO_2^--N concentrations are relatively low (below 3mgN/l) for st.6, st.7, st.8. Further downstream, a significant increase (almost 10 times) is observed between st.6 and st.3. From that station to st.1 the concentrations continue rising, but with much lower rate. At st.1, where the highest NO_3^--N and NO_2^--N concentration for the whole Lundgårds bæk is measured, the average value is 9.81mg N/l, when for st.3 the value is 7.67mg N/l (around 1.3 times lower than in st.1) (see Figure 54).

Water Temperature Measurements in the Stream

On 6th and 7th of December the temperature of the water in the stream has been measured at 92 points upstream from Villestrup Å to the st.3, with average distance between the points around 75m (see Figure 55).

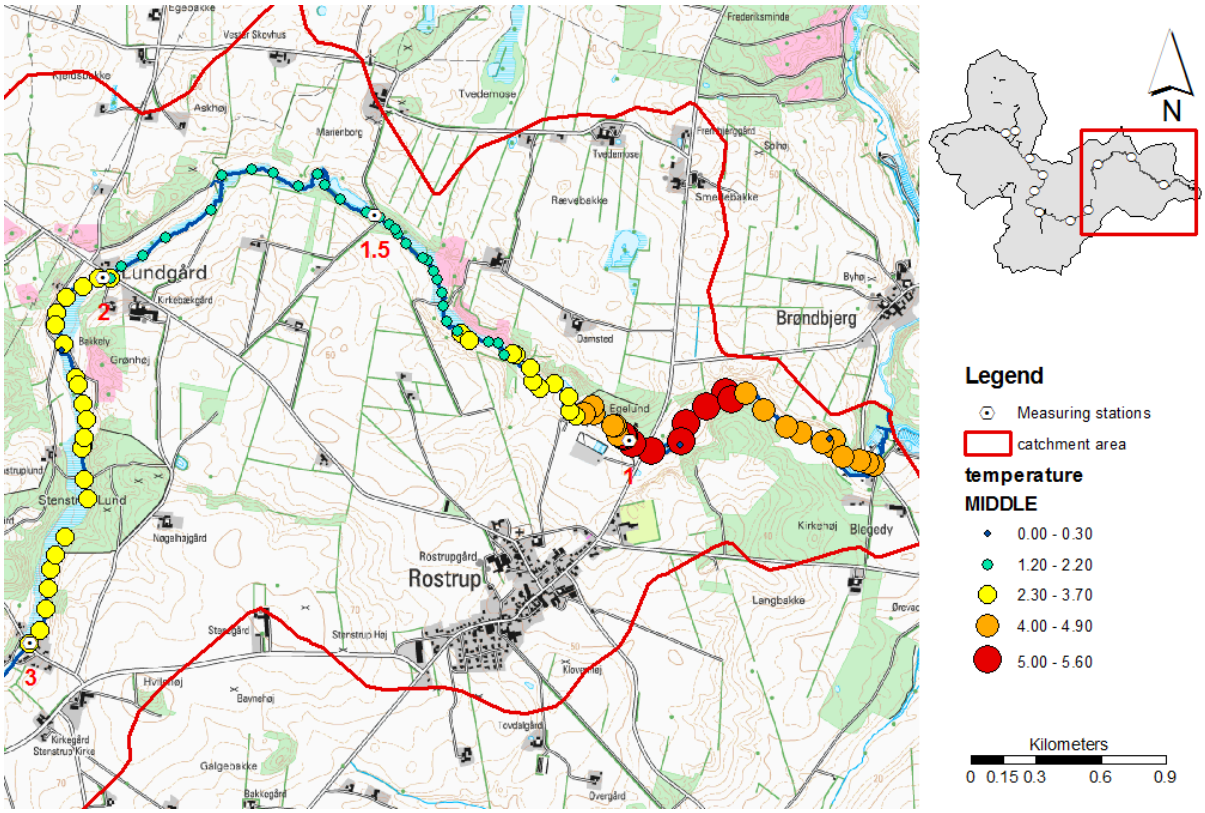

Figure 55: Water temperature measurements at Lundgårds bæk (6th, 7th December 2010); (data: Miljøcenter ,Aalborg)

For each point the temperatures of the water close to the banks and in the middle is measured. The temperatures measured in the middle of the stream are shown on Figure 55. From those, the highest temperatures are observed around st.1 (5-5.6°C). Around the middle in between st.1 and st1,5 the water cools down to 1.2-2.2°C. From that point to st.2 the water temperature stays in the range of 1.2-2.2°C, but from st.2 to st.3 it warms again to 2,3-3,7°C. Further upstream, the temperature of the water at st.4 and st.5 was measured to be respectively 1.5°C and 3.2°C. All the measurements are presented on Figure 157 (p.169).

Field Investigation and Sampling from the Sources (Groundwater Springs, Diffuse Groundwater Flow, Pipes etc. in Lundgårds bæk's Riparian Zone)

Field investigation for detecting groundwater (springs, diffuse groundwater flow) and other sources (sewage or drain pipes, inlets) is performed in the period between 22nd February and 1st March 2011 (5 working days). The used methods for this investigation are observing for visible groundwater discharge and thermo imaging. The thermo imaging is used for detecting a groundwater discharge from the banks and from the riparian zone of Lundgårds bæk. The difference in the surface water and groundwater temperatures is used for detecting those places. The ground water in the region is with almost constant temperatures in the year - around 8-9°C, whereas the temperature of the surface water is more influenced by the air temperature and differs in day/night and also seasonally. Generally, in the winter the groundwater is warmer than the surface water. Thermo images are made by using thermo camera Fluke Ti25 (calibrated for the interval from -22°C to 125°C) and processed with the software SmartView 1.9.0.21 (Fluke, 2006-2007). In addition the water temperature and the oxygen concentration in the stream are measured, and samples for nitrates and phosphates are taken from the groundwater sources.

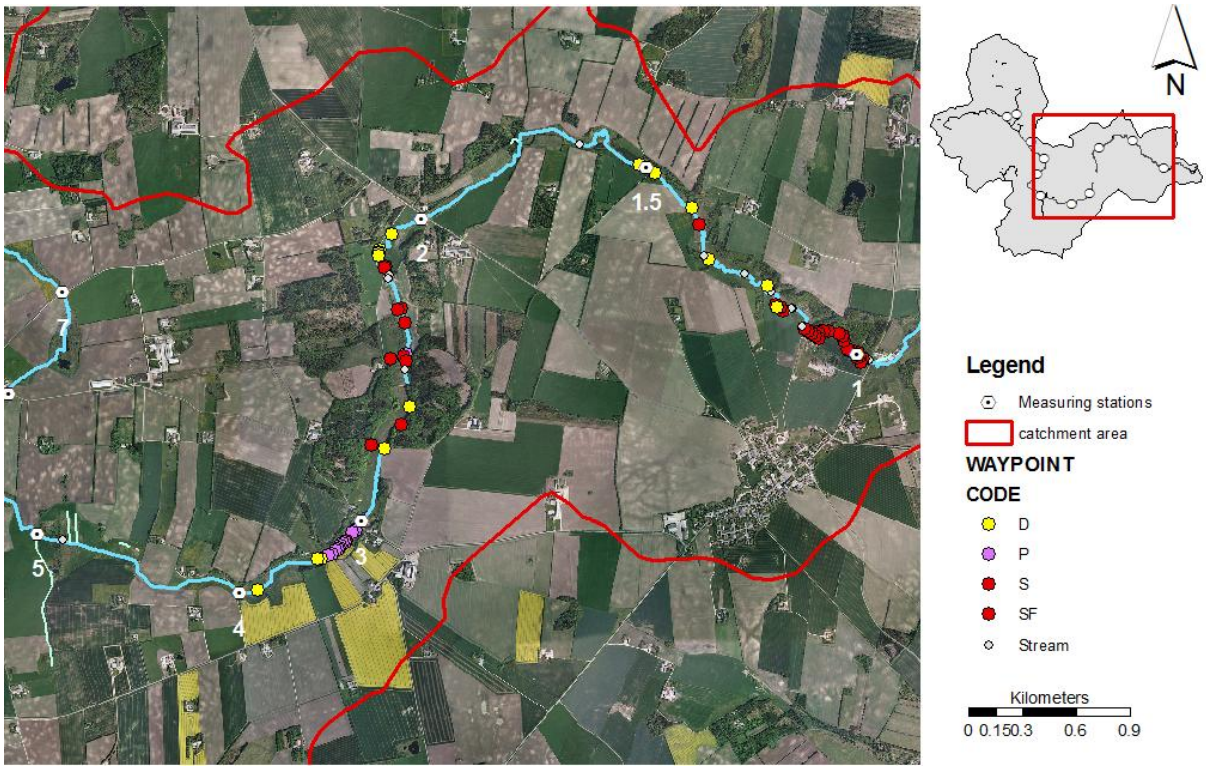

Figure 56: Investigated area (used codes: diffuse groundwater flow "D", pipes "P", groundwater spring "S", groundwater spring field "SF")

The investigated area between st.1 and st.5 with an overview of the gathered information about the sources is presented on Figure 56. The focus of this field investigation is on the region between st.5 and st.1, because the previous measurements of the temperature in the stream showed that this is the region, where something happens. A more detailed view of the field investigation is presented next.

Thermo Imaging and Field Observations

Figure 57 presents the findings from the field observation from the first 200m, close to st.1:

- the warm banks with diffusing groundwater and the groundwater spring areas;
- the measured water temperature at the springs and in the stream;
- some photos and thermo images, giving an example of the diffuse groundwater flow and the groundwater springs.

The figures, presenting the rest of the observed area, are given in “Appendix: Field Observations and Thermo Imaging” (p.155). The one presented on the next page, particularly, is part of the region where most of the groundwater discharge is concentrated. As it is seen from Figure 57 the measured water temperature in the stream is around 4.8°C, whereas the temperature in the small groundwater springs in the vicinity of the stream is warmer with 2 to 4°C.

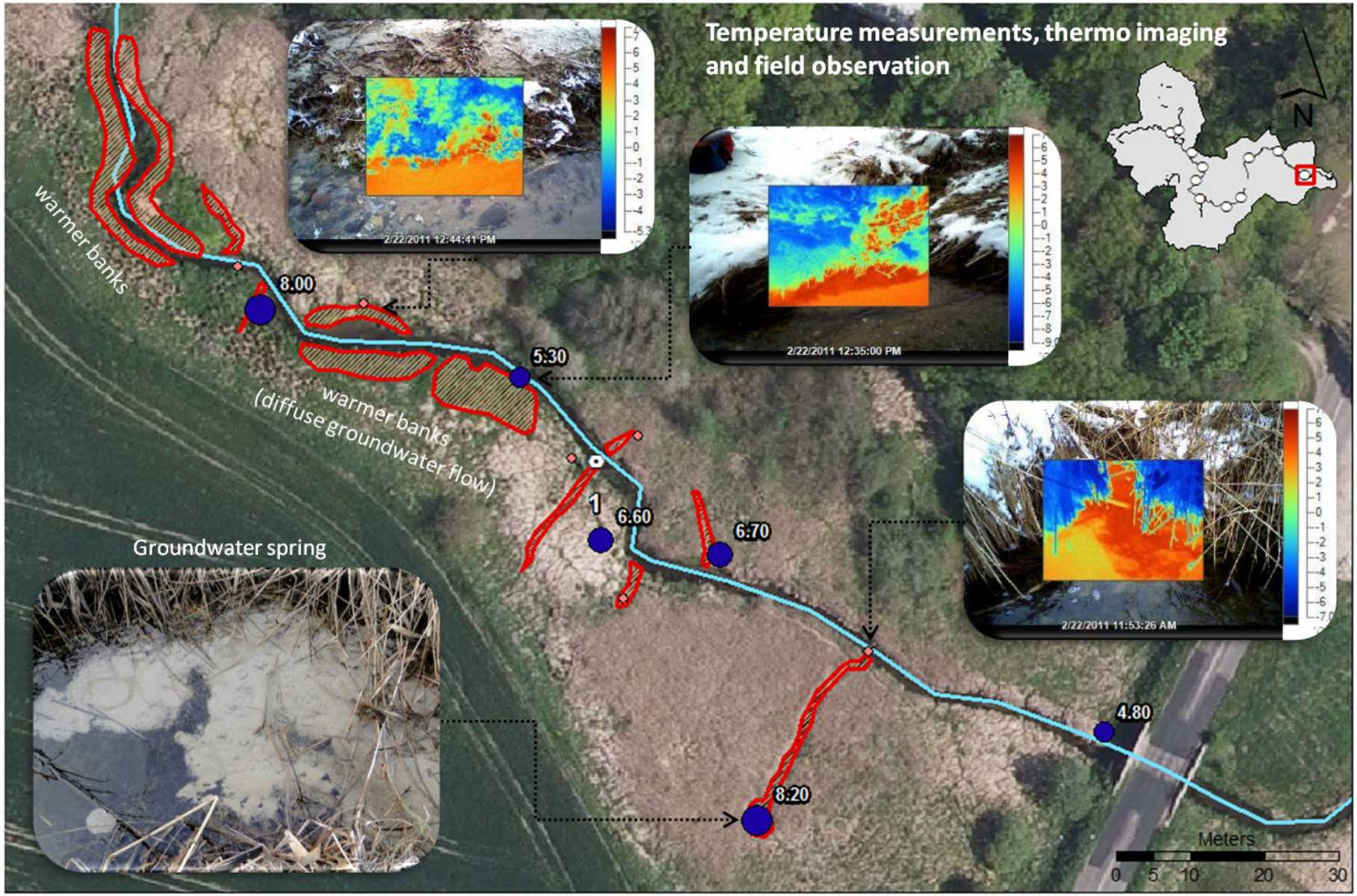

Figure 57: Field observation, temperature measurement, and thermo imaging (1/11)

Nitrate-N and Nitrite-N Concentrations in the Groundwater Springs

19 samples for analysis are taken from the investigated area, from which 16 are from a groundwater springs or spring fields, where the groundwater discharge is visible, and 3 from places where it was not (diffuse flow under the roots or small puddles). The results are presented below:

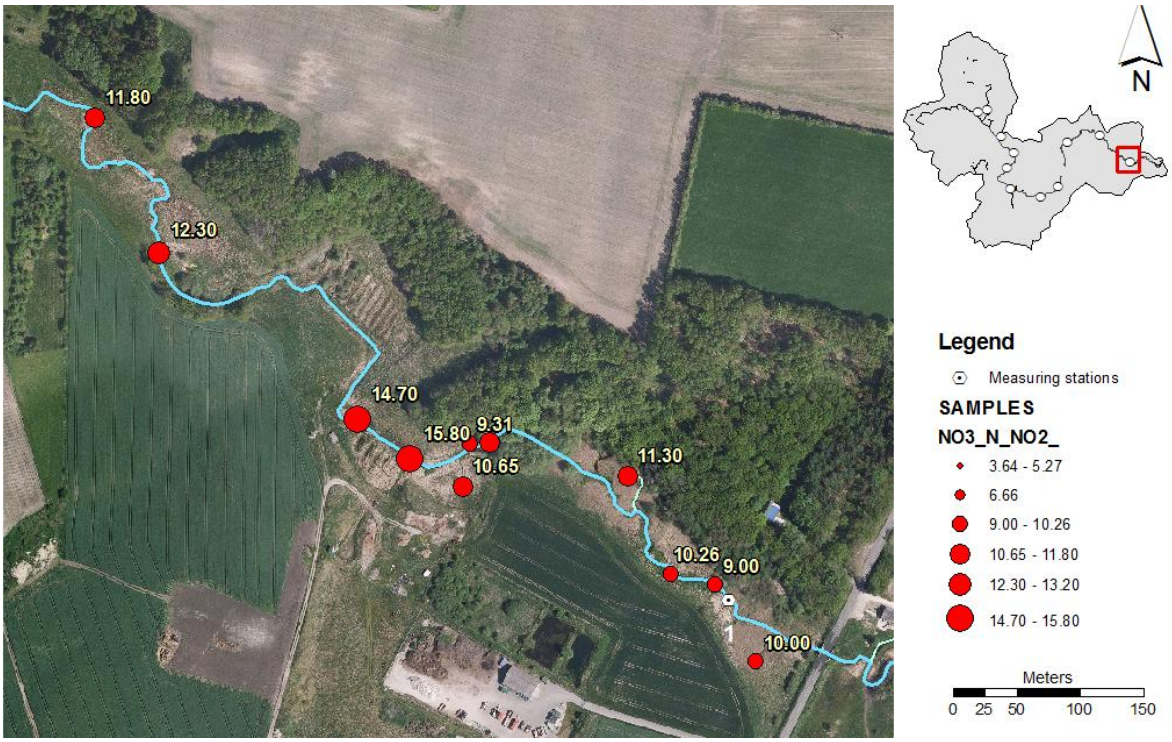

Figure 58: Measured NO_3-N and NO_2-N concentrations at the groundwater sources in the vicinity of st.1 (the concentrations are in mgN/l)

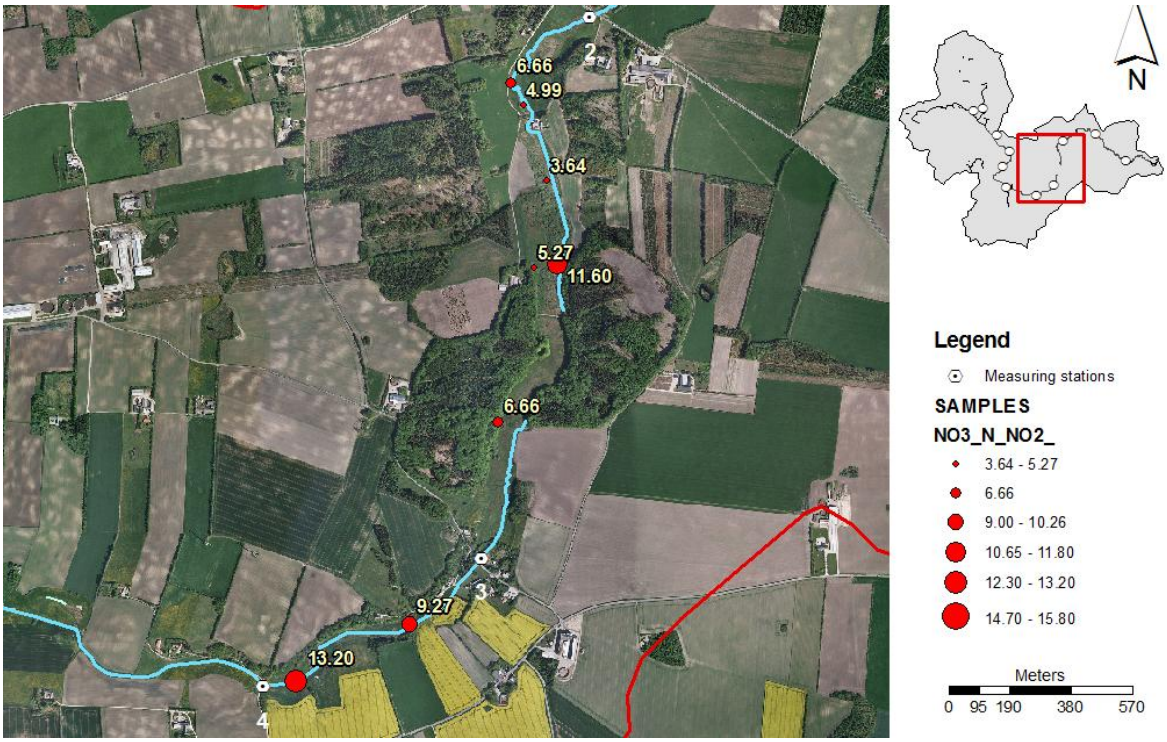

Figure 59: Measured NO_3-N and NO_2-N concentrations at the groundwater sources in the area between st.2 and st.4 (the concentrations are in mgN/l)

From Figure 58 can be seen that the measured NO_3^--N and NO_2^--N concentration in the springs close to st.1 are in the range 10.00-15.80mg N/l. As a comparison, the measured NO_3^--N and NO_2^--N concentration in the stream at st.1 on 21st February (couple of days earlier) is 10.5mgN/l. On the next figure (see Figure 59) the region between st.2 and st.4 is shown, where two types of concentrations have been measured: bellow 7mg/l and above 9mg/l. Possible reasons for those low concentrations are that the groundwater was diluted by the stream water (in cases where there was a sample taken from a places with a contact with the stream) or that there was a denitrification (in cases with the small ponds with decaying organic matter and almost still-standing water). As a comparison, the measured NO_3^--N and NO_2^--N concentrations in st. 2, st.3, and st.4 are respectively 6.88mgN/l, 7.8mgN/l, and 5.6mgN/l. The results from the measured oxygen concentrations, temperature and NO_3^--N and NO_2^--N from the sources can be seen at the "Appendix: Field Measurements" (p. 167), Figure 158 and Table 23. A good correlation exists between the measured temperatures in the sources and the NO_3^--N and NO_2^--N concentrations (R=0.75), which means that high temperatures correspond to high concentrations.

Overview and discussion of the results from the field work

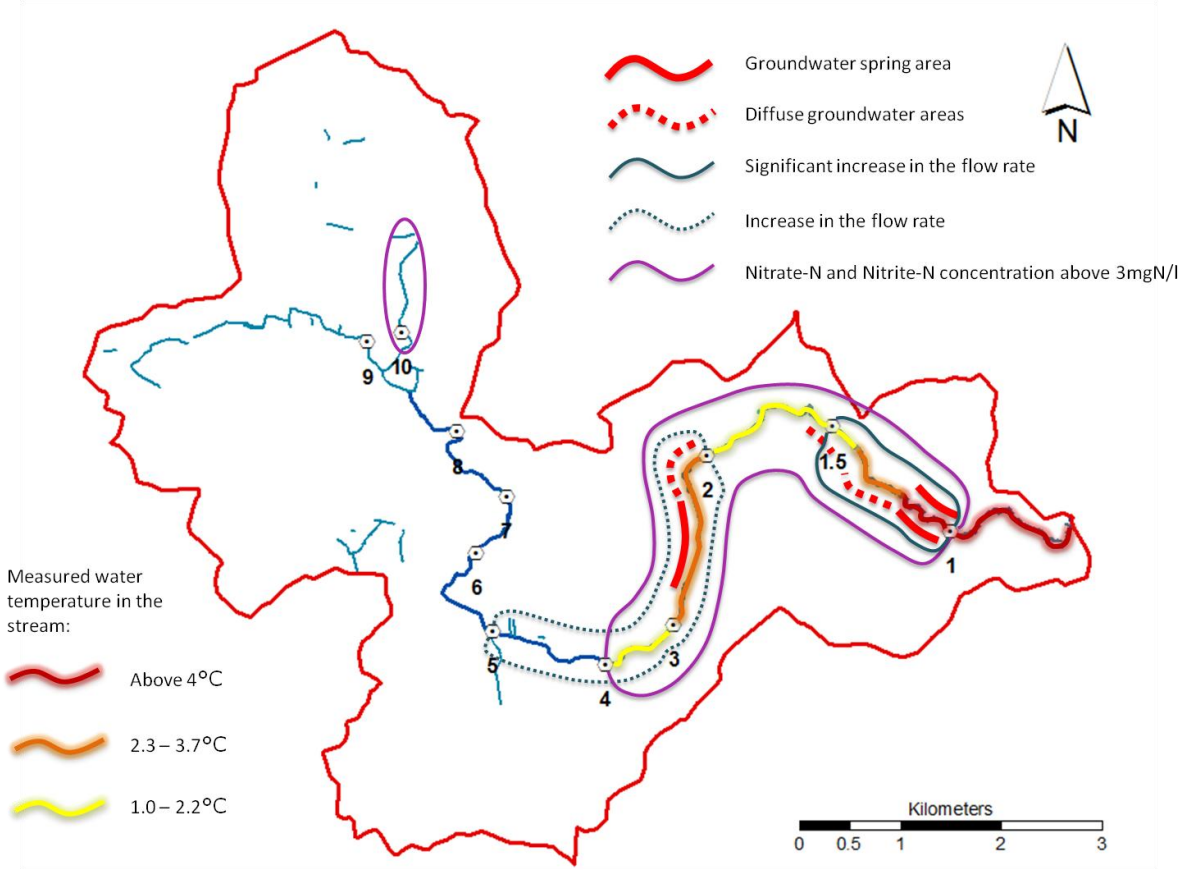

Figure 60: Overview of the results from the field work

Figure 60 depicts an overview of the performed field work with the zones, where:

- groundwater springs or diffuse groundwater is observed;
- there is a significant increase in the flow rate;
- where were NO_3^--N and NO_2^--N concentrations higher that 3mgN/l are found;
- and where the temperature in the stream is warmer.

Groundwater springs are found mainly in the first part between st.1 and st.2 (from both banks), and also between st.2 and st.3 (only from one of the banks) but not with such high density as in the first part. It is observed that at the parts where there are a lot of spring, there are also quite a lot of diffuse flow areas, but also to some extend there are regions, where only diffuse water is found. Such places are found all the way between st.1 and st.1,5, also close to st.2.

The flow rate starts increasing from st.5 to st.2.Then, from st.1,5 to st.1 there is a significant increase in the flow rate – around 3 times bigger at st.1 than at st.1,5 or st.2.

The NO_3^--N and NO_2^--N concentrations in the region between st.4 and st.1 are measured to be higher than 3mgN/l. Also an increase in the concentrations is observed from st.4 to st.1. The measured concentrations at st.10 differ significantly from one measuring session to the next. A possible reason for this significant difference could be a storm-runoff from the small village Arden situated north of this station.

In addition, the measured water temperatures in the stream are shown with tree colours (red- above 4°C; orange – from 2.3 to 3.7°C; and yellow – form 1 to 2.2°C). These measurements are also in a consensus with the findings from the field observation for the groundwater sources. The highest water temperature in the stream is observed in the region, where there was also high density of groundwater springs, directly discharging to the stream.

As a conclusion can be said that the results from the field work showed that the groundwater is one of the main sources of water (warmer) and of NO_3^- pollution in the winter season.

F. Analysis of the Catchment and the Sub-catchment Areas

Introduction

The purpose of this part of the project is to delineate the sub-catchment areas of each sampling station along Lundgårds bæk. In the previous part were shown the areas, where the groundwater discharges to the stream and the different flow path types were discussed. In this part the focus is on the catchment areas as the sources of the water and the NO_3^- entering the stream. For being able to make land-use analysis for each part of the catchment, first the sub-catchments are delineated. Further in the report, based on those sub-catchments, the leaching from the area is evaluated. A brief explanation on the used methods is given next, followed by the results and some discussion.

The sub-catchment analysis is made by using two different methods: one for the topographical catchment areas and one for the hydrogeological catchment areas (as it is called further). The difference between the two types of catchment areas is that the hydrogeological catchment area takes into account only the area where the groundwater has been formed. In other words, this is the area where the groundwater flow, which is discharged to the stream, has started from. On the other hand, the topographical catchment area is also taking into account the other types of water feeding the stream, like surface runoff etc.

Method

Topographical Sub-catchment Areas

The topographical sub-catchment areas of each measuring station are created by using the software CatchmentSIM v.2.30(Catchment, 2008). CatchmentSIM is a stand-alone GIS based program, which automatically delineates sub-catchments and calculates their properties. The digital elevation model of the area with 10m resolution (provided by NIRAS) is used as input information for the terrain. To ensure flow connectivity and proper work of the delineation algorithm, the pit and flat removal is applied. As addition, a stream burning is used to lower the pixels underlying the stream with 1m below the terrain. In that manner it is guaranteed that the simulated flow paths don't differ from the watercourse path.(Catchment, 2002-2010)

Hydrogeological Sub-Catchment Areas

The hydrogeological sub-catchment areas are delineated in GIS environment by using as input the flow paths simulated in GMS. The GMS model was built and calibrated by NIRAS. For the geological base in the GMS modelling, the 3D stratigraphic model of the area built as part of this master thesis together with Miljøcenter Aalborg is used (see "Appendix: Building a 3D Geological Model of the Project Area", p.123). Further, the flow paths (together with the residence times) (Figure 61) and their starting and ending points (Figure 62) are analysed in GIS.

Some remarks should be made about the used data (flow paths, starting, ending point):

1) The flow paths are generated with applying one starting point for each cell from the grid of the GMS model. With other words, each point represents a cell, where the cell size of the GMS model is 100m. On Figure 62 with blue dots are shown only the starting points of the flow paths, which end at the stream or at the catchment area of the stream. The selection is made by joining the two shape files in GIS and applying the condition "keep only the matching records".

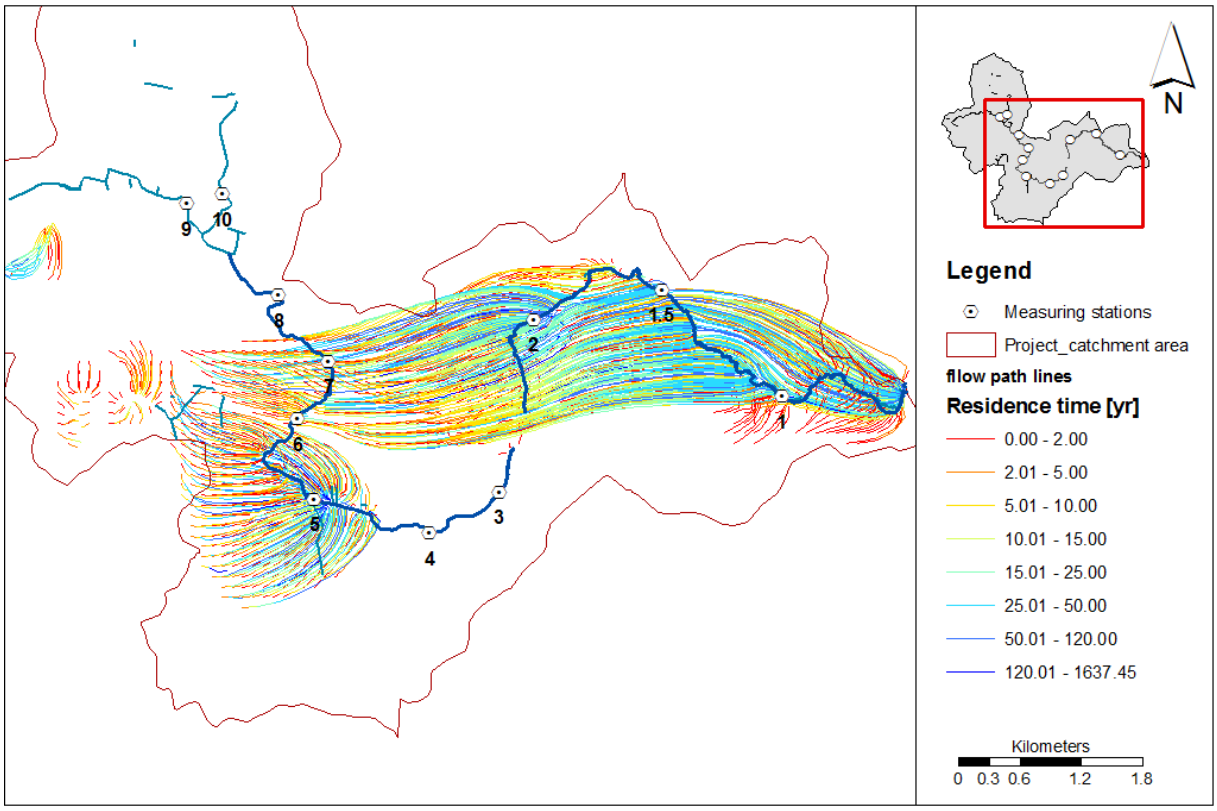

Figure 61: Generated with GMS flow paths (shape file source NIRAS)

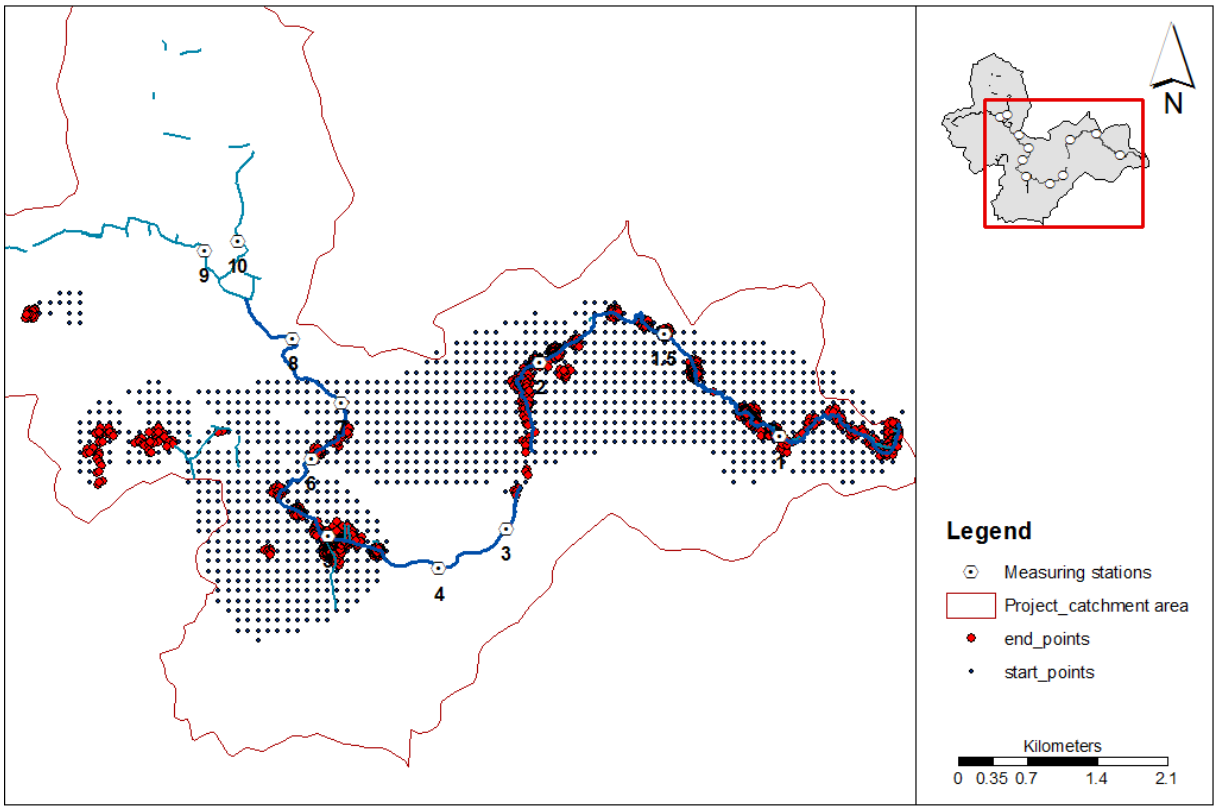

Figure 62: Starting and ending points of the flow paths (shape files: NIRAS)(with red dots – ending points; blue – starting points)

2) To validate the GMS model, the results from it are compared with the measurements in the stream. To make the comparison it is calculated what part of the flow particles (volume of water) end in the stream between two stations as a %, on one side. On the other side, it is calculated, based on the flow rate measurements, how much is the change in the flow in between two stations as % from the flow at the end of the stream (st.0) . The low rate in st.0 is not measured as part of the field work. The value is estimated as it is assumed that the flow rate changes with the same rate as in the part between st.1,5 and st.1. The results are presented in Figure 63:

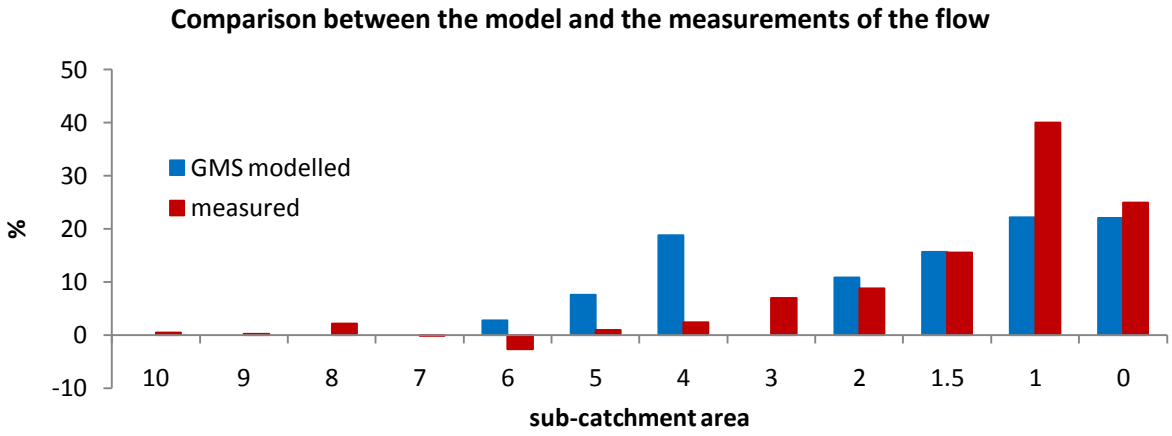

Figure 63 Comparison between the modelled and the measured volume of water

Figure 63 shows that the results from GMS model and the measurements are close for st.0, st.1.5, st.2, but differ significantly in st.1, st.4.

3) The flow path directions are modelled and calibrated in GMS (NIRAS), but the residence times (or the travelling time) of one particle from the starting point to the end point is highly dependent on the effective porosity and this hasn't been calibrated (only sensitivity analysis were made). The used effective porosity in the model is:

- For sand and clay - 20%
- For limestone – 5%

All the residence times shown further in the report are calculated with that effective porosity. The relation between those two follows the formula:

$$2 * n_{eff\%} = 2 * t$$

where $n_{eff\%}$ is the effective porosity and t is the residence time.

4) To delineate the hydrogeological catchment and sub-catchment areas it was taken into account that each starting point represents a cell, so buffer zones with radius 50m around each starting point are created in GIS environment. The hydrogeological catchment area is then drawn as an outer contour of the buffer zones. An illustration of the explained procedure is given on Figure 64.

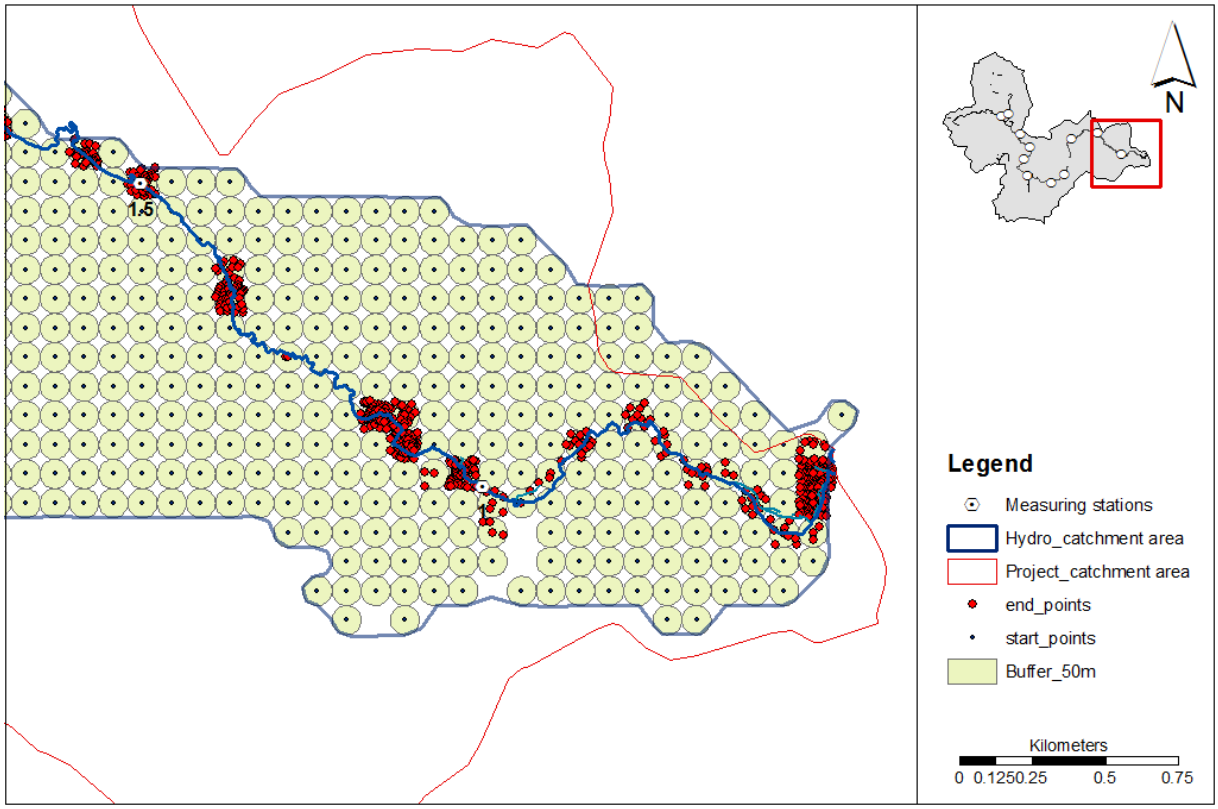

Figure 64: Illustration for hydrogeological catchment delineation (around each start point is drawn a buffer, the outer contour of the buffer zones is the catchment)

With the used method there is a little underestimation of the size of the catchment area, because the cells in GMS are rectangular 100/100m, so the hydrogeological catchment area should be with sharp edges. It was taken into account when the method was chosen that in the reality it is not likely to have sharp edges and 90 degree angles between the contributing areas and the ones that have no contribution to the groundwater formation.

Results

Catchment Areas of Lundgårds Bæk

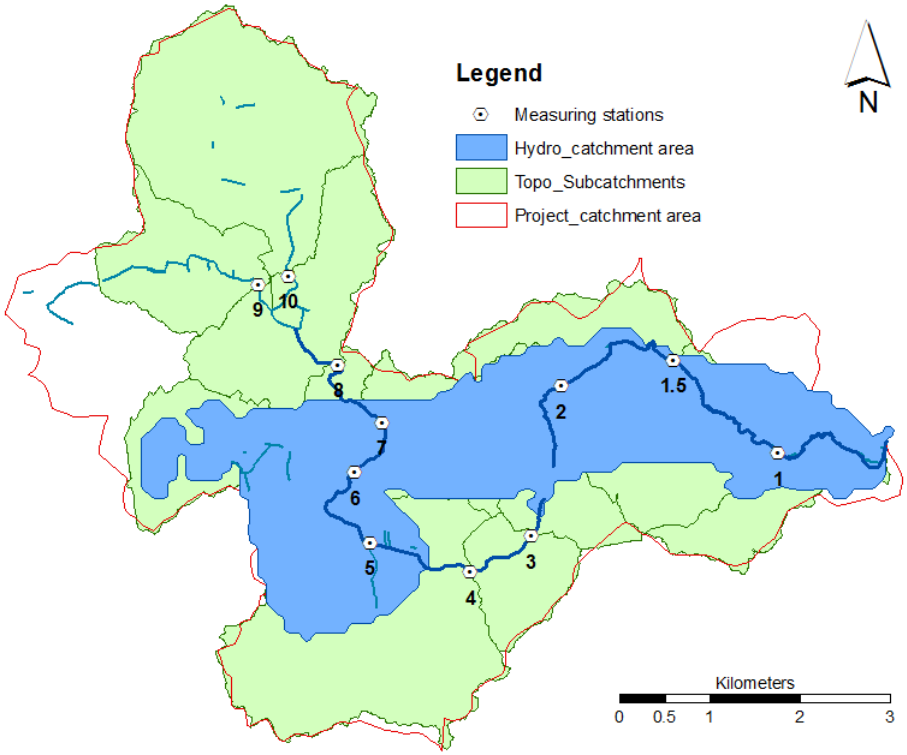

Figure 65: Project area (red contour), topographical (green)and hydrogeological (blue) catchment areas

Figure 65 shows the project area (with red contour) together with the topographical catchment area made in CatchmentSim (Catchment, 2008), and the hydrogeological catchment area based on in GMS model (NIRAS). As it was mentioned before the hydrogeological catchment is the area which contributes to the groundwater discharge to the stream. On the other hand, the topographical area is the drainage basin where the surface water joins the stream.

As it is seen on Figure 65 the hydrogeological catchment is significantly smaller than the topographical one. The areas of the different catchments are given in Table 7:

Table 7: Area of the different catchments in square kilometres

Type	Area [km^2]
Project area	35.00
Topographical catchment area	31.60
Hydrogeological catchment area	12.09

The project area is the initial, manually delineated from old map, catchment area. As it is seen the difference between the manually delineated and the digitally delineated one is 3.4km^2, which compared with the difference between the hydrogeological and the topographical area is not significant. The topographical catchment area is 2.6 times bigger than the hydrogeological catchment area.

Sub-catchment Areas

Figure 66 depicts the topographical catchment area and the different sub-catchment areas of the sampling points. Each sub-catchment is named by the sampling point to which it belongs, for instance the zone with number 1 is the catchment area of the 1st sampling point. One more point (0) was added, so the area between Villestrup Å (the place where Lundgårds bæk ends) and the st.1 is included in the sub-catchment area analysis.

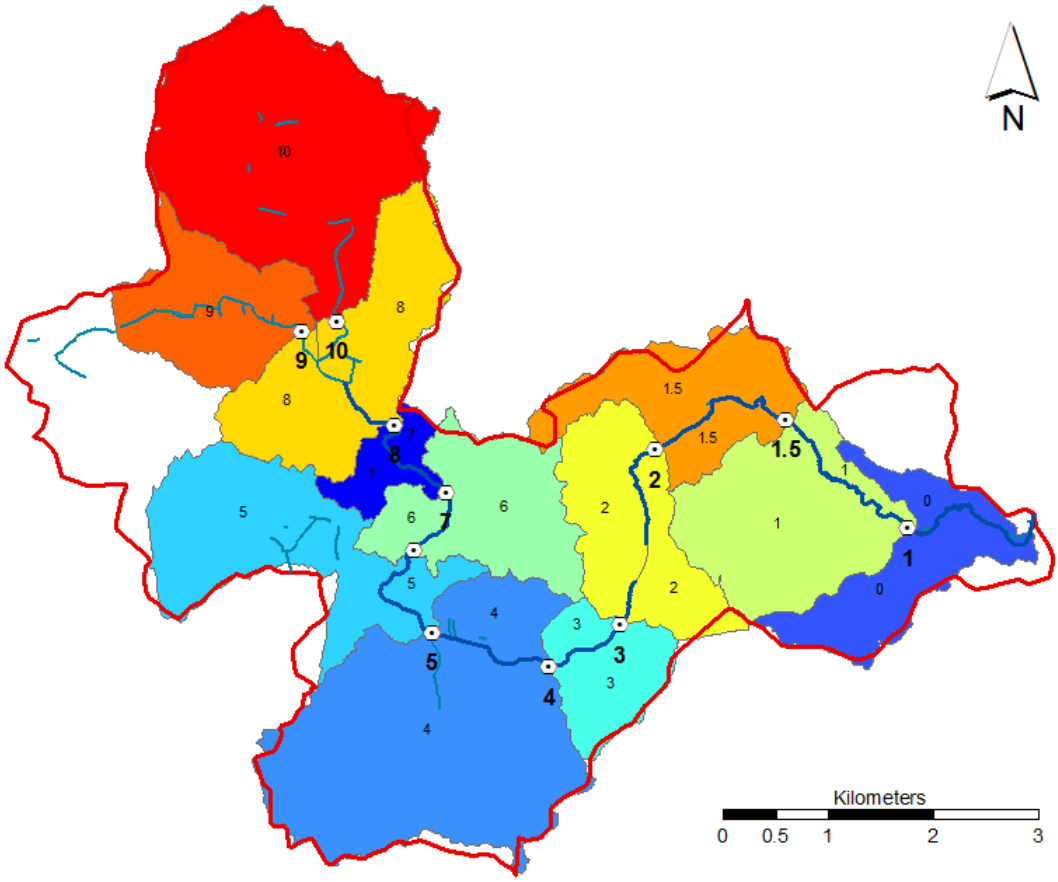

Figure 66: Topographical sub-catchment areas (the red contour shows the project area; with small numbers are given the labels of the sub-catchments of each sampling/measuring point)

The same system for labelling the sub-catchment areas is applied for the hydrogeological sub-catchments areas. The sub-catchments are presented with different colours on Figure 67. The used method of delineation is the one described earlier (see Figure 64, p.72). As it is seen on Figure 67 the sampling stations 3, 7, 8, 9, and 10 doesn't have hydrogeological catchment areas, which means that there are no flow paths ending at the stream between: st.3 and 4; around st.4; around st.8; between st.8 and st.9 /st.10 and to the beginning of the 2 first order tributaries of Lundgårds bæk. One of the differences between the topographical and the hydrogeological catchment areas is that the borders between the topographical areas are more obvious, because they represent the water divides. The hydrogeological sub-catchments are interlacing each other.

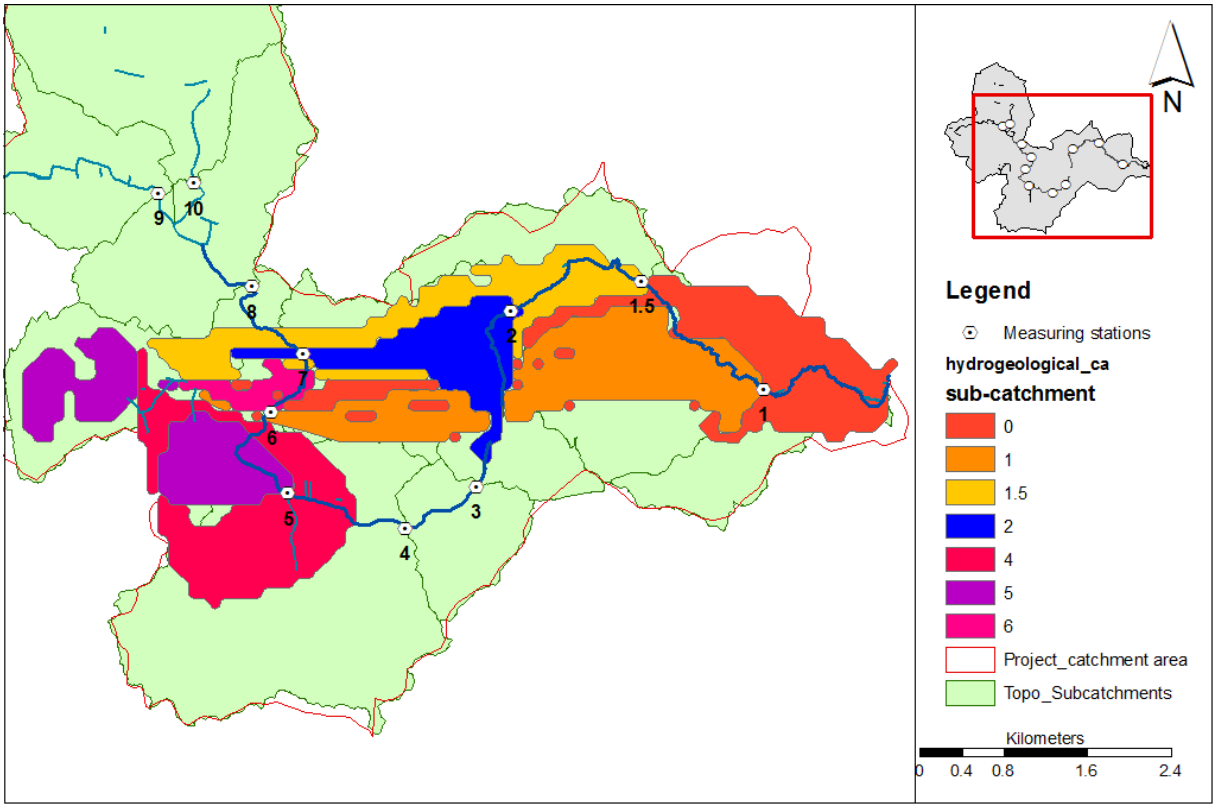

Figure 67: Hydrogeological sub-catchment areas

A comparison between the area of the hydrogeological and the topographical sub-catchments is made in order to evaluate how big the difference is and how exactly is distributed in the sub-catchment level. The results can be seen in Figure 68, where the only zone where the hydrogeological sub-catchment has a bigger area (0.57km^2 bigger) than the topographical sub-catchment is at the st.0 (the point where Lundgårds bæk ends in Villestrup Å). Then, the difference at the catchments of the st. 1 and st.1,5 is almost the same (around 0.3 km^2). The biggest difference is at the 4th zone, where the topographical area is 2.6 times bigger than the hydrogeological.

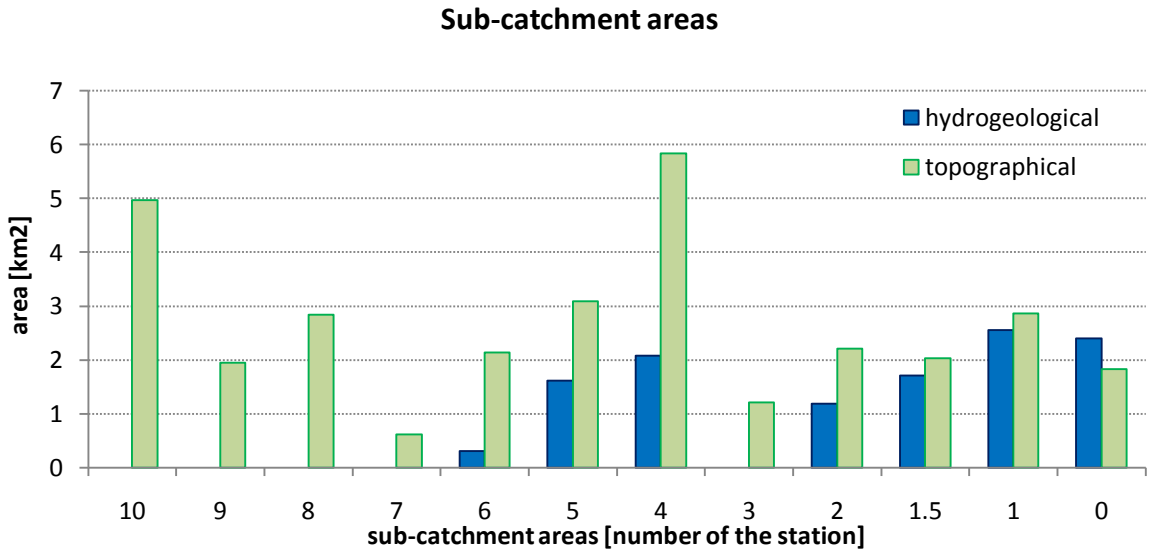

Figure 68: Comparison of the hydrogeological and topographical sub-catchments

The distribution of the area of the sub-catchments as a percentage of the whole catchment area is given on Figure 69. The biggest hydrogeological sub-catchment is the one of st.1 with 22% of the whole area, followed by st.0 with 20% and st.4 with 17%. The biggest topographical sub-catchment is the one of st. 4, followed by st.10 with 16% and st. 5 with 10%.

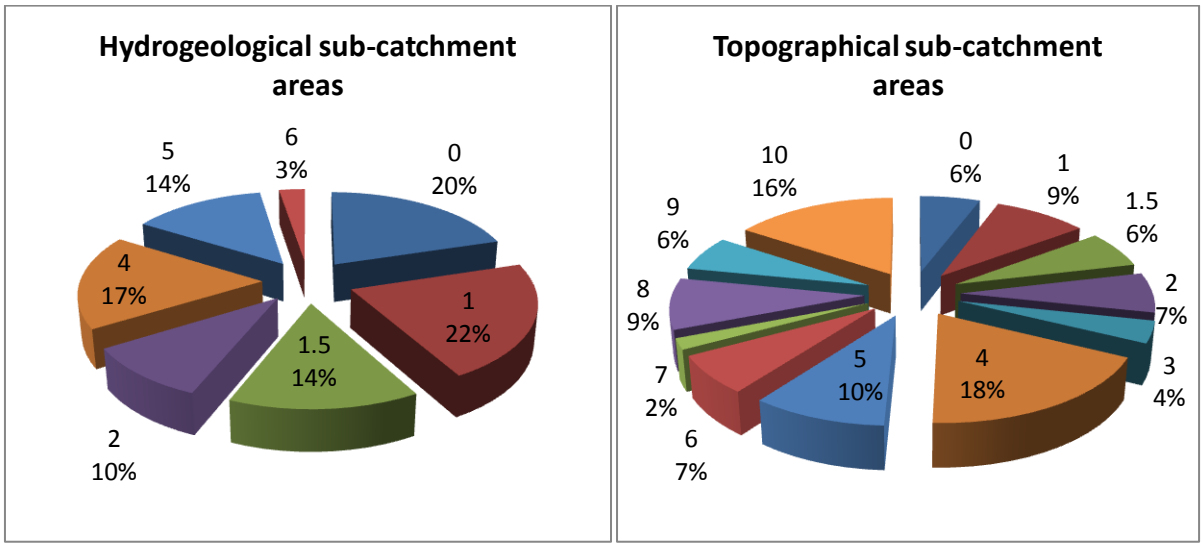

Figure 69: Area distribution of the sub-catchments as a percentage of the whole catchment area (the area label and the % are given)

Groundwater-flow Residence Time

The hydrogeological catchment with all the starting points of the flow paths which end at the stream are presented on Figure 70, showing also the travelling time of each particle to the stream. The warm colours are representing the short travelling times, or the areas which form the relatively young groundwater. For example, the red colour represents the areas from which the flow particle travels from 0 to 2 years. Opposite, the cold colours are representing the long travelling times. It is seen that the closer the area to the stream, the shorter the travelling time, in general. For more detailed view of the residence times, maps for each sub-catchment are given in “Appendix: Residence Times” (p.171).

In order to analyse the similarities and differences between the sub-catchment areas in respect to the residence time of the groundwater flow-particles, the distribution of the particles to groups with different time period for each sub-catchment is plotted (see Figure 71). The groundwater flow particles, starting from each sub-catchment, are distributed in 4 groups of particles which are travelling:

- from 0 to 2 years;
- from 2 to 10 years;
- from 10 to 25;
- and above 25 years before they reach the stream.

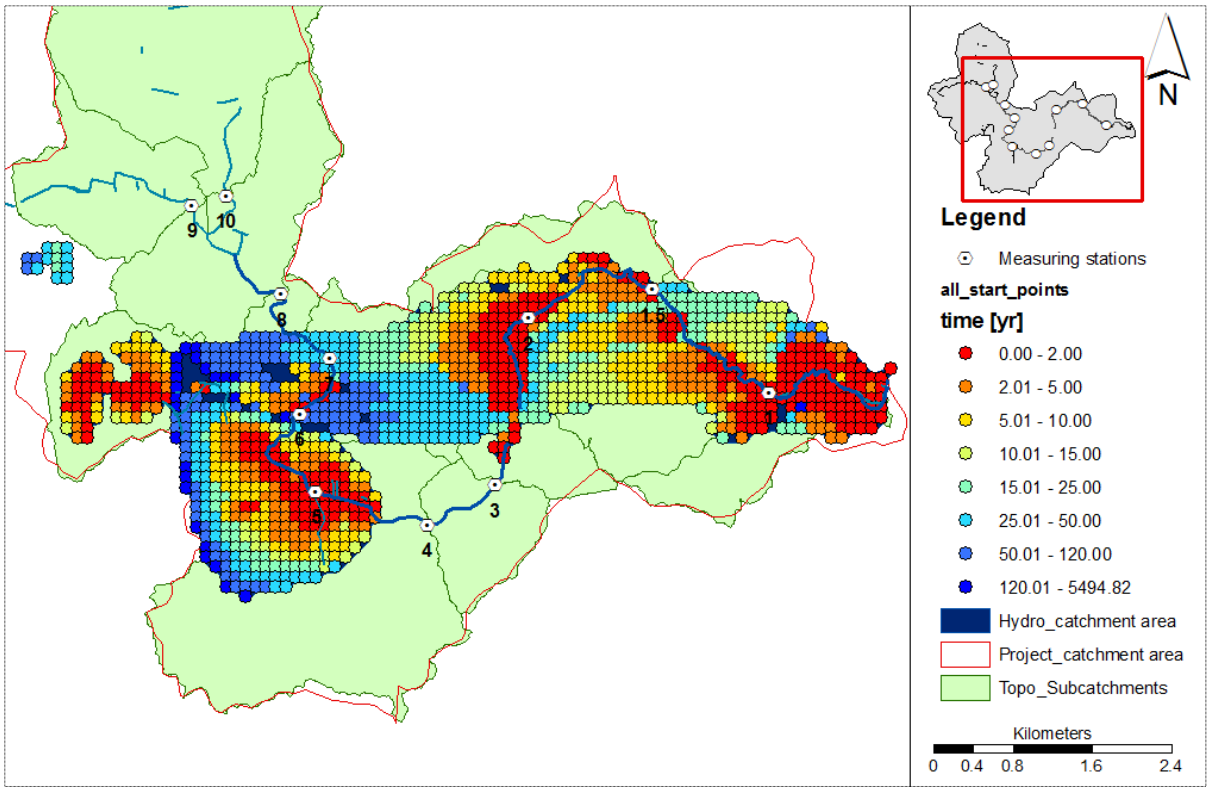

Figure 70: Residence times of the groundwater flow

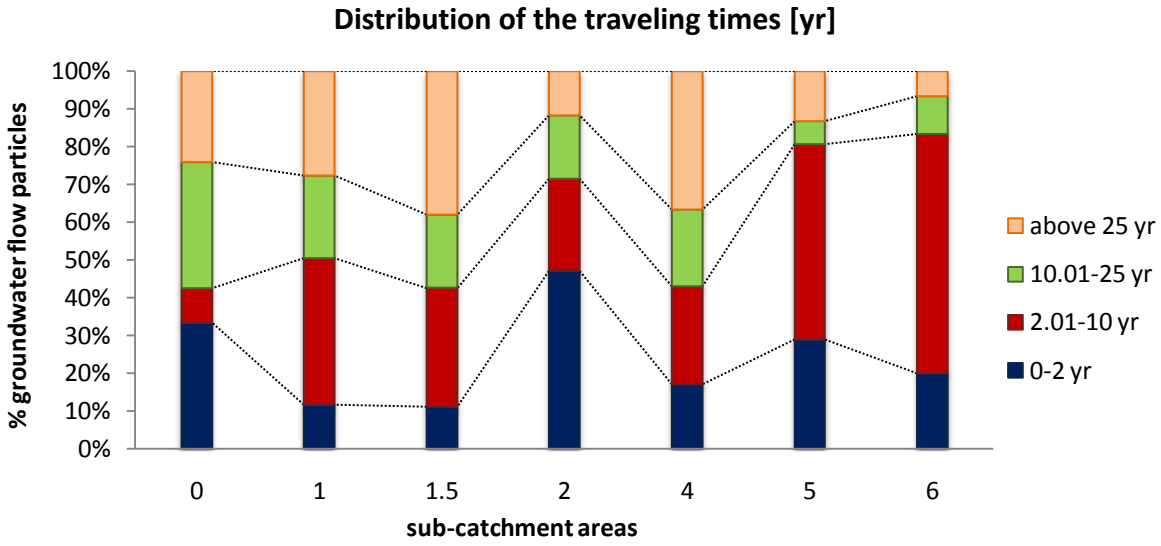

Figure 71: Distribution of the groundwater flow particles in respect to their travelling time to the stream for each hydrogeological sub-catchment

A couple of observations can be made based on Figure 71:

- the zones with **shortest travelling times** for the groundwater are the sub-catchment of st.0 and st.2, with respectively 33.33% and 47.06% of the particles of that zones ending at the stream after 0 to 2 years. The difference between these two sub-catchments is that the one of st.0 has almost equal amount of particles ending at the stream for 0 to 2 years and for 10

to 25 years, but the group 2 to 10 years is not so much present, whereas that is not the case with st.2, where there is no big domination between the 3 left groups (2-10, 10-25, above25).

- the sub-catchments of st.5 and st.6 look alike: more than half of the particles (respectively, 51.81% and 63.33%) travel between 2 and 10 years before they reach the stream;
- for the group 10 to 25 years, the sub-catchment of st.0 is represented with 33.33%, followed by the sub-catchments of st.1, 1.5, 2, and 4, which have between 16% and 22% of the particles travelling in this time interval.
- the zones with the longest travelling times are the sub-catchments of st. 1,5 and st.4 with respectively 38.01% and 36.59% of the particles of that zones travelling more than 25 years before they reach the stream.

Figure 72 illustrates the listed above observations about how the groundwater flow particle travelling times are distributed for each of the hydrogeological sub-catchment areas:

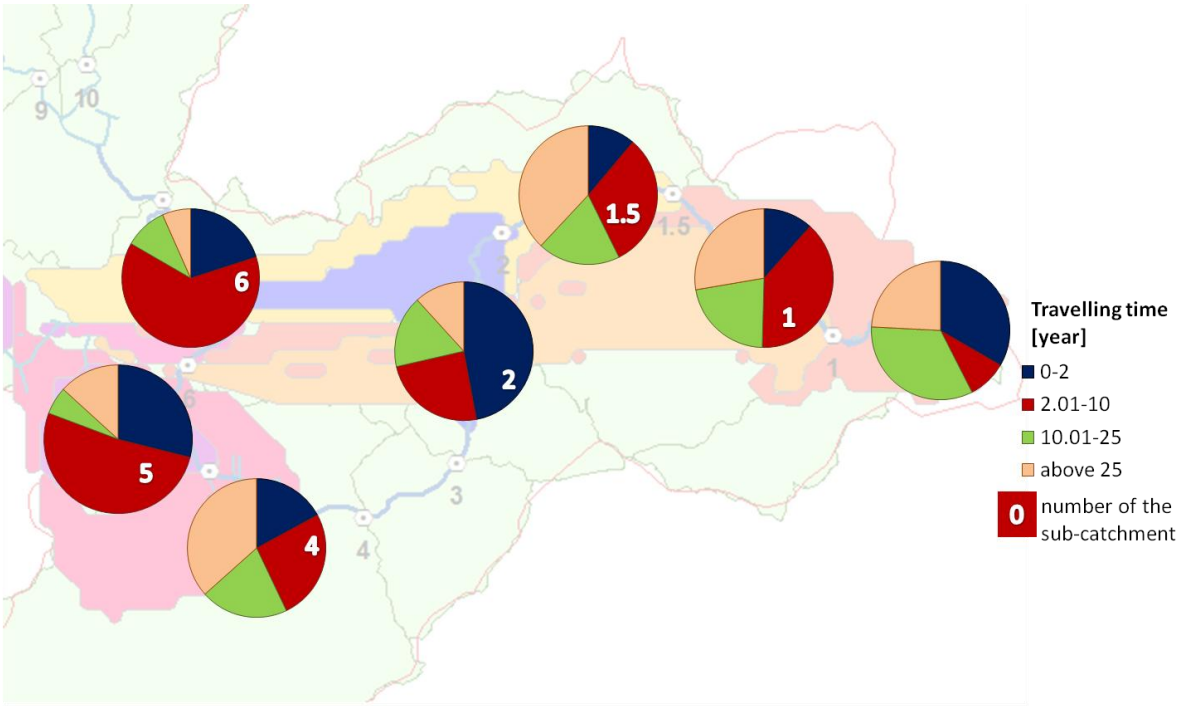

Figure 72: Illustration of the groundwater flow particles travelling times for each hydrogeological sub-catchment zone

G. Estimation of the Nitrate Leaching from the Sub-catchment Areas

Introduction

The purpose of this part of the project is to estimate how much NO_3^--N leaches from the root zone to the groundwater for each of the topographical sub-catchment areas for one year. Weighted averages of the NO_3^--N leaching from each sub-catchment are calculated. The following calculations are made for the topographical sub-catchment areas, because in that way the leaching to the sub-surface (shallow) groundwater is also included.

Method

To be able to estimate NO_3^--N leaching for a year from the sub-catchment areas of Lundgårds bæk is used combination of different methods. A step-by-step explanation of the used procedure follows.

Leaching from the Agricultural Areas

As a base for the analysis, the GIS theme providing with information about the NO_3^--N leaching [kg N/ha] from the root zone for 2008 is used (Figure 29, p.40). To be able to estimate how much is the leaching from each sub-catchment, first, this theme is spatially joined to the GIS theme of the topographical sub-catchment areas. Then, all agricultural parcels in the borders of one sub-catchment are grouped together (see Figure 73)

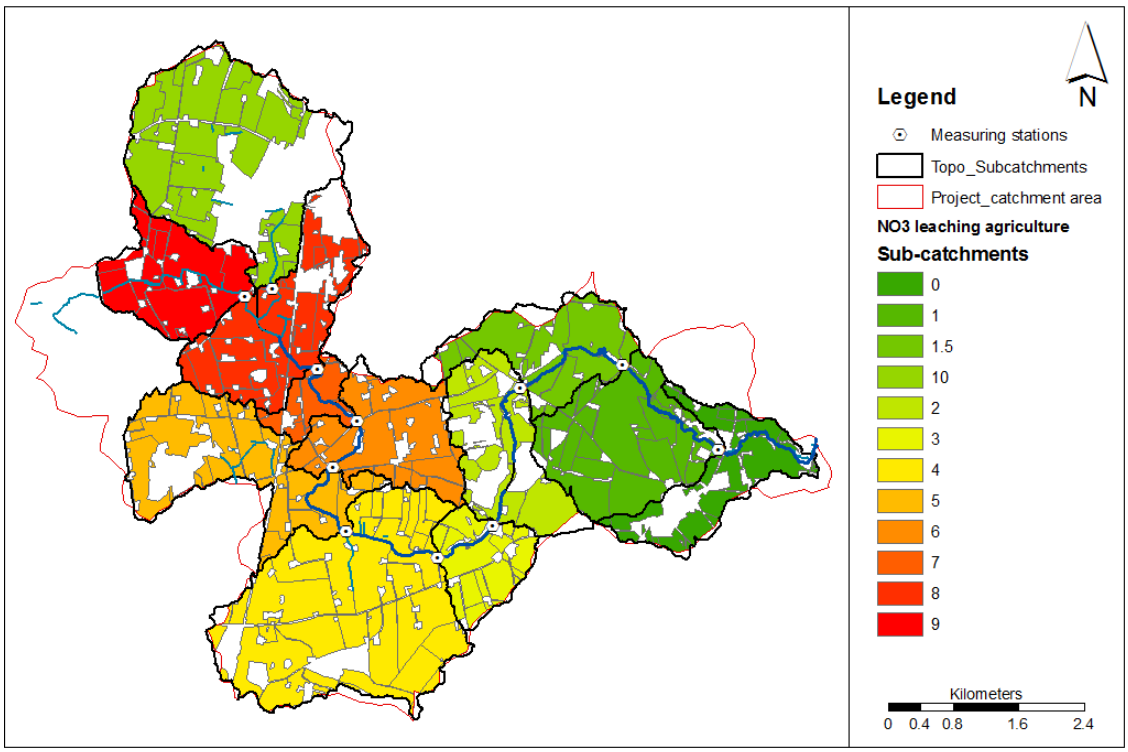

Figure 73: NO_3-N leaching from the root zone: agricultural parcels, grouped to each sub-catchment area

As the purpose is to estimate the total NO_3^--N leaching from sub-catchment area, there is a need to include the NO_3^--N leaching from non agricultural sources or with other words: to fill the white gaps from Figure 73.

Leaching from Non-agricultural Land

As there is no GIS information about the leaching from non-agricultural sources present, there are 2 main issues to be discussed. First, what kind of non-agricultural areas are there, and second, how much NO_3^--N leaches from the different areas. To be able to solve the first problem, the modified GIS theme for the leaching from agricultural land (Figure 73) is spatially joined with the landuse theme (Figure 24, p.36). In that way the "white gaps" from Figure 73 are filled (see Figure 74) and also the information about each parcel is saved in the same attribute table.

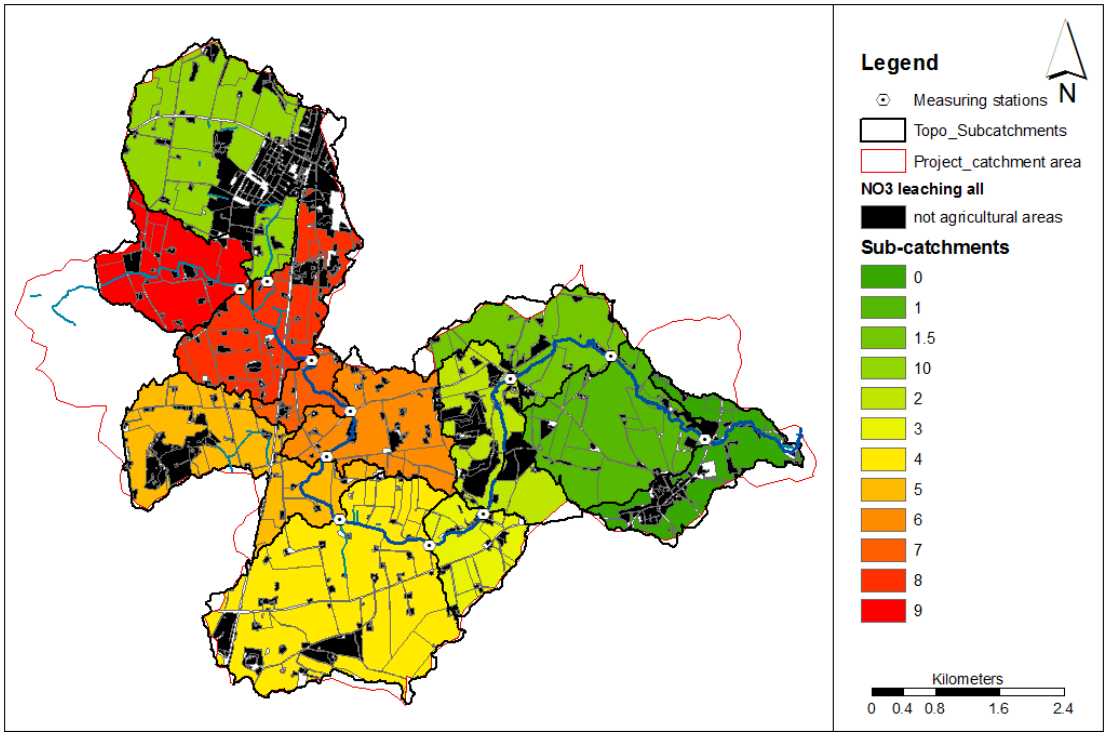

Figure 74: Filling the gaps of the agricultural leaching theme with the non-agricultural parcels

After the joining is possible to evaluate and compare the sub-catchment areas in respect to the land use (see Figure 75).

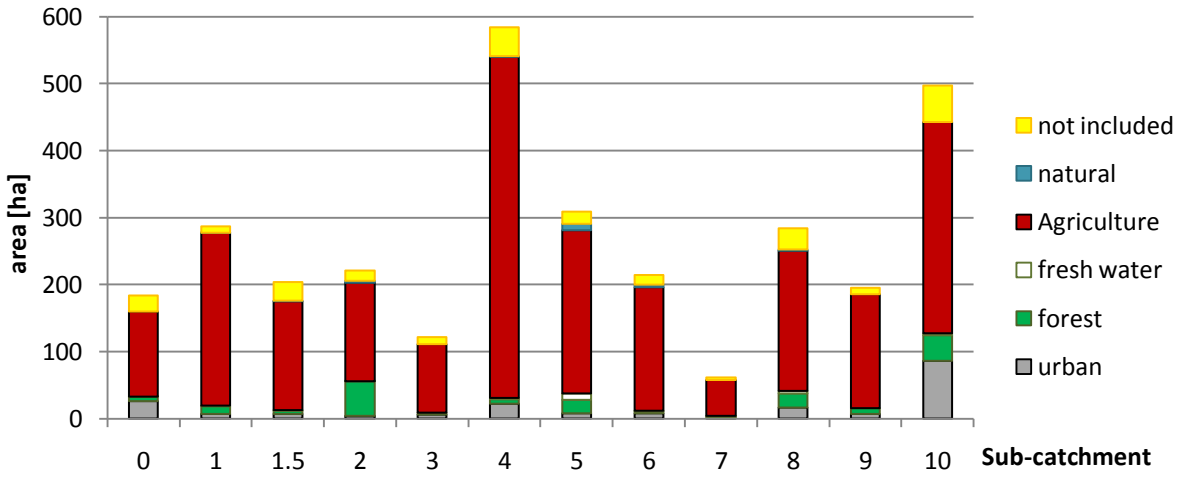

Figure 75: Landuse for each sub-catchment area

A distinction is made between 5 different landuse types: natural areas; agricultural areas; fresh water; forests; and urban areas. Even after the followed procedure there are some areas, which aren't included in the analysis (yellow on Figure 75). These not included areas are: the roads in the sub-catchment; the difference between the project area and the topographical sub-catchment (the extend of the project area doesn't include the whole topographic sub-catchment in some places); and the very few areas without specified landuse type.

Because there was no information found about the NO_3^--N leaching from non-agricultural areas for the Lundgårds bæk catchment for 2008 present, literature sources are used. Detailed explanation of the chosen values and the used studies are presented in "Appendix: Non-agricultural Sources for Nitrate Leaching", p.181. The values for NO_3^--N leaching from non-agricultural sources to the groundwater, presented in Table 8, are used further in the calculations of the weighted average and total leaching from the root zone.

Table 8 Used values for NO3-N leaching from the different areas and reason (see "Appendix: Non-agricultural Sources for Nitrate Leaching", p.181, for further explanations)

Type of area	NO3-N [kg/ha/yr]	source
Agriculture	Different for each parcel	see Figure 29, p.40
Fresh water	0	see Chapter B, p.13
Forests	5.00	(Callesen et al., 1999)
Natural	5.00	assumed to be like in "forests"
Urban	21.00	(Wakida & Lerner, 2005)

Not only the values are from different sources, but also the used methods for estimating them and the periods of time are different. It should be remarked that the following calculation for the weighted average leaching and total leaching from each sub-catchment can be used only for orientation or for initial step of one more precise and preventative study.

Weighted Average Leaching and Total Leaching for Each Sub-catchment Area

It is decided to calculate weighted averages (instead of the arithmetic ones) because in that manor the size of the parcel will be taken into account and it will result in a more realistic value.

Following equation is used to calculate the weighted average leaching for each sub-catchment area:

$$WANL = \frac{\sum_{i=1}^{n}(A_i.NL_i)}{\sum_{i=1}^{n} A_i} = \frac{(A_1.NL_1 + A_2.NL_2 + \cdots + A_n.NL_n)}{(A_1 + A_2 + \cdots + A_n)}$$

were:

- $WANL$ is the weighted average for the NO_3^--N leaching for each sub-catchment area for a year [kgN/ha/yr];
- A_i is the area of each parcel, where i is the index for the number of the parcel [ha];
- NL_i is the NO_3^--N leaching from each parcel, where i is the index for the number of the parcel [kgN/yr];

Next to the weighted average leaching, the total leaching for one year for each sub-catchment is calculated. To calculate those values, the following equation is used:

$$TNL = \frac{\sum_{i=1}^{n} NL_i}{1000}$$

where:

- $TNL$is the total NO_3^--N leaching from each sub-catchment for one year [tonN/yr]
- NL_i is the NO_3^--N leaching from each parcel, where i is the index for the number of the parcel [kgN/yr]

Results

After the explained above procedure is used, the weighted average NO_3^--N leaching is calculated for each sub-catchment area and the results are presented in Figure 76:

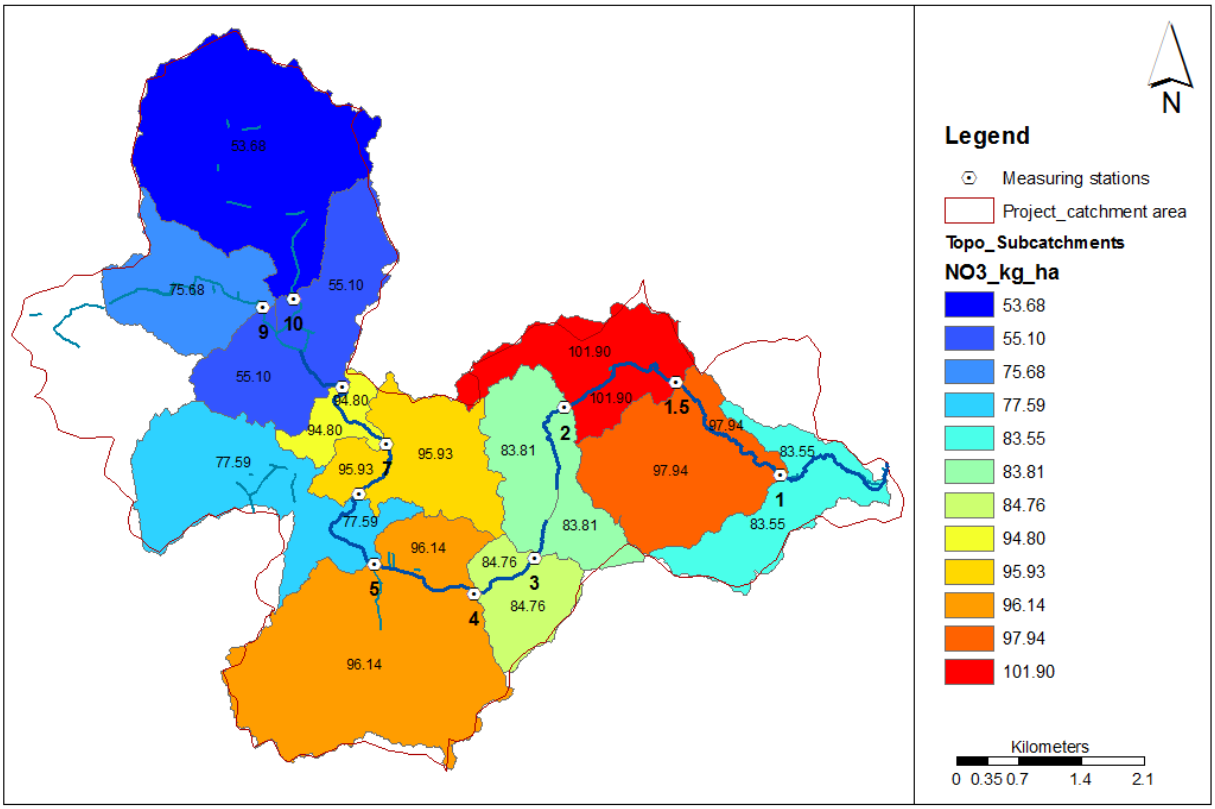

Figure 76: Weighted average of the leaching NO3-N for each topographic sub-catchment (kgN/ha for year)

From Figure 76 is seen that the sub-catchment area of st.1,5 is with the highest NO_3^--N leaching (101.90kg N/ha), followed by the sub-catchments of st.1 (97.94 kg N/ha) and st.4 (96.14kg N/ha). The areas with average NO_3^--N leaching above 80kg N/ha are the sub-catchments of st.0, st.2, st.3, st.6, and st.7. The lowest leaching is from the sub-catchment of st.10 – 53.68kg N/ha. It can be explained with the relatively big non-agricultural area. The result for this sub-catchment area gives a good example for the importance to include the non-agricultural sources, when the NO_3^--N leaching is evaluated on a catchment scale.

As addition the total NO_3^--N leaching for each sub-catchment is calculated and the results are presented in Figure 77:

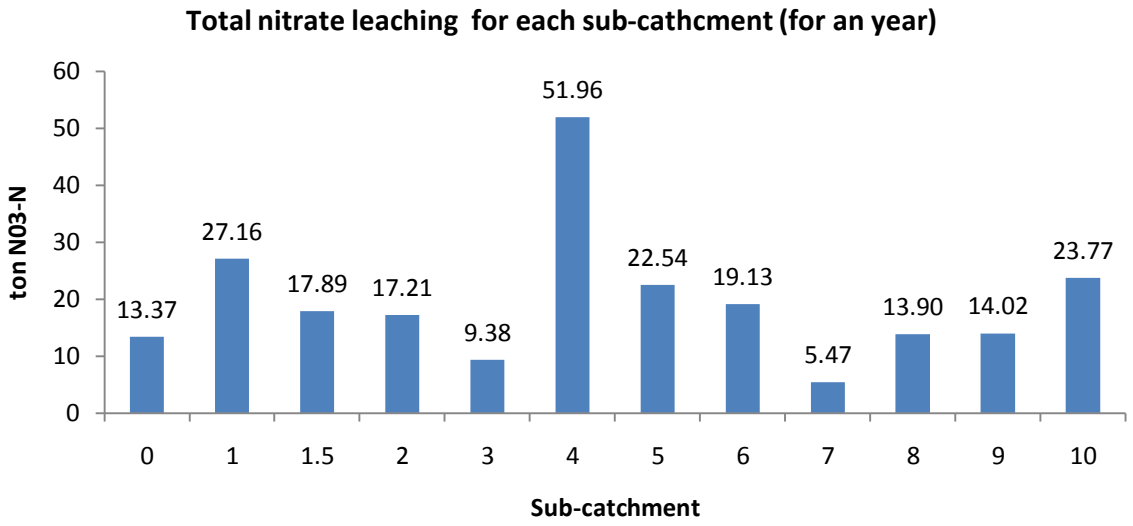

Figure 77: Total NO_3-N leaching from each sub-catchment area for an year, [t N/yr]

The total leaching shouldn't be used independently, without taking into account the area of the sub-catchment. The bigger the sub-catchment area is, the bigger the leaching from this area is. The relationship between the total leaching and the area is presented in Figure 78:

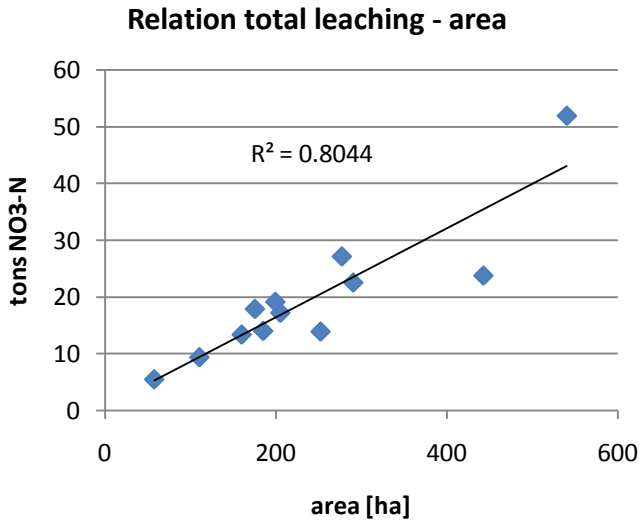

Figure 78: Relation between the total NO_3-N leaching and the area of the sub-catchment

As it is seen from Figure 78, the correlation between the total leaching and the area of the sub-catchments is very strong (R^2=0.8044) as it should be. The R^2 is influenced of the differences in the landuse of each sub-catchment. If the land-use was the same the R^2 should have been 1.

[empty page]

H. Application of Two Methods, Found in Literature Sources, for Estimating Reduction Capacities

Application of the Dahl's GSI Typology as a Tool for Estimating the Reduction Capacities of the Riparian Zone for the Sub-catchment Areas

Introduction

The Dahl's groundwater-surface water interaction typology (GSI) is a way to conceptualize the real system in order to evaluate the risk or to assess the status of the dependent eco-systems. The GSI typology with its three levels is presented as part of Chapter B on p.32. The application of the typology, however, could be a time-consuming task if initially there is not enough data for the target catchment. Moreover, the proper application of the typology is very much dependant on the skills and the knowledge of the person who makes the analysis, because it is not always obvious which type of interactions are present and the data can be interpreted differently. Two reports give guidance for applying the typology by the Danish Nature agencies: the (Hinsby & Dahl, 2010) gives a GSI mapping guidance, and (Dahl et al., 2010) gives the procedure step-by-step. These guidances have been more or less followed in the project, as the purpose was to getter as much information about the catchment area as possible.

The riparian hydrogeological types (2nd level GSI typology) may be used as a basis for evaluating the eco-hydrological interactions and further as a tool to delineate the riparian zones, receiving a NO_3^- free- or polluted groundwater. The riparian flow types assist with the evaluation of the denitrification capacities of the catchment areas.(Dahl et al., 2007)

The GSI typology can be used as a tool providing the frame when a comparison between different catchment areas is needed; however, the process of GSI typology application is not a straight forward process when already established rules can be followed. As (Dahl et al., 2007) are concluding in their review, there is a need of developing methods to estimate the flow path distribution through the riparian zones, as this controls the quality of the groundwater passing through them. A combination of methods for evaluation on the different scales is also needed. This requires broad knowledge in different areas: geology, microbiology, hydrology etc.

An attempt to apply the GSI typology on the catchment area of Lundgårds bæk as a step forward to the risk assessment and the land-use management of the area has been made in this part of the project.

Critical Sub-catchments

As initial step of the analysis (Hinsby & Dahl, 2010) suggest that a screening sampling for NO_3^- concentrations in the watershed should be done, preferable in the winter, when the highest concentrations are expected to be found. The authors separate the sub-catchments to critical and not-critical, based on the measured NO_3^- concentrations in the receiving waters. According to them, if the NO_3^- concentration exceeds 10mg/l (converted to NO_3^--N concentration is 2.3mgN/l), then there is need for applying an NO_3^- reduction measures in that sub-catchment area. For this purpose, the results from the sampling for each station from December 2010 and February 2011 are combined and the sub-catchment areas where a concentration lower than 2.3mgN/l is measured are considered critical and the ones with concentrations above 2.3mg/l are considered not critical. There

are also 2 sub-catchments for which there should be a warning: the sub-catchment of st.10, because the difference between the measured concentrations from the two sampling sessions is too big (1.29 and 6.01mgN/l); and the sub-catchment of st. 5, where the measured concentrations are just above the 2.3mgN/l border, so it might be considered that this is caused by the inaccuracy of the method. The critical area delineation is presented in Figure 79:

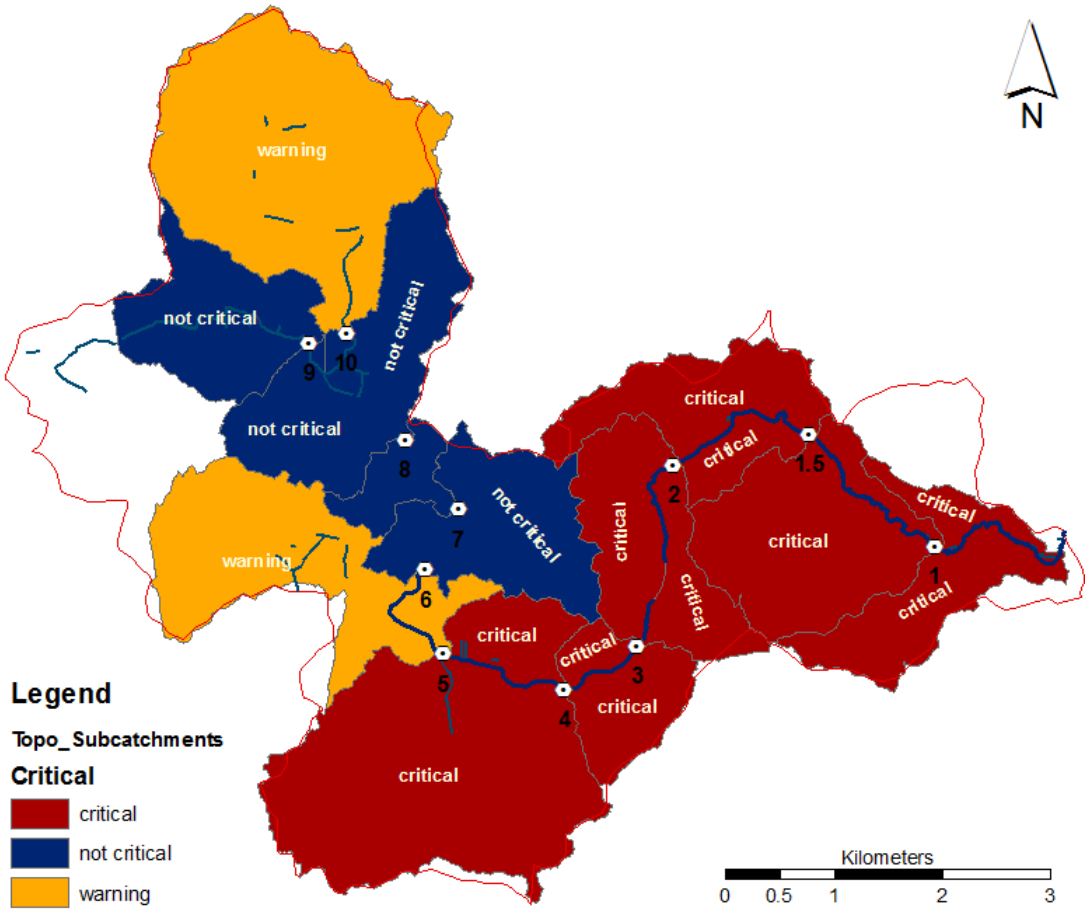

Figure 79: Critical areas (where NO_3^--N and NO_2^-- N concentrations exceed 2.3mg/l)

The meaning of this separation is that in the "blue" areas (Figure 79) there is no need for further action, which could be more sampling or applying a NO_3^- reducing measures (without specifying what kind of measures). For the sub-catchment area of st.10, maybe samples should have been taken more times or other factors should be also included in the evaluation. For sub-catchment 5, there might not be need for any reduction measures, but the confidence interval of the sampling method should be checked. All the "red" areas should be further evaluated (according to the guidance procedure) and that is what it was done in the field observation (Chapter E, p.59).

GSI 2nd Level: Riparian Hydrogeological Types

The riparian hydrogeological types are presented in Chapter B, p.32. The delineation is based on the topographical sub-catchment areas. For applying the typology, knowledge based on:

- the results from the GMS model (hydrogeological sub-catchments and travelling times),
- the field observations and measurements,
- and the understanding about the geology of the area is used.

The different riparian hydrogeological types presented in the catchment area of Lundgårds bæk are given in Figure 80, where also the GSI codes are used. Further explanation about the GSI codes can be found in the Chapter B, p.33.

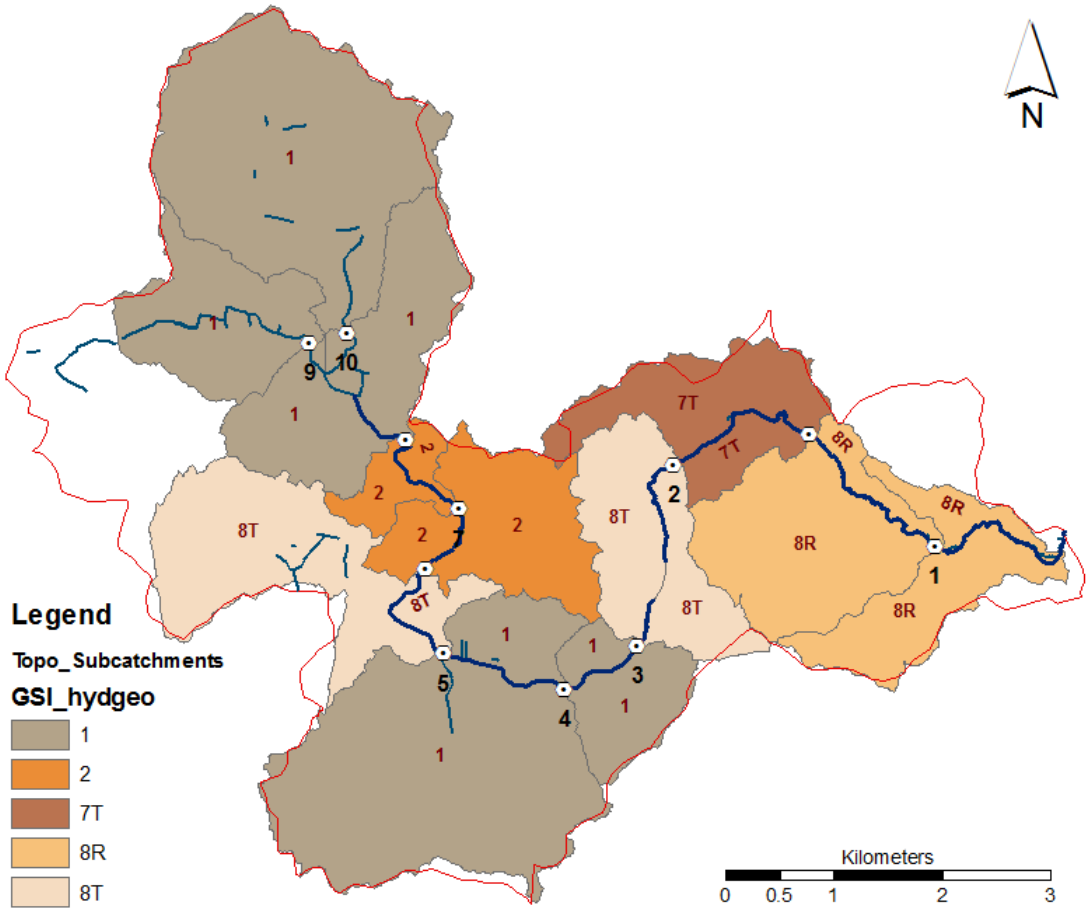

Figure 80: GSI typology, 2nd level: riparian hydrogeological types (1 – runoff/surface; 2 – disconnected; 7T – unconfined, side, local groundwater body; 8T – unconfined, local groundwater body; 8R – unconfined, regional groundwater body)

As it is seen from Figure 80 the sub-catchments of st.0 and 1 are receiving a groundwater from a regional groundwater body. In this case "regional" is used in the meaning that the groundwater recharge might be not in the vicinity of the stream, or it is assumed to be the "deeper" and "older" groundwater. The catchment area of st.1.5 is chosen to be 7T, because most probably there is some groundwater discharge from the local groundwater body (in the winter observations, a groundwater source wasn't found, but the soil in the riparian areas was frozen), but it is not as much as in the previous two zones and is more than in the sub-catchments 5, 6, 7. The sub-catchment of st.2 is chosen to be 8T, because it is assumed that the groundwater body is different from the one in sub-catchments 0 and 1, but still some groundwater springs were found in the area. For the sub-catchments of 6, and 7 the 2nd type (disconnected) was chosen. Since actually the stream is losing in this area, but this is not included as a possibility in the typology. The sub-catchment of st.5 is chosen to be the same type as the one for st.5, because the GMS model was showing quite a lot of groundwater discharging to the lake in the area. It is believed that the lake is connected to the stream by pipe, so the typology was applied based on the lake groundwater-surface water interactions.

a more detailed study on the geology of each of the sub-catchment areas should have been made for more representative results for this level of the typology. For instance, hydrogeological profiles for each sub-catchment areas can be drawn and based on them the typology could be applied in a better way. This wasn't part of this master thesis, so the result is based on the interpretation of the field observations (Chapter E, p.59).

GSI 3rd Level: Riparian Flow Path Types

The GSI typology distinguishes between 4 types of riparian flow path-types: diffuse, overland, direct, and drainage. More explanations about them are given in the Chapter B, p. 28. For applying the typology, the data from the field observations and measurements is used (Chapter E). Especially helpful for finding the zones, where a diffuse flow is present was the use of thermo-imaging. Based on Figure 60 (p.67), the 3rd level of GSI is made and presented in Figure 81:

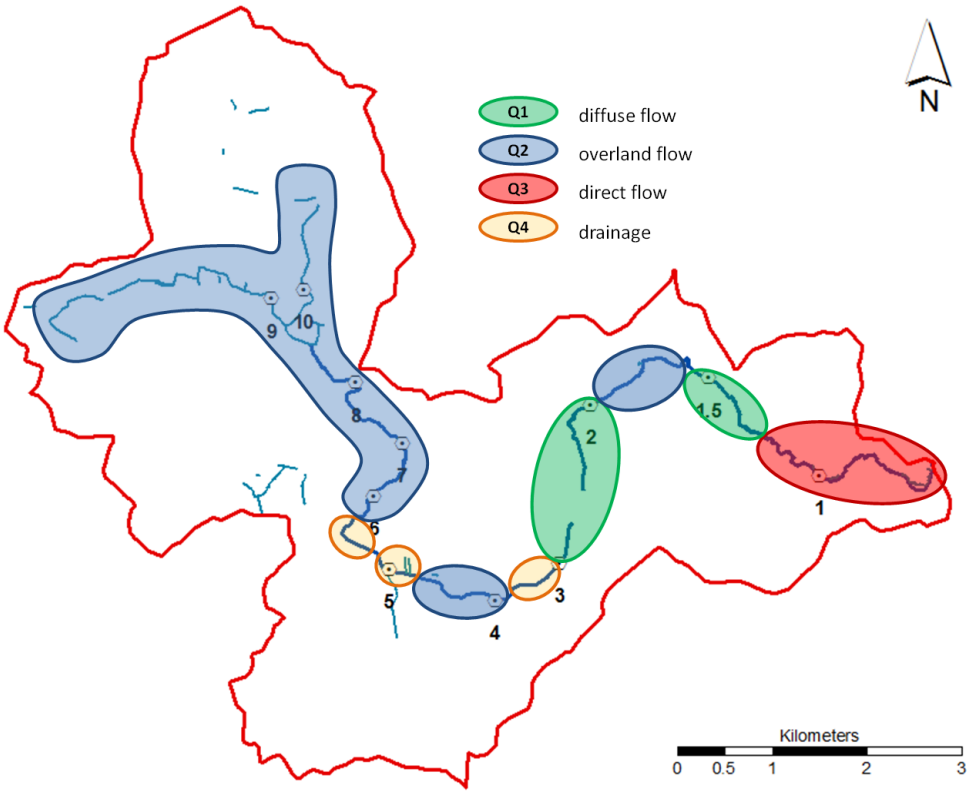

Figure 81: GSI typology, 3rd level: Riparian flow path types (Q1 – diffuse flow; Q2 – overland flow; Q3 – direct flow; Q4 – drainage)

Figure 81 shows the different zones, with the dominating type of flow. Between st.2 and st.3 there were also some direct flow observed, but the dominating type was the diffusive groundwater flow. Between st.3 and 4 the drain pipes were mapped as part of the field observation, but at st.5 and close to st.6 – it is assumed that there the dominating type of flow is the drainage. (see Appendix: Field Observations and Thermo Imaging, p.155)

After Dahl's GSI typology was applied for Lundgårds bæk, some conclusions about reduction capacities of the riparian zones can be made based on (Dahl et al., 2007).

Reduction Capacities of the Riparian Zone (Based on Dahl's GSI Typology)

The GSI typology gives the opportunity to determine the reduction capacities of the riparian zones in the catchment area. However, the method is quite simplified and should be used only as part of initial screening. The factors which are taken into account are: 1) the riparian flow type; 2) the organic matter content and for some cases 3) the interaction with the organic deposits (see Figure 82).

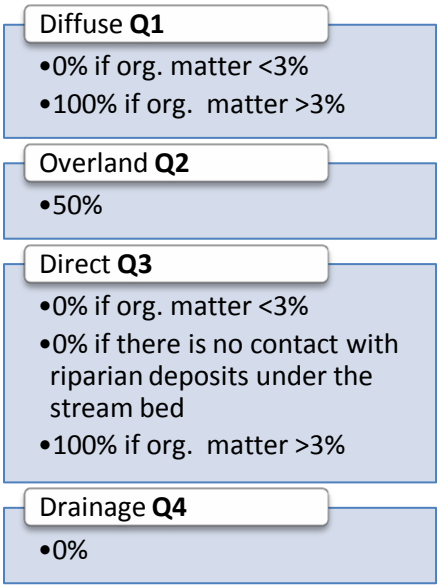

Figure 82: Methodology for determining the reduction capacities of the riparian zone

The result of the application of the methodology from Figure 82 is presented in Figure 83:

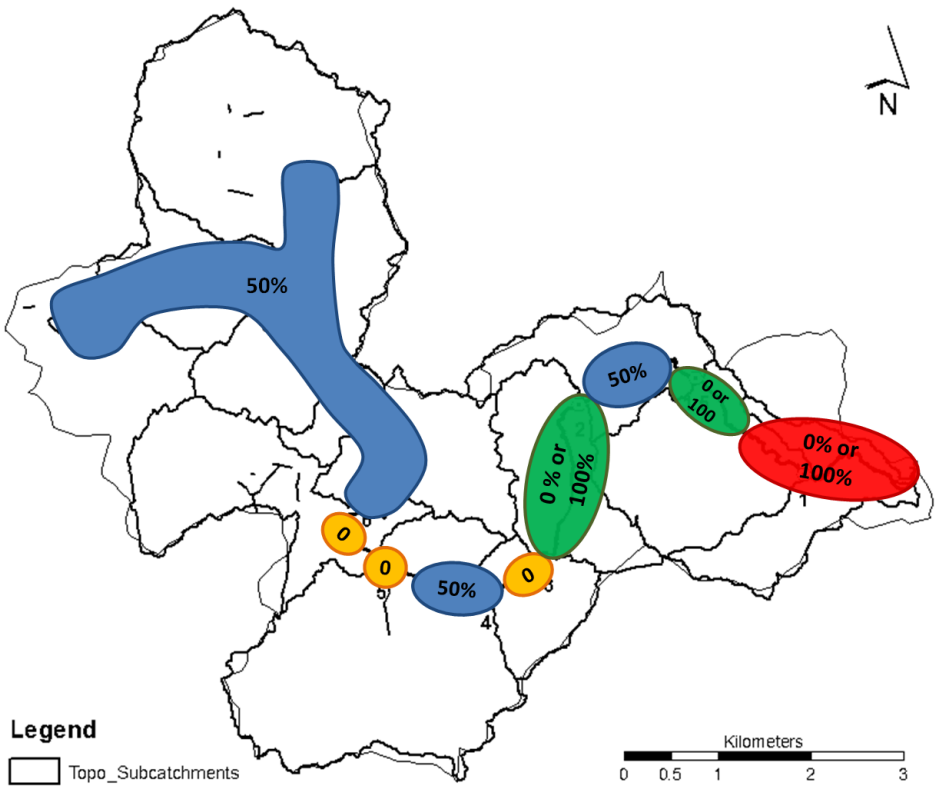

Figure 83: GSI typology: reduction capacities of the riparian zone

As it is seen for Q1 and Q3 there is need to know the organic content of the soil in the riparian zone to be able to determine the reduction capacity. On Figure 83, the green areas are with dominating diffuse flow, and as it is seen from Figure 168 (p.179) there is organic soil resent, so the reduction capacity of the riparian zone in this part should be 100%. For the red zone (Figure 83), based on the field observations, it is assumed that there is no contact between the groundwater and the organic sediment, so the reduction capacity according to Dahl's GSI typology should be 0%. It should be remarked that in the typology is not specified what is meant by using the term "riparian zone". It is not distinguished between the size of the riparian zone or the type. According to the understanding about the term, riparian zone is the undisturbed natural land in the stream valley, which has both the characteristics of the terrestrial and aquatic environment. In some parts of the catchment area there are wetlands in the stream valley (see Figure 167, p.178), but in other parts there is almost no buffer zone between the agricultural land and the stream. This shortcoming of Dahl's GSI typology can be essential for the estimation of the reduction capacities on a sub-catchment level.

In the next part another attempt to conceptualise the system and to estimate the NO3-N reduction capacities of the riparian zone is presented, by taking into account the landscape.

Application of the Vidon & Hill Conceptual Model as a Tool for Estimating the Reduction Capacities of the Riparian Zones for the Sub-catchment Areas

Introduction

A conceptual model of the riparian zones has been developed, which links the landscape hydrogeological characteristics to the riparian groundwater hydrology and to the NO_3^- removal efficiency of the riparian zone(Vidon & Hill, 2006). The result of the application of this conceptual model is to estimate how wide should be the riparian buffer zone in order to remove 90% of the NO_3. More about the conceptual frame can be found in Chapter B on p.30.

According to the understanding for riparian zone (Chapter B, p.23), the stream valley in its whole width has the potential to be a riparian zone of the stream. However, the riparian zone is only the undisturbed (natural) part of it. In the small catchment area of Lundgårds bæk the most of the land in the stream valley is used for agricultural purposes (see Table 9). Thus, the riparian zone is the part, which includes the 2m buffer (see below Table 9 for further explanation) and the natural areas, which represents 14.40% of the stream valley. Maps with the stream valley can be found in "Appendix: Stream Valley Characteristics".

Table 9: Stream valley area

	Area [ha]	% from the project area
Stream valley, from which:	181.68	5.19
- forests/natural areas (actual riparian zone)	21.65	0.62
- agricultural land	155.51	4.44
- 2m buffer	4.52	0.13

According to the Danish legislation (from 1992) there should be a 2 meters buffer zone from the upper edge of the stream bed, where agricultural activities are not allowed (see Figure 84).

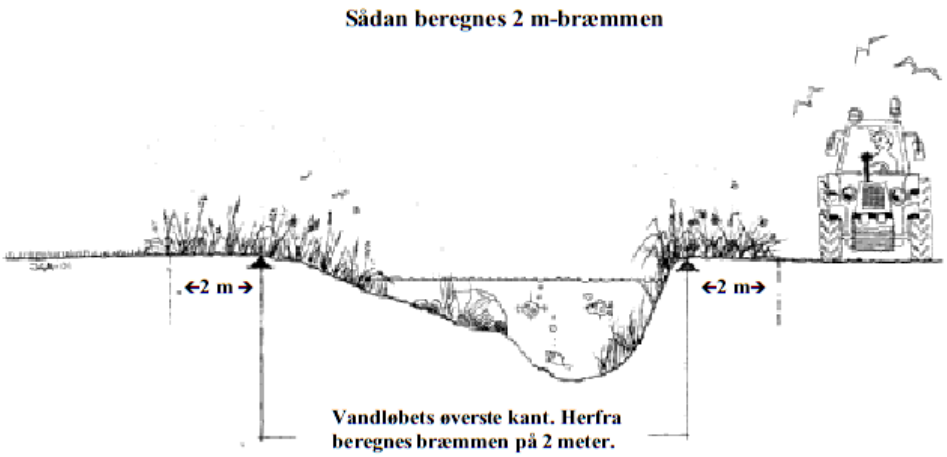

Figure 84: Scheme of the 2m buffer zone according to Danish legislation (Miljøministeriet, 2002)

In that manner, by law it is guaranteed that the riparian zone in agricultural land should be not less than 2m from the upper edge of the banks.

Even though, there is a legal buffer established, not everywhere in the catchment area of Lundgårds bæk a buffer of 2m from the edge to the agricultural land is found. It can be interesting to research if the 2m buffer is enough to ensure N removal and to what extent.

The results of applying (Vidon & Hill, 2006) conceptual model of the removal efficiency are presented further.

Needed Width of the Riparian Buffer Zone for 90% Removal of the Nitrate Removal

According to (Vidon & Hill, 2006) if the slope is from 0 to 5% (which is the case with Lundgårds bæk) then for 90% NO_3^- removal, the riparian buffer zone should be:

- <20m if the depth of the permeable sediments is 1-2m;
- >20m if the depth of permeable sediments is above 2m and the soil is coarse sand and gravel;

The soil texture in the stream valley (see Figure 168, p.179) is mostly humus (organic soil), fine sand and loamy sand, so the needed buffer for 90% NO_3^- removal is less than 20m. Still, the soil in the area between st.3 and st.6 is mainly coarse sand, so in that part the buffer zone should be bigger than 20m.

From Figure 85 can be seen that the stream valley is almost everywhere with width more than 20m. This means that, if this stream valley was not used for agricultural purposes, then the riparian zone would have the capacity to reduce 90% of the NO_3^-. However, at the present moment only 14.4% from the stream valley are having the conditions of a riparian zone.

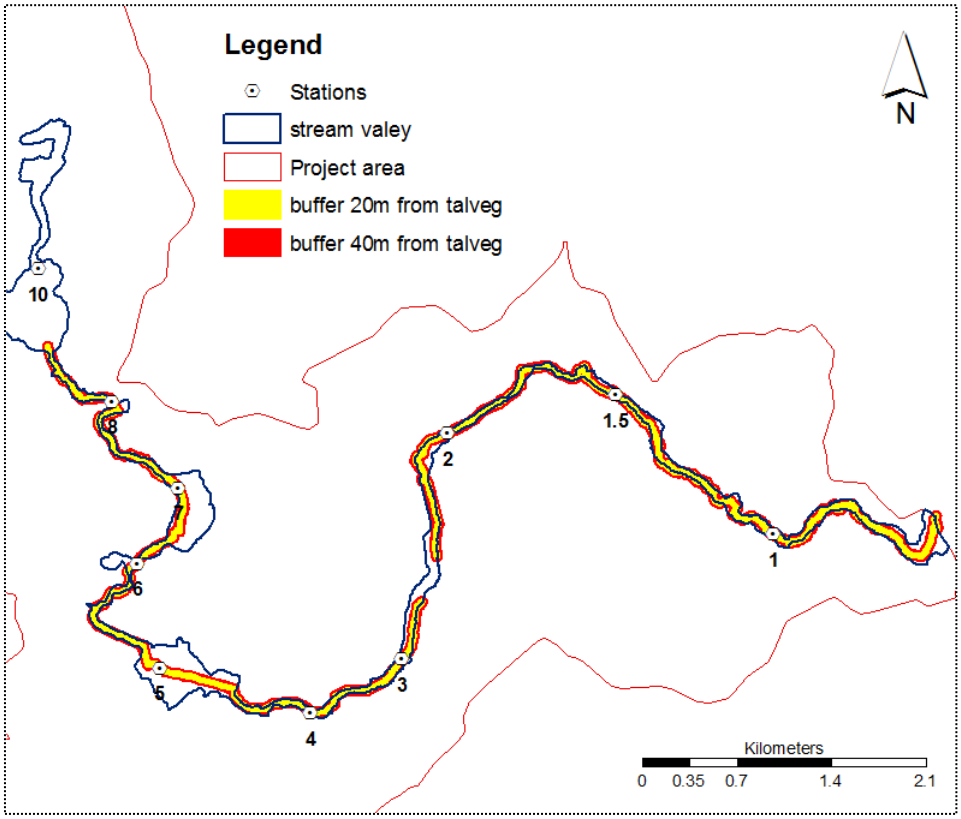

Figure 85: Map presenting the stream valley together with the 20m and 40m buffer zones

If the stream valley was a natural area everywhere, not only there would be 90% NO_3^- removal, but also there would be less NO_3^- leaching to the stream. As it is seen from Table 10, the total leaching from the stream valley is 13579 kgN/yr, but if the land use in the stream valley is changed – then the total leaching would be 908kgN/yr, or this is 93% less than the amount leaching in the present moment from that part of the catchment area.

Table 10: Total leaching from the stream valley

	Total leaching at the present [kgN/yr]	**Total leaching stream valley = natural area [kgN/yr]**
Stream valley, from which:	13579	908
- forests/natural areas (actual riparian zone)	108	108
- agricultural land (Figure 169, p.179)	13449	778
- 2m buffer (natural area, p.81)	23	23

To calculate the leaching from the 2m buffer zone, 5kg N/ha leaching (p.81) is used, but if the values from the GIS theme (Figure 169, p.179) are used, then the leaching from the 2m buffer is 449kg N/yr.

As it was mentioned before, there are some places, where even the 2m buffer zone is not present. On Figure 86 it is presented a map with the 2m, 20m, and 40m buffers drawn in GIS from the thalweg of the stream together with example of two parcels, where the 2m buffer from the upper edge of the stream valley are not present.

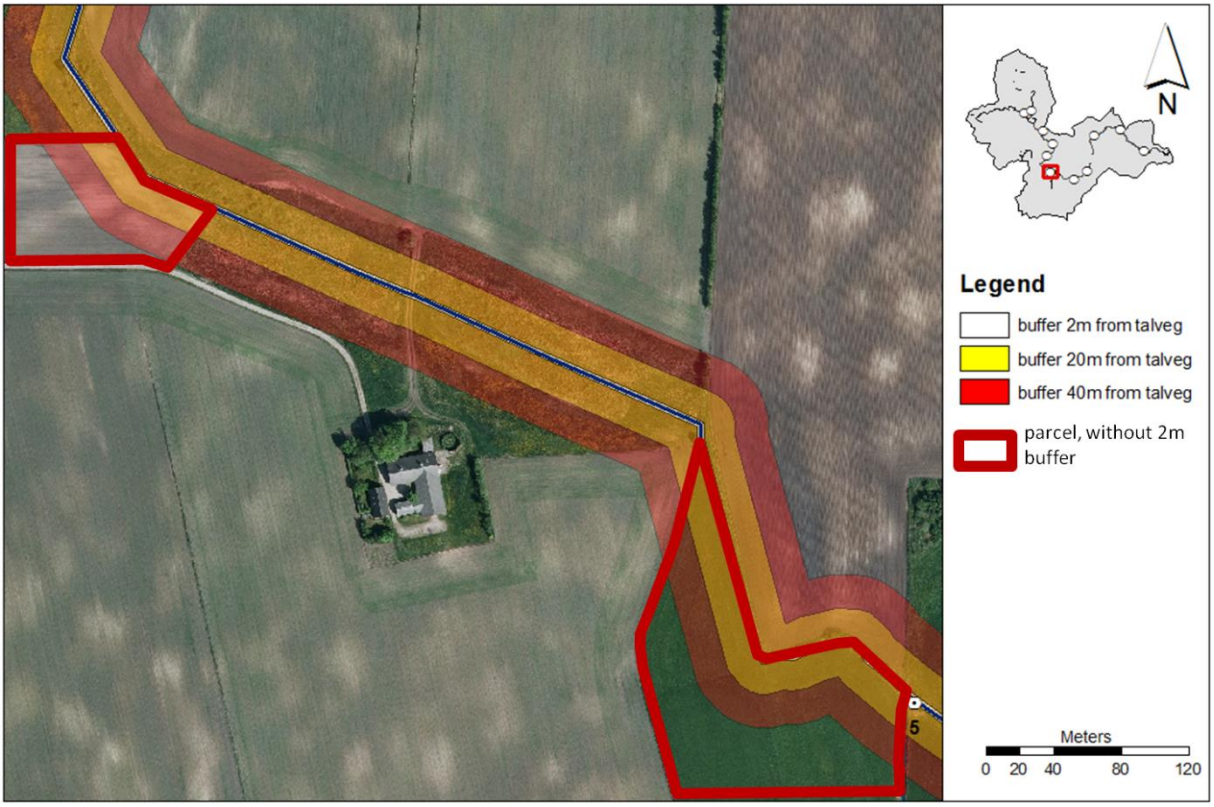

Figure 86: Map, showing the 2, 20, and 40m buffer zone, together with two parcels, where even 2m buffer is not present

Conclusion

Both of the two presented systems for conceptualising the groundwater-surface water interactions as a tool to estimate reduction capacities have shortcomings. However, they can be used together so more representative results are gathered. For example, the 20m buffer zone rule can be applied only in the areas, where the reduction capacities from Dahl's typology are 0%. Further, research should be made in order to find if the rule for the 2m buffer zone is 1) followed, and 2) good enough to ensure NO_3^- removal in the rates proposed from (Vidon & Hill, 2006) and (Dahl et al., 2007).

In the next part it is made an attempt to develop a new methodology for estimating reduction capacities on a sub-catchment scale.

[empty page]

I. Reduction Capacity on Sub-catchment Scale

Introduction

The purpose of this part of the project is to develop a methodology for building a reduction map on a sub-catchment level. Further the methodology is used for calculating the reduction capacities of each sub-catchment area of Lundgårds bæk. A thorough explanation of used method is presented below.

Method

The used method for calculating the NO_3^- reduction capacity of the system (catchment area/sub-catchment area) is a mass balance: what comes in the system minus what goes out of the system equals the reduction happening in the system (see Figure 87). With the following method all the processes, which could be reducing NO_3^- concentrations in one or another part of the catchment area are grouped together in one "reduction capacity" value for the whole catchment (sub-catchment) area. With this method the system and the processes have been simplified and the results should be carefully used, keeping in mind all the assumptions, which were made during the process.

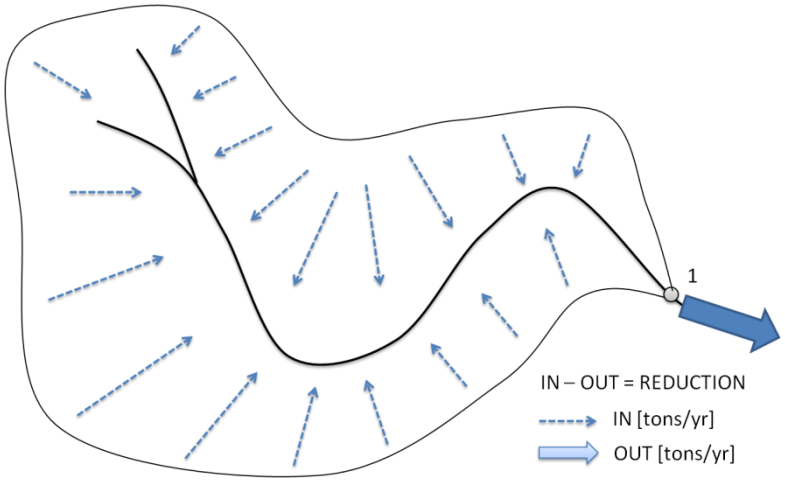

Figure 87: Mass-balance scheme on a catchment scale)

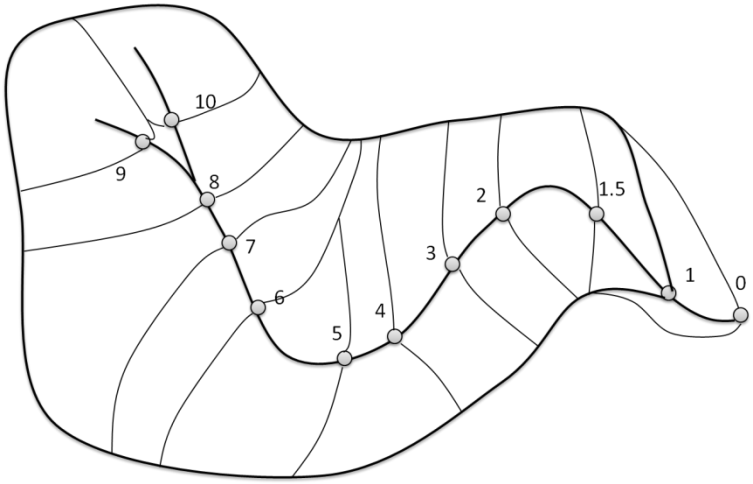

Figure 88: Dividing the catchment area to sub-catchments

As the idea is to get a reduction capacity value for each sub-catchment area, the system is divided to 12 connected sub-systems and the mass balance is made for each of the areas (see Figure 88).

The delineation of the sub-catchment areas is presented in Chapter F (p.69), where an explanation about the method is also given.

The reduction capacities are further calculated for each sub-catchment by applying a mass balance method for each of the areas, starting from the sub-catchments 9 and 10, where the stream begins. Some explanations about the mass-balance of the areas are given further.

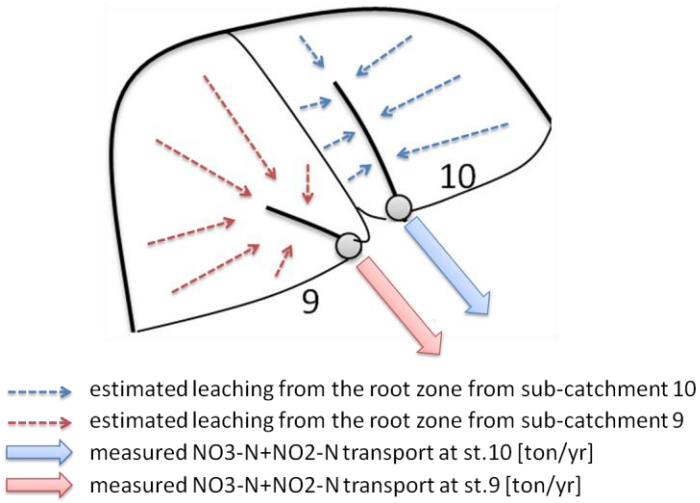

Figure 89: Mass-balance scheme for sub-catchment 9 and sub-catchment 10

Figure 89 presents schematically the mass-balance for sub-catchments 9 and 10. The reduction capacity for those 2 areas is calculated by applying the equation:

$$RED_{(9\ or\ 10)} = EL_{(9\ or\ 10)} - NO3L_{(9\ or\ 10)}$$

where:

- $RED_{(9\ or\ 10)}$ is the reduction capacity of sub-catchment 9 or sub-catchment 10 [tons N/yr]
- $EL_{(9\ or\ 10)}$ is the estimated leaching from the root zone from sub-catchment area 9 or 10 [tons N/yr]
- $NO3L_{(9\ or\ 10)}$ is the NO_3^--N and NO_2^--N load calculated from the measurements of the concentration and the flow rate at the st.9 or st.10 [tons N/yr]

The mass balance for sub-catchment area 8 is schematically presented on Figure 90 and the reduction capacity is calculated with the equation:

$$RED_{(8)} = NO3L_{(9)} + NO3L_{(10)} + EL_{(8)} - NO3L_{(8)}$$

where:

- $RED_{(8)}$ is the reduction capacity of sub-catchment 8 [tons N/yr]
- $EL_{(8)}$ is the estimated leaching from the root zone from sub-catchment area 8 [tons N/yr] (in the mass-balance as part of "IN")
- $NO3L_{(8)}$ is the NO_3^--N and NO_2^--N load calculated from the measurements of the concentration and the flow rate at the st.8 [tons N/yr] (in the mass-balance as part of "OUT")

- $NO3L_{(9)}$ is the NO_3^--N and NO_2^--N load calculated from the measurements of the concentration and the flow rate at the st.9 [tons N/yr] (in the mass-balance as part of "IN")
- $NO3L_{(10)}$ is the NO_3^--N and NO_2^--N load calculated from the measurements of the concentration and the flow rate at the st.10 [tonsN/yr] (in the mass-balance as part of "IN"

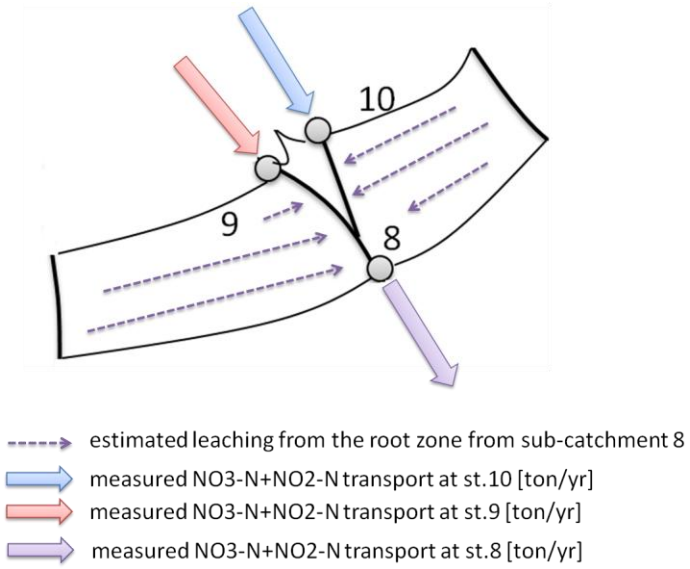

Figure 90: Mass-balance scheme for sub-catchment 8

The rest of the sub-catchment areas have similar mass-balance schemes, so only one is presented as an example (see Figure 91).

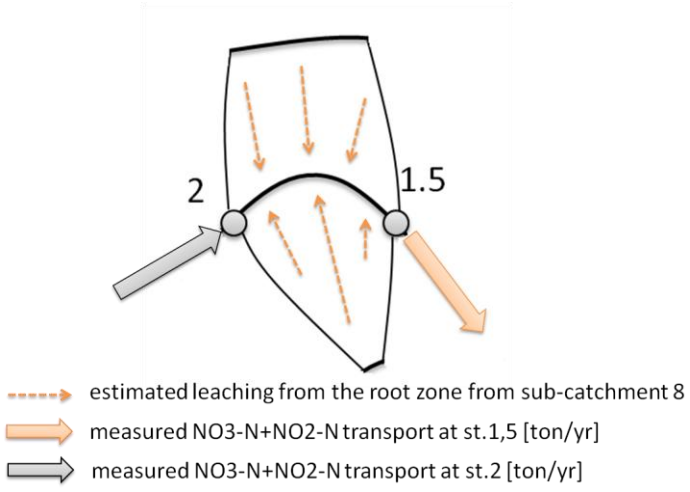

Figure 91: Mass-balance scheme for "standard" sub-catchment (sub-catchment 1,5)

The reduction capacity of the "standard" areas can be calculated analogically by using the equation for sub-catchment 1,5, given below:

$$RED_{(1.5)} = NO3L_{(2)} + EL_{(1.5)} - NO3L_{(1.5)}$$

where:

- $RED_{(1.5)}$ is the reduction capacity of sub-catchment 1,5 [tons N/yr]

- $EL_{(1.5)}$ the estimated leaching from the root zone from sub-catchment area 1,5 [tons N/yr] ("IN")
- $NO3L_{(1.5)}$ is the NO_3^--N and NO_2^--N load calculated from the measurements of the concentration and the flow rate at the st.1,5 [tons N/yr] ("OUT")
- $NO3L_{(2)}$ is the NO_3^--N and NO_2^--N load calculated from the measurements of the concentration and the flow rate at the st.2 [tons N/yr] ("IN")

As input data in the mass balance are used following data:

- **Total leaching from each sub-catchment, corrected for the "lag" time**. The explanations about the method and the results for the total leaching are presented in Chapter G (p.79). Further some corrections are made, see the explanations bellow.
- **NO_3^--N and NO_2^--N transport in the stream (load)**, calculated from the measured NO_3^--N and NO_2^--N concentrations and flow rate at each station (see p.99).

Correction Coefficients

In order to be able to "compare" the leaching from the area (based on the data for 2008) with the transport of the stream (calculated for the winter of 2010/2011) it should be taken into account that there is a delay in the response of the system and also that there was a trend for lowering the leaching in the past (see Chapter 35, p.36).

For being able to come up with correction coefficients, the age of the water/NO_3^- should have been investigated, so it is possible to calculate how long the delay in the response of the system is. Because this hasn't been part of the project, two main assumptions have been made:

1. The trend of fertiliser application is the same as the one for LOOP2 (Figure 26 and Figure 27, p.38).
2. The proportions of the different travelling times, calculated with GMS for the hydrogeological sub-catchment areas, are the same as the ones of the topographical sub-catchment areas. (Figure 71, p.77, and Figure 72, p.78). For the sub-catchment areas, where there is no hydrogeological sub-catchment area it is assumed that there is only "young" groundwater, so no correction is applied.

Based on these two assumptions the groundwater and respectively the leached NO_3^- amounts are divided in 3 groups for each sub-catchment area and for each of these 3 groups a different correction coefficient is applied. Those groups represent the travelling time of the modelled groundwater flow particles, or with other words, the age of the ground water transporting the NO_3^-. And if the logic of "as far it is the recharge area from the stream, as long is the travelling time of the groundwater/ NO_3^- particles to the stream" can be applied, these 3 coefficients give also a spatial correction to the used input data. Thus, the $EL_{(i)}$ can be calculated by applying the equation:

$$EL_{(i)} = \sum EL_{(i)j} \,.\, k_j = k_1 . EL_{(i)1} + k_2 . EL_{(i)2} + k_1 . EL_{(i)3}$$

where:

- $EL_{(i)}$ is the corrected total leaching from the root zone of sub-catchment (i), where $i = 1, 1.5, 2, 3, 4, 5, 6, 7, 8, 9, 10$
- $EL_{(i)1}$ is the part of the leached NO_3-N from the first age group etc.
- k_1 is the correction coefficient for the first group etc.

The calculation sheet with more explanations is presented in "Appendix: Correction Coefficients Calculations" (p.183). The calculated correction coefficients can be seen in Table 11:

Table 11: Calculated values for the correction coefficients

Correction coefficient	Value [-]
k_1	1.00
k_2	1.35
k_3	1.88

Nitrate-N and Nitrite-N Transport in the Stream (load)

The calculations for the transport are based on the measurements of the flow and the concentration, measured as part of this project (Chapter E). The data from the measurements in December 2010 and February 2011 are used and the results for the transport are presented in Figure 92:

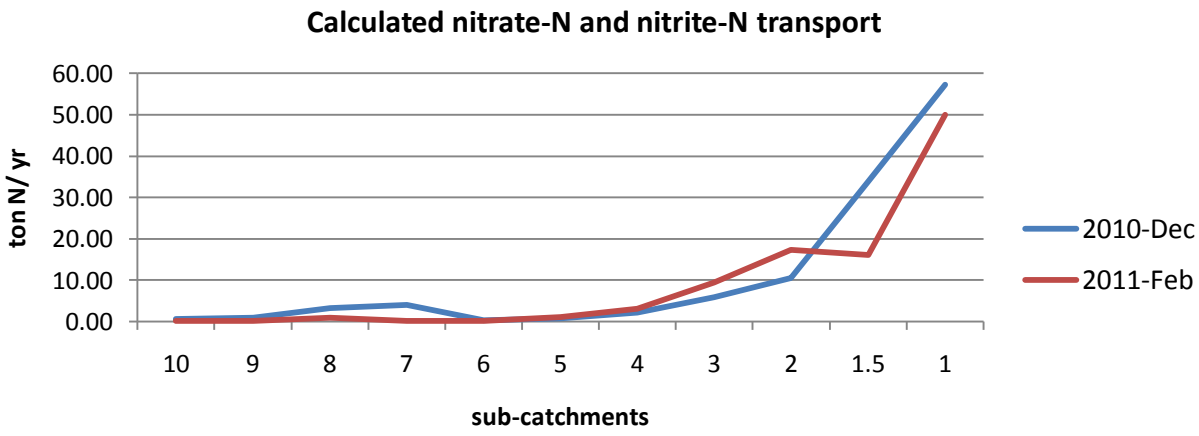

Figure 92: Calculated NO_3^--N and NO_2^--N in for each station for December 2010 and February 2011

For the purposes of the mass-balance calculations, an average from those two sets of values is calculated and is presented in Figure 93:

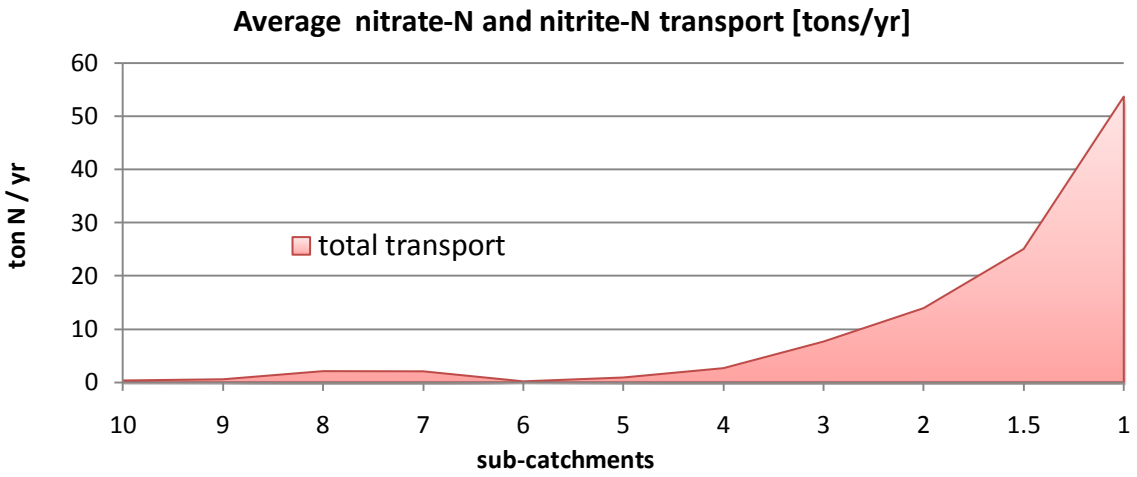

Figure 93: Average NO_3-N and NO_2-N transport calculated for each station

From Figure 93 can be seen that at st.1 the calculated load is 53.65 tons N/yr (which is comparable with the calculated annual load from the monitoring data at Egelund). For the period 1992-2003, the annual load, calculated from monthly values is in the range 44.75 tons N/yr to 87.84tons N/yr. Because there is no similar data available for the load in the other stations of the stream, it is assumed that the calculated average values (Figure 93) are representative. Therefore they are used in the mass-balance calculations.

After the method and all the parameters, included in the mass-balance, have been explained, the reduction capacity for each zone is calculated as absolute values and as % of the corrected values of the estimated leaching for each sub-catchment. Further the results are mapped in GIS and a reduction map in a sub-catchment level is plotted.

Before presenting the results, a brief summary of the assumptions made in this simplified mass-balance is given:

1. Ground water is formed in the whole area of the topographic sub-catchment;
2. The groundwater age is assumed to be similar to the one modelled with GMS for the hydrogeological sub-catchment areas; in that way the "lag" time is also included in the calculations;
3. As the groundwater is the main source of the NO_3^- pollution to Lundgårds bæk, it is assumed that the potential leaching from the root zone is transported with the groundwater to the stream (unless it undergoes through reduction)
4. The same trends of NO_3^- leaching as the one for LOOP2 (Figure 27, p.38) are observed in Lundgårds bæk catchment area.
5. The reduction capacity includes the reduction of NO_3^- by different processes, without specifying which ones.

Results

Following the explained procedure and bearing in mind all the assumptions made, the reduction capacities of the sub-catchment areas are calculated. The results are given in Table 12:

Table 12: Calculated reduction capacities for each sub-catchment

Station/ sub-catchment	NO3L(i)	EL(i) corrected	Red(i)	Red(i)
	ton/yr	*ton/yr*	*ton/yr*	*%*
10	0.35	23.77	23.43	98.55
9	0.57	14.023	13.45	95.94
8	2.10	13.91	12.72	91.50
7	2.06	5.47	5.51	100.63
6	0.18	21.59	23.47	108.72
5	0.90	26.21	25.48	97.24
4	2.66	74.96	73.20	97.66
3	7.65	9.38	4.38	46.76
2	13.93	20.98	14.70	70.08
1.5	25.04	25.92	14.81	57.13
1	53.65	36.92	8.31	22.51
0	71.53	19.28	1.39	7.23

As it is seen the reduction for sub-catchment areas 7 and 6 is calculated to be bigger than the corrected leaching from the area. This can be explained by the fact that from st. 8 to st.6 the stream is losing, so the decrease in the flow is influencing the load, calculated for these stations. This is more likely to be the reason for reduction capacities higher than 100%.

When the reduction map is prepared it is assumed that the reduction capacities for an area can be maximum 100%, so for sub-catchment area 7 and 6 100% is taken instead of 100.63% and 108.72%, respectively.

The reduction map on sub-catchment scale is presented in Figure 94:

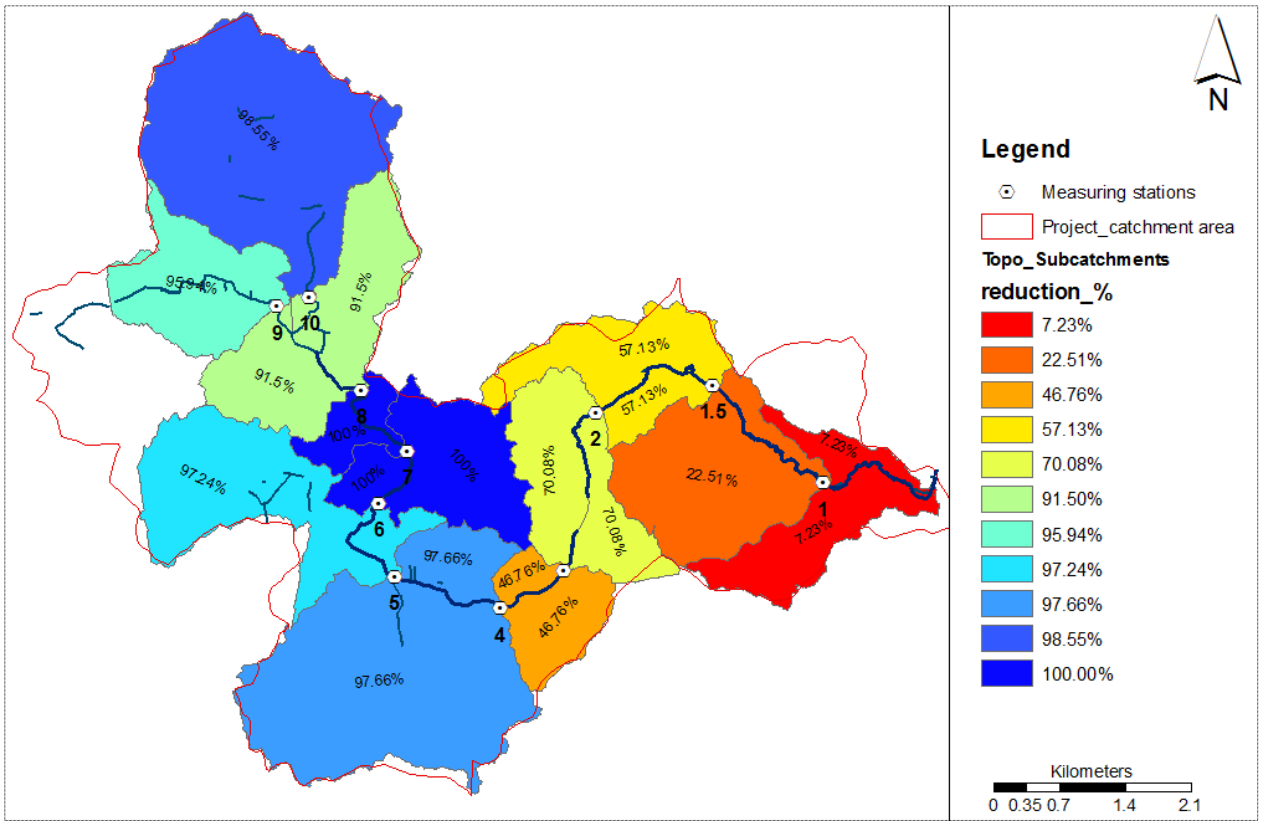

Figure 94: Reduction map on a sub-catchment scale for Lundgårds bæk

From the reduction map it is seen that the vulnerable areas, with low reduction capacities (bellow 60%) are the sub-catchment of st.0, st.1, st.1.5, and st.3, followed by the sub-catchment of st. 2., with 70%. it is also seen that the reduction capacities of the rest of the catchment area are above 90%. It should be pointed out that if reduction analysis on such a small-scale should be made, then the data used for the analysis should be more detailed. For some of the sub-catchment areas, the non-agricultural sources of NO_3^- may have a big influence. For example the sub-catchment of st.2 might have a lower reduction capacity if a different value for the leaching from forests is chosen. Or, for the sub-catchment area of st.10 the leaching from urban areas can play an important role. However, if this method should be applied for other areas, then an evaluation of the method should be performed and more reliable input data should be obtained.

Overview and Discussion

A method for estimation of the reduction capacities on a sub-catchment scale has been developed in this part of the project. The method is a simplified mass balance, even though the leaching from the different sub-catchments is included in the method, some corrections for the response time of the system are made, and the data from the field work are taken into account. It should be noticed, that as smaller the scale gets as much processes/data should be included in the balance. An overview/summary of the reduction capacities is presented bellow, where the sub-catchments are grouped in 3 reduction groups (see Figure 95).

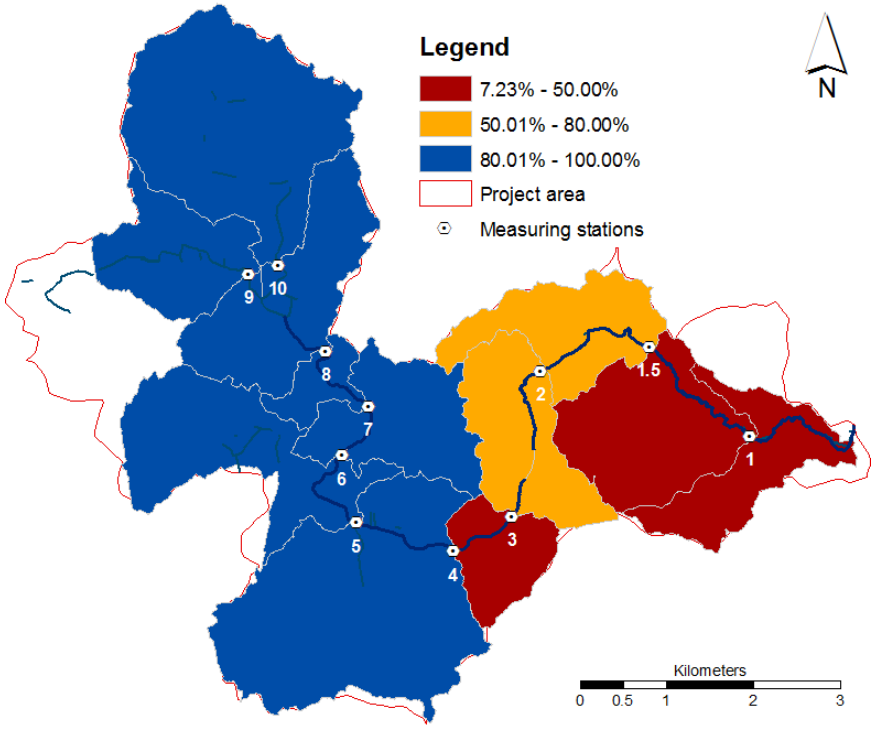

Figure 95: Summary of the reduction capacities: 3 reduction groups: below 50% reduction; 50-80% reduction; above 80% reduction capacity of the sub-catchment area

Further, if some NO_3^- reduction measures should be taken, it should be in the sub-catchment areas, where the reduction capacities are lower than 80%. Even though the reduction capacities are calculated on a sub-catchment area basis, it should be taken into account that most probably different parts of the sub-catchments contribute in a different way to the NO_3^- pollution of the stream. In the next chapter is made analysis in order to find critical zones.

[empty page]

J. Critical Areas for Nitrate Pollution

Introduction

The purpose of this part of the project is to define the critical areas, contributing to the NO_3^- contamination of the stream. To achieve that, the NO_3^- reduction capacities, found in Chapter I (p.101), are used together with the knowledge gathered as part of the field observations.

In Chapter I, where the reduction capacities were calculated, it wasn't specified which processes are responsible for the calculated reduction capacities. To be able to delineate the critical areas, contributing to the NO_3^- pollution in the stream, first this topic should be discussed.

Where Does the Calculated Nitrate Reduction Take Place?

It is believed that the NO_3^- reduction capacities of the sub-catchments of Lundgårds bæk are result of the processes happening in the groundwater zone (2nd zone of interest, p. 21). The reasons why the other 2 zones are excluded are:

- The processes happening in the **upland zone** (1st zone of interest, p. 15) are already included in the calculation of the leaching from the root zone (see p.40)
- The processes happening in the **riparian zone** (2nd zone of interest, p.23) are influencing directly the measured NO_3^- concentrations in the stream. However, in this case, when the reduction capacities are based on the winter measurements, the plant uptake can be excluded because then it is the dormant season of the plants. The denitrification in the riparian zone can be neglected, because of the sub-zero temperatures and the frozen soil. There may be some denitrification and plant uptake in the so called warm areas, where groundwater springs or diffuse groundwater was found (see "Thermo Imaging and Field Observations", p. 63).

If the NO_3^- reduction is taking place in the groundwater zone, then it is expected to happen in the deep sub-surface below the redox front. As part of the general understanding about that, it is expected that the relatively old ground water should be reduced.

Method

To delineate the areas which are contributing to the NO_3^- contamination in the stream, the reduction capacities for each sub-catchment area are applied to the flow particles (modelled with GMS) for each hydrogeological sub-catchment area. For example, the reduction capacity for sub-catchment 1.5 is 57.13% and because it is assumed that this reduction is happening in the deep subsurface, it is calculates which fraction of the particles starting in hydrogeological sub-catchment 1.5 is giving around 57% from all of the groundwater flow particles for that sub-catchment. Further, after it has been estimated which groundwater particles should be reduced, it is delineated the area around the starting points of the not reduced groundwater. In that way the far-away areas, where the reduced groundwater comes from, are excluded. The areas which are left are believed to be the ones contributing to the NO_3^- contamination in the stream. As it was shown in Chapter F (p.74), not for each of the topographical sub-catchments a hydrogeological sub-catchment area is present. For those cases it has been excluded area from the topographical sub-catchment, proportional to the reduction capacity area.

Results and Discussion

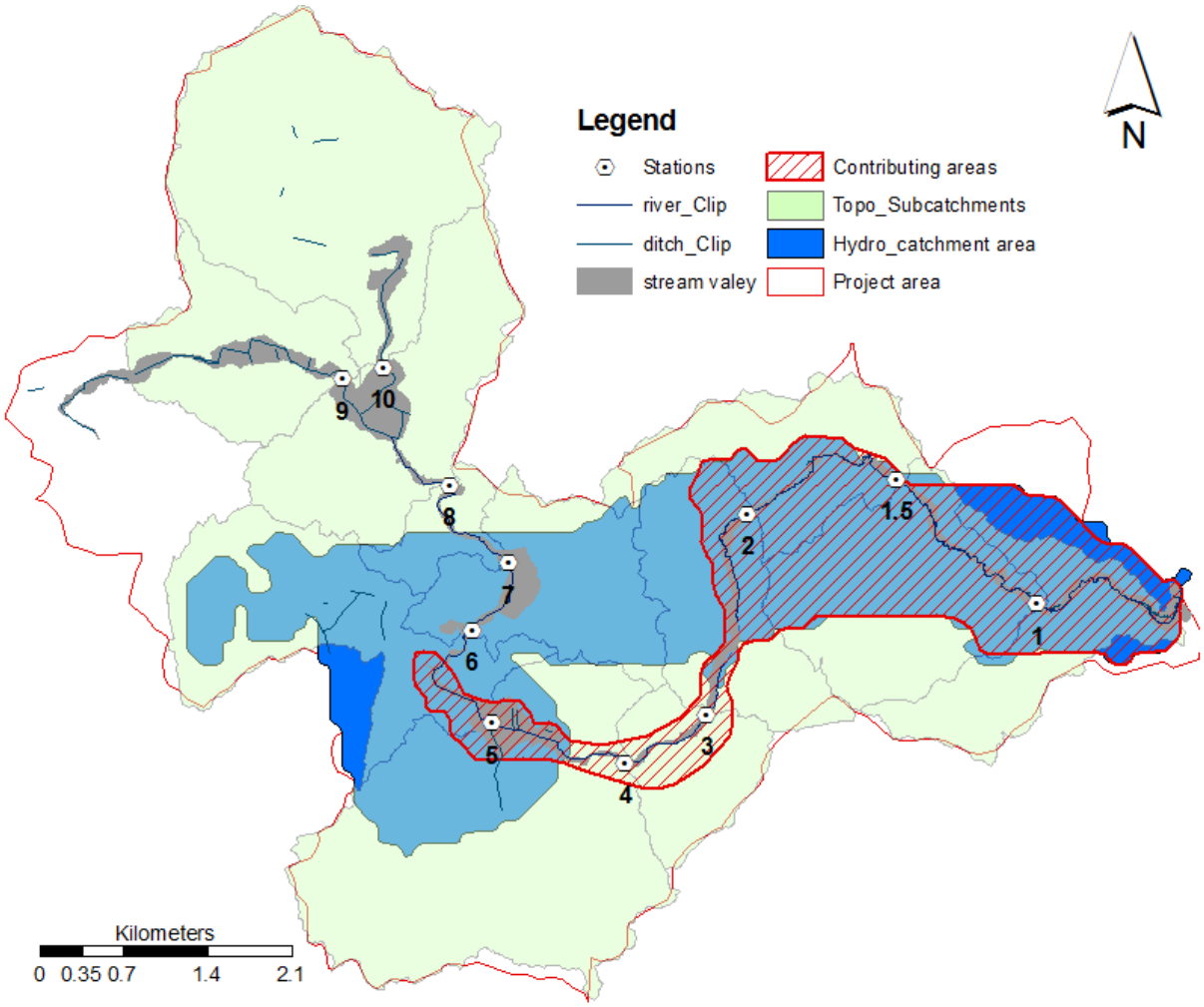

Figure 96: Contributing areas to the NO_3^- contamination of the stream (critical areas)

Figure 96 depicts the critical area contributing to the NO_3^- contamination in the stream together with the two types of catchment areas (topographical and hydrogeological) and with the stream valley. The contributing area (red hatch) is 6.10km^2 and represents half of the hydrogeological catchment area and one fifth of the hydrogeological area (Table 13:)

Table 13: Contributing area as % of the different catchment areas

Type of area	Area [km^2]	Contributing area [%]
Project area	35.00	17.4%
Topographical catchment area	31.60	19.3%
Hydrogeological catchment area	12.09	50.5%

K. Summary and Conclusions

As the purpose of the project was to research and develop a methodology for estimating the NO_3^- reduction capacities, a combination of methods and approaches had to be used. Moreover, the NO_3^- reduction is a subject which can be approached from different angles and researched on different scales: from the micro-scale of the microbiological activity to the macro scale (regional scale) of the land-use management. One of the challenges of the project was to determine on which scale this problem should be investigated and how much of processes happening on a micro level can be neglected in order to evaluate the effects on the so called "small" scale – the sub-catchments of a 1st order stream.

To conclude the report, based on the project made in the two last semesters of the master program "Water and Environment", a summary of the results is schematically presented in Table 14:

Table 14: Summary of the project (the groundwater age is divided in 3 age groups and for each sub-catchment the % of dominating groundwater age is presented; where there is no dominating age group, the %of the mostly presented age groups is given)

sub-catchment areas	**measured** temperatures in the stream	increase in the **measured** flow rate	**measured** nitrate concentrations	**calculated** weighted average leaching	travelling time of the gw flow praticles (GMS)	**calculated reduction** sub-catchments	critical areas (ref)	**reduction** rip-zone (Dahl's GSI typology)	90% **reduction** in rip-zone (Vidon&Hill)
0		-	-		40%/40%				
1					50%/30%				
1.5					40%/40%				
2					70%				
3					100%				
4					40%/40%				
5					80%				
6					80%				
7					100%				
8					100%				
9					100%				
10					100%				
legend	<2.2°C	no	<3mg/l	<80kg/ha	0-10yr	80-100%	no	100%	yes
	2.3-3.9°C	increase	-	80-95kg/ha	10-15yr	50-80%	warning	50%	-
	>4°C	sufficent	>3mg/l	>95kg/ha	>15yr	<50%	yes	0%	no

Table 14 gives summary of the results from: the stream measurements (1st, 2nd, 3rd column), the total NO_3^--N leaching, the travelling times, the reduction calculations (4th,5th, 6th), the applied conceptual models (7th, 8th, 9th) for each sub-catchment area.

The most important findings of this project are:

- The high NO_3^- concentrations in Lundgårds bæk are caused by the NO_3^- polluted groundwater, discharging directly in the stream. The NO_3^- concentrations measured in the stream differ significantly in the different part of the stream. (see Chapter D and Chapter E)

- Based on calculated total leaching from the catchment area and on the measurements performed as part of the field work, an NO_3^- reduction capacity map has been developed. This map shows that only around 30% of the catchment area of Lundgårds bæk has less than 80% NO_3^- reduction capacity; (see Chapter I)
- Based on the calculated reduction capacities and on the modelled residence times of the groundwater, the contributing to the NO_3^- pollution of the stream areas has been mapped. It has been shown that the leaching from 80% of Lundgårds bæk catchment area is not affecting the water quality of the stream. (see Chapter J)

If some measures for reducing NO_3^- should be taken, they can be either in the stream valley (3rd zone of interest) or upland (1st zone of interest). If applying any measures upland, it would be most effective to use the contributing area map together with the leaching from the agricultural land. In that way can be found on a parcel level where some kind of change in the land-use management would be most appropriate.

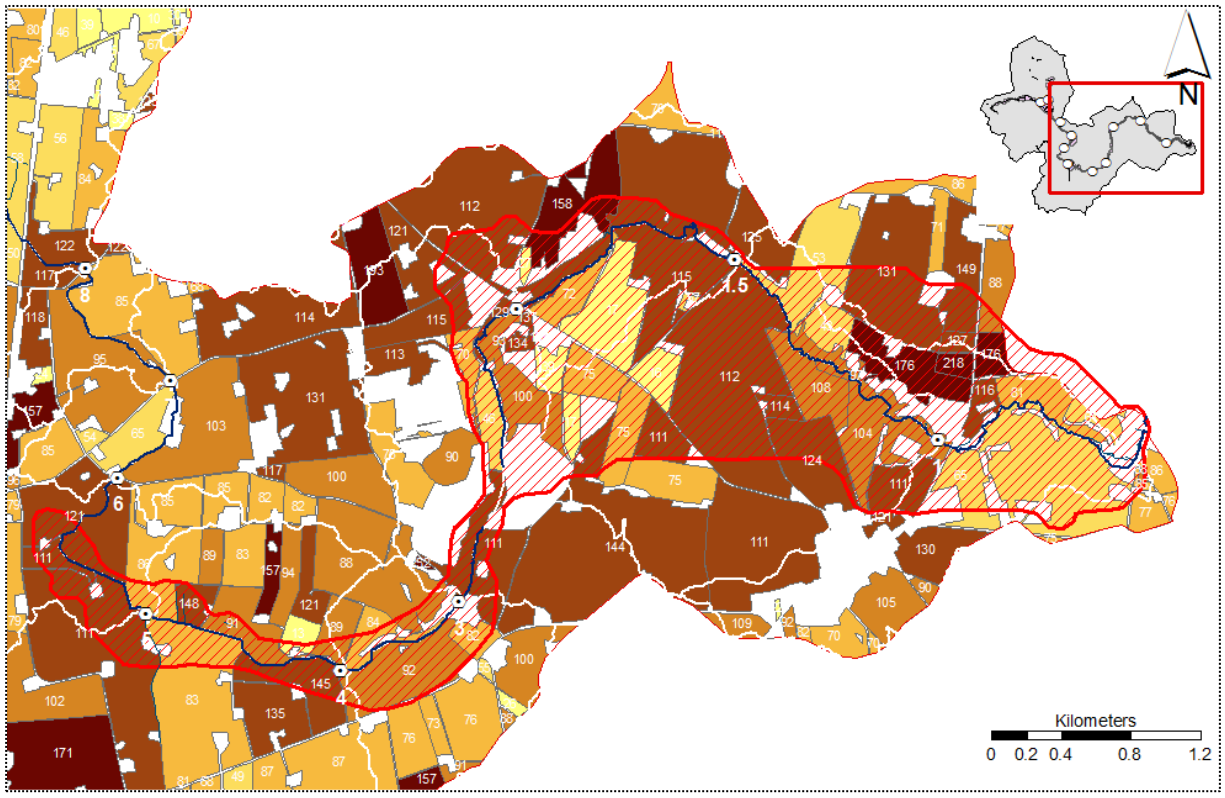

Figure 97: Contributing areas to the water quality in the stream (NO_3^- contamination) together with the NO_3^--N leaching from each parcel (kg N/ha/yr)

If applying any measures in the 3rd zone of interest, then it would be more effective to focus on the part of the stream lying downstream from st.4. The importance of the riparian zone as a protection buffer zone, where NO_3^- attenuation happens, is discussed in Chapter B and Chapter H.

Based on all said, it can be concluded that small-scale NO_3^- reduction maps are possible to be made and can be used as a step forward to the good land-use management practices.

L. Future Perspectives

In the process of working on this project, other suggestions and ideas for further investigation came across.

As part of the field work and sampling:

- Collecting of soil samples from the stream valley – soil type characterisation and measuring organic matter content;
- Eh and pH measurements – to locate the redox front (further reading: (Spalding & Parrott, 1994));
- Mapping stream bed temperatures in order to delineate groundwater discharge or recharge zones and to quantify groundwater – surface water interactions; can be used also in the groundwater springs to measure the groundwater flow rate (further reading (Schmidt et al., 2007) (Kalbus et al., 2006))
- Hydrograph separation based on environmental tracer methods; by using isotopic and geochemical tracers can be provided information on the temporal and spatial origin of the flow; it can be used to determine the fractions of the sub-surface flow paths (further reading (Kalbus et al., 2006))
- Examining the sources and the fate of NO_3^- on a landscape scale with application of stable N isotopes (further reading: (Bedard-Haughn et al., 2003))

As part of the calculating NO_3^- leaching on a sub-catchment level:

- Determination of the leaching from non-agricultural sources and especially for the sub-catchments, where the urban areas are present to a bigger extend; to take into account the size of the residential areas and if the NO_3^- leaching is dependent on it.
- Determination of the leaching from the forest areas, taking into account the type of forest, the size and the historical aspect;

As part of the mass-balance approach:

- the flow and NO_3^--N concentration along the stream can be measured more times, so the data is representative for certain period of time;
- data from tracer measurements can be used for taking into account the “lag” time;
- the mass-balance can be applied for one and the same catchment area with data for the leaching for more than 1 year, in order to compare the differences in the reduction capacities calculated based on different years;
- a “sensitivity” analysis can be performed in order to evaluate how big is the difference in the reduction capacities, if the different parameters are changed;
- a map about the needed reduction of the Nitrogen input from different sources can be produced based on the reduction capacity map;

The method can be used also for comparing different catchments and finding if there is a general rule about the reduction capacities in different parts of the catchment areas. As a final point: the small scale reduction maps can be used nationwide if a general rule can be found.

[empty page]

M. Bibliography

Alley, W.M., Reilly, T.E. & Franke, O.L., 1999. *Sustainability of Ground-Water resourses*. US Geological survey circular 1186. Denver, Colorado: U.S. Government Printing Office US Geological Survey.

Bedard-Haughn, A., van Groenigen, J.W. & van Kessel, C., 2003. Tracing 15N through landscapes: potential uses and precautions. *Journal of Hydrology*, (272), pp.175-90.

Brodie, R.S. & Hostetler, S., n.d. A review of thechniques for analysing baseflow from stream hydrographs.

CAB International, 2008. *Ecohydrology: Processes, Models and Case studies: an aproach to the sustainable management of water resourses*.

Callesen, I., Raulund-Rasmussen, K., Gundersen, P. & Stryhn, H., 1999. Nitrate concentrations in soil solutions below Danish forests. *Forest Ecology and Management*, (114), pp.71-81.

Catchment, S.S., 2002-2010. *CatchmentSIM: Web help*. [Online] Available at: http://www.csse.com.au/catchsim_online_help/index.html?introduction.htm [Accessed 19 April 2011].

Catchment, S.S., 2008. CatchmentSIM.

Chapelle, F.H. & Lovely, D.R., 1995. Deep subsurface microbial processes. *Review of geophysics*, pp.365-81.

Commonwealth of Australia, 2006. *Scale issues in connectivity*. [Online] Available at: http://www.connectedwater.gov.au/contacts.html [Accessed 10 February 2010].

Cooper, A.B., 1990. Nitrate depletion in the riparian zone and stream chanel of a small headwater catchment. *Hydrobiologia*, pp.13-26.

Dahl, M., Hinsby, K. & Refsgaard, J.C., 2010. *GOI typologiens anvendelsesmuligheder - med fokus pa beskyttelse af overfladevand og okosystemer i relation til vand og naturplaner*. By- og Landskabsstyrelsen.

Dahl, M., Nilsson, B., Langhoff, J.H. & Refsgaard, J.C., 2007. Review of clacification systems and new multy scale typology of groundwater-surface water interaction. *Journal of Hydrology*, pp.1-16.

DeBusk, W.F., White, J.R. & Reddy, K.R., 2001. Chapter 3: "Carbon and Nitrogen Dynamics in Wetland Soils". In M.J. Shaffer, L. Ma & S. Hansen, eds. *Modeling Carbon and Nitrogen dynamics for Soil Management*. Lewis Publishers. pp.27-53.

Duff, J.H. & Triska, F.J., 2000. Nitrogen Biogeochemistry and Surface-Subsurface Exchange in Streams. In J.B. Jones & P.J. Mulholland, eds. *Streams and Ground Waters*. Academic Press.

Endreny, T.A., 2003. *Fluvial Geomorphology Module*. [Online] Available at: http://www.fgmorph.com/fg_4_1.php [Accessed 11 February 2011].

Fetter, C.W., 2001. *Applied Hydrogeology*. 4th ed.

Fluke, 2006-2007. *SmartView 1.9.0.21 (Fluke thermography)*. [Online].

GEUS, n.d. *Jupiter - Danmarks geologiske and hydrologiske database*.

Grant, R. et al., 2010. *Landovervågningsoplande 2009*. Faglig rapport fra DMU nr. 802. Danmarks Miljøundersøgelser, Aarhus Universitet.

Grant, R. et al., 2000. *Landovervågningsoplande 1999*. Faglig rapport fra DMU nr. 334. Danmarks Miljøundersøgelser.

Hansen, B., Thorling, L., Dalgaard, T. & Erlandsen, M., 2011. Trend Reversal of Nitrate in Danish Groundwater - a Reflection of Agricultural Practices and Nitrogen Surpluses since 1950. *Environmental Science & Technology*, 45(1), pp.228-34.

Harvey, J.W. & Wagner, B.J., 2000. Quantifying Hydrologic Interactions between Streams and Their Subsurface Hyporheic Zones. In J.B. Jones & P.J. Mulholland, eds. *Streams and Ground Waters*. Academic press.

Hill, A.R., 2000. Stream Chemistry and Riparian Zones. In J.B. Jones & P.J. Mulholland, eds. *Streams and Ground water*. Academic Press.

Hinsby, K. & Dahl, M., 2010. *Udpegning af kritiske deloplande for nitratbelastning af okosystemer via grundvandsforekomster*. By- og Landskabsstyrelsen.

I-GIS, n.d. *GeoScene3D – Modelling and visualization of Geological Data (software)*. Denmark.

K. M. van der Heijde, P., 1988. Chapter 11: "Spatial and Temporal Scales in Groundwater Modelling". In T. Rosswall, R.G. Woodmansee & P.G. Risser, eds. *SCOPE 35: Scales and Global Change - spatial and temporal variability in biospheric and geospheric processes*. M S Swaminathan Research Foundation, Chennai, India (electronic version).

Kalbus, E., Reinstorf, F. & Schirmer, M., 2006. Measuring methods for groundwater-surface water interactions: a review. *Hydrology and Earth Sciences*, (10), pp.873-87.

Kronvang, B., Grant, R., Laubel, A.R. & Pedersen, M.L., 2002. Quantifying Sediment and Nutrient Pathways within Danish Agricultural Catchments. In P.M. Haygarth & S.C. Jarvis, eds. *Agriculture, Hydrology and Water Quality*. CAB International Publishing. pp.281-301.

Miljøministeriet, 2002. *Vejledning om bræmmer langs vandløb og søer*. Guidence. København Ø: Skov- og Naturstyrelsen, Miljøministeriet Miljøministeriet.

Nieder, R. & Benbi, D.K., 2008. *Carbon and Nitrogen in the Terrestrial Environment*. Springers.

Pedersen, J.K., Bjerg, P.L. & Christensen, T.H., 1991. Correlation of nitrate profiles with groundwater and sediment characteristics in a shalow sandy aquifer. *Journal of Hydrology*, pp.263-77.

Pfeifer, S.M., Bahr, J.M. & Beilfuss, R.D., 2006. Identification of groundwater flowpaths and denitrification zones in a dynamic flood plain aquifer. *Journal of Hydrology*, pp.262-72.

Ranalli, A.J. & Macalady, D.L., 2010. The importance of the riparian zone and in-stream process in nitrate attenuation in undisturbed and agricultural watersheds - A review of the scientific literature. *Journal of Hydrology*, pp.406-15.

Schmidt, C., Conant Jr., B., Bayer-Raich, M. & Schirmer, M., 2007. Evaluation and field-scale application of an analytical method to quantify groundwater discharge using mapped streambed temperatures. *Journal of Hydrology*, (347), pp.292-307.

Shabaga, J.A. & Hill, A.R., 2010. Groundwater-fed surface flow path hydrodynamics and nitrate removal in three riparian zones in southern Ontario, Canada. *Journal of Hydrology*, pp.52-64.

Shaffer, M.J. & Ma, L., 2001. Chapter2: "Carbon and Nitrogen Dynamics in Upland Soils". In M.J. Shaffer, L. Ma & S. Hansen, eds. *Modeling Carbon and Nitrogen dynamics for Soil Management*. Lewis Publishers.

Spalding, R.F. & Parrott, J.D., 1994. Shallow groundwater denitrification. *The Science of the Total Environment*, pp.17-25.

USDA, 1987. Module 3: "USDA Textural Soil Classification". In *Soil Mechanics Level 1*. United States Department of Agriculture; Soil Concervation Service.

Vidon, F.G.F. & Hill, A.R., 2004. Landscape controls on the hydrology of stream riparian zones. *Journal of Hydrology*, pp.210-28.

Vidon, P.G. & Hill, A.R., 2006. A landscape-based approach to estimate riparian hydrological and nitrate removal functions. *Journal of the American Water Resources Association*, pp.1099-112.

Wakida, F.T. & Lerner, D.N., 2005. Non-agricultural sourses of groundwater nitrate: a review and case study. *Water Research*, (39), pp.3-16.

N. Appendixes

1. Appendix: Nitrate Reduction Potential Map
2. Appendix: Rosgen Stream Bed Classification
3. Appendix: Six Geological Profiles (initial geological study)
4. Appendix: Building a 3D geological model of the project area
5. Appendix: Base Flow Separation
6. Appendix: Basic Theory for the Statistical Analysis (after TGP, 2005)
7. Appendix: Nitrate Concentrations Plotted vs. Flow Rate (annually and monthly)
8. Appendix: Regression Analysis (additional figures)
9. Appendix: Field Observations and Thermo Imaging
10. Appendix: Field Measurements
11. Appendix: Residence Times
12. Appendix: Stream Valley Characteristics
13. Appendix: Non-agricultural Sources for Nitrate Leaching
14. Appendix: Correction Coefficients Calculations

1 Appendix: Nitrate Reduction Potential Map

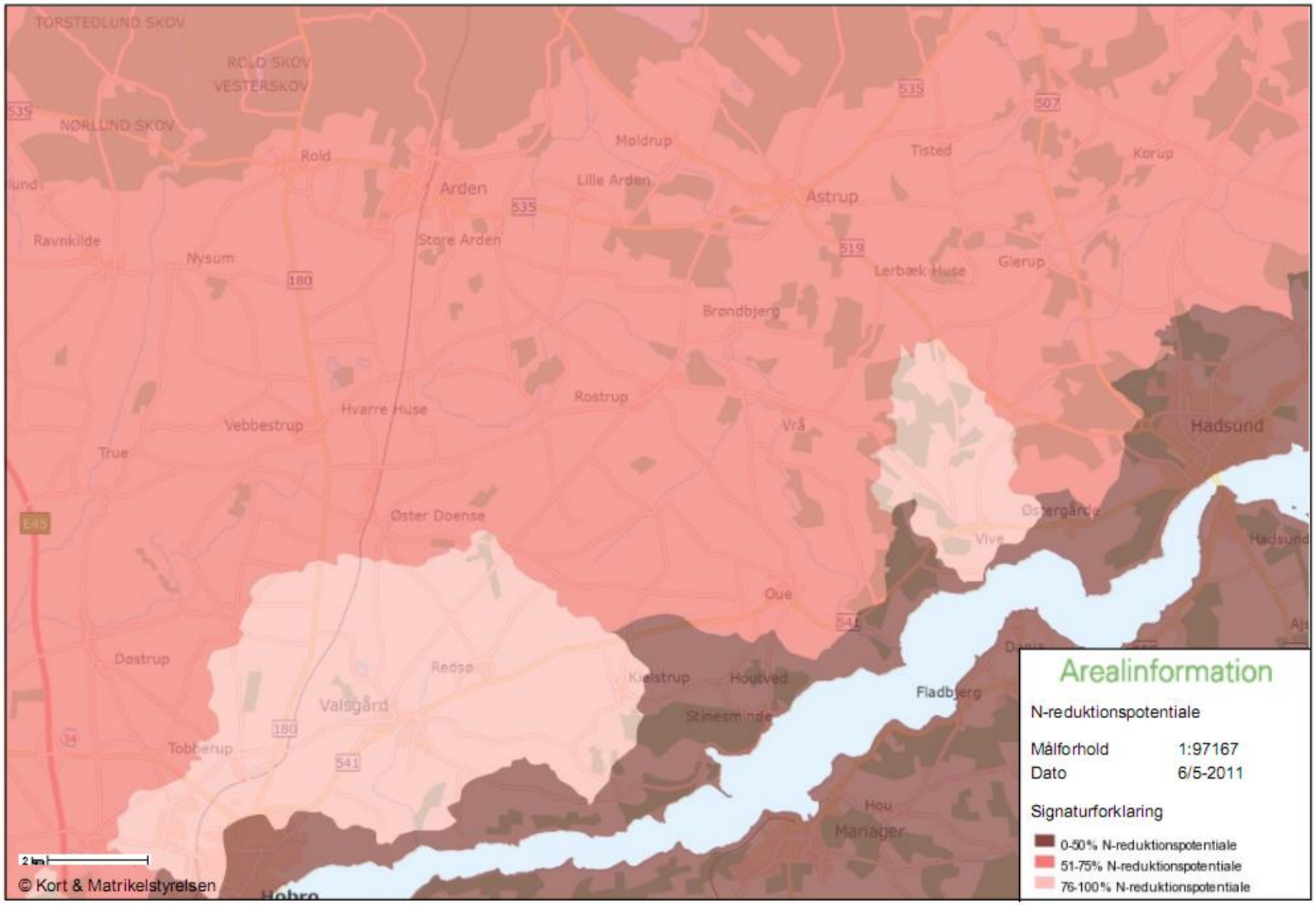

Figure 98: Nitrate-reduction-potential map

2 Appendix: Rosgen Stream Bed Classification

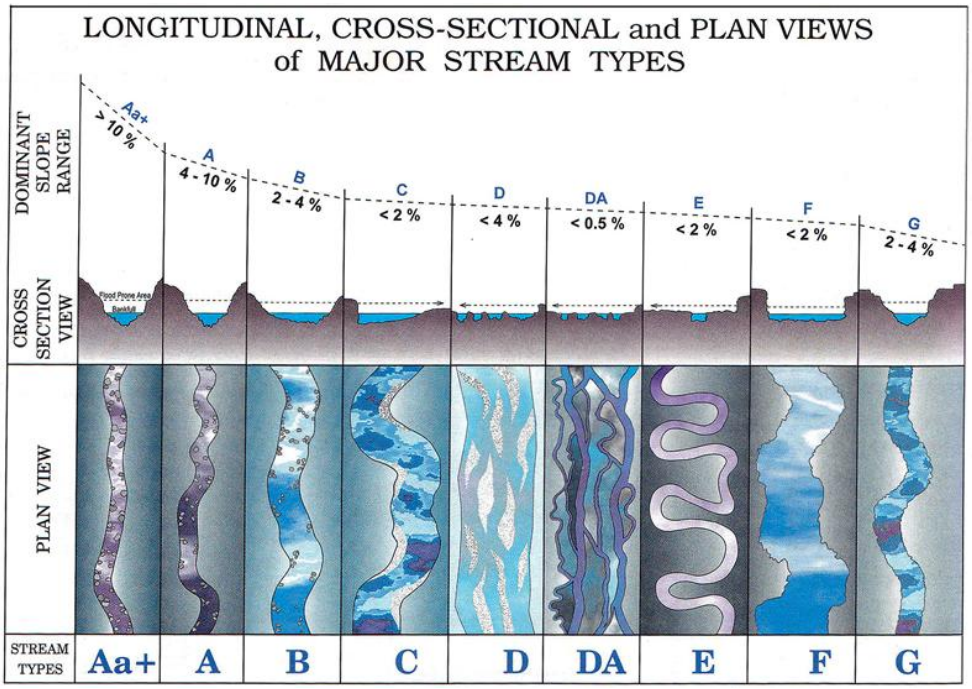

Figure 99: Rosgen's simplified classification, where A and B describe steeper sloped headwater streams; C – meandering channels; D and DA – braided channels; E – highly sinuous vegetation lined channels; F – wide and shallow channels; G – gully like channels.(Endreny, 2003)

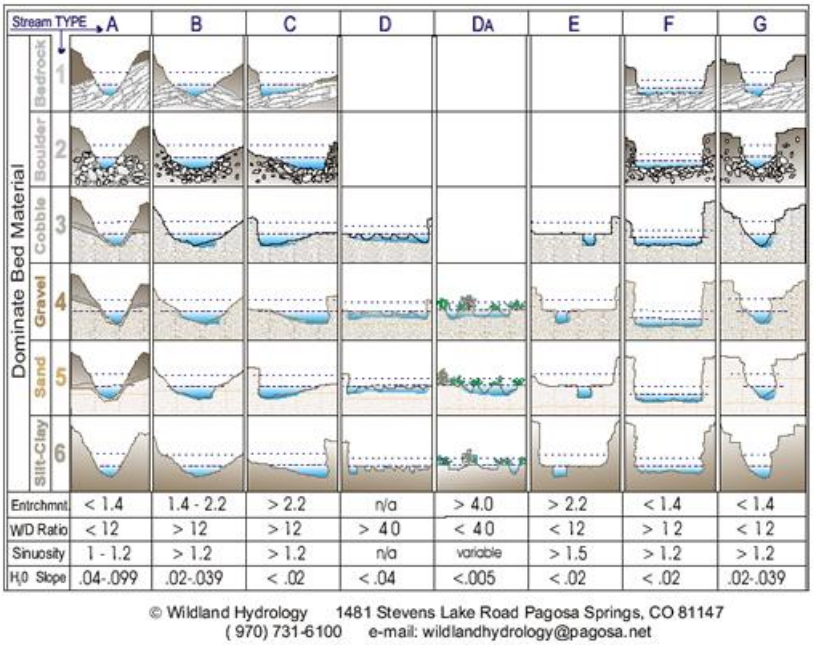

Figure 100: Rosgen's classification with included characteristics of the dominant bed material, where 1 is for bedrock, 2 - boulders, 3 - cobble, 4 - with gravel, 5 - sand, and 6 - silt and clay(Endreny, 2003)

3 Appendix: Six Geological Profiles (Initial Geological Study)

Profil 4

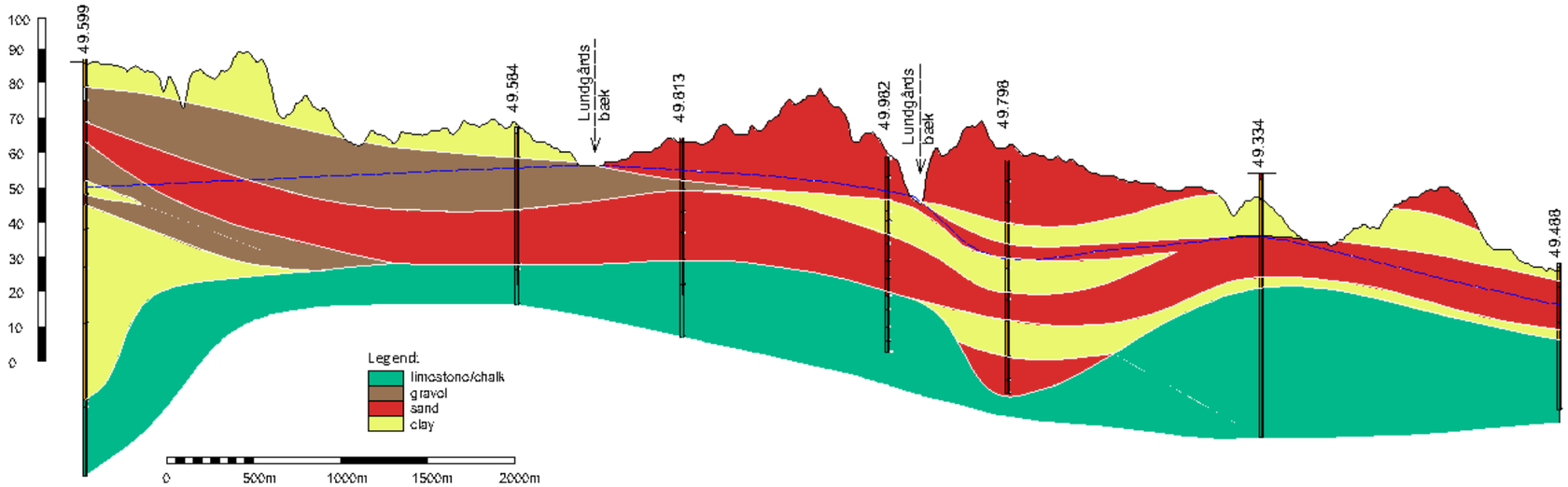

Profil 1

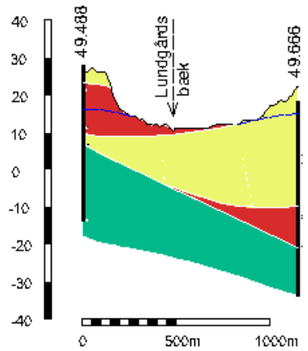

Profil 5

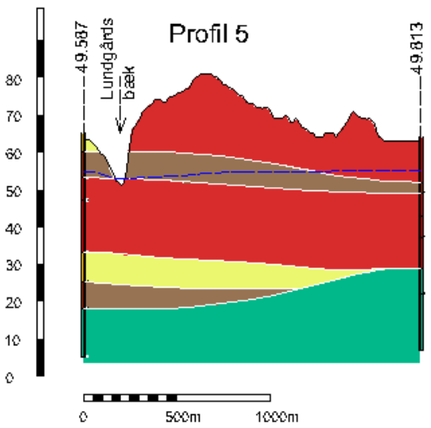

Profil 7

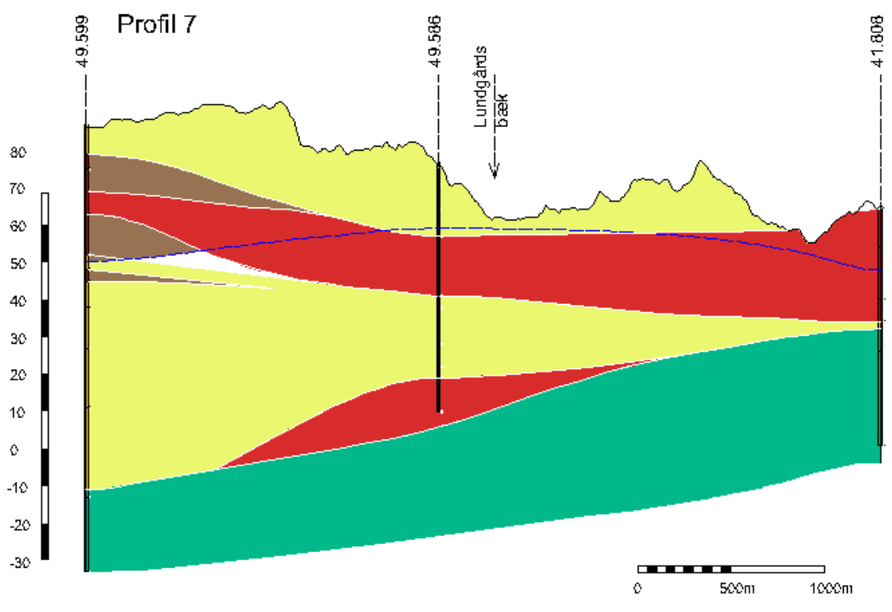

Profil 6

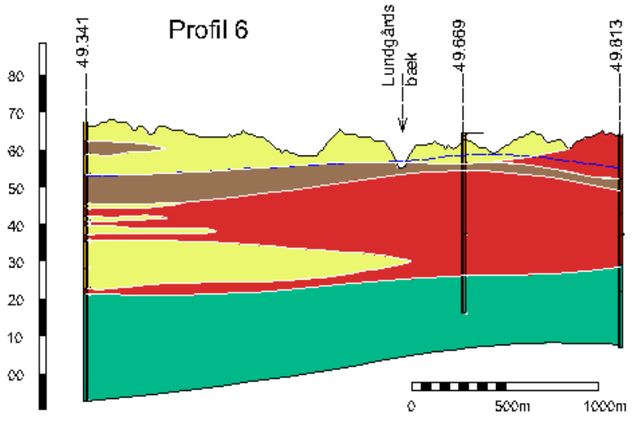

Profil 2

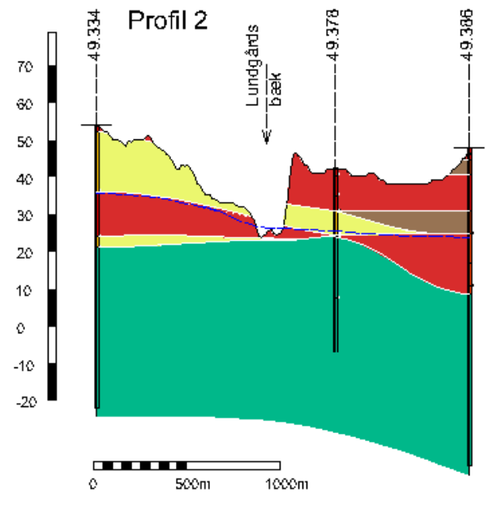

4 Appendix: Building a 3D Geological Model of the Project Area

Introduction

The 3d geological model was build together with NIRAS and Miljøcenter for the purposes of the project. Further it is used as a base for building the groundwater model in GMS.

Method

The program GeoScene3D (I-GIS, n.d.) is used for building the 3D geological model of the area. Different sets of data are used as input information, provided by NIRAS:

- Terrain model;
- Per Smed map (gives information about the landscape origin)
- 1055 borehole reports from Jupiter (GEUS, n.d.)
- 23838 SkyTem models (5 layers) (geophysical data) together with a layer giving information about the reliability of the geophysical data and a layer for the "good conductor"
- Limestone surface and pre-quaternary surface (NOVANA)

For building the model the given procedure bellow is followed:

1. Building a conceptual model of the geological system of the area – how many and what kind of geological layers are present;
2. Loading the data-sets to GeoScene3d;
3. Creating a system of profiles;
4. Adding digitalisation points for each of the geological layers on the profiles;
5. Interpolating the digitalisation points in order to build a surface (upper and bottom borders of a geological layer)
6. Revising the surfaces and checking if they fit to the borehole and geophysical data; adding new digitalisation points or deleting some;
7. Using Surfer for the final interpolation of the surfaces (done by NIRAS)
8. Adjusting the layers in GMS (done by NIRAS)

An overview of GeoScene3D window with the project area and the profile system is presented on Figure 101. The 3D geological model extend includes area much bigger than the catchment area of Lundgårds bæk. This was decided mainly because of the further use of the model as a base for GMS modelling. It was needed for the GMS modelling to take into account that the closer to the edges of the model the bigger uncertainty of the model.

The digitalisation points are drawn in two stages: first, based only on the borehole information, and second, based also on the geophysical data. An example of how the profiles looked like before any digitalisation points are added is given in Figure 102.

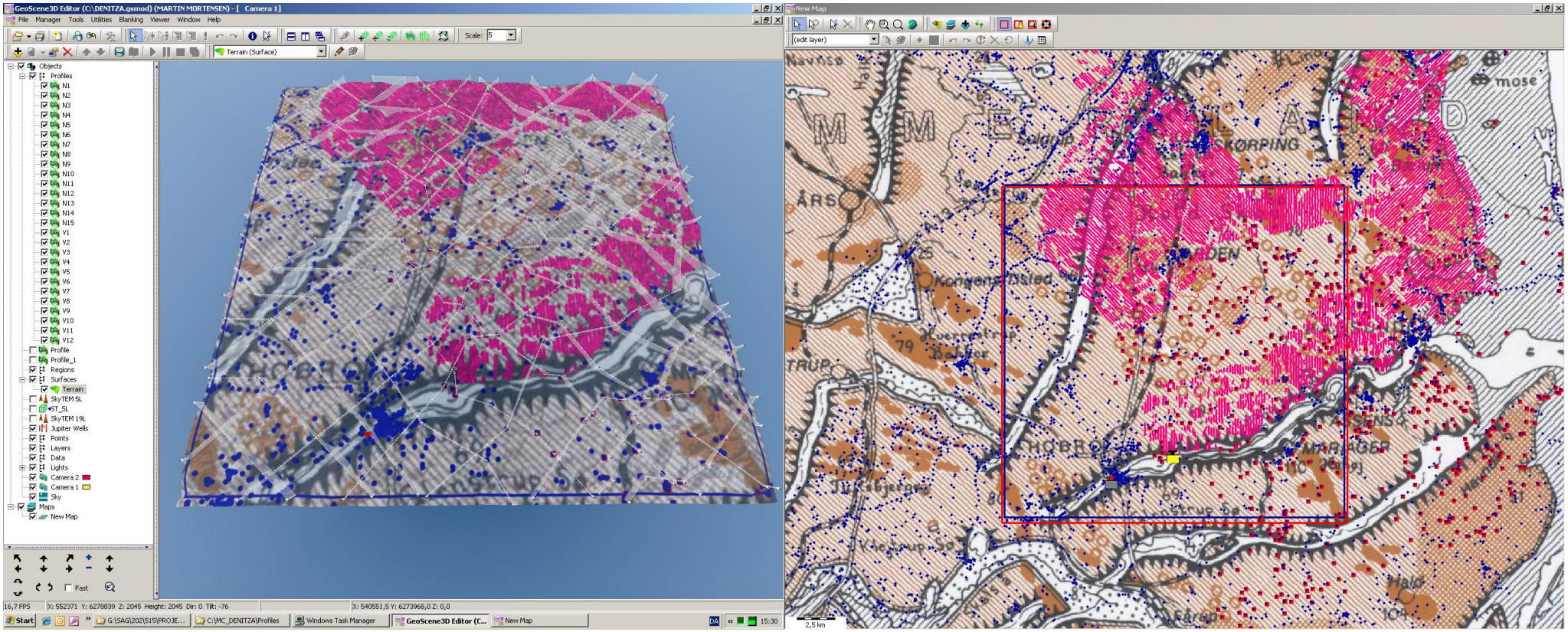

Figure 101: GoeScene3D window (the project extend is given with a red rectangle; the blue dots are the boreholes, the red dots are only the boreholes deeper than 30m (see on the right map); the pink lines are the geophysical models; the white diagonal lines are the profiles, which were used through the procedure of digitalising, together with one moving profile)

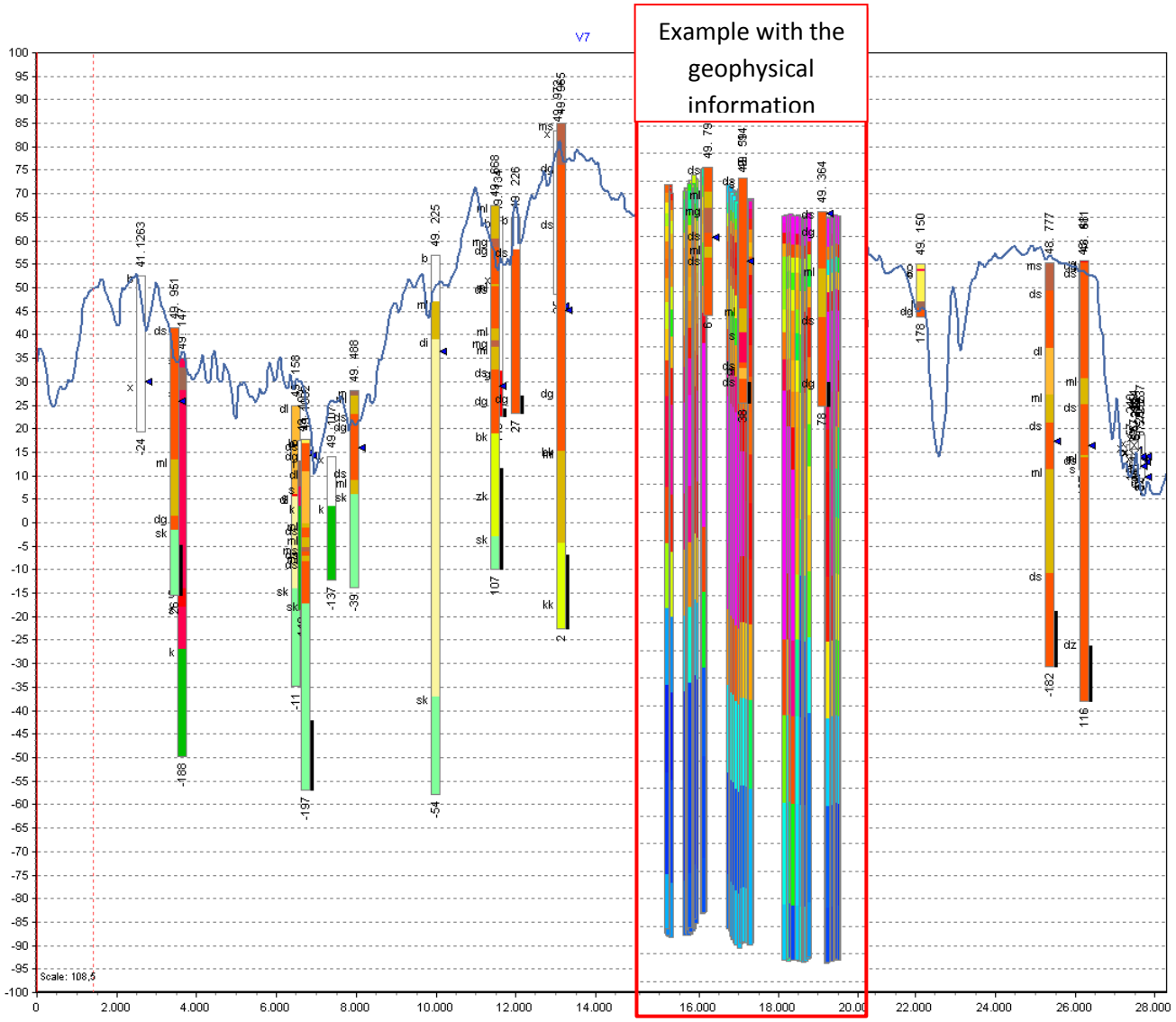

Figure 102: Example of profile (V7) with borehole data and geophysical data

As it is seen from Figure 102, the data from the Jupiter is displayed with different colours and in addition short names for each soil type are used (e.x.: kk, dg, sl). The different short names and their meaning are given in Table 15:

Table 15: Description of the used short names in the boreholes reports (translation: NIRAS)

SHORT	DANSK BESKRIVELSE	ENGLISH DESCRIPTION
a	grundfjeld	Bedrock
ak	turonien kalk, arnager kalk	Turonien limestone, Arnager limestone
al	turonien ler, ler i arnager kalk	Turonien clay, clay in arnager limestone
b	brønd	Well (no geol. description)
bl	coniacien-santonien ler, ler i bavnodde	coniacien-santonien clay
dg	glacial smeltevandsgrus	Glacial melt water gravel
di	glacial smeltevandssilt	Glacial melt water silt
dk	campanien-maastrichtien kalksten	campanien-maastrichtien limestone
dl	glacial smeltevandsler	Glacial melt water clay
ds	glacial smeltevandssand	Glacial melt water sand
dv	glacial vekslende små smeltevandslag	Small alternating glacial melt water deposits
dz	glacial smeltevandssten	Glacial melt water rocks
es	postglacial flyvesand	Post-Glacial aolean sand
f	konglomerat, fosforitkonglomerat	Conglomerate
fi	postglacial ferskvandssilt	Post-Glacial freshwater silt
fl	postglacial ferskvandsler	Post-Glacial freshwater clay
fp	postglacial ferskvandsgytje	Post-Glacial freshwater gytja
fs	postglacial ferskvandssand	Post-Glacial freshwater sand
ft	postglacial ferskvandstørv	Post-Glacial freshwater peat
g	grus, sand og grus	gravel and sand
gk	cenomanien kalk	Cenomanien limestone
hg	postglacial saltvandsgrus	Post-Glacial saltwater gravel
hi	postglacial saltvandssilt	Post-Glacial saltwater silt
hl	postglacial saltvandsler	Post-Glacial saltwater clay
hp	postglacial saltvandsgytje	Post-Glacial saltwater gytja
hs	postglacial saltvandssand	Post-Glacial saltwater sand
hv	postglacial vekslende små saltvandslag	Small alternating saltwater deposits
i	silt klæg, meller	Silt
il	interglacial ferskvandsler	Inter-Glacial freshwater clay
ip	interglacial ferskvandsgytje	Inter-Glacial freshwater gytja
j	lersten, siltsten, okker lerjernsten, al	Lias claystone
jl	lias ler	Lias clay
jq	lias sandsten	Lias sandstone
k	kalk, kridt kalksten	Limestone
ks	miocæn kvartssand	Miocene quartssand
l	ler	clay
m	muld	top soil
mg	glacial morænegrus	glacial gravel, gravely till
mi	glacial morænesilt (siltet till)	glacial silt, silty till
ml	glacial moræneler (leret till)	glacial clayey, till
ms	glacial morænesand (sandet till)	glacial sandy, till
mv	glacial vekslende små morænelag	Small alternating glacial till deposits
nl	cenomanien ler, ler i arnager grønsand	Cenomanien clay
o	fyld	Earth fill
p	gytje, dynd, slam	Gytja, sludge, ooze
q	sandsten	sandstone

qg	interglacial, interstadial saltvandsgrus	Inter-Glacial saltwater gravel
qi	interglacial, interstadial saltvandssilt	Inter-Glacial saltwater silt
ql	interglacial, interstadial saltvandsler	Inter-Glacial saltwater clay
qs	interglacial, interstadial saltvandssand	Inter-Glacial saltwater sand
qv	intergl., -stadial veksl. små saltv.lag	Small alternating Inter-Glacial saltwater deposits
s	sand	Sand
sk	campanien-maastrichtien skrivekridt	Campanien-maastrichtien chalk
t	tørv	Peat
ti	senglacial ferskvandssilt	Late glacial freshwater silt
tk	coniacien-santonien kalksten	Coniacien-santonien limestone
tl	senglacial ferskvandsler	Late glacial freshwater clay
ts	senglacial ferskvandssand	Late glacial freshwater sand
u	ler, sand og grus	clay, sand and gravel
ul	dogger-malm ler	dogger-malm clay
uv	dogger-malm vekslende små lag	Small alternating dogger-malm deposits
v	vekslende små lag	Small alternating layers
vi	nedre kridt silt, silt i jydegård fm	lower cretaceous, silt
vj	nedre kridt ler-, silt- og lerjernsten	lower cretaceous, claystone
vs	nedre kridt sand	lower cretaceous, sand
vv	nedre kridt veksl.små lag, i jydegård fm	lower cretaceous, small varying layers
w	evaporitter	Evaporites
wl	nedre kridt ler, ler i jydegård fm	lower cretaceous,clay
x	ukendt lag, oplysninger mangler	Unknown
yg	senglacial saltvandsgrus (yoldia)	Late glacial saltwater gravel (yoldia gravel)
yi	senglacial saltvandssilt (yoldia)	Late glacial saltwater silt (yoldia silt)
yl	senglacial saltvandsler (yoldia)	Late glacial saltwater clay (yoldia clay)
ys	senglacial saltvandssand (yoldia)	Late glacial saltwater sand (yoldia sand)
yv	senglacial vekslende små saltvandslag (yoldia)	Small alternating Late glacial saltwater deposits (yoldia)
z	sten, flint	stone, silicium minerals usually in the limestone кремък
zs	post/senglacialt, terrestrisk/marint ned	Post-/late- glacial, terrestial/marine sand

The geophysical data is displayed only by different colour (Figure 102), where the colour represents certain electrical resistivity [Ω/m]. However, based on different literature studies, one and the same soil type has different range of resistivity (see Figure 103)

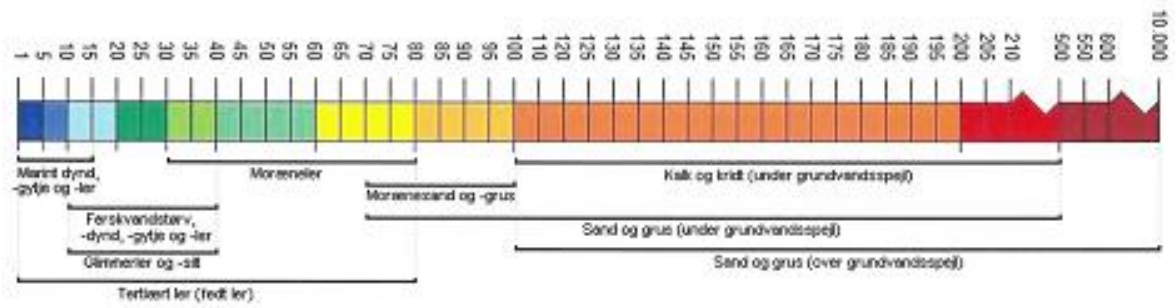

Figure 103: Colour palette with the electrical resistivity of the different soil types [ohm/meter](NIRAS)

The conceptual geological model is built in the next section.

Conceptual Geological Model

To be able to build the geological conceptual model all the available data was reviewed. The aim was to find how many and which layers are present almost everywhere in the studied area. When analysing this, it was taken into account that in 3DGeoScene surfaces are built and those surfaces have to be continuous in the whole area with no gaps aloud. So if a geological layer disappears from place to place, the digitalisation points are drawn on the top or bottom surface, so the thickness of the layer is close to 0. Further, some adjustments are made in GMS, so there are no layers which cross each other, or the terrain. As part of these adjustments, the 3D geological model has been changed, so even if there is no layer present, in the numerical model (GMS) this layer is with a minimum thickness of 1m which is not always as in the reality. The followed procedure is schematically presented in Figure 104

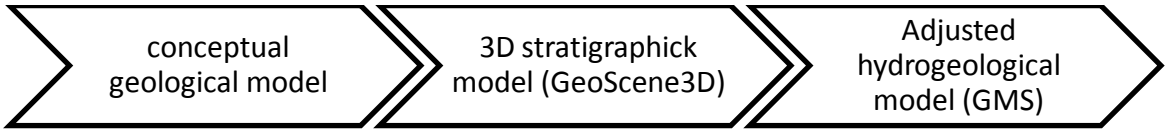

Figure 104: followed procedure of building a geological model of the area: 1) conceptual model; 2) adding digitalisation points and building the upper and bottom surfaces of the different geological layers, followed by interpolation in Surfer; 3)Adjusting the surfaces in GMS, so they don't cross each other or the terrain, minimum thickness 1m

Figure 105 presents the conceptual model, where:

1. Clay – not present in the whole area
2. Sand/gravel
3. Clay lenses – it was decided to not build that layer
4. Sand/gravel
5. Clay/silt
6. Sand/gravel
7. Clay lenses - it was decided to not build that layer
8. Sand/gravel
9. Clay/silt – not present everywhere; but in some places in the area there is a thin clay layer above the limestone surface
10. Limestone/chalk

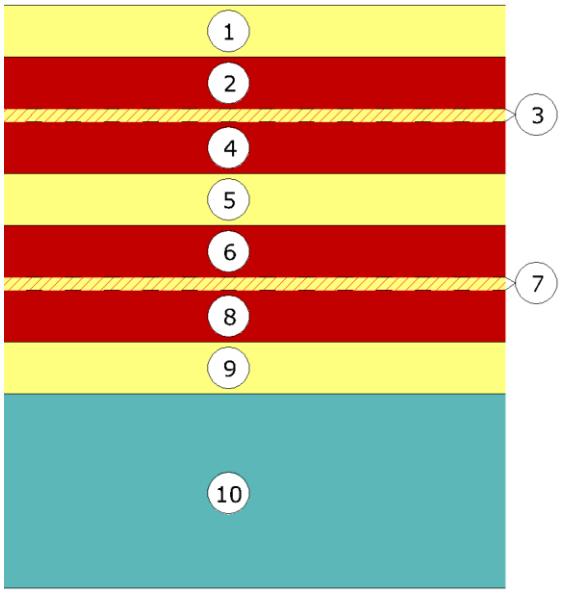

Figure 105: Conceptual geological model

It was decided that the there is not enough data to build Layer 3 and Layer 7, so in GeoScene3D digitalization points are made for the bottom of the 1st layer, 4th layer, 5th layer, 8th layer, and 9th layer.

For the purposes of the GMS modeling after the adjustments of the layers and giving them at least 1m thickness, 2 more layers (peat) are added above the 1st clay layer and the limestone is divided to two limestone layers.

The interpolation of the digitalization points to surfaces is done in Surfer by NIRAS. The surfaces were checked in GeoScene3D if they fit to the data. The followed adjustments in GMS are made by NIRAS.

Further are presented the results after the adjustments, as those are the surfaces used in GMS to build the hydrogeological model and to simulate the flow paths and the residence times, which are used in this master thesis.

Results

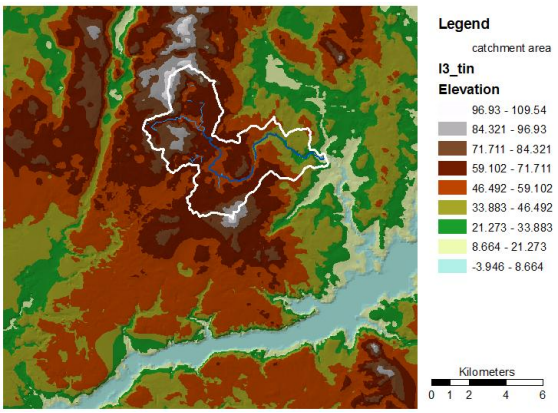

Figure 106: Bottom surface of 1st clay layer

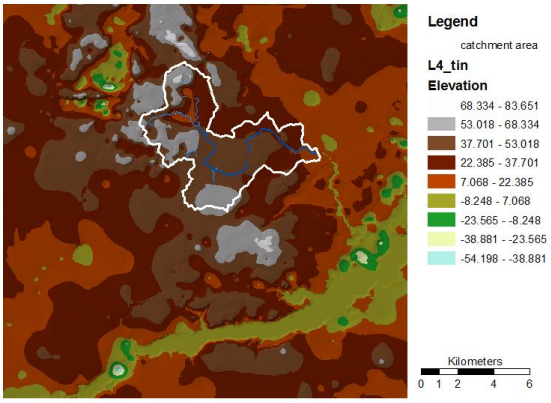

Figure 107: Bottom surface of 1st sand layer (layer 4 from the conceptual model)

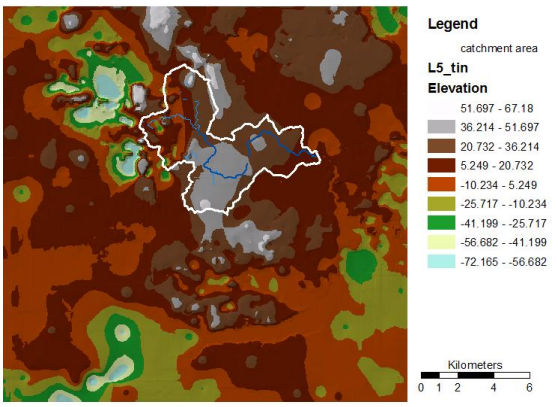

Figure 108: Bottom surface of 2nd clay layer (layer 5 from conceptual model)

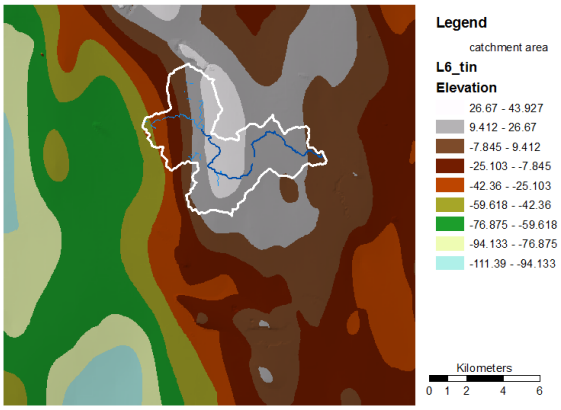

Figure 109: Bottom surface of 2nd sand layer (layer 8 from conceptual method)

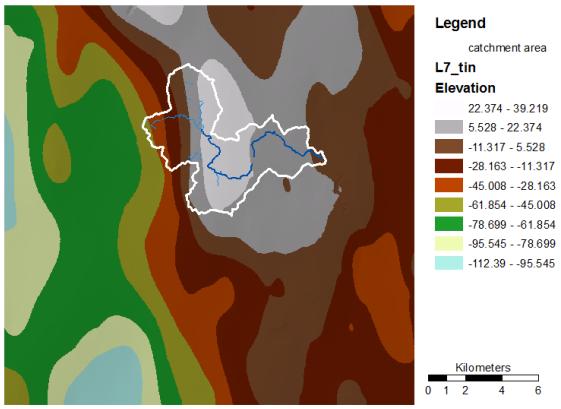

Figure 110: Bottom surface of 3rd clay layer – upper limestone surface (layer 9 from conceptual model)

Figure 106 to Figure 110 present the surfaces after their adjustment in GMS. Some profiles were drawn to illustrate how the geology in the project looks like. For this purpose is chosen to use the same profiles as the ones for the initial geology study (see Figure 111)(ref).

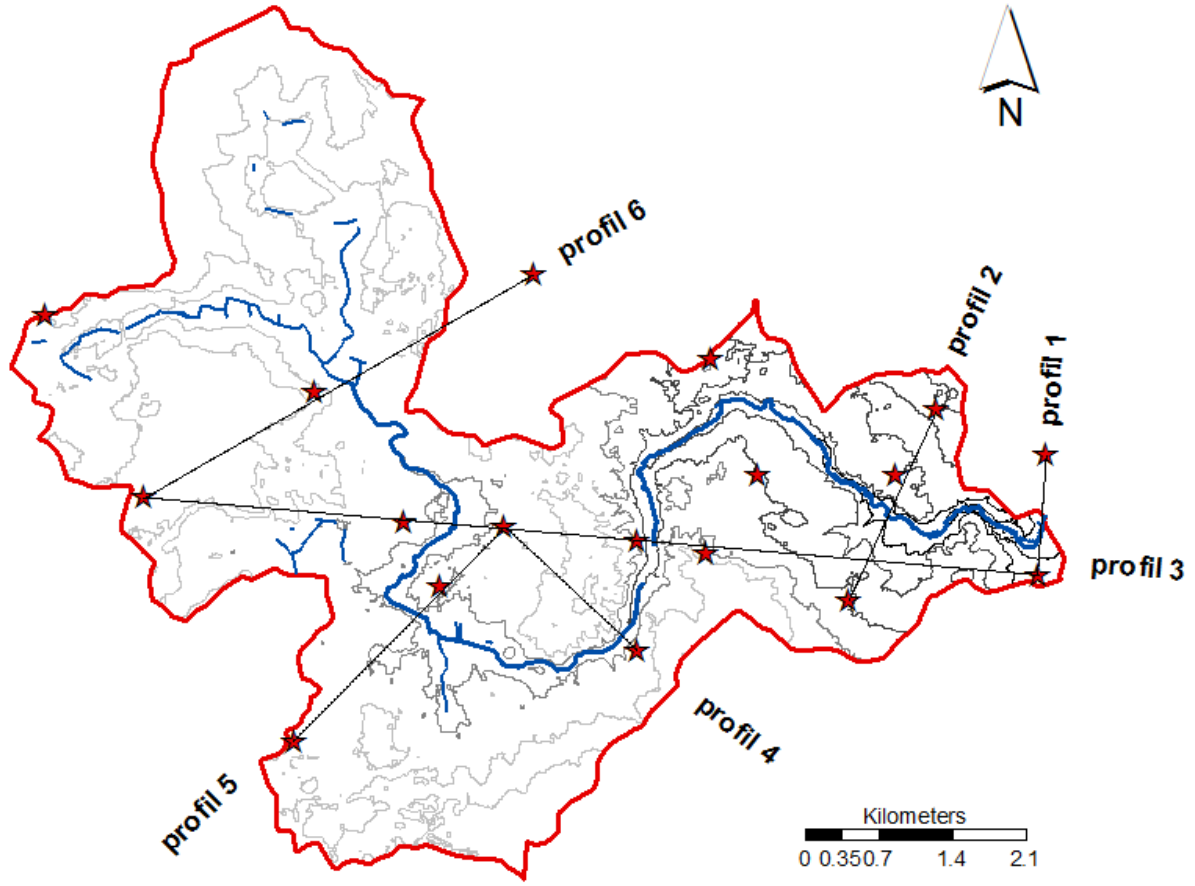

Figure 111: Placement of the profiles (used for the initial geological study)

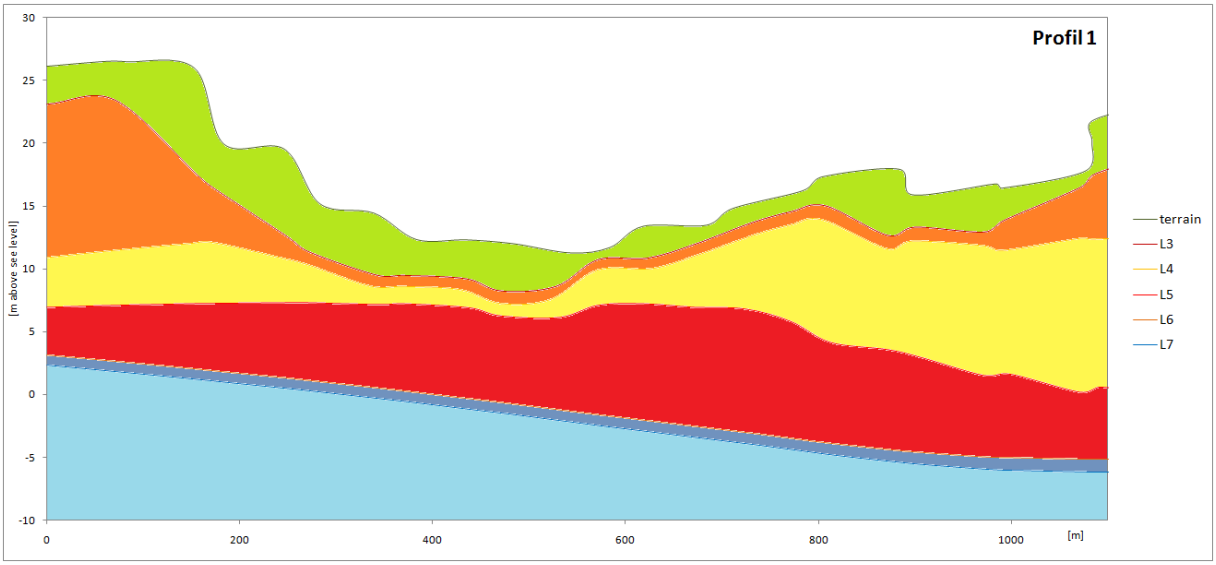

Figure 112: Profile1 : green – clay+2 peat layers; orange and red – sand; yellow – clay; dark blue – clay; light blue- limestone (L3 - bottom 1st clay layer + 2 peat layers; L4 - bottom sand layer; L5 - bottom clay layer; L6 - bottom sand layer; L7 - bottom clay layer and upper limestone)

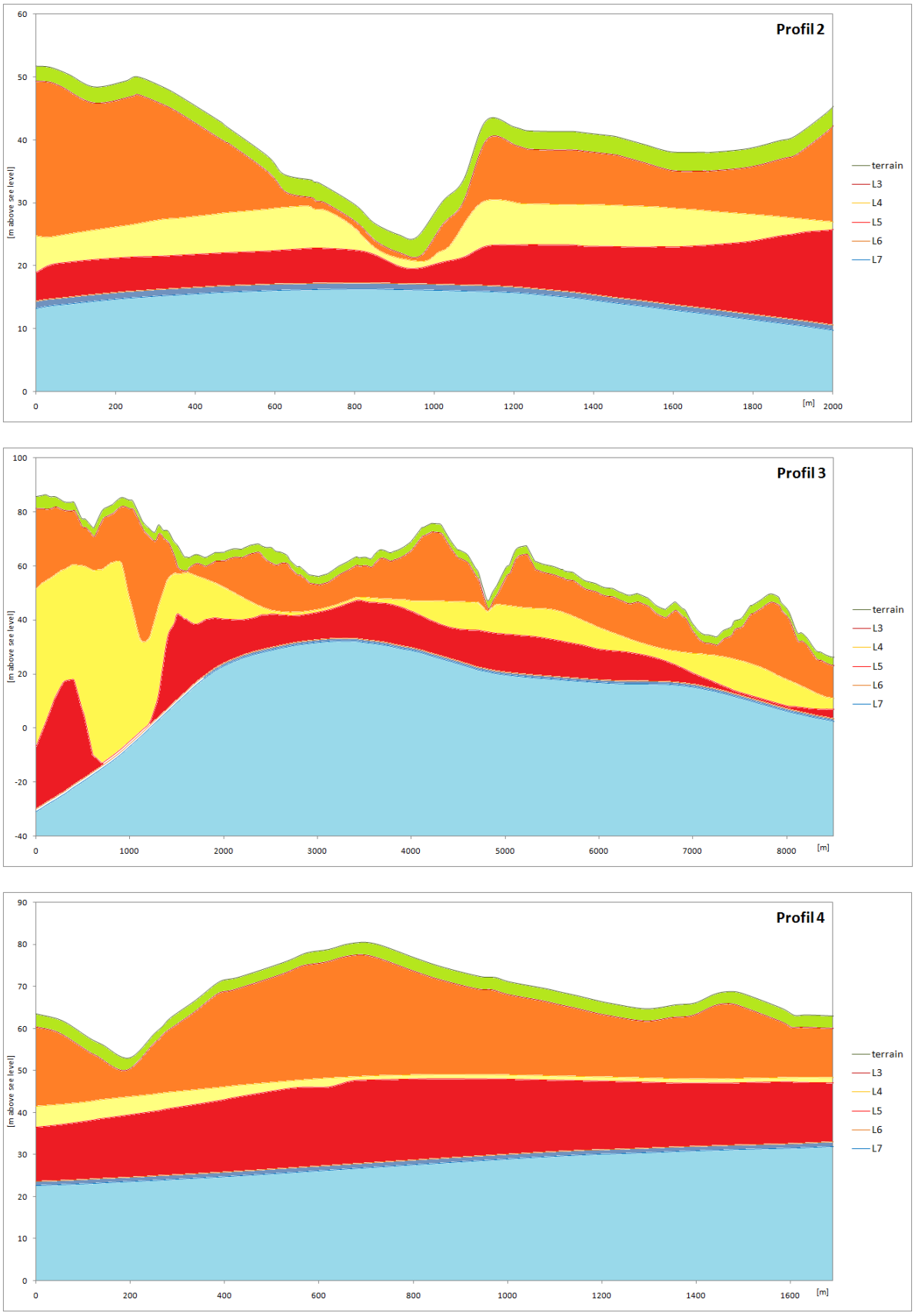

Figure 113: Profiles 2, 3, and 4: green –1m clay+2m peat layer; orange and red – sand; yellow – clay; dark blue – clay; light blue- limestone

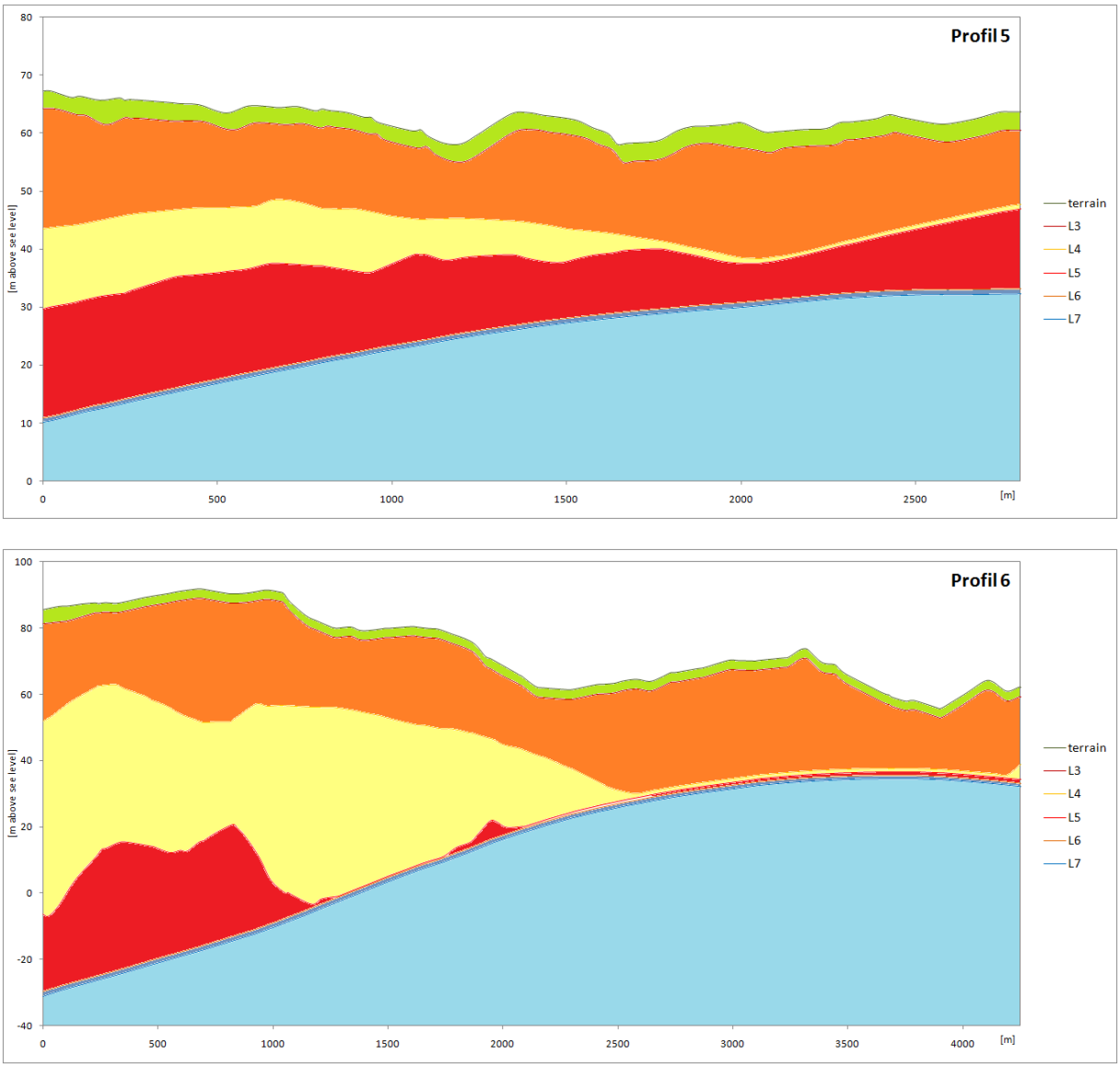

Figure 114: Profiles 5 and 6: green –1m clay+2m peat; orange and red – sand; yellow – clay; dark blue – clay; light blue- limestone

5 Appendix: Base Flow Separation

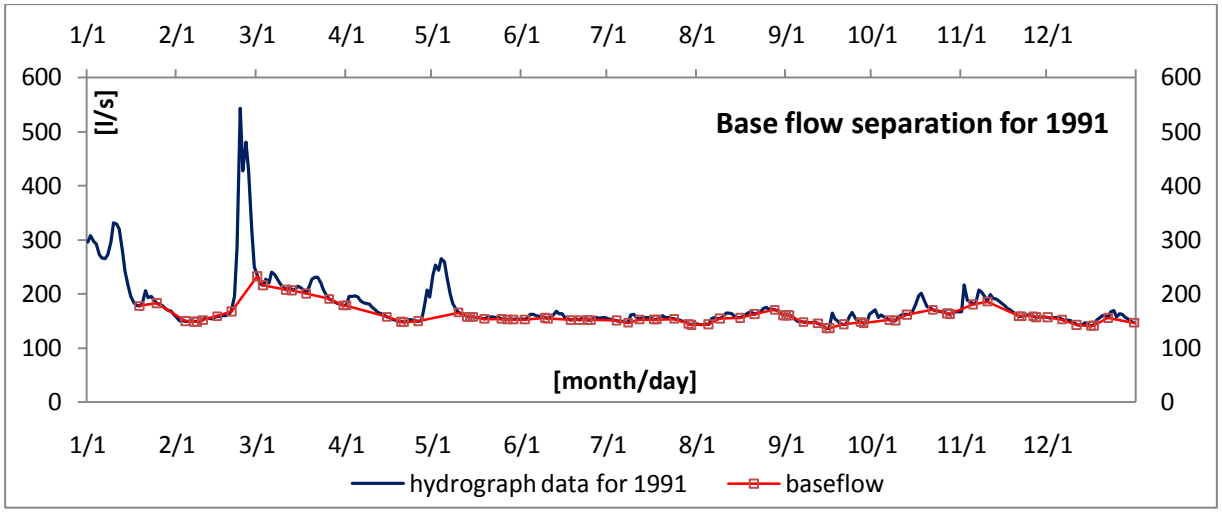

Figure 115: Base flow separation of Lundgårds Bæk for 1991

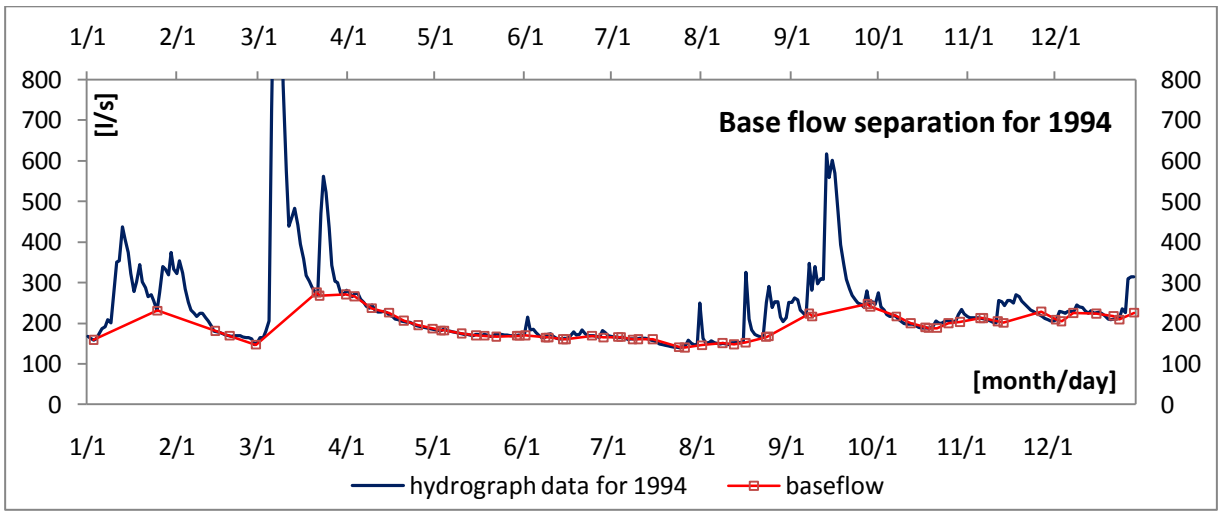

Figure 116: Base flow separation of Lundgårds Bæk for 1994

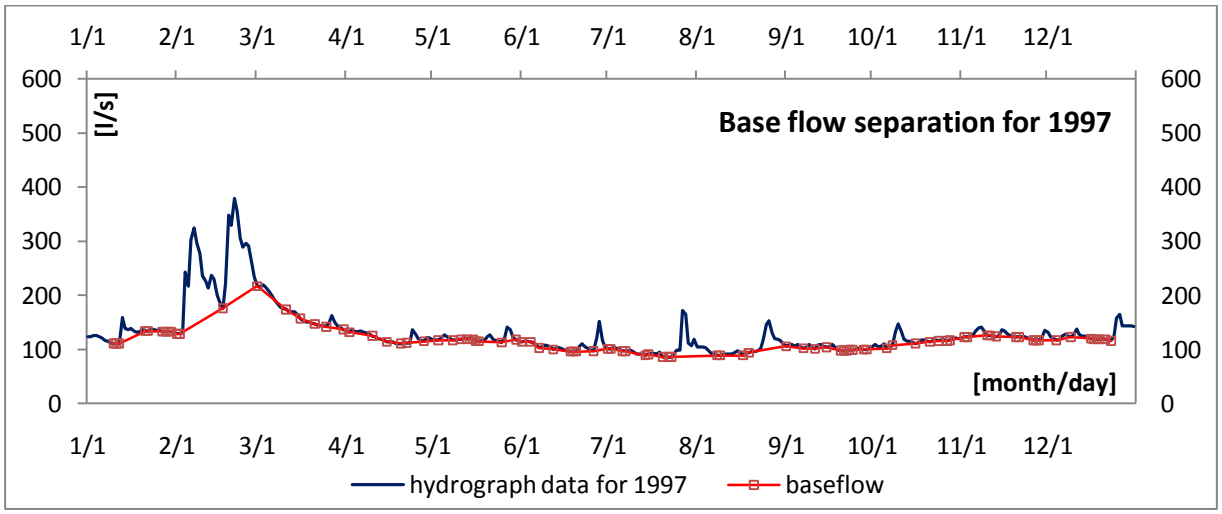

Figure 117: Base flow separation of Lundgårds Bæk for 1997

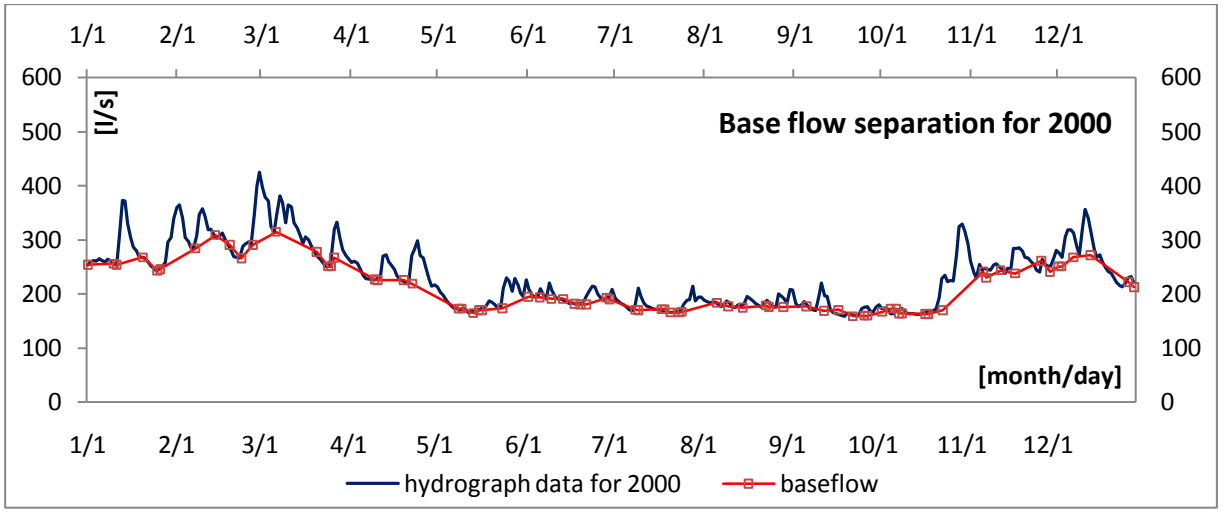

Figure 118: Base flow separation of Lundgårds Bæk for 2000

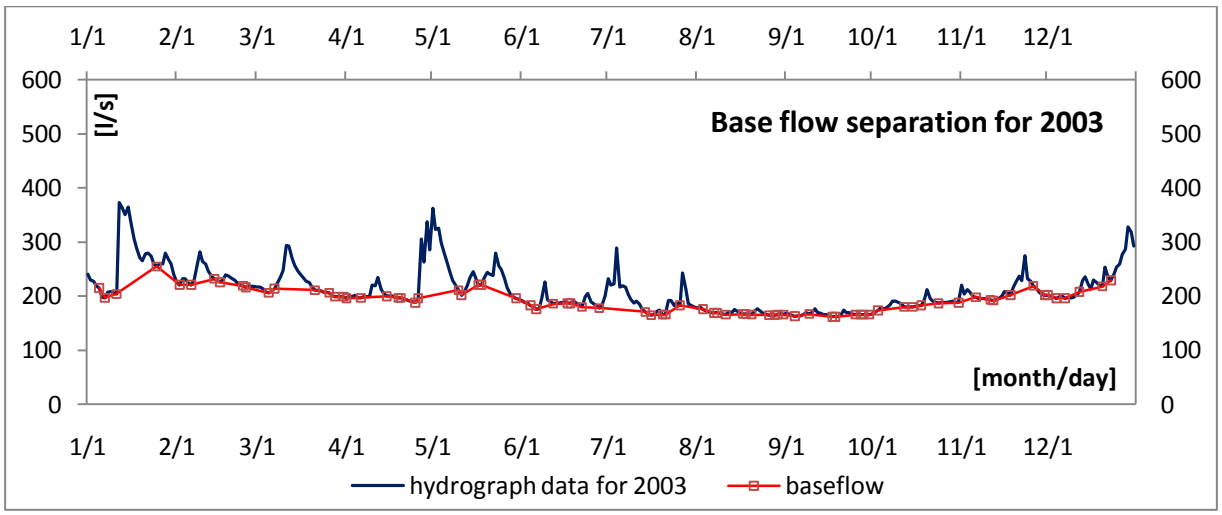

Figure 119: Base flow separation of Lundgårds Bæk for 2003

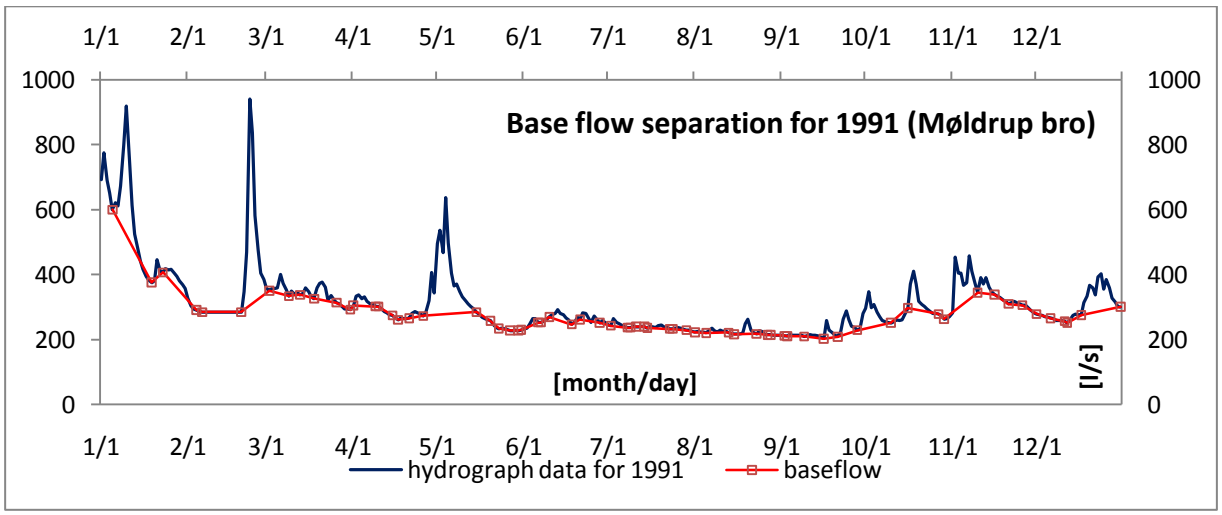

Figure 120: Base flow separation of Villestrup Å for 1991 (Møldrup bro)

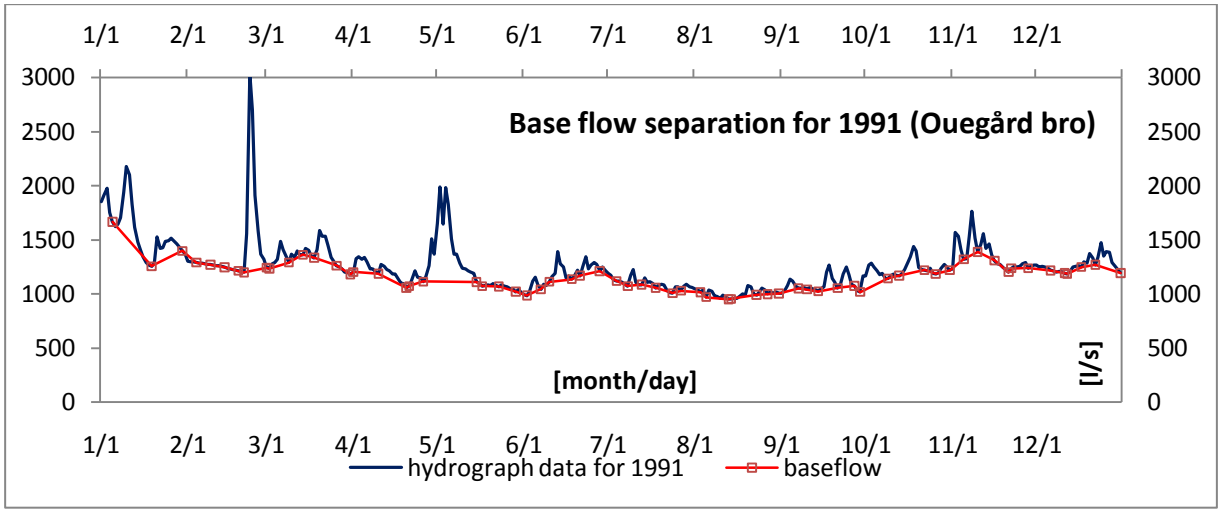

Figure 121: Base flow separation of Villestrup Å for 1991 (Ouegård bro)

6 Appendix: Basic Theory for the Statistical Analysis (after TGP, 2005)

Linear regression basics

To perform a linear regression means to fit a linear model to the existing data. The linear function can be described by the equation:

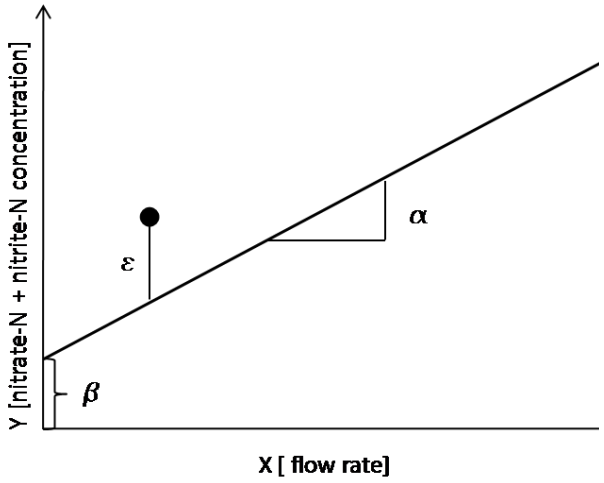

$$Y = \alpha X + \beta + \varepsilon,$$

Where:
Y – the dependent variable, output (in this case: the NO_3-N+NO_2-N concentration),
X – the independent variable, input (in this case: the flow rate (Q)),
α - the slope,
β – the intercept with "y" axis
ε - the random errors for the y-values;

Figure 122: Constants of the linear function

If a data set of measurements is present, it is of interest to find the α and the β from these data. It can be expressed by:

$$Y_{est} = AX + B + e_i,$$

Where:
Y_{est} - the estimated values for Y

Each data will fulfil the relation:

$$y_i = Ax_i + B + \varepsilon_i,$$

Where:
A – the sample estimate for α,
B – the sample estimate for β,
$e_i = y_i - y_{i,est}$: the residue, the vertical distance between the measured value and the estimated value from the straight line.
$_i$ – index: moves from 1 to N, where N is the number of the values in the data set.

The best fit is normally found by minimising the SSE, where SSE is the sum of the standard errors:

$$SSE = \sum_{i=1}^{N} e_i^2 = \sum_{i=1}^{N} \left(y_i + y_{i,est}\right)^2$$

This method, when using the SSE for finding the best fit is called Least squares or Ordinary least squares (OLS).

When evaluating the goodness of a fit, different parameters can be used to help quantifying the uncertainty. The once used in the following calculations are the correlation coefficient (R), the coefficient of determination (R^2) and the root mean square error (RMSE).

Correlation coefficient (R)

It is also called product moment correlation coefficient or Pearson's coefficient. It can take values between -1 and 1. Can be calculated by using the equation:

$$R = A\sqrt{\frac{S_{xx}}{S_{yy}}} = \frac{S_{xy}}{\sqrt{S_{xx}S_{yy}}} = \frac{\sum_{i=1}^{N}(x_i - m_x)(y_i - m_y)}{\sqrt{\sum_{i=1}^{N}(x_i - m_x)^2 \sum_{i=1}^{N}(y_i - m_y)^2}}$$

Where m_x and m_y are the mean values for X and Y.

Coefficient of determination (R^2)

It is a general measure of influence and it is found as the square of R. Both (R and R^2) are dependent on the estimated slope (A) and as larger is the slope as larger are R and R^2. R^2 equal to 0,9 will mean that 90% of the variation in Y (f.ex.: NO_3^--N and NO_2^--N concentration) can be explained by the Y's linear dependency on X (flow rate). Because of the dependency to the estimated slope, R and R^2 don't give an absolute measure of how good is one fit for a linear model.

Root mean square error (RMSE)

When the purpose is to measure the goodness of a fit, RMSE can be used instead of R and R^2. RMSE can be calculated by using the formula:

$$RMSE = \sqrt{\frac{SSE}{N}} = \sqrt{\frac{\sum_{i=1}^{N}(y_{i,est} - y_i)^2}{N}}$$

Non-linear regression

Non-linear regression is to fit a non-linear model to existing data. The mode can be exponential, logarithmic, polynomial or other. The nonlinear regression was performed with using the SOLVE function in EXCEL. This method can be used also for performing a linear regression. The followed procedure is:

1. Arrange the data set in a table in spreadsheet as in Table 16:

Table 16 Example how to arrange the data in the spread sheet

Y (concentration)	X (flow rate)	Yest (estimated conc.)	SE squared errors	$RMSE = \sqrt{\frac{SSE}{N}}$
y_1	x_1	$y_{1,est}$	$(y_{1,est} - y_1)^2$	parameters:
y_2	x_2	$y_{2,est}$	$(y_{2,est} - y_1)^2$	a_0
...	...	...	...	a_1
y_N	x_N	$y_{N,est}$	$(y_{N,est} - y_1)^2$	a_2
			SSE=$\sum(y_{N,est} - y_1)^2$	a_3

2. Chose a model equation and number of fitting constants;

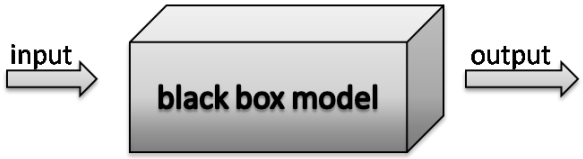

Figure 123 black box model concept

The used method is similar to the black box model concept, where the used equation is empirically derived and it doesn't have theoretical background. In this case the input is the flow rate measurements (x_i) and the output is the estimated NO_3-N and NO_2-N concentration an ($y_{i,\,est}$). The purpose is to find a function which would describe in the best way the transformation which happens in the black box, so the RMSE of the estimated and measured concentrations is as smaller as possible. As it was mentioned before the function could be: linear, power, exponential, logarithmical etc. Together with the choice of function also a number of fitting constants are chosen (a_0, a_1, a_2, a_3).

3. Make a initial guess about the parameters (fitting constants), so $y_{i,est}$ is calculated;
4. Use SOLVE function to find $y_{i,est}$, so the RMSE value becomes as small as possible;

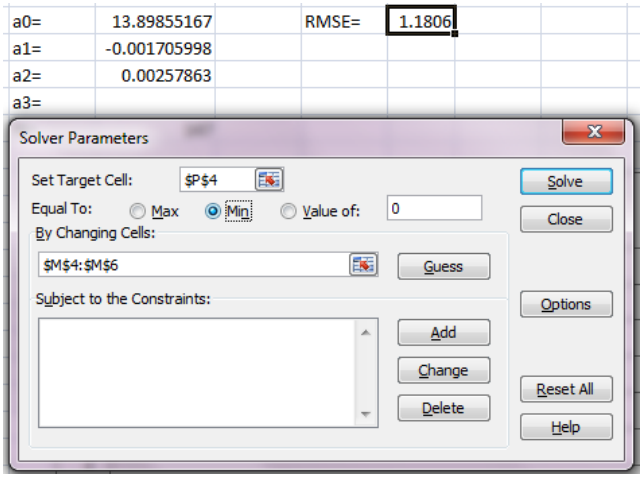

Figure 124: SOLVER dialog box (Microsoft Office Excel 2007)

On Figure 124 the dialog box of the SOLVER function (Microsoft Office Excel 2007) is given. The target cell is the RMSE equation, and the goal is by changing the cells of the fitting constants to make the RMSE as smaller as possible with choosing "min" in the "equal to" conditions.

5. The procedure is iterative and the results of the SOLVE function depend on the initial guess for the fitting constants. Different initial values are chosen until the solution doesn't change significantly. The purpose is to avoid the local minima in RMSE.

7 Appendix: Nitrate Concentrations Plotted vs. Flow Rate (Annually and Monthly)

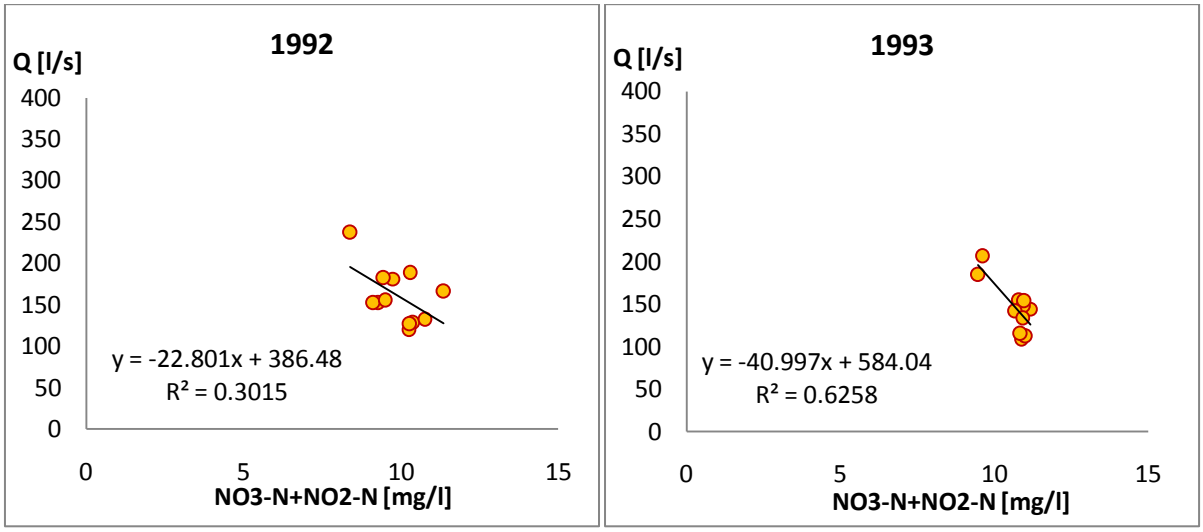

Figure 125: Flow rate vs. NO3-N + NO2-N concentrations for 1992 (left) and 1993 (right)

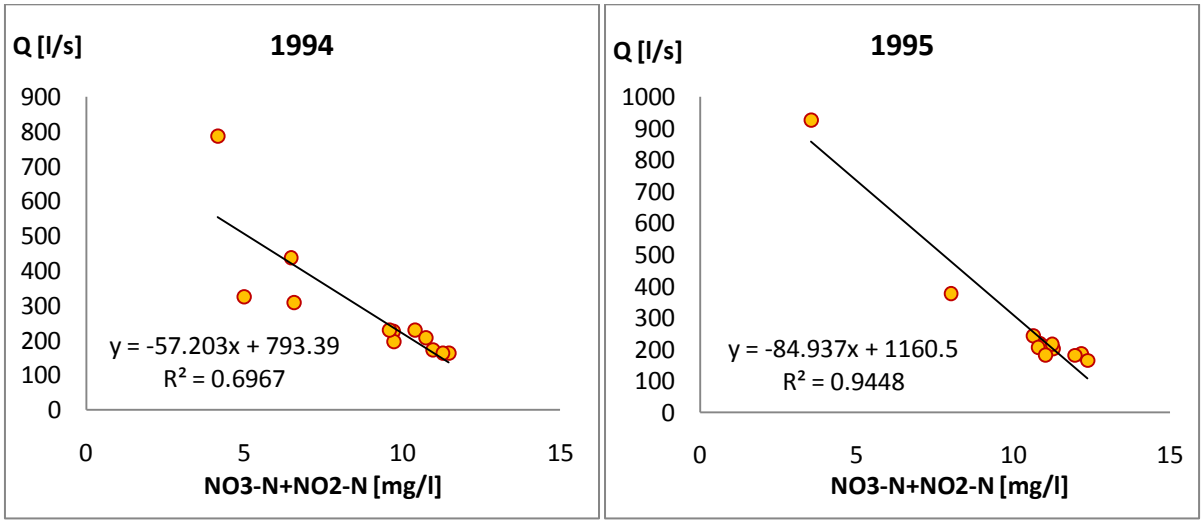

Figure 126: Flow rate vs. NO3-N + NO2-N concentrations for 1994 (left) and 1995 (right)

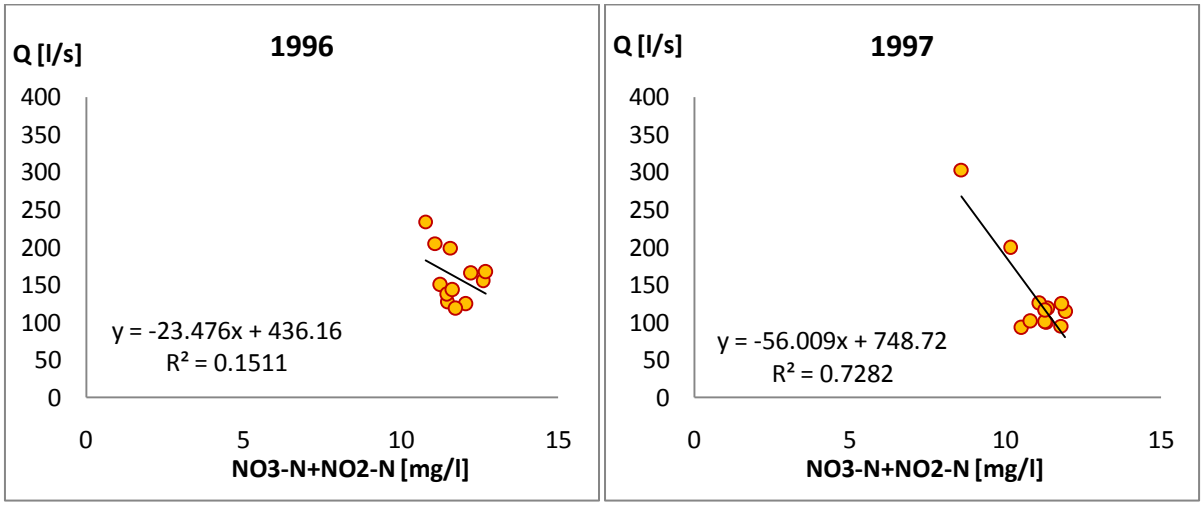

Figure 127: Flow rate vs. NO3-N + NO2-N concentrations for 1996 (left) and 1997 (right)

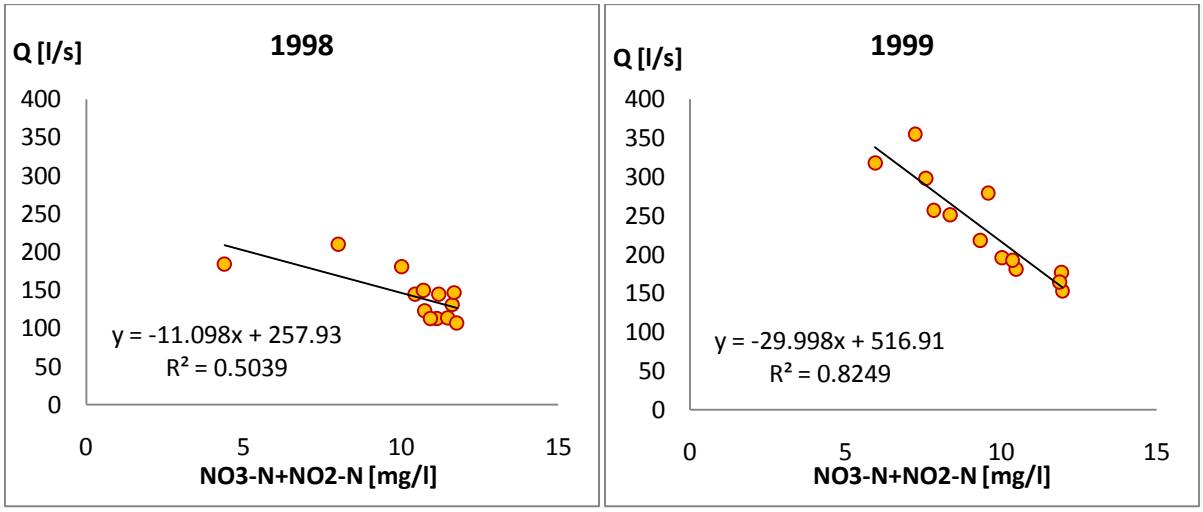

Figure 128: Flow rate vs. NO3-N + NO2-N concentrations for 1998 (left) and 1999 (right)

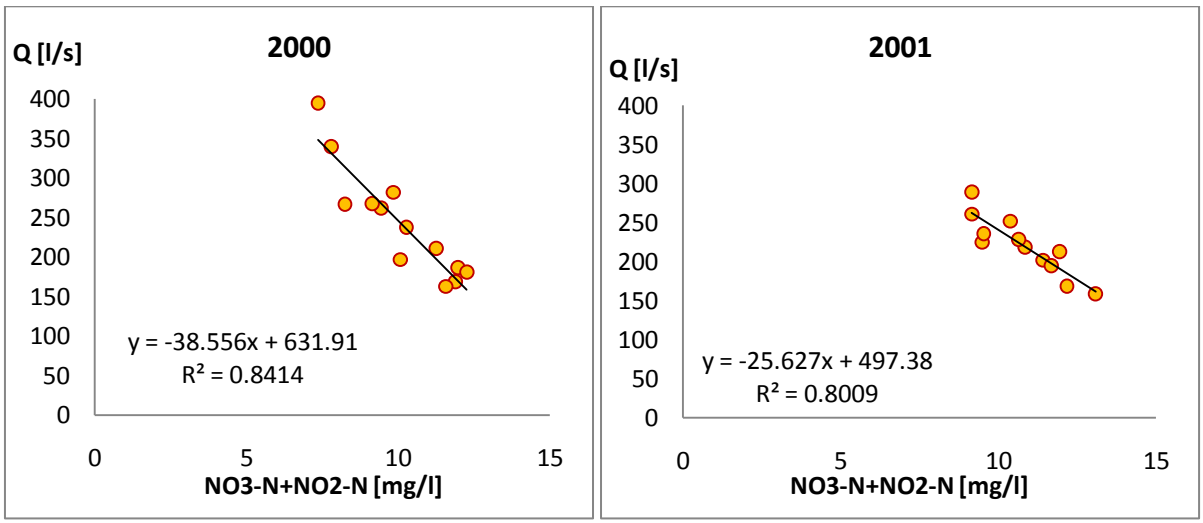

Figure 129: Flow rate vs. NO3-N + NO2-N concentrations for 2000 (left) and 2001 (right)

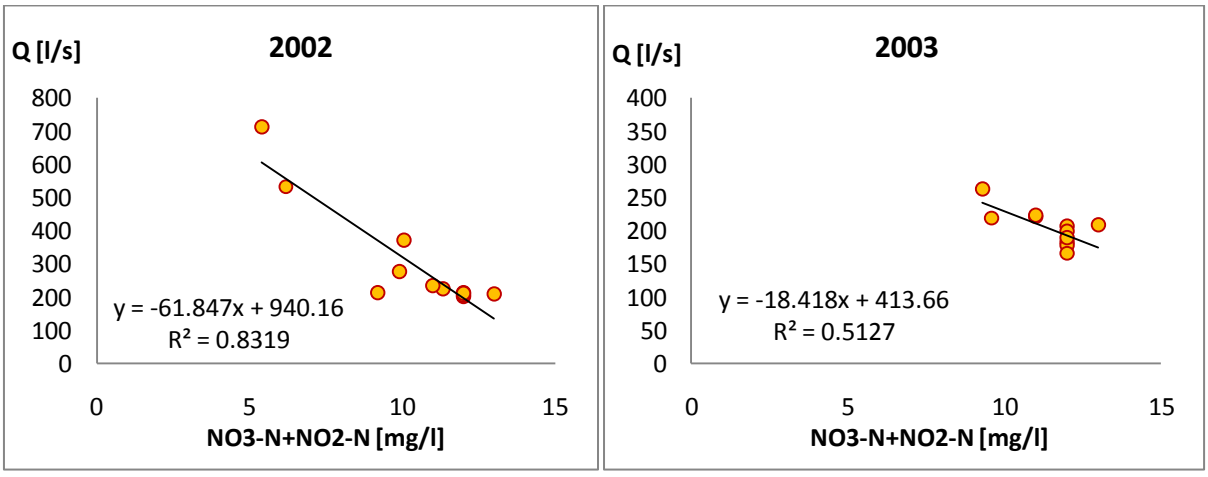

Figure 130: Flow rate vs. NO3-N + NO2-N concentrations for 2002 (left) and 2003 (right)

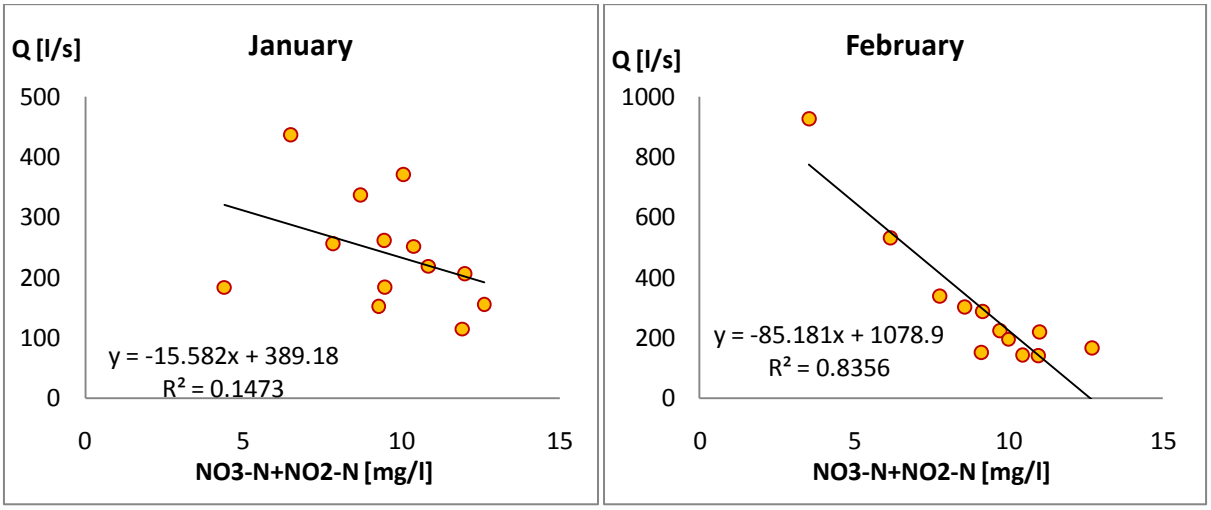

Figure 131: Flow rate vs. NO3-N + NO2-N concentrations for January (left) and February (right)

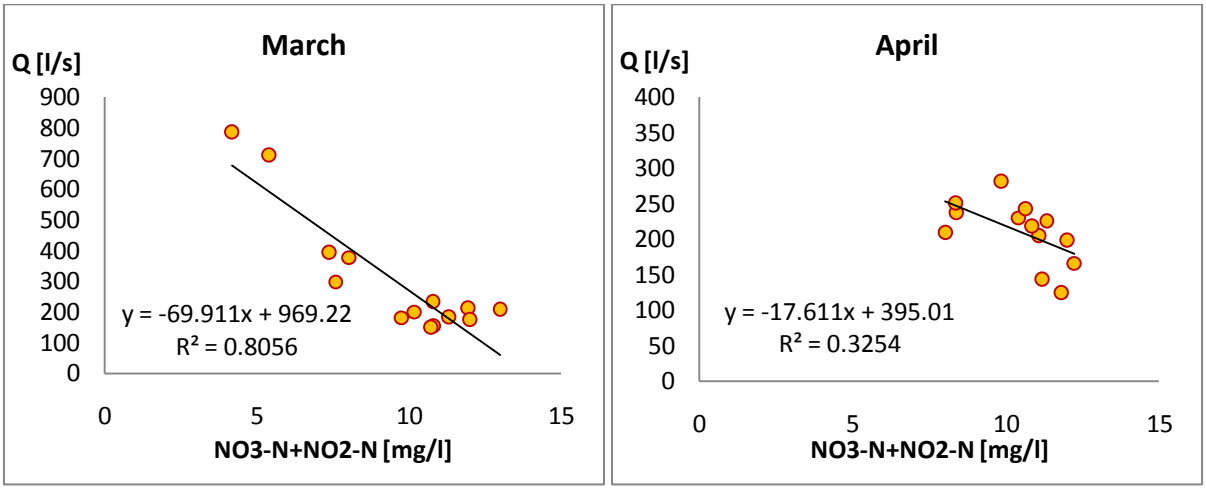

Figure 132: Flow rate vs. NO3-N + NO2-N concentrations for March (left) and April (right)

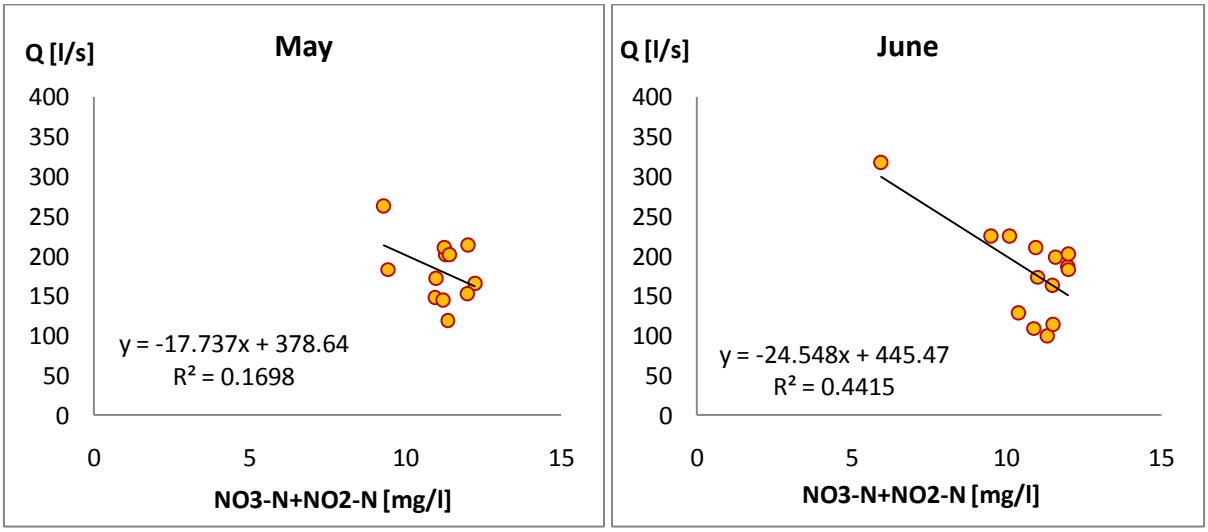

Figure 133: Flow rate vs. NO3-N + NO2-N concentrations for May (left) and June (right)

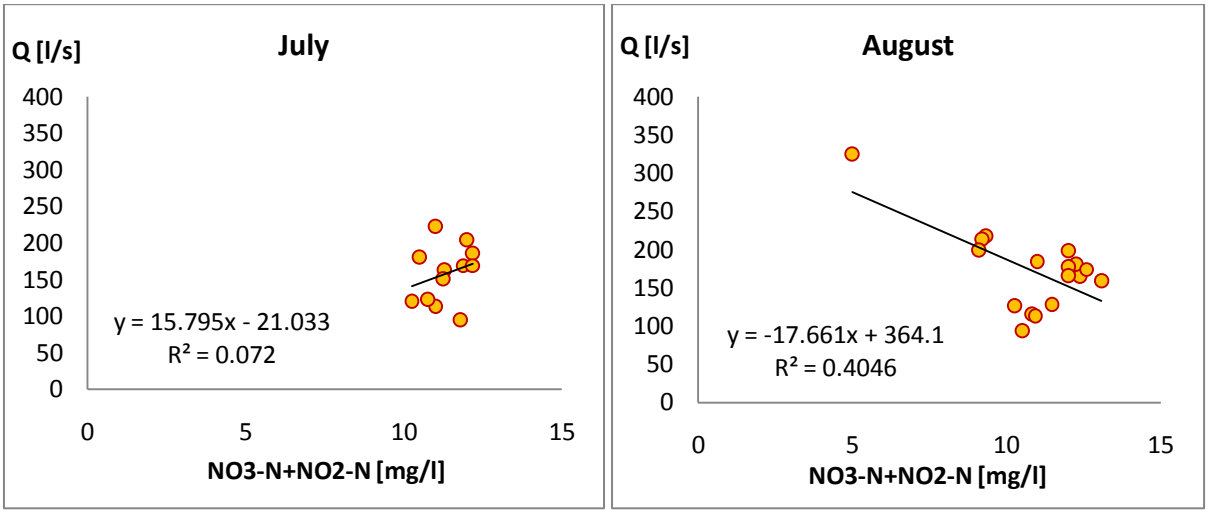

Figure 134: Flow rate vs. NO3-N + NO2-N concentrations for July (left) and August (right)

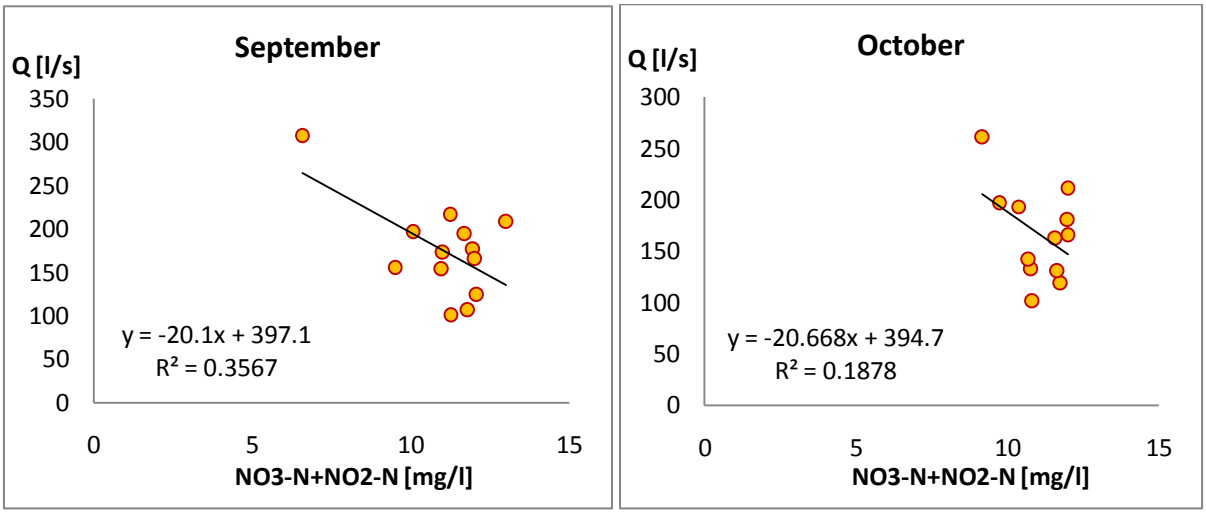

Figure 135: Flow rate vs. NO3-N + NO2-N concentrations for September (left) and October (right)

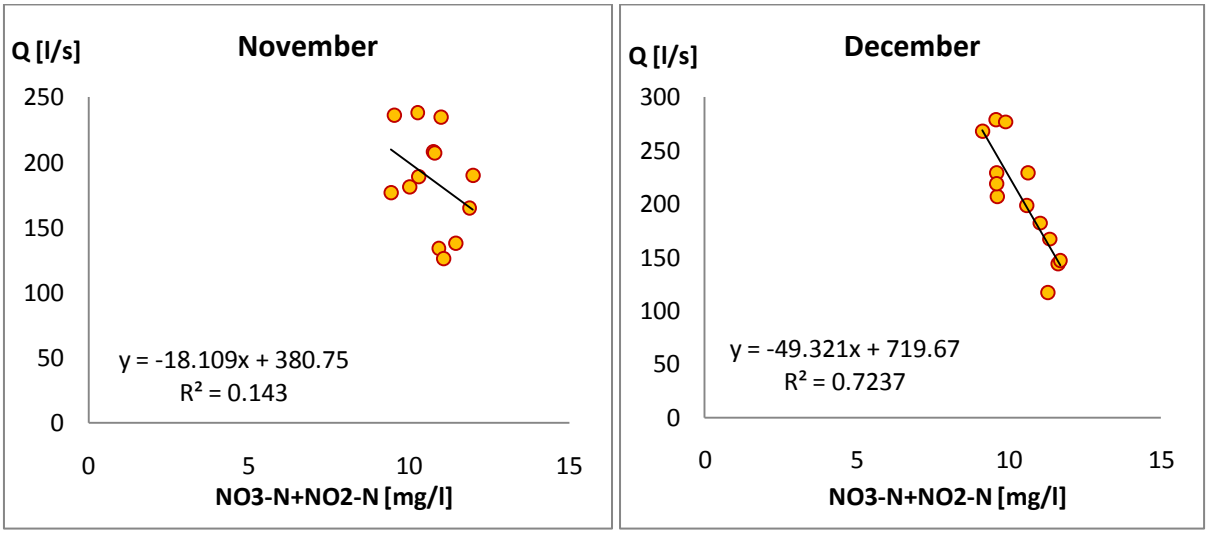

Figure 136: Flow rate vs. NO3-N + NO2-N concentrations for November (left) and December (right)

8 Appendix: Regression Analysis (Additional Figures)

Linear regression (original data set)

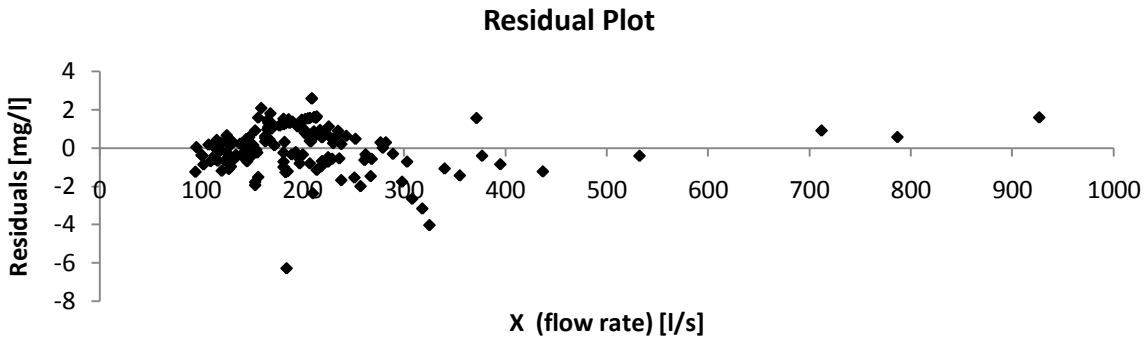

Figure 137: Residual plot of the linear regression (original data set)

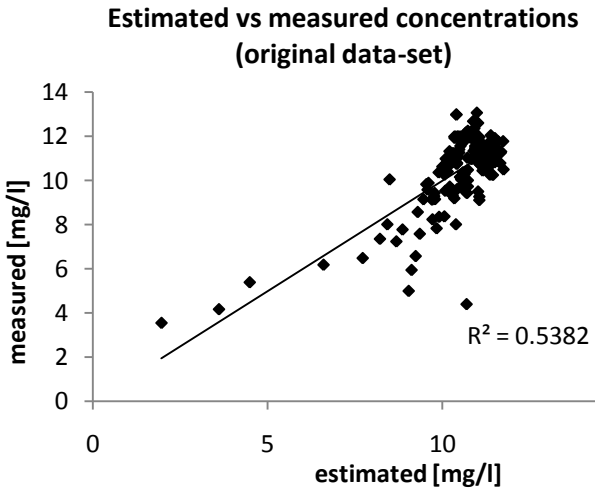

Figure 138: Estimated vs. measured concentrations (original data-set)

Table 17: Regression summary output (original data-set)

Regression Statistics	
R	0.734
R^2	0.538
RMSE	1.225
Observations	147

Linear regression (changed data set)

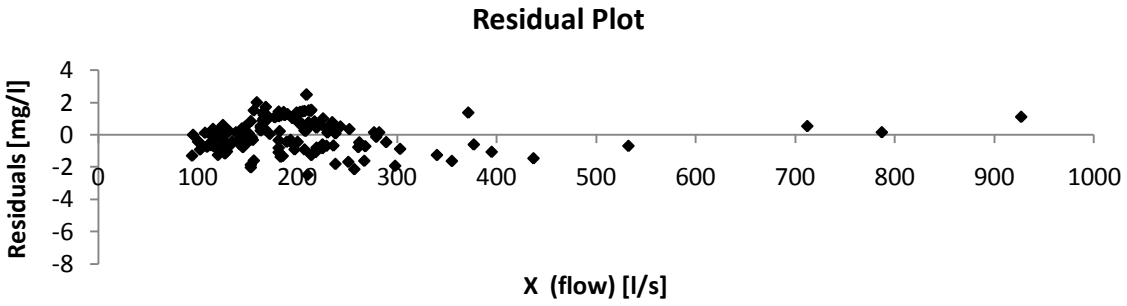

Figure 139: Residual plot of the linear regression (changed data-set)

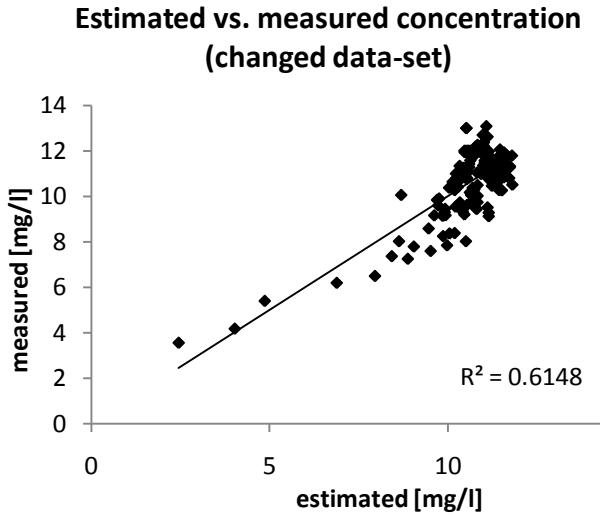

Figure 140: Estimated versus measured concentrations (changed data-set)

Table 18: Regression summary output (changed data-set)

Regression Statistics	
R	0.784
R^2	0.615
RMSE	1.003
Observations	143

Non-linear regression (original data set)

Table 19: Non-linear regression equations and regression coefficients (original data set)

equations	RMSE	regression constants		
		a_0	a_1	a_2
$Y_{est}=a_0+a_1/X_i\text{^}2$	1.601	9.212738	34417.67	-
$Y_{est}=a_0+a_1/X_i\text{^}a_2$	1.600	9.138019	34417.67	1.987965
$Y_{est}=(\exp(a_0*X))*a_1+a_2$	1.203	-0.00093	18.27922	-4.72213
$Y_{est}=a_0*\exp(a_1*X_i)$	1.207	13.867	-0.00142	-
$Y_{est}=a_0*\exp(a1*X_i)+a2*X_{i-1}$	**1.181**	**13.899**	**-0.0017**	**0.0026**

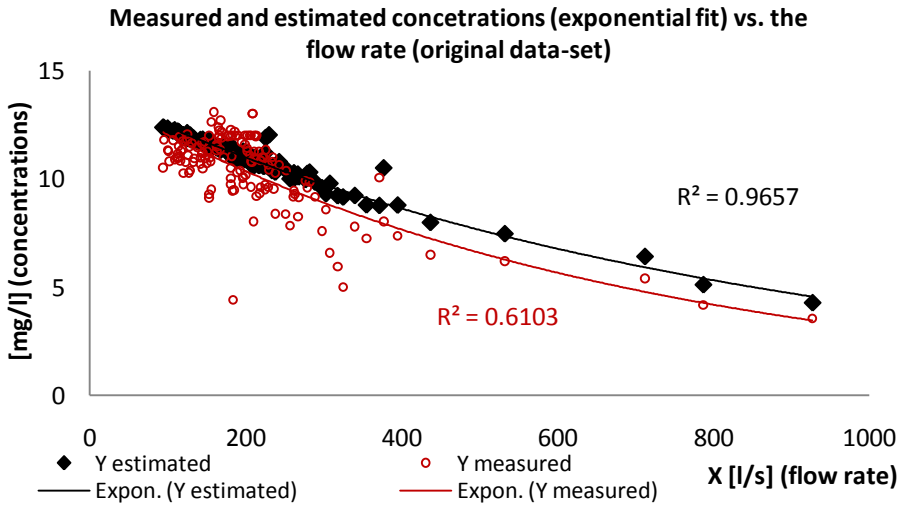

Figure 141: Measured and estimated concentrations (exponential fit) vs. flow rate (original data set)

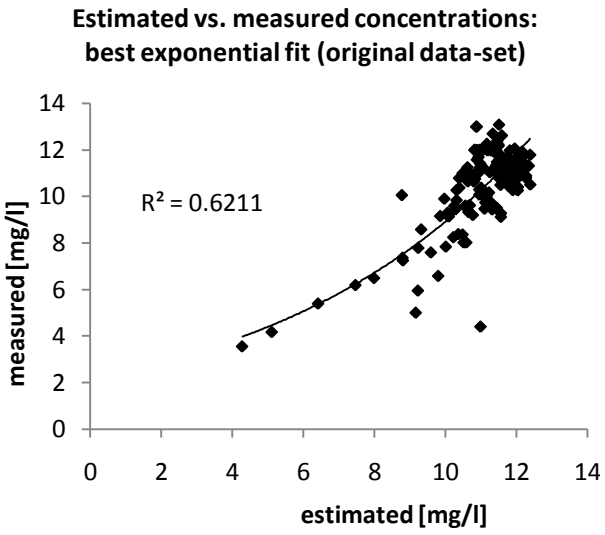

Figure 142: Estimated versus measured concentrations: best exponential fit (original data set)

Table 20: Regression summary for the exponential best fit (original data set)

Regression Statistics	
R	0.788
R Square	0.6211
RMSE	1.181
Observations	147

Non-linear regression (changed data set)

Table 21: Non-linear regression equations and regression coefficients (changed data-set)

equation	RMSE	regression constants		
		a_0	a_1	a_2
Y_{est} =a0*exp(a1*x)	1.360	14.007	-0.001	-
Y_{est} =a0*exp(a1*x)	1.005	13.68024	-0.0013	-
$Y_{est} = a_0 * \exp(a_1 * x_i) + a_2 * x_i$	**0.993**	**13.1748**	**-0.0007**	**-0.00427**
$Y_{est} = a_0 * \exp(a_1 * x_i) + a_2 * x_{i-1}$	0.988	13.67857	-0.00149	0.001859

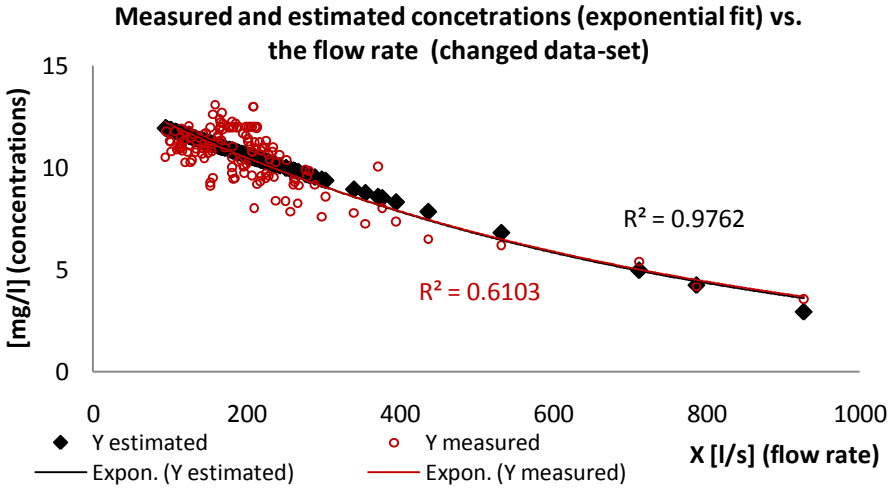

Figure 143: Measured and estimated concentrations (exponential fit) vs. flow rate (changed data-set)

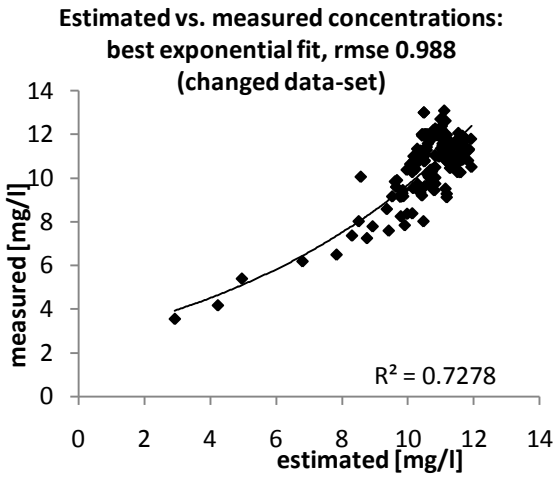

Figure 144: Estimated versus measured concentrations: best exponential fit (changed data set)

Table 22: Regression summary for the exponential best fit (changed data set)

Regression Statistics	
R	0.853
R Square	0.728
RMSE	0.993
Observations	143

9 Appendix: Field Observations and Thermo Imaging

The following observations were made together with Nature Agency (Aalborg) and some of the pictures were taken by them.

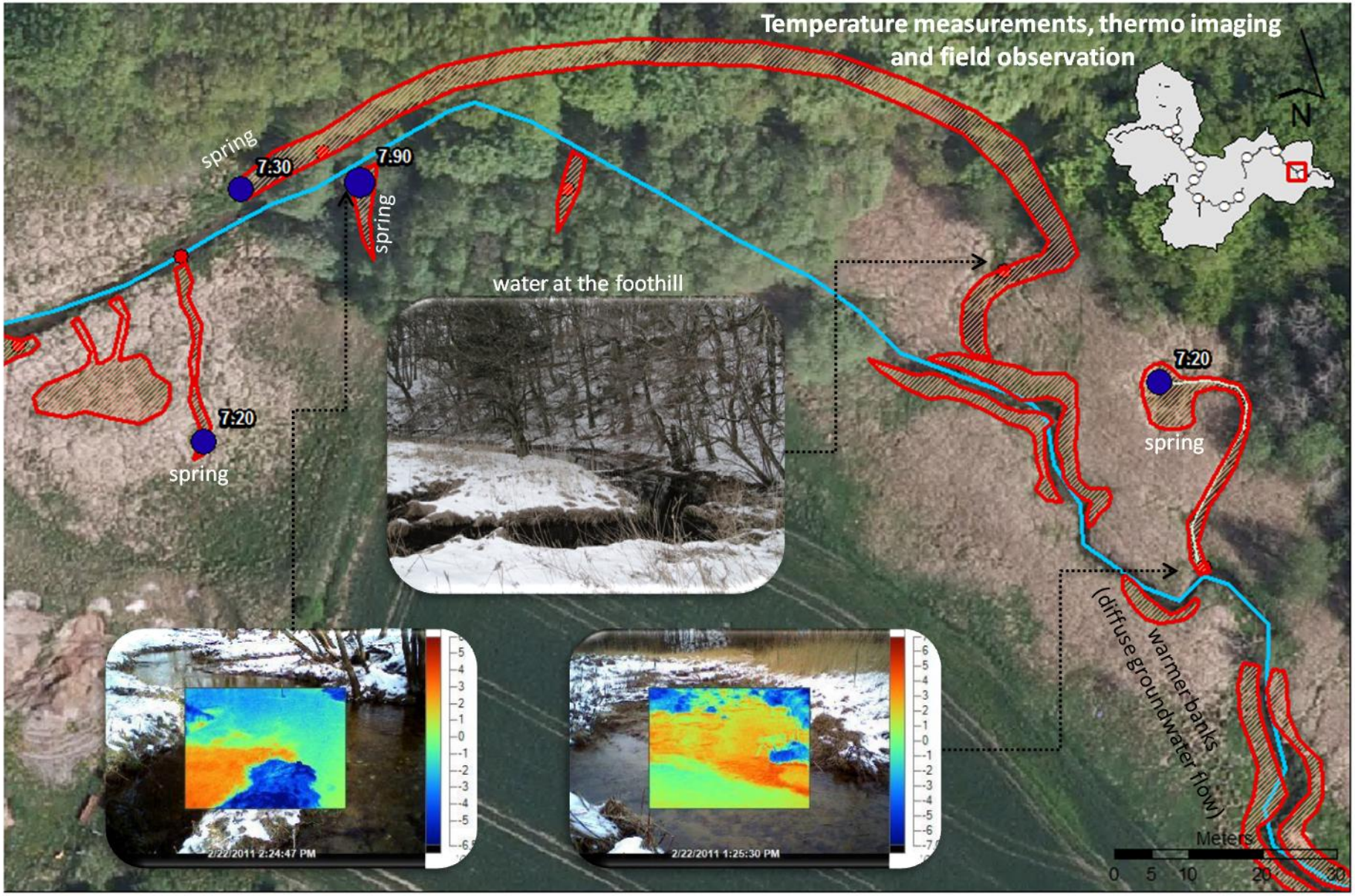

Figure 145: Field observation, temperature measurements, and thermo imaging (2/11)

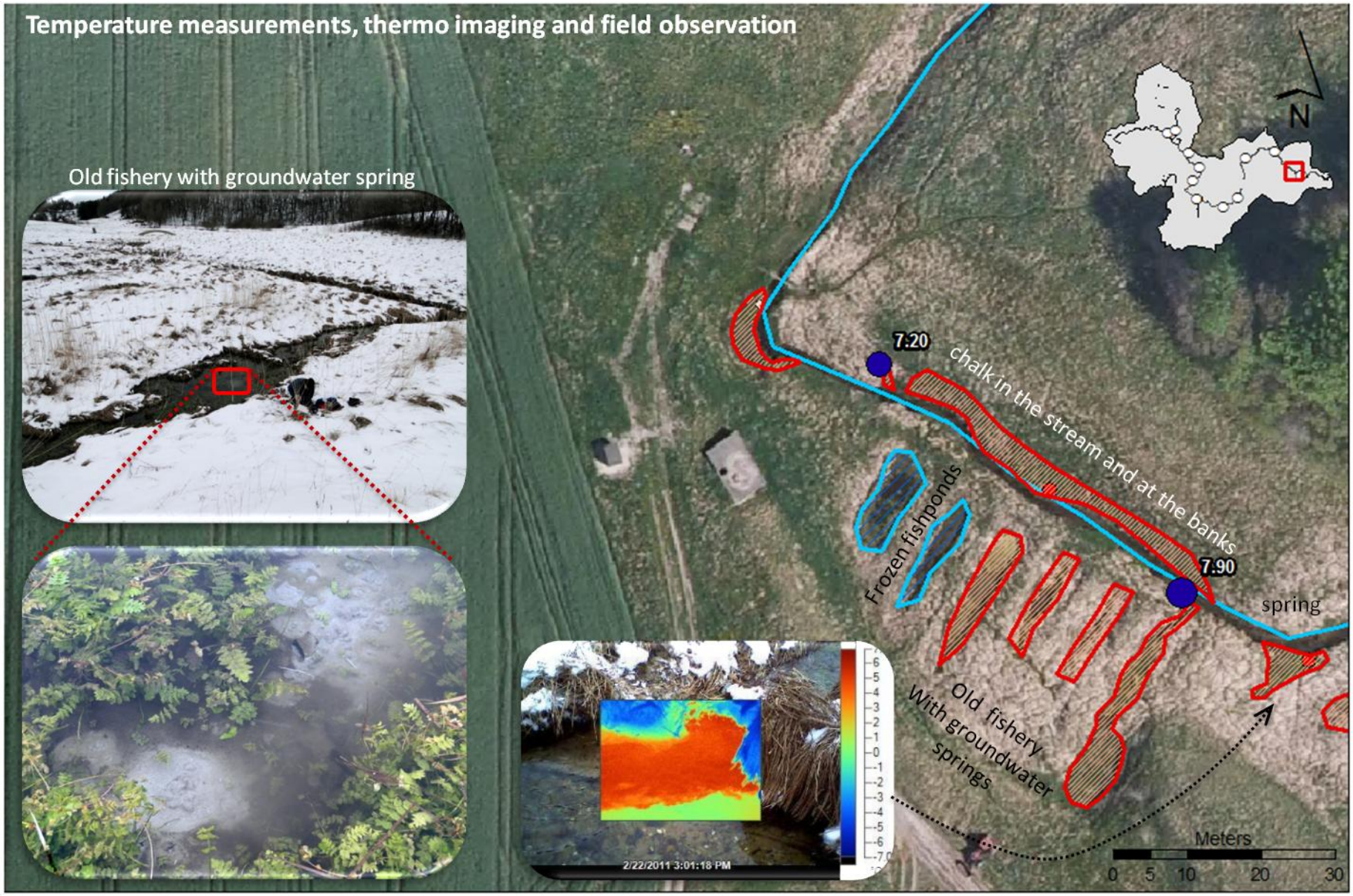

Figure 146: Field observation, temperature measurements, and thermo imaging (3/11)

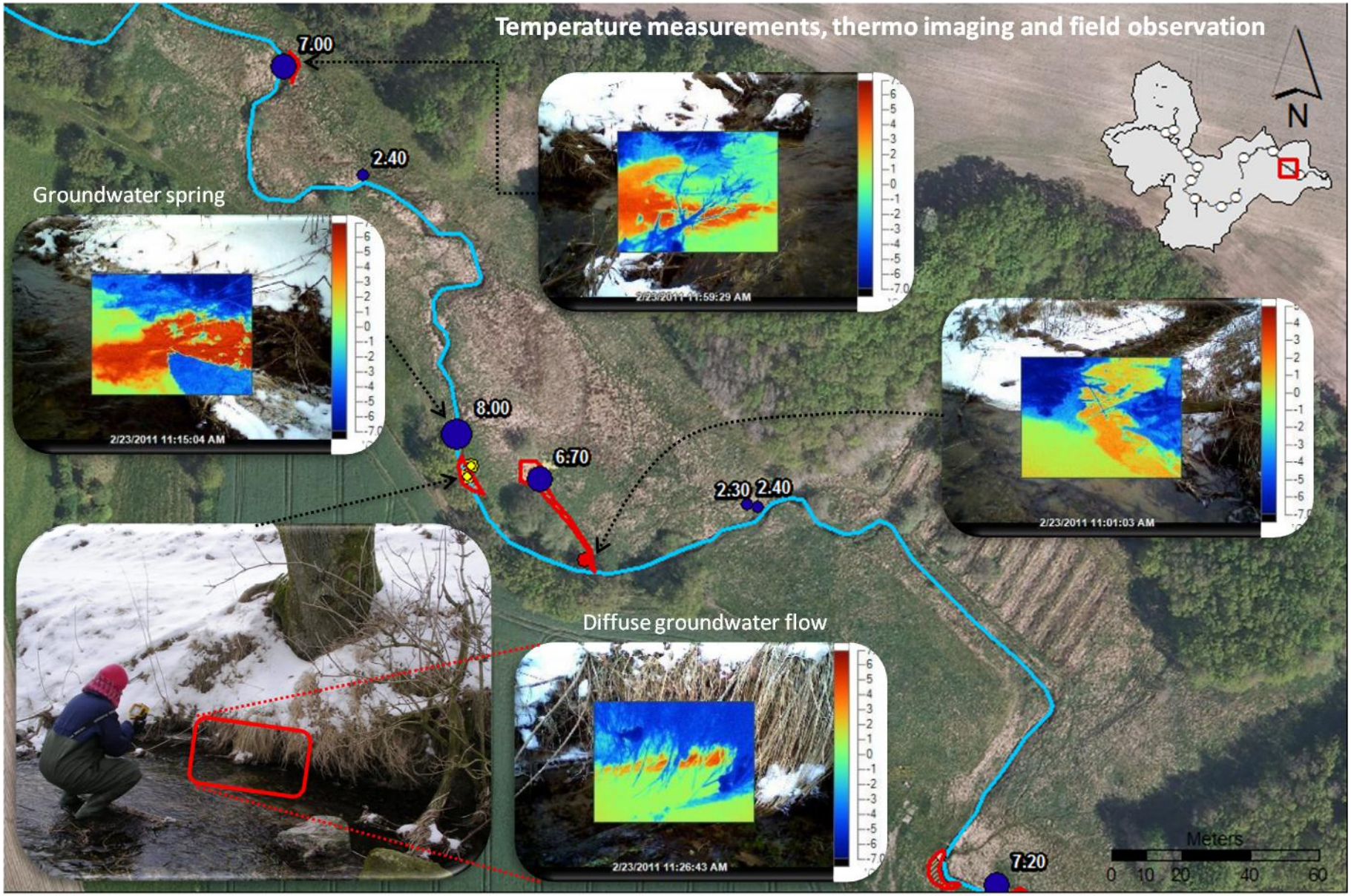

Figure 147: Field observation, temperature measurements, and thermo imaging (4/11)

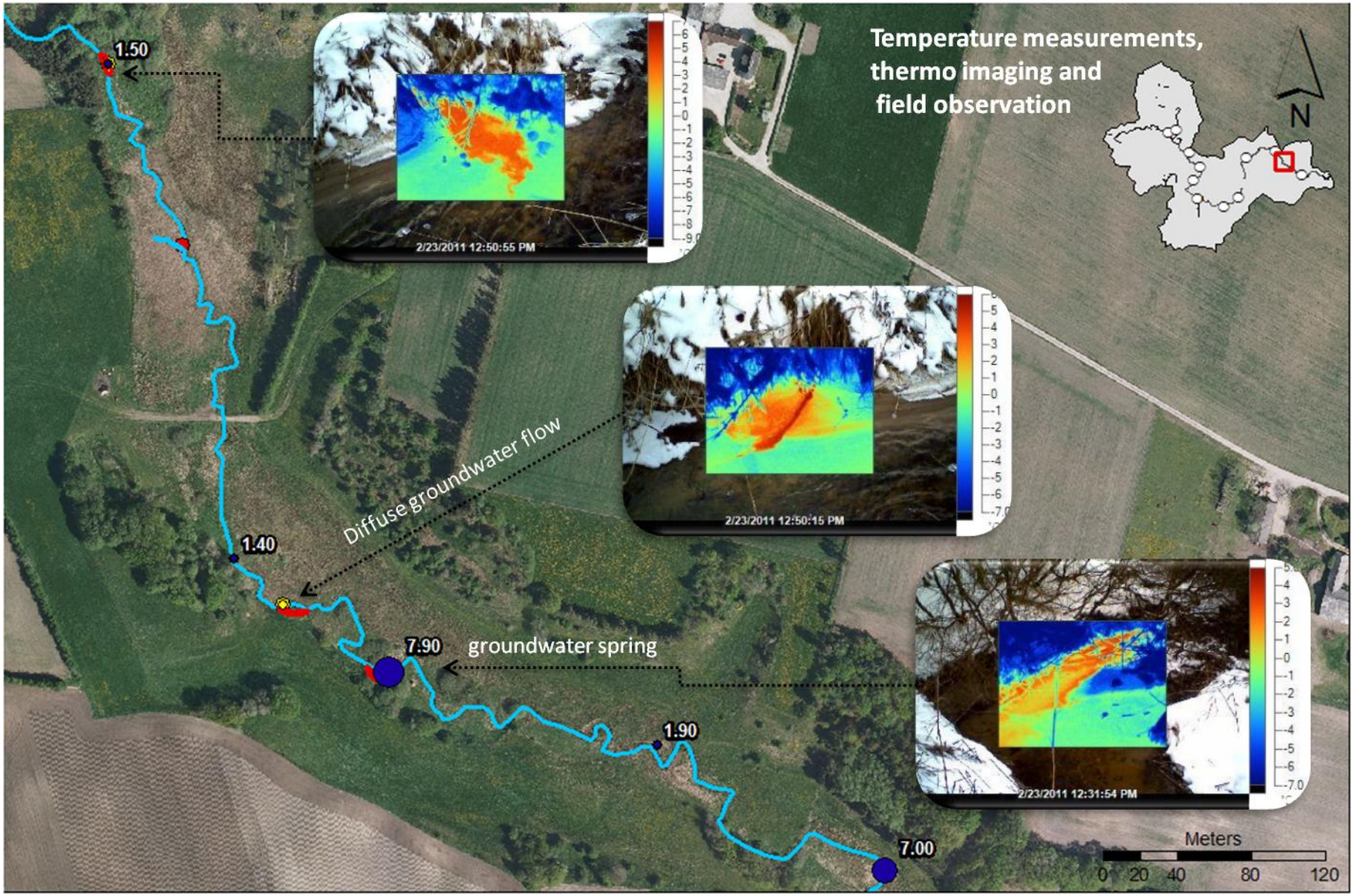

Figure 148: Field observation, temperature measurements, and thermo imaging (5/11)

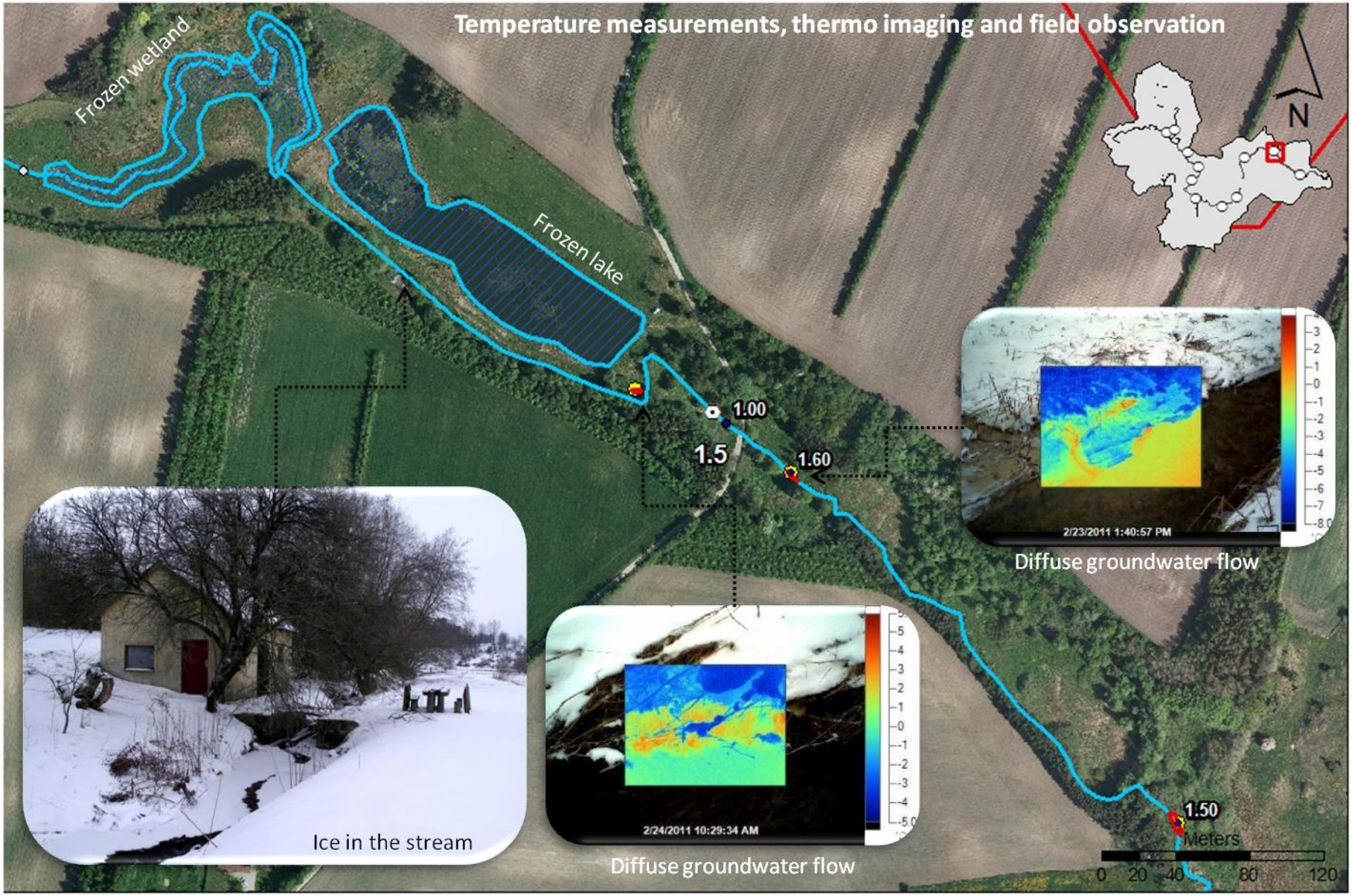

Figure 149: Field observation, temperature measurements, and thermo imaging (6/11)

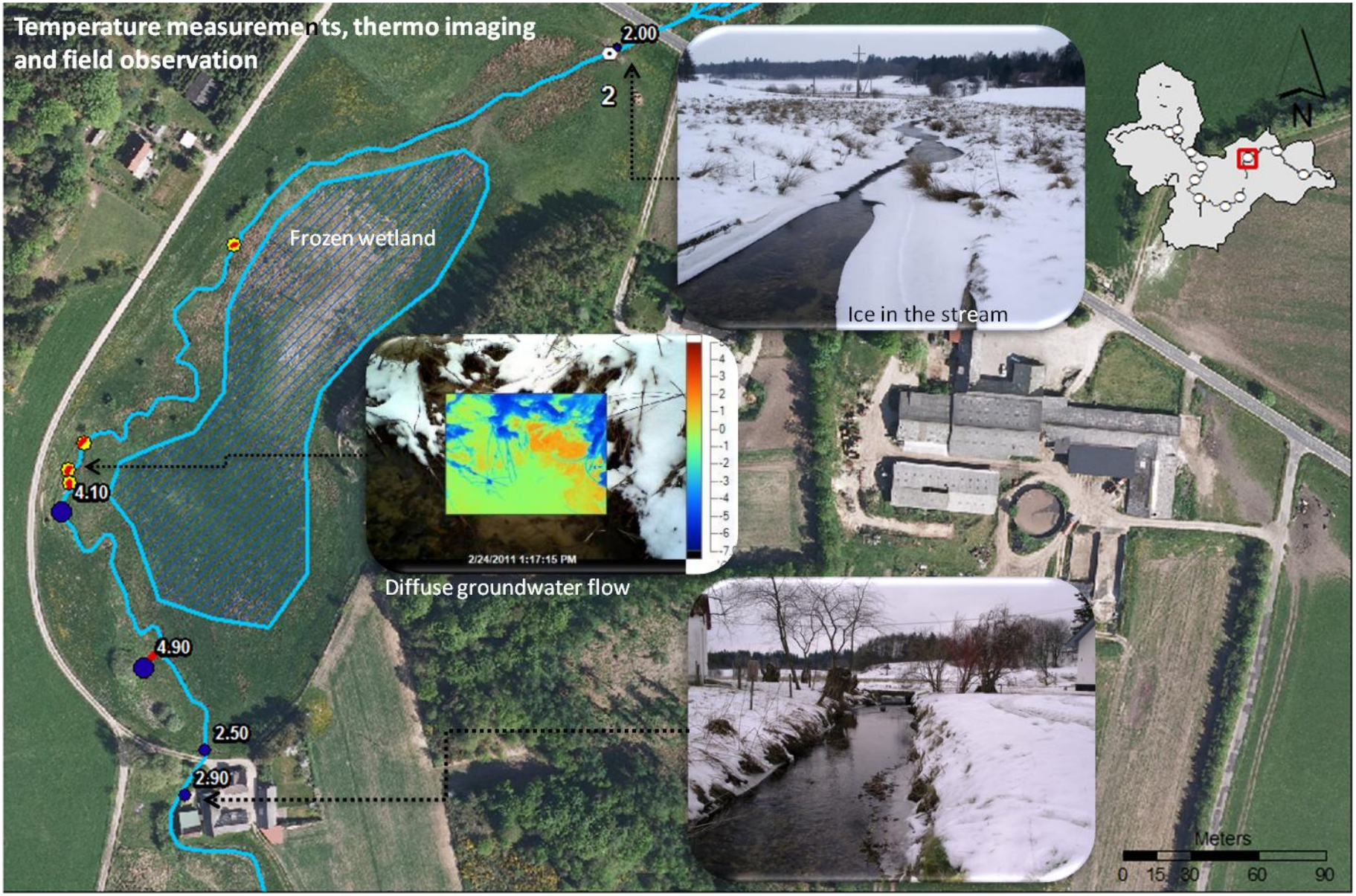

Figure 150: Field observation, temperature measurements, and thermo imaging (7/11)

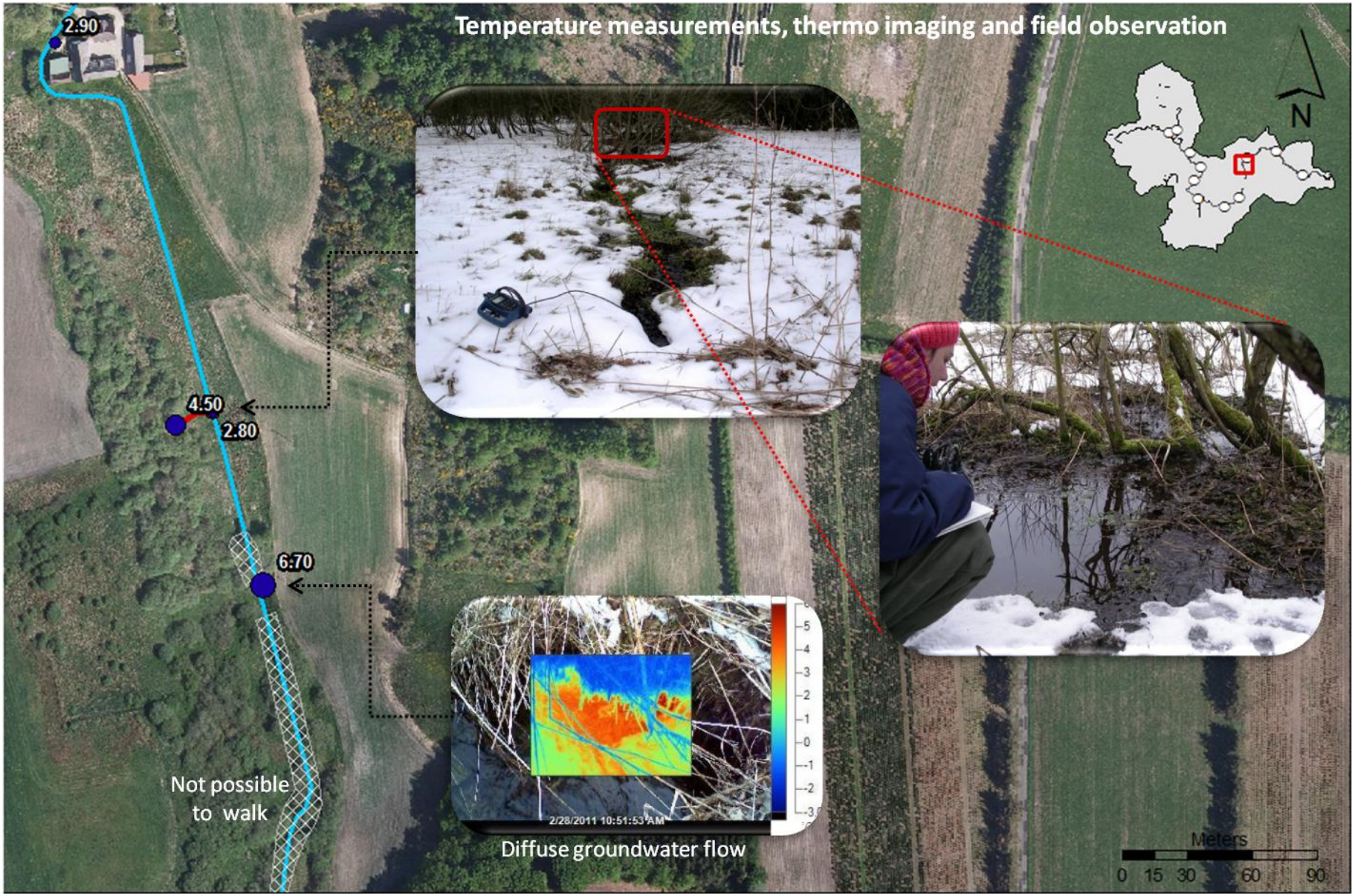

Figure 151: Field observation, temperature measurements, and thermo imaging (8/11)

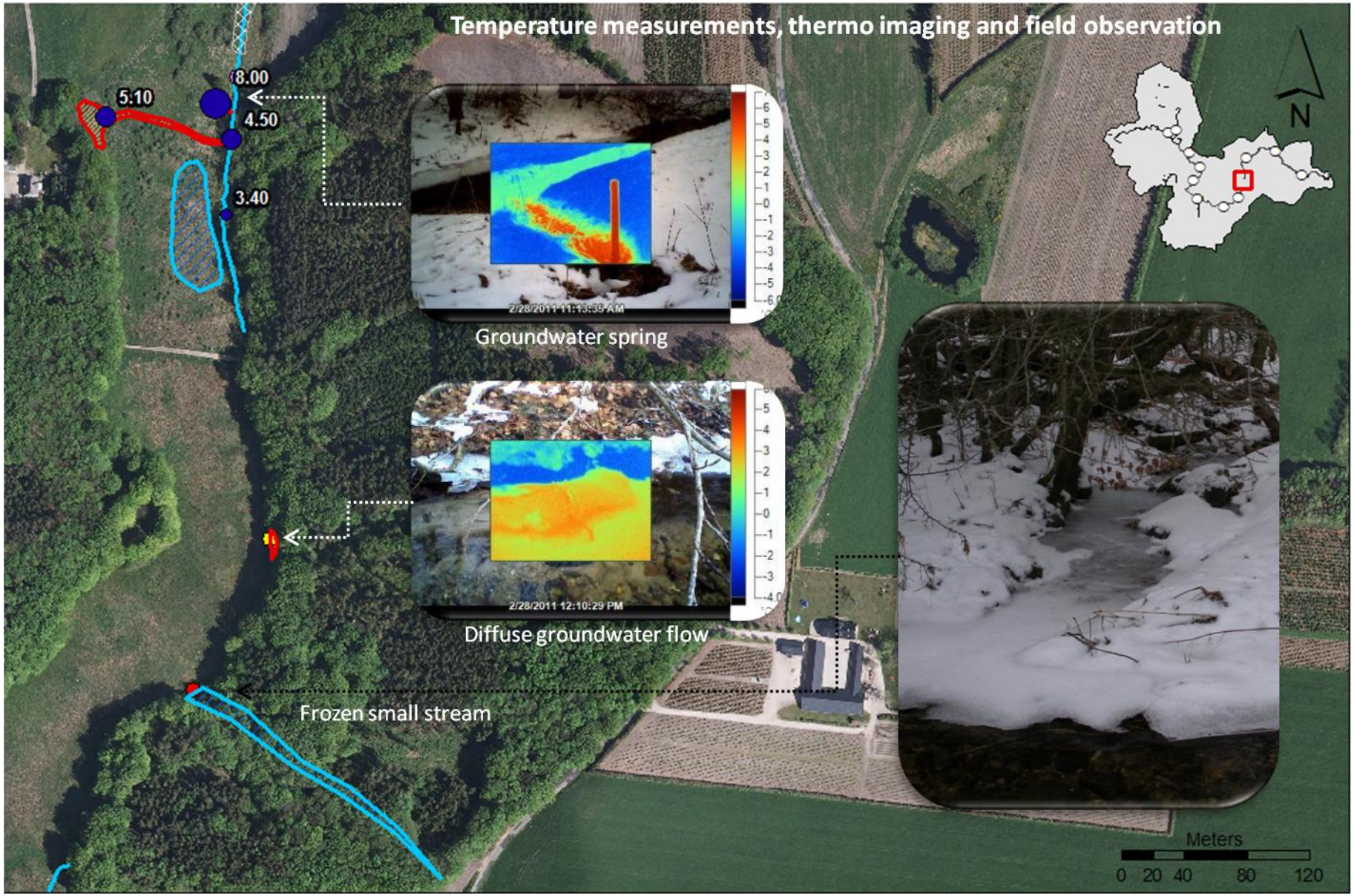

Figure 152: Field observation, temperature measurements, and thermo imaging (9/11)

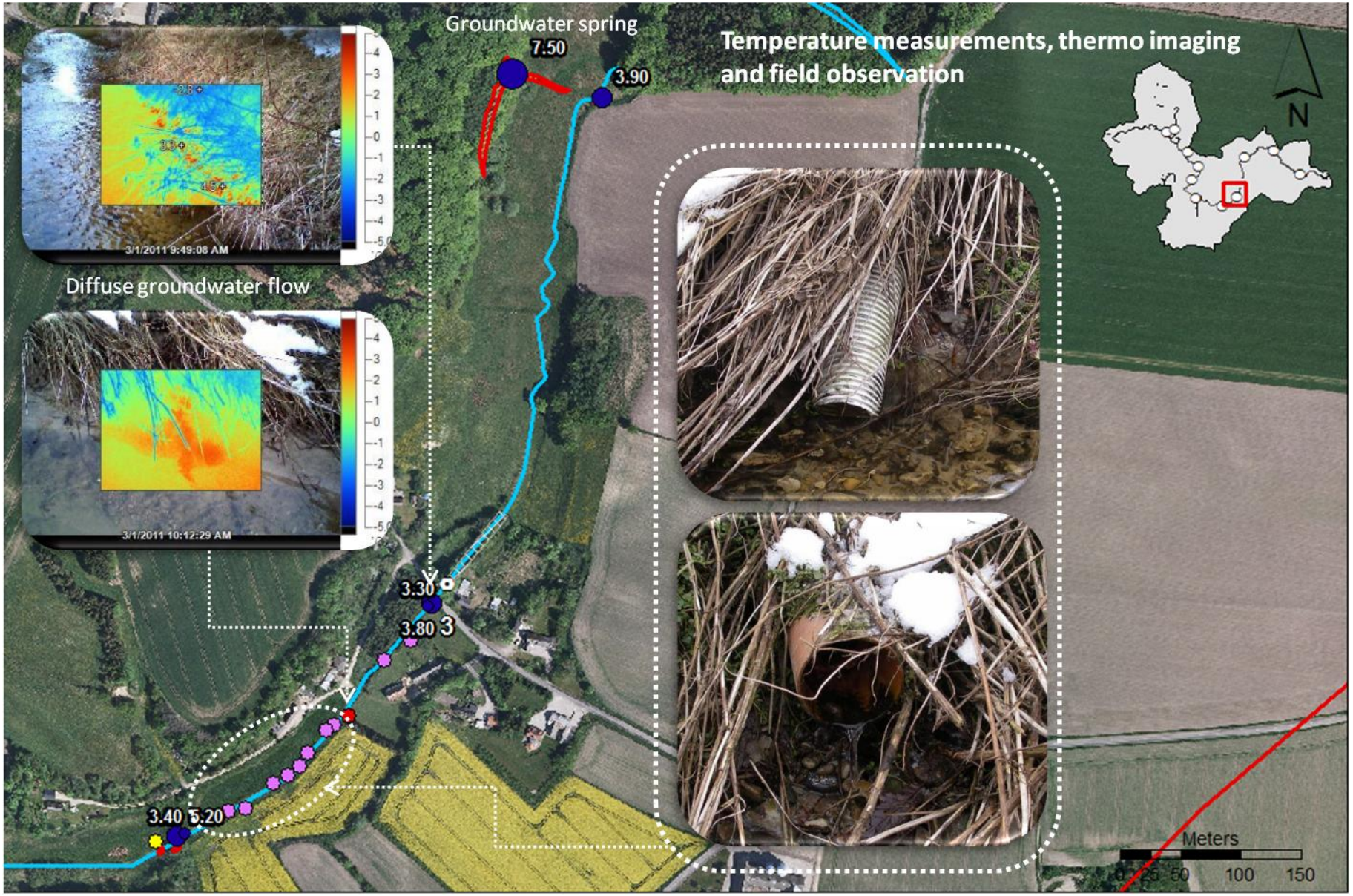

Figure 153: Field observation, temperature measurements, and thermo imaging (10/11)

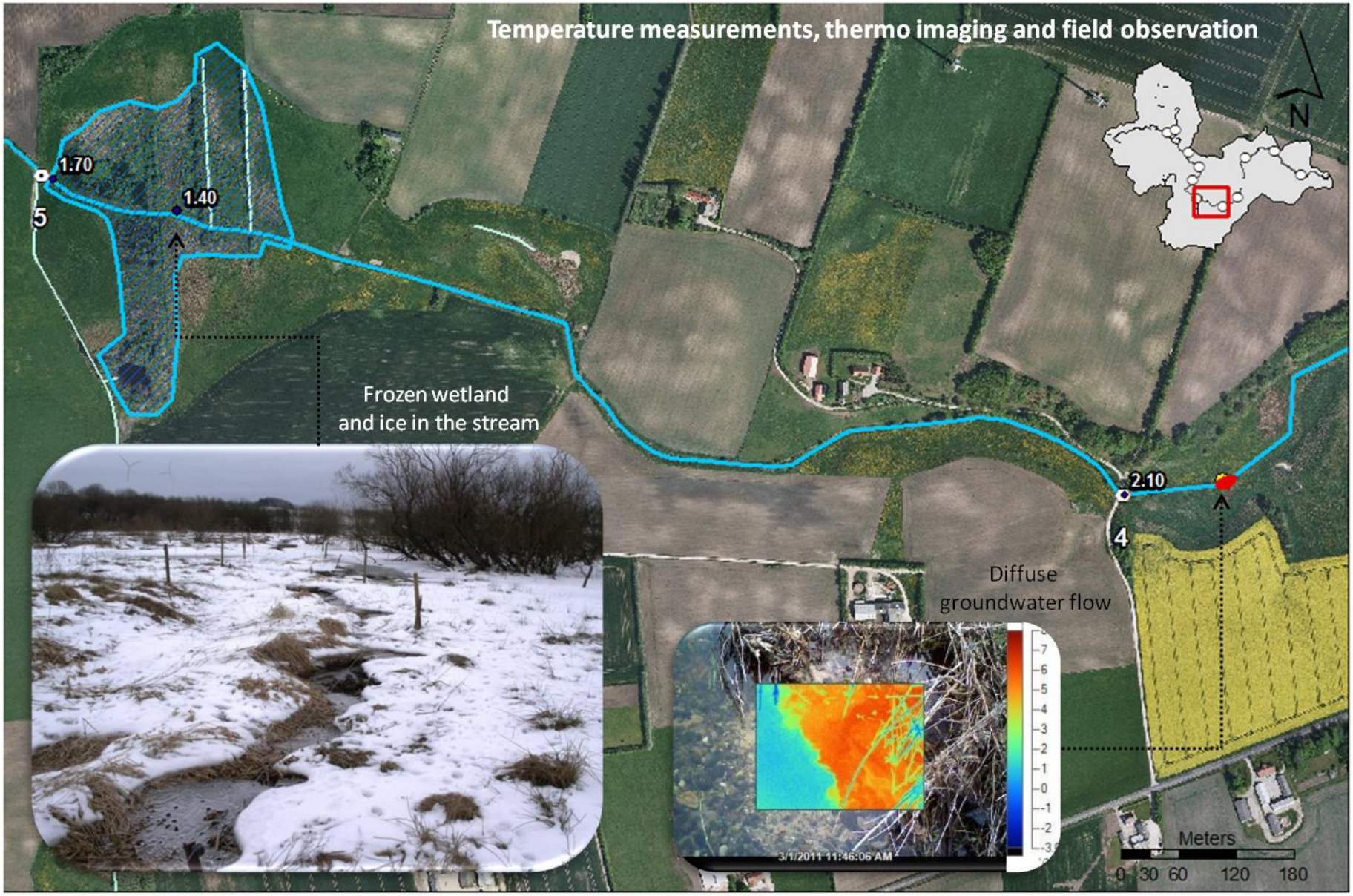

Figure 154: Field observation, temperature measurements, and thermo imaging (11/11)

10 Appendix: Field Measurements

Nitrate-n and Nitrite-N Measurements at the Stream (11stations)

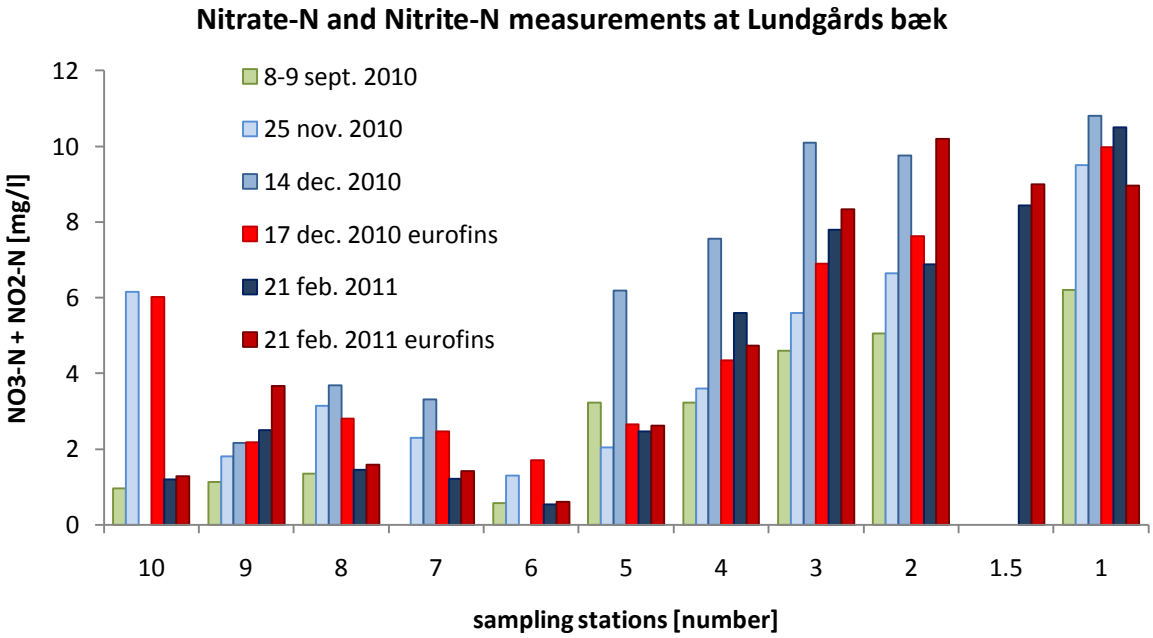

Figure 155: NO3-N-N and NO2-N-N concentrations for the sampling stations (st.1-st.10)

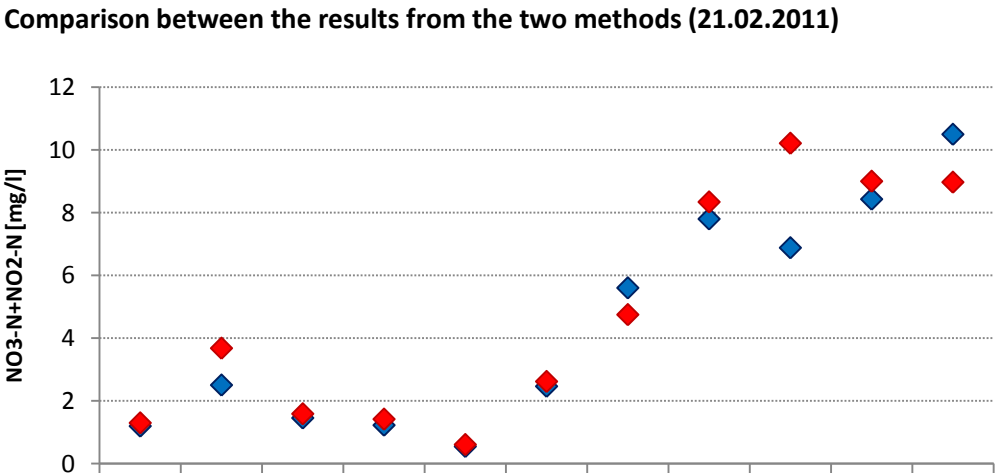

sampling st.	10	9	8	7	6	5	4	3	2	1.5	1
photometer	1.19	2.5	1.45	1.22	0.54	2.46	5.6	7.8	6.88	8.43	10.5
eurofins lab	1.29	3.67	1.58	1.41	0.6	2.61	4.74	8.33	10.2	8.99	8.96

Figure 156: Comparison between the results from the two methods used to analyse the samples from 21st February 2010

Measured temperatures at the stream

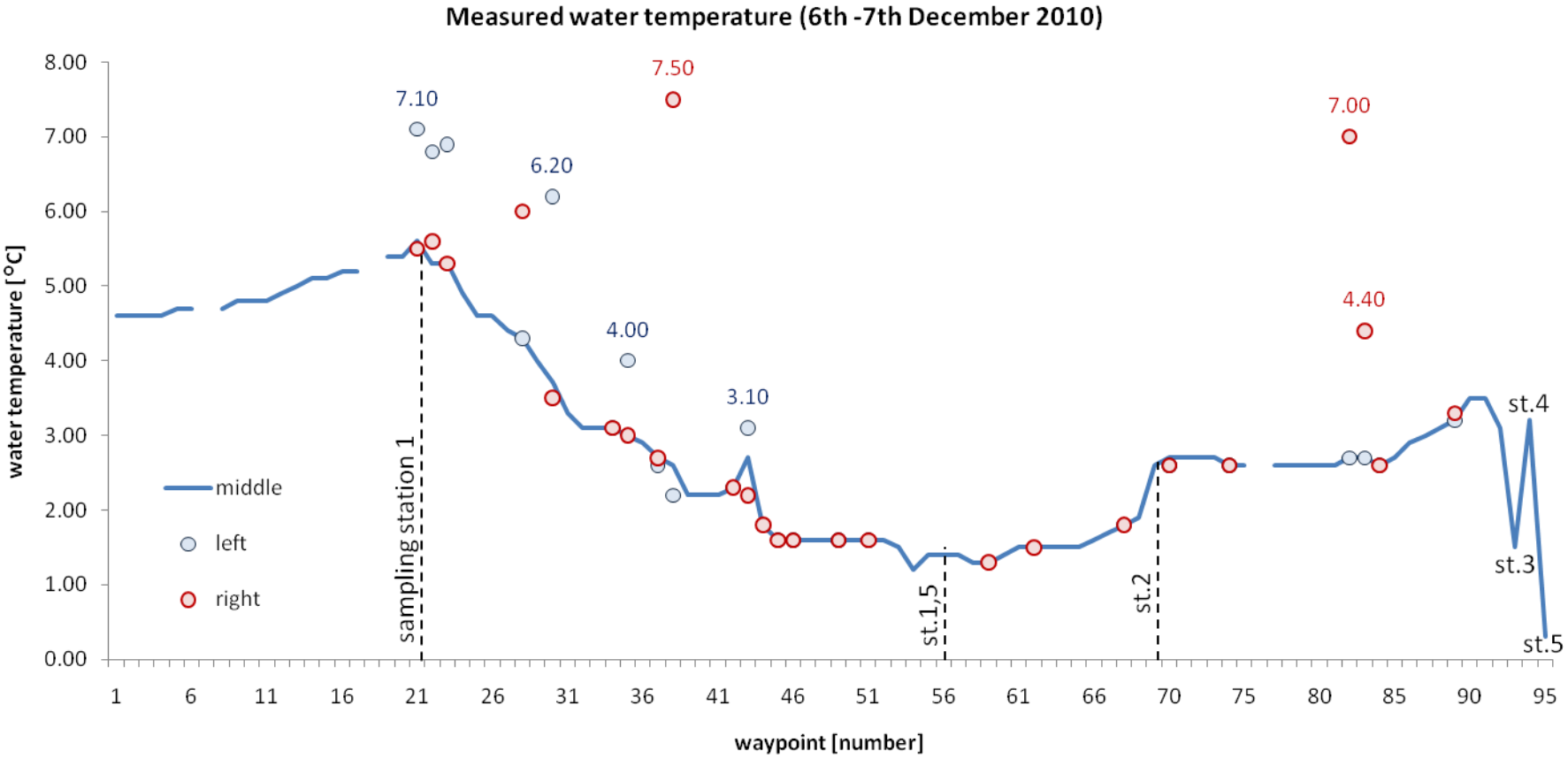

Figure 157: Measured water temperatures of (6th-7th December 2010); the left and right directions are when looking against the water flow direction (data: Miljøcenter,2010)

Groundwater springs – results from the measurements

Table 23: Results from the measurements for the groundwater springs

Sample number	Waypoint number	NO3-N+NO2-N mgN/l	PO4-P mgP/l	temperature °C	oxygen mg/l
1	3	10.00	0.08	8.20	4.50
2	9	9.00	0.11	5.30	5.60
3	11	10.26	0.10	8.00	5.40
4	14	11.30	0.07	7.20	5.90
5	18	9.31	0.08	7.30	5.40
6	19	11.65	0.06	7.90	5.80
7	22	10.65	0.13	7.20	4.60
8	24	15.80	0.11	7.90	7.30
9	26	14.70	0.06	7.20	5.60
1	34	12.30	0.11	**8.00**	**11.80**
2	37	11.80	0.08	**7.00**	**8.70**
3	40	11.60	0.11	**7.90**	**7.50**
1	61	6.66	0.06	**4.10**	**4.70**
2	63	4.99	0.09	**4.90**	**9.40**
1	67	3.64	0.09	**4.50**	**1.90**
2	70	11.60	0.13	**8.00**	**1.70**
3	72	5.27	0.12	**5.10**	**8.60**
4	79	6.66	0.09	**7.50**	**6.10**
1	95	9.27	0.05	-	-
2	99	13.20	0.17	-	-

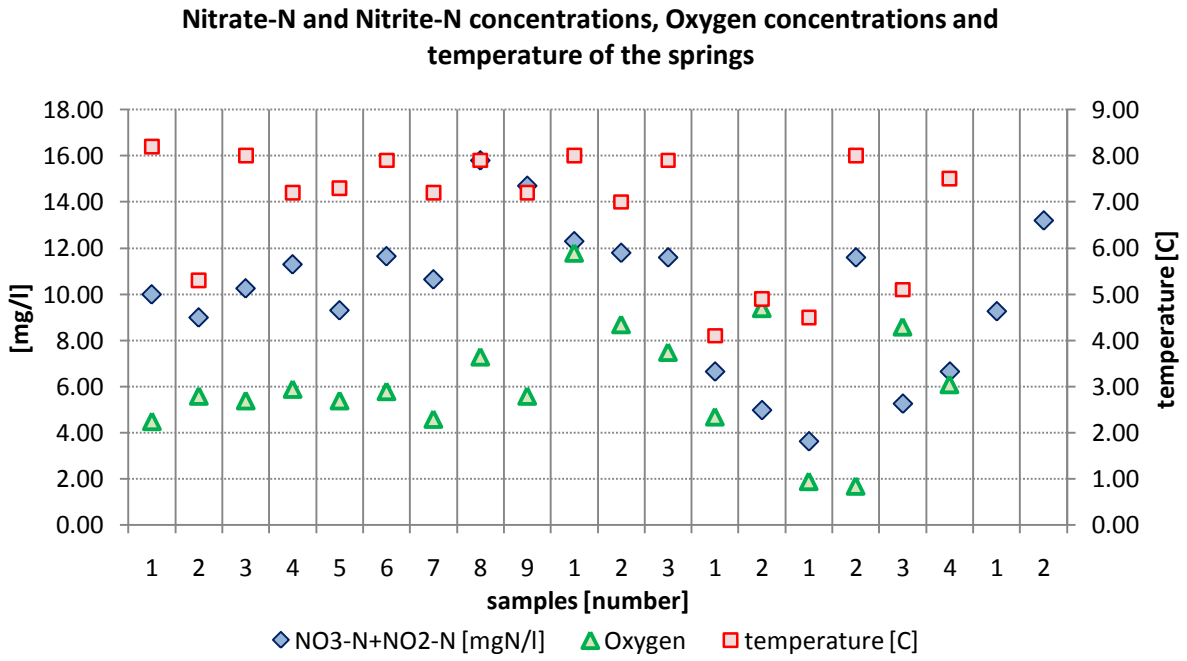

Figure 158: Measured NO3-N-N and NO2-N-N concentrations, Oxygen concentrations and temperature

11 Appendix: Residence Times

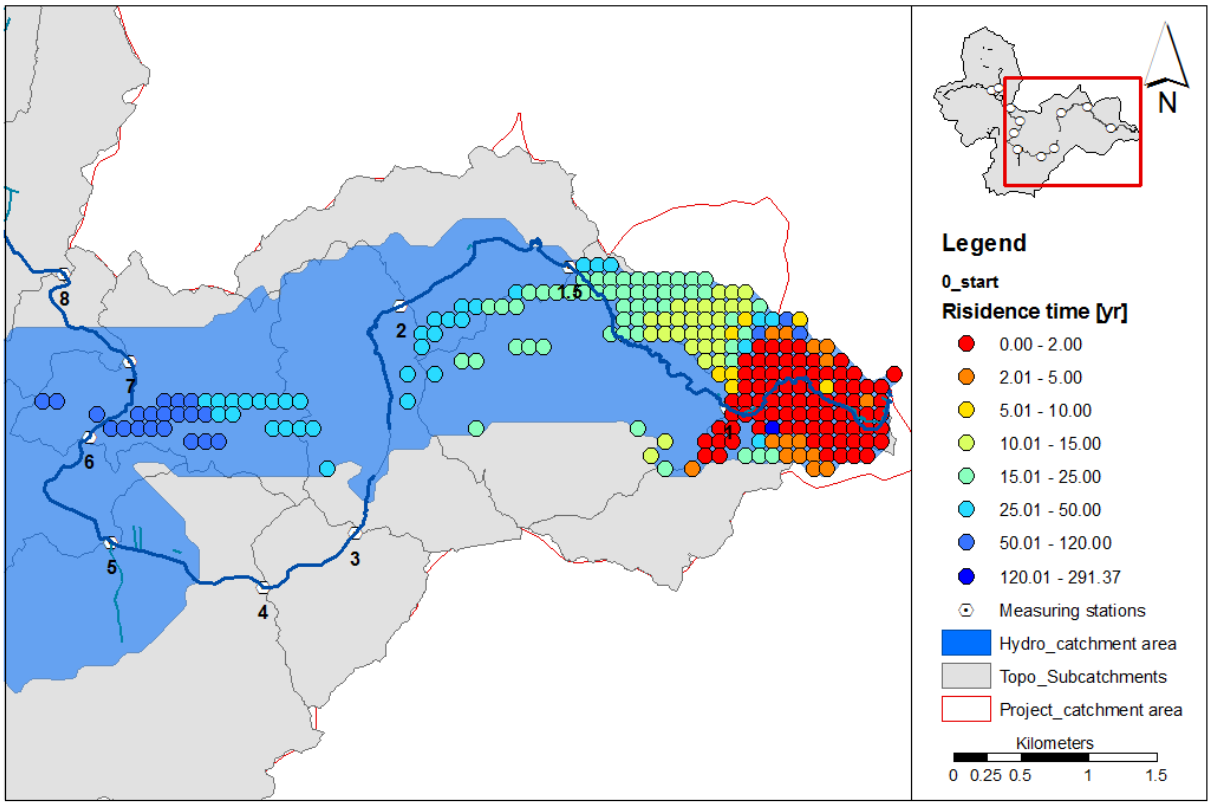

Figure 159: Residence times for hydrogeological sub-catchment of st.0

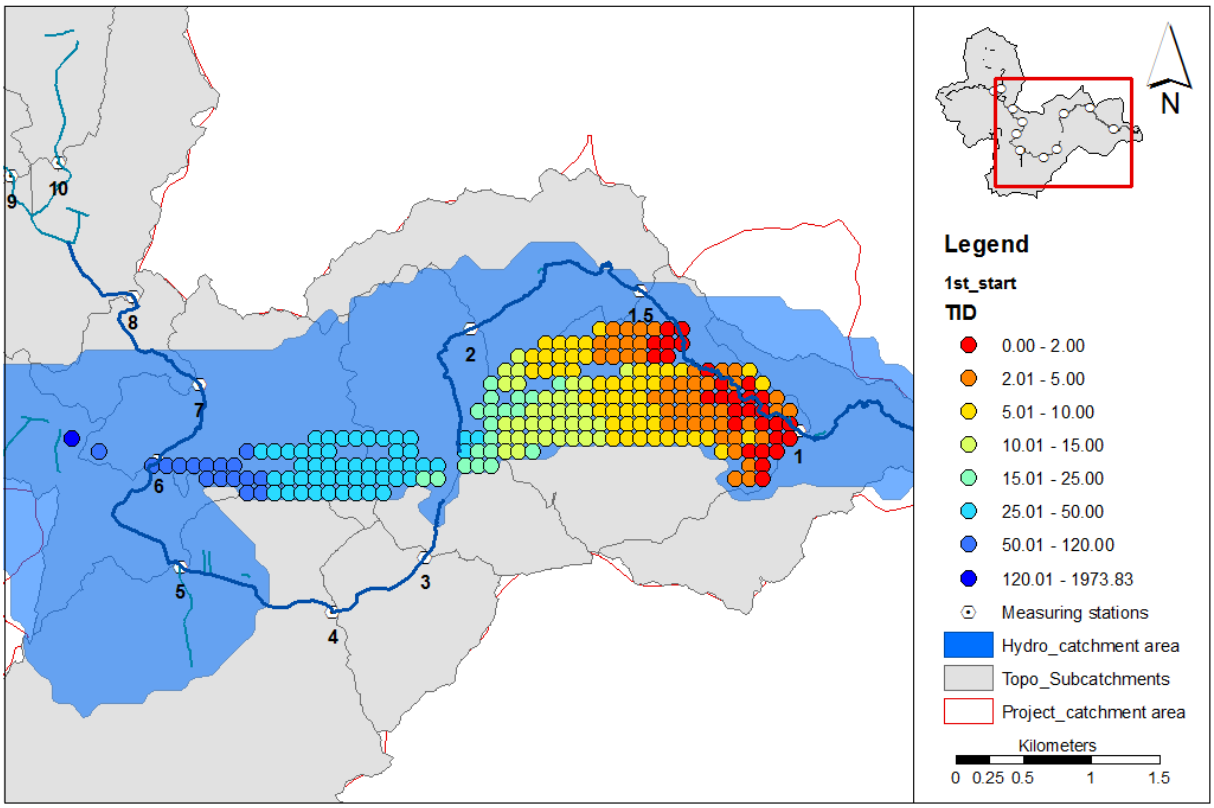

Figure 160: Residence times for hydrogeological sub-catchment of st.1

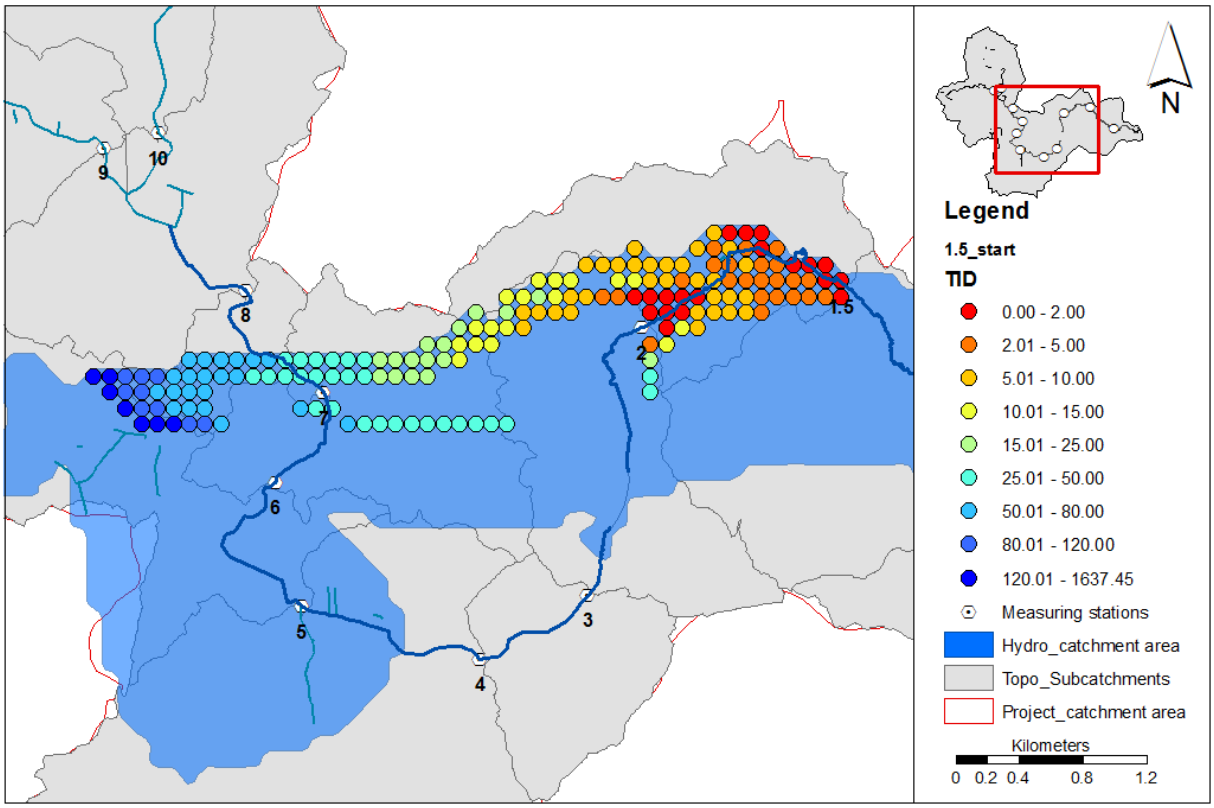

Figure 161: Residence times for hydrogeological sub-catchment of st.1,5

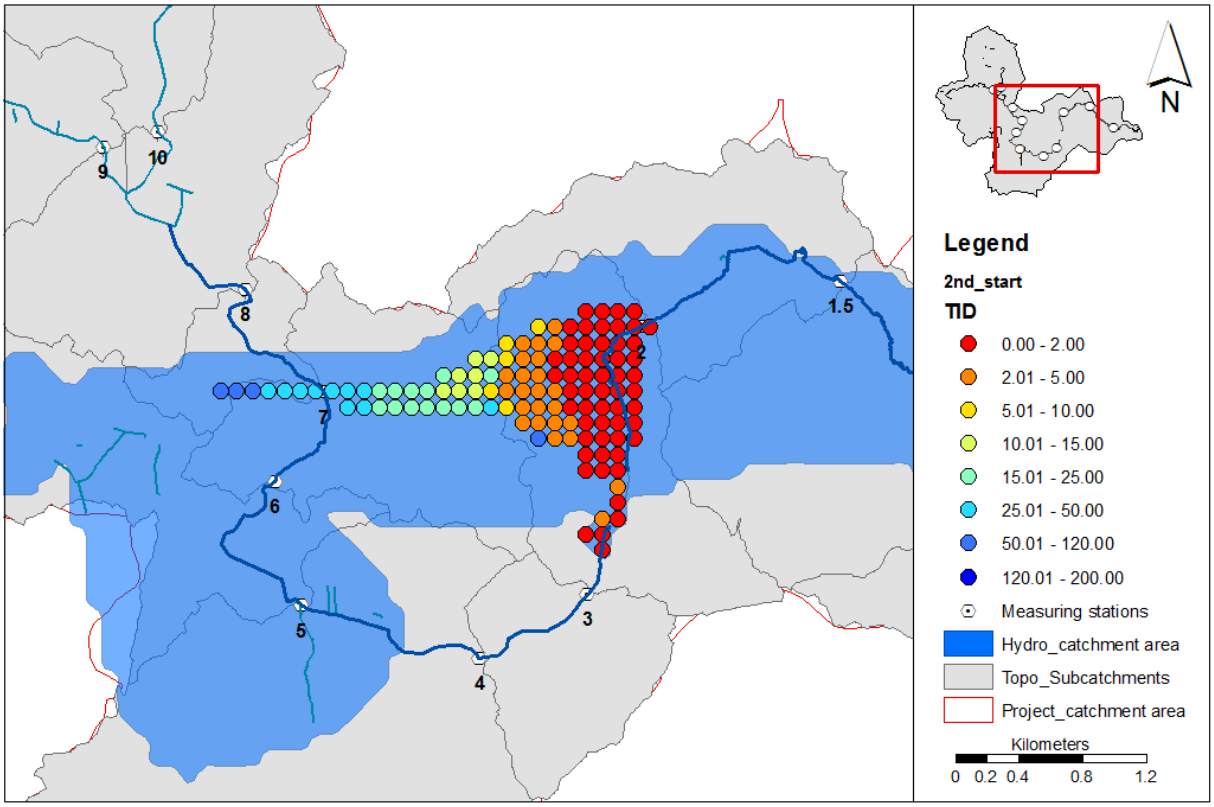

Figure 162: Residence times for hydrogeological sub-catchment of st.2

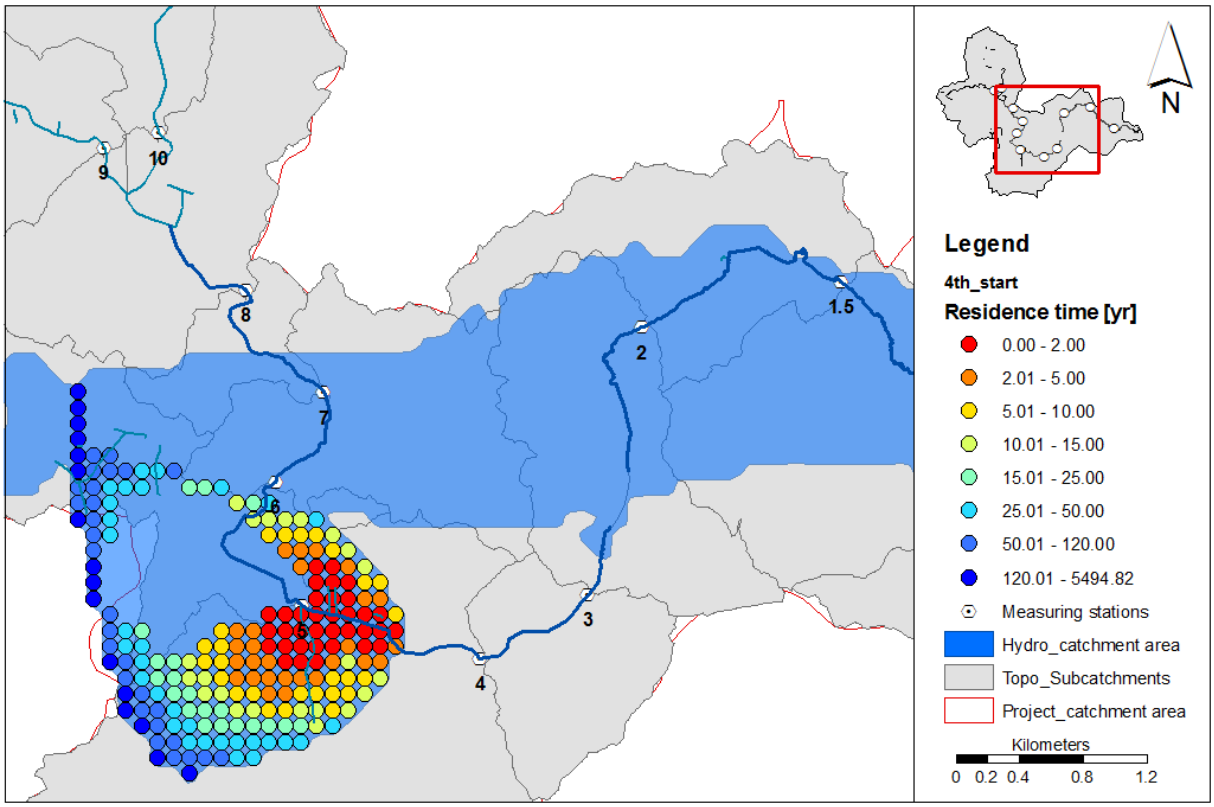

Figure 163: Residence times for hydrogeological sub-catchment of st.4

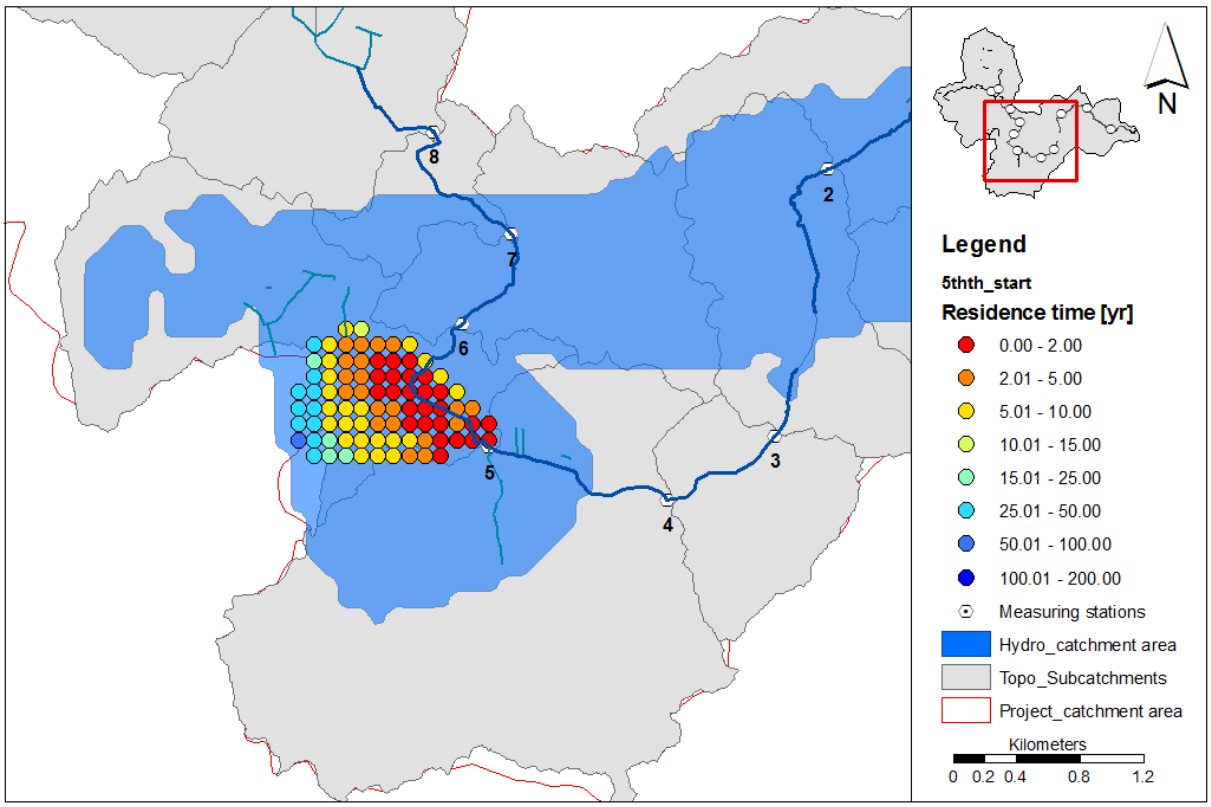

Figure 164: Residence times for hydrogeological sub-catchment of st.5

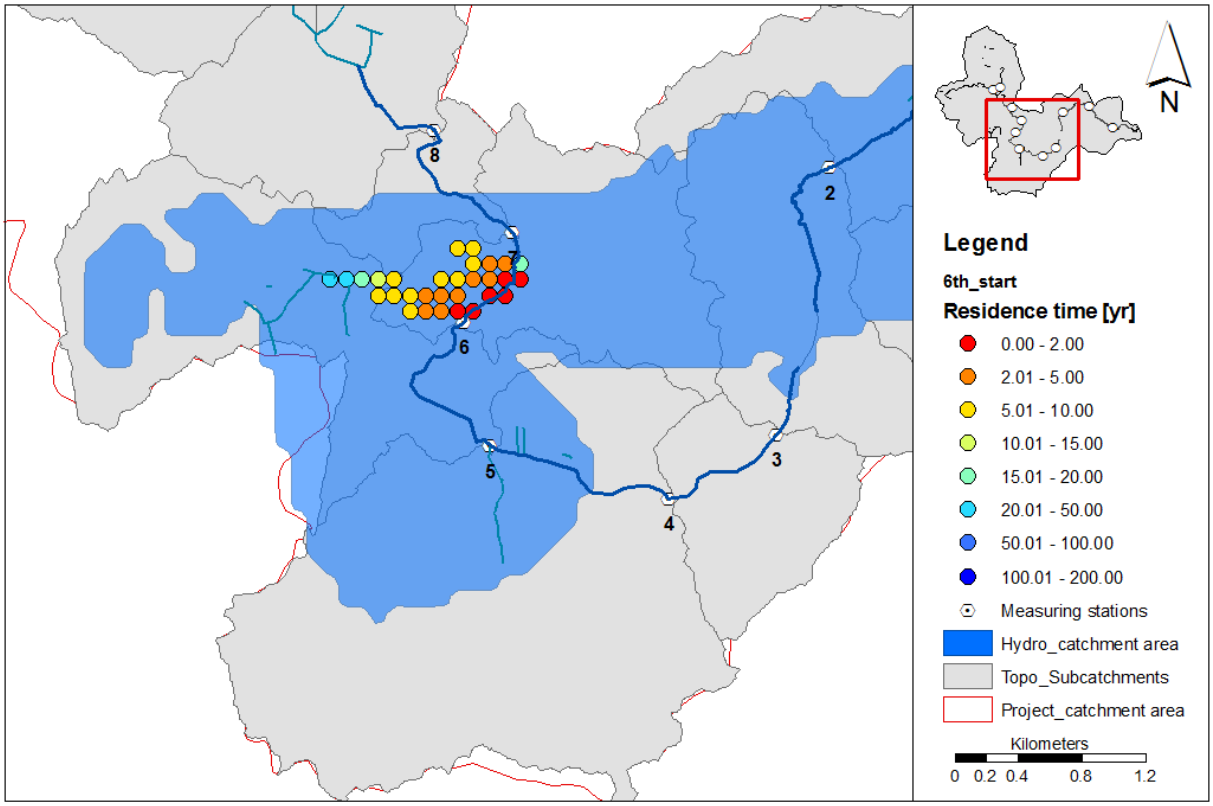

Figure 165: Residence times for hydrogeological sub-catchment of st.6

Table 24: Distribution of the groundwater flow particles to different groups

Range [years]	elements per zone						
	0	1	1.5	2	4	5	6
0-2	80	28	19	56	35	24	6
2.01-5	15	45	23	24	27	20	9
5.01-10	7	49	31	5	26	23	10
10.01-15	28	34	17	7	22	1	1
15.01-25	52	19	16	13	20	4	2
25.01-50	34	50	28	10	31	10	2
50.01-120	23	16	30	4	28	1	0
above 120	1	1	7	0	16	0	0
count[elements]	240	242	171	119	205	83	30
mean	20.86	25.34	67.91	8.6	72.24	9.08	7.19
median	13.73	9.58	13.97	2.18	12.99	4.34	4.93
st.dev.	30.54	126.96	236.92	12.97	436	12.32	7.89
element = starting point of the groundwater flow particles, ending to the stream in that sub-catchment zone							

12 Appendix: Stream Valley Characteristics

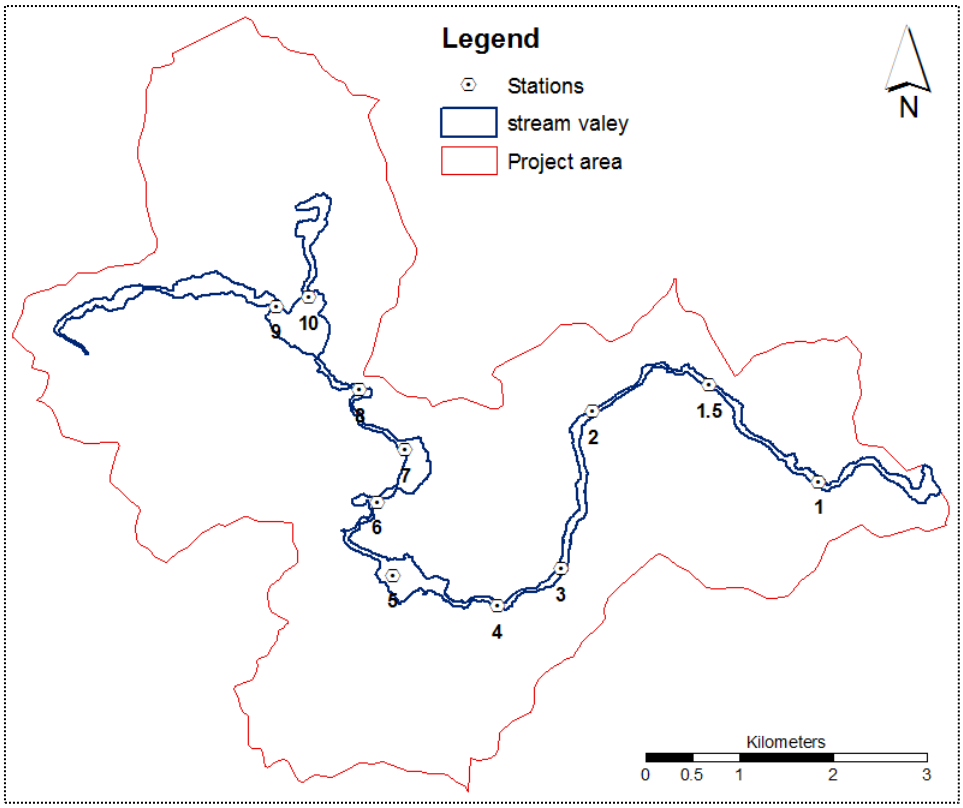

Figure 166: Stream valley (Nature Agency, Aalborg)

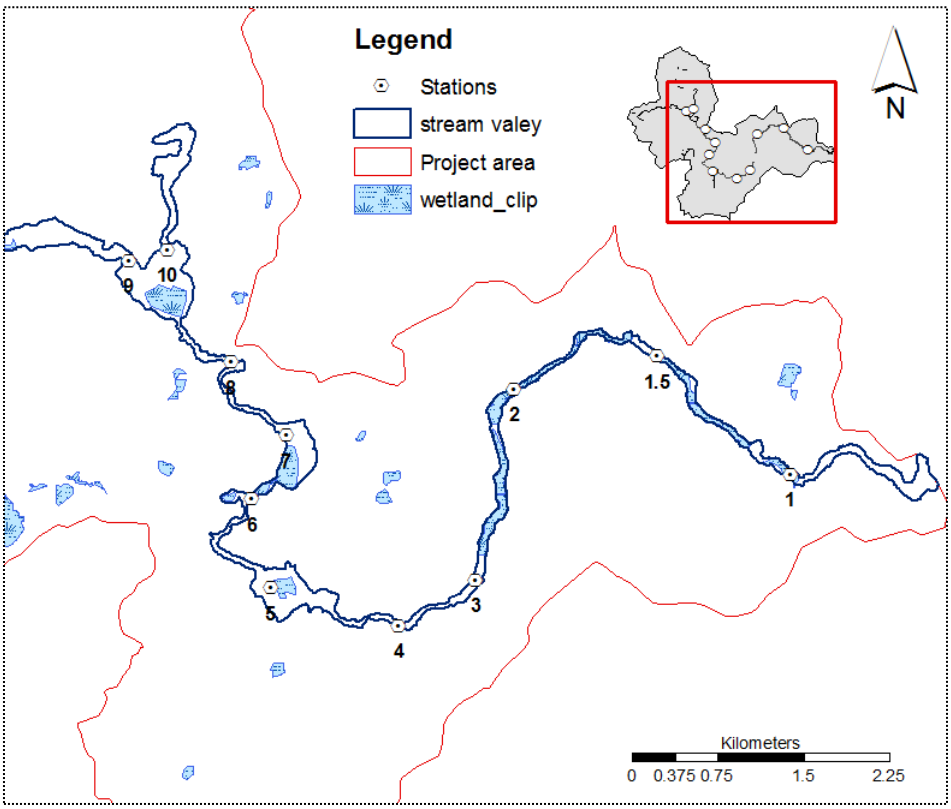

Figure 167: Stream valley together with the wetlands (according to (Ranalli & Macalady, 2010) the hydric soils, which are present in the wetlands, have NO3-N removal capacity above 80% (see Literature study))

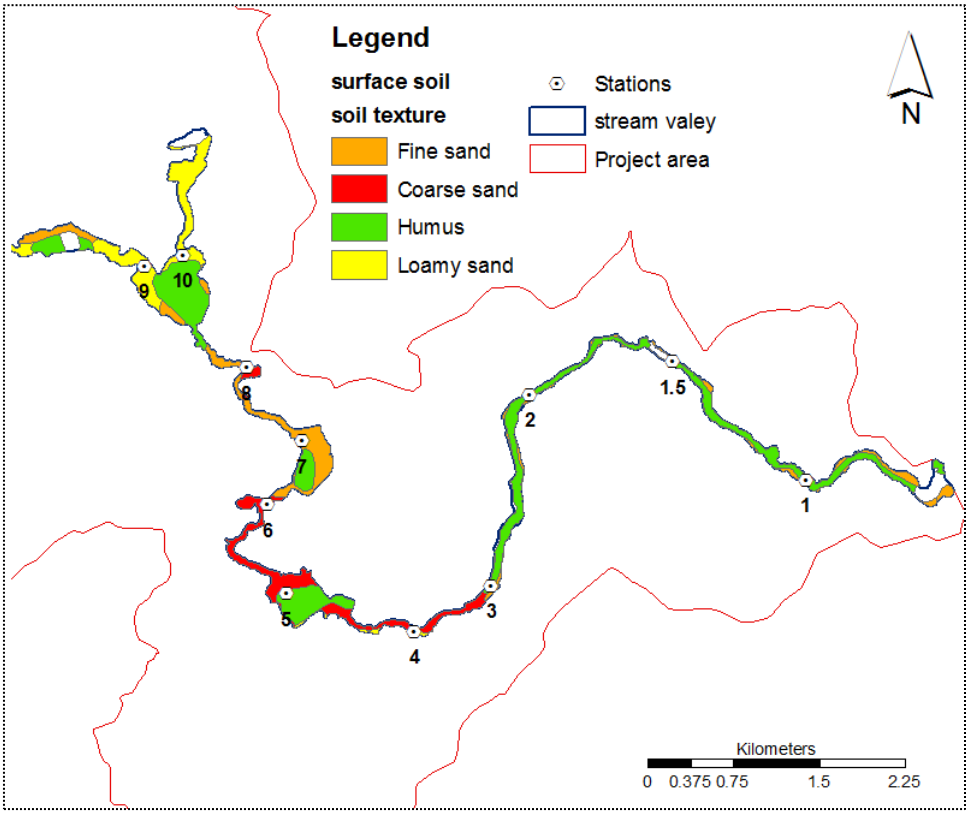

Figure 168: Soil texture in the stream valley

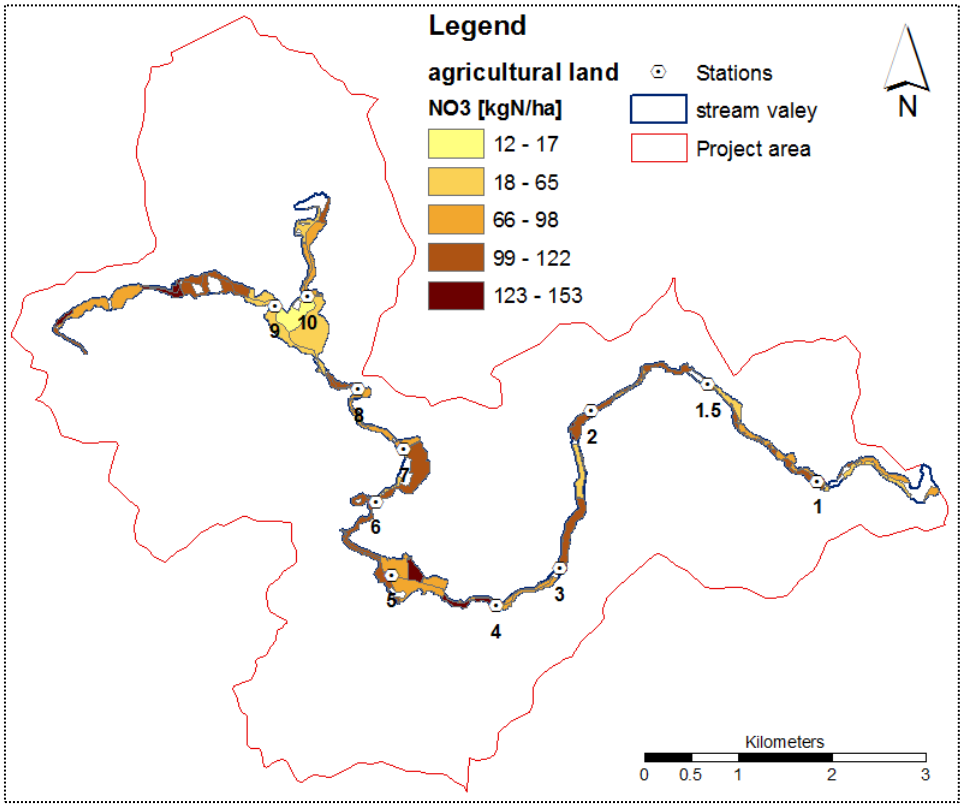

Figure 169: Leaching from the agricultural land in the stream valley

13 Appendix: Non-agricultural Sources for Nitrate Leaching

Fresh water areas

It is decided that the leaching from the "fresh water" areas (small lakes) will be 0kg/ha, because the denitrification occurring in the anoxic sediments.

Natural areas

No value for the leaching from "natural" areas is found from a literature source, so it is assumed, that the leaching will be the same as from the "forest" areas.

Forests

A value for the "forests" is found from a study based on sampling from 111 points in forests in the winters of 1986-1993, as part of the Danish national monitoring program (Callesen et al., 1999). The soil samples from 75-100cm were analysed as this was the depth considered as potential for leaching and it was found that the range of NO_3^--N concentrations is from 0 to 141mgNO_3^--N /dm^3, with a mean value 1.51mgNO_3^--N /dm^3. Callesen et all. (1999) found also that at 7% of the sites the drinking water standard is exceeded and 30% of the sites had a median concentration above 2mgNO_3^--N /dm^3. The authors of the article have calculated that with the precipitation surplus in Denmark in the range 100-300mm/yr these sites will leach more than 2-6kgN/ha/yr.(Callesen et al., 1999) For the purposes of the project, where the leaching from forests is not the main focus, it was chosen that the forests in the catchment area of Lundgårds bæk will leach in the proposed range - 5kgN/ha. It has to be remarked, that this assumption is giving a very rough estimation about the leaching of the forest areas in the region. If a more scientific approach has to be used, than it should be distinguished between forest size, forest type, soil-type and some sampling should be done in order to measure the NO_3^--N leaching from this catchment area. According to (Callesen et al., 1999) the concentrations in forests smaller than 10ha are significantly higher (almost 2 times) than in forests bigger than 50ha. As it is typical for Denmark to have a fragmentary forest cover in the agrarian landscapes, the forest edges (where the higher deposition rates are found) will constitute a high proportion of the forest area. In order to not underestimate the influence of the forest areas, no matter that those represent only 10% of the catchment of Lundgårds bæk further investigation is needed.

Urban areas

Relevant information for the "urban" areas isn't found, neither for the project site, nor for Denmark. That's why it is used a literature source explaining the significance of the non-agricultural Nitrogen for the groundwater quality and presenting a case study of NO_3^- leaching to the oxic aquifer of Nottingham (Wakida & Lerner, 2005). The estimation of the NO_3^- leaching from urban areas is a complicated task, mainly because the complexity of the recharge in those areas and the wide range of pollutant sources. The sources in the urban areas are mixture of point-, multipoint-, and diffuse sources. Wakida and Lerner (2005) build and calibrated a groundwater flow model and three solute transport models for Nottingham, from which as outcome they got the estimates for the total recharge, subdivision of the recharge to different sources, and average N content in the recharge. For the period 1959-1995 the average recharge over the area is calculated to be 211mm/yr. The average Nitrogen concentration in the urban area (Nottingham) for the same period was from 3-17mgN/l, which equivalents to loading of 21kgN/ha/yr. Because the aquifer is mostly oxic, the authors assumed that the main Nitrogen form leaking to the groundwater would be NO_3^--N. The estimated loading is distributed to 5 different sources: 37% to leaking water mains (7.7kgN/ha/yr); 13% to leaking sewers (2.7kgN/ha/yr); 3% N released during house building (0.7kgN/ha/yr); 9% to leaching from gardens, parks etc. (1.9kgN/ha/yr); and 38% to contaminated land, including landfills, industrial land and chemical spills (8.0kg/ha/yr).(Wakida & Lerner, 2005) As the focus of the project is not on the urban areas and their impact on the groundwater quality, it was decided to use the value found in the literature source (21kg/ha). If a more scientific approach should be used, then a similar evaluation for the urban areas in the catchment of Lundgårds bæk should be made.

14 Appendix: Correction Coefficients Calculations

Correction coefficient calculation

The calculation sheet is presented on the next page, where following can be seen:

- In **Table A**: the calculated in GMS travelling times, distributed in 9 time periods for each hydrogeological sub-catchment area (more explanations in Chapter F, p.76)
- In **Table B**: the estimated total NO_3^--N leaching amounts for each sub-catchment, separated in the 3 time groups (0-10years; 10-15 years; above 15 years), $EL_{(i)j}$, by taking into account the % distribution given in Table A;
- The correction coefficients k_j together with the respective time period and the average value for the fertiliser application for LOOP2 (Figure 26, p.38) are also presented.
    - The correction coefficient for the first time period 1998-2008 (0-10years) is $k_1 = 1.00$. In this period the fertiliser application for LOOP2 is in the same range, without obvious upward or downward trend (Figure 27, p.38) with average 80kgN/ha. This is the period, where the estimated for Lundgårds bæk values fall, as they are based on the data for 2008;
    - The correction coefficients for the two other periods are calculated as: the average values of the leaching for the second and third time group are compared with the first one. For example: the average leaching for the period 1993-1997, which corresponds to 10 to 15 years travelling time , is 108 kgN/ha. This is 1.35 times more than in the first period, so the correction coefficient $k_2 = 1.35$
- In **Table C** are calculated $k_j . EL_{(i)j}$ for each sub-catchment, where the values from Table B are multiplied by the correction coefficients for the time period

zone	coefficients	period		[kgN/ha/y]	average NO3-N-n and NO2-N-n over the period (see (Grant et al., 2010))
1	1.00	2008	0	80	
		2007	1		
		2006	2		
		2005	3		
		2004	4		
		2003	5		
		2002	6		
		2001	7		
		2000	8		
		1999	9		
		1998	10		
2	1.35	1997	11	108	
		1996	12		
		1995	13		
		1994	14		
		1993	15		
3	1.88	1992	16	150	
		1991	17		
		1990	18		
		1989	19		
		1988	20		
		1987	21		
		1986	22		
		1985	23		
		1984	24		
		1983	25		

Table A **calculated travelling time distribution in % for each sub-catchment**

traveling time of gw particle	% per sub-catchment 0	1	1.5	2	3	4	5	6	7	8	9	10
0-2	33.33	11.57	11.11	47.06		17.07	28.92	20.00				
2.01-5	6.25	18.60	13.45	20.17		13.17	24.10	30.00				
5.01-10	2.92	20.25	18.13	4.20		12.68	27.71	33.33				
10.01-15	11.67	14.05	9.94	5.88		10.73	1.20	3.33				
15.01-25	21.67	7.85	9.36	10.92		9.76	4.82	6.67				
25.01-50	14.17	20.66	16.37	8.40		15.12	12.05	6.67				
50.01-120	9.58	6.61	17.54	3.36		13.66	1.20	0.00				
above 120	0.42	0.41	4.09	0.00		7.80	0.00	0.00				

Table B **estimated NO3-N leaching divided proportionally to 3 travelling groups**

sub-catchment	0	1	1.5	2	3	4	5	6	7	8	9	10
GIS estimated	13.37	27.16	17.89	17.21	9.38	51.96	22.54	19.13	5.47	13.90	14.02	23.77
gr. 0 - 10	5.68	13.69	7.64	12.29	9.38	22.30	18.20	15.94	5.47	13.90	14.02	23.77
gr.10 - 15	1.56	3.82	1.78	1.01		5.58	0.27	0.64				
gr. Above 15	6.13	9.65	8.47	3.90		24.08	4.07	2.55				
control	13.37	27.16	17.89	17.21	9.38	51.96	22.54	19.13	5.47	13.90	14.02	23.77

Table C **corrected leaching with the coefficient for the different travelling times**

sub-catchment	0	1	1.5	2	3	4	5	6	7	8	9	10
gr. 0 - 10	5.68	13.69	7.64	12.29	9.38	22.30	18.20	15.94	5.47	13.90	14.02	23.77
gr.10 - 15	2.10	5.13	2.39	1.36		7.50	0.37	0.86				
gr. Above 15	11.49	18.09	15.89	7.32		45.15	7.64	4.78				